







FACULTY OF PHARMACEUTICAL SCIENCES

Ghent University

Faculty of Pharmaceutical Sciences

**SPECTROSCOPIC PROCESS MONITORING FOR QUALITY  
ASSESSMENT, VISUALIZATION AND UNDERSTANDING OF  
PHARMACEUTICAL HOT-MELT EXTRUSION**

**LIEN SAERENS**

Pharmacist

Thesis submitted to obtain the degree of Doctor in Pharmaceutical Sciences

2013

Promoter:

Prof. Dr. Thomas De Beer

Laboratory of Pharmaceutical Process Analytical Technology, Ghent University

Co-promoter:

Prof. Dr. Chris Vervaet

Laboratory of Pharmaceutical Technology, Ghent University



The author, the promoter and the co-promoter give the authorization to consult and to copy parts of this thesis for personal use only. Any other use is limited by the Laws of Copyright, especially concerning the obligation to refer to the source whenever results are cited from this thesis.

Ghent, August 10, 2013

The author

The promoter

The co-promoter

Lien Saerens

Prof. Dr. Thomas De Beer

Prof. Dr. Chris Vervaet



# ACKNOWLEDGEMENTS

---

*These past four years turned out to be an overwhelming experience, coloured by the people around me. Completing this PhD could not have been possible without the help, patience, support and encouragement of numerous people, who inspired me and each contributed to this work in their own way.*

*First of all, I would like to express my sincerest appreciation to my promoter, Prof. Dr. Thomas De Beer. Thank you for giving me the opportunity to start this PhD, for the enthusiastic guidance and advice during this period, for the freedom you gave me to interpret and manage the project in my own way, and for the opportunities and challenges to perform parts of this research abroad.*

*I am grateful to my co-promoter, Prof. Dr. Chris Vervaet, and to Prof. Dr. Jean Paul Remon, for their constructive input and revisions of this work, for their interest in the topic and for providing financial support for this PhD.*

*Special thanks go to Anneleen, Margot and Tinne, my allies in the PAT lab, with whom I shared an 'office' from the very beginning. Your friendship, encouragements, scientific assistance, the many conferences we have spent together, our brainstorm sessions and the countless fun moments were inspiring, priceless, and helped me through the more difficult parts of this project. My gratitude also goes out to Laurent, Ana, Fien and Laurens for their constant interest, their support, for brightening up meetings and lunch breaks and for making the PAT lab an enjoyable place to work.*

*I would like to thank all the colleagues from the lab of Pharmaceutical Technology for their advice and helping hands, and in particular Lien, An-Katrien, Thomas and Ana for their scientific input and assistance with the extrusion experiments. The help from Claudine, Katharine and Ilse, who took care of the administrative tasks, is also greatly appreciated.*

*During this PhD, Dr. Elaine Brown gave me the opportunity to perform a part of the presented research in the IRC in Polymer Science & Technology at the University of Bradford, for which I am incredibly grateful. The warm welcome I received from everyone in the department, and the help and scientific feedback during experiments from Dr. Adrian Kelly, Dr. Tim Gough, Prof. Dr. Anant Paradkar, Dr. Ravi Dhumal and Prafulla Apshingekar is genuinely appreciated.*

*I also wish to acknowledge the people at Brabender® Pharma, and in particular Dr. Dima Ghanam and Dipl. Ing. Jane Schwarz, for inviting me to perform experiments at the Brabender® Pharma site in Duisburg, and for their guidance and assistance during the experimental work.*

*Sincere thanks go to FWO (Fonds Wetenschappelijk Onderzoek – Vlaanderen) for providing the necessary funding to successfully complete this project.*

*I am particularly grateful for my friends, who succeeded in taking my mind of work as much as possible. Whether they distracted me by going on memorable holidays or weekends with me (Romy, Wannes, Thomas, Bart, Joachim, Anneke, Greet, Evelien, Annemieke, Severine), by joining me on the volleyball court to reduce the stress levels (Yati, Daphne, Evi, Tine, Lynn, Dolfien) or just by being there as my roommates (Lorijn, Eline), these past four years would have been much tougher without them. Special thanks go to Hanneleen, for her help with the layout and cover design.*

*And finally, my deepest gratitude goes out to my family, and in particular to my parents, my brothers Tijs and Toon, my grandparents and tante Trees. Thank you for your endless support and encouragements, and for the many opportunities you have given me!*







---

# TABLE OF CONTENTS

---

<b>LIST OF ABBREVIATIONS .....</b>	<b>1</b>
 <b>CHAPTER 1</b>	
<b>INTRODUCTION AND OBJECTIVES .....</b>	<b>5</b>
1.1. INTRODUCTION AND OBJECTIVES .....	7
1.2. REFERENCES .....	11
 <b>CHAPTER 2</b>	
<b>HOT-MELT EXTRUSION AS A PHARMACEUTICAL PRODUCTION PROCESS .....</b>	<b>13</b>
2.1. HOT-MELT EXTRUSION .....	15
2.2. PROCESS AND EQUIPMENT .....	17
2.3. REFERENCES .....	20
 <b>CHAPTER 3</b>	
<b>PROCESS MONITORING AND VISUALIZATION SOLUTIONS FOR HOT-MELT EXTRUSION.....</b>	<b>23</b>
3.1. INTRODUCTION .....	25
3.2. PROCESS ANALYTICAL TECHNOLOGY .....	27
3.3. PROCESS ANALYTICAL TECHNIQUES APPLIED FOR PHARMACEUTICAL HOT-MELT EXTRUSION .....	30
3.3.1. NIR spectroscopy .....	30
3.3.2. Raman spectroscopy .....	37
3.3.3. Monitoring of torque and power consumption .....	40
3.4. MONITORING OF POLYMER MELT EXTRUSION .....	42
3.4.1. Spectroscopic techniques .....	42
3.4.1.1. NIR spectroscopy .....	42
3.4.1.2. UV-VIS spectroscopy .....	45
3.4.1.3. Fluorescence spectroscopy .....	52

3.4.1.4.	Terahertz (THz) spectroscopy .....	55
3.4.1.5.	Dielectric spectroscopy .....	56
3.4.1.6.	Optical detectors .....	57
3.4.1.7.	Nuclear magnetic resonance (NMR) spectroscopy .....	58
3.4.2.	Ultrasonic techniques .....	58
3.4.3.	Rheological techniques.....	61
3.4.4.	Other process analytical techniques .....	65
3.4.5.	Combinations and comparison of complementary process analytical techniques .....	66
3.5.	CONCLUSION .....	68
3.6.	REFERENCES .....	69

#### **CHAPTER 4**

#### ***RAMAN SPECTROSCOPY FOR THE IN-LINE POLYMER-DRUG QUANTIFICATION AND SOLID STATE CHARACTERIZATION DURING A PHARMACEUTICAL HOT-MELT EXTRUSION PROCESS***

.....	73	
4.1.	INTRODUCTION .....	75
4.2.	MATERIALS AND METHODS .....	77
4.2.1.	Materials and hot-melt extrusion .....	77
4.2.2.	Raman spectroscopy .....	78
4.2.3.	Differential scanning calorimetry (DSC) .....	78
4.2.4.	Attenuated total reflectance Fourier transform infrared (ATR FT-IR).....	79
4.3.	RESULTS AND DISCUSSION .....	80
4.3.1.	In-line API concentration monitoring.....	80
4.3.2.	In-line solid state monitoring .....	82
4.4.	CONCLUSION .....	92
4.5.	REFERENCES .....	93

**CHAPTER 5****VALIDATION OF AN IN-LINE RAMAN SPECTROSCOPIC METHOD FOR CONTINUOUS API**

<b>QUANTIFICATION DURING PHARMACEUTICAL HOT-MELT EXTRUSION</b> .....	95
5.1. INTRODUCTION .....	97
5.2. MATERIALS AND METHODS .....	99
5.2.1. Materials.....	99
5.2.2. Hot-melt extrusion .....	99
5.2.3. Raman spectroscopy .....	99
5.2.4. Development of the Raman calibration models .....	100
5.2.5. Validation of the Raman method and estimation of its uncertainty .....	103
5.2.6. Evaluation of the robustness of the Raman calibration models .....	105
5.3. RESULTS AND DISCUSSION .....	107
5.3.1. Development of the Raman calibration models .....	107
5.3.2. Validation of the Raman method and estimation of its uncertainty .....	108
5.3.3. Evaluation of the robustness of the Raman calibration models .....	114
5.4. CONCLUSION .....	116
5.5. REFERENCES .....	117

**CHAPTER 6****VISUALIZATION AND PROCESS UNDERSTANDING OF MATERIAL BEHAVIOUR IN THE EXTRUSION BARREL DURING A HOT-MELT EXTRUSION PROCESS USING RAMAN**

<b>SPECTROSCOPY</b> .....	119
6.1. INTRODUCTION .....	121
6.2. MATERIALS AND METHODS .....	124
6.2.1. Materials.....	124
6.2.2. Hot-melt extrusion .....	124
6.2.3. Raman spectroscopy .....	125
6.2.4. Fourier transform infrared spectroscopy (FT-IR).....	127
6.2.5. Differential scanning calorimetry (DSC) .....	128
6.3. RESULTS AND DISCUSSION .....	129

6.3.1.	Influence of MPT concentration on the solid state of the extrudates .....	129
6.3.2.	Influence of the barrel temperature on the solid state of the extrudates .....	136
6.3.3.	Influence of the rotational screw speed on the solid state of the extrudates.....	138
6.4.	CONCLUSION .....	142
6.5.	REFERENCES .....	143

## **CHAPTER 7**

<b><i>IN-LINE SOLID STATE PREDICTION DURING PHARMACEUTICAL HOT-MELT EXTRUSION IN A 12 MM TWIN SCREW EXTRUDER USING RAMAN SPECTROSCOPY</i></b> .....		145
7.1.	INTRODUCTION .....	148
7.2.	MATERIALS AND METHODS .....	150
7.2.1.	Materials.....	150
7.2.2.	Hot-melt extrusion .....	150
7.2.3.	Raman spectroscopy .....	152
7.2.4.	Data collection, alignment and analysis .....	154
7.2.5.	Differential scanning calorimetry .....	155
7.2.6.	X-ray powder diffraction .....	156
7.3.	RESULTS AND DISCUSSION .....	157
7.3.1.	In-line monitoring of solid state .....	157
7.3.2.	Influence of die pressure on in-line collected Raman spectra .....	165
7.4.	CONCLUSION .....	168
7.5.	REFERENCES .....	169

## **CHAPTER 8**

<b><i>IN-LINE NIR SPECTROSCOPY FOR THE UNDERSTANDING OF POLYMER-DRUG INTERACTION DURING PHARMACEUTICAL HOT-MELT EXTRUSION</i></b> .....		171
8.1.	INTRODUCTION .....	173
8.2.	MATERIALS AND METHODS .....	176
8.2.1.	Materials.....	176
8.2.2.	Hot-melt extrusion .....	176
8.2.3.	NIR spectroscopy .....	177

8.2.4.	Raman spectroscopy .....	179
8.2.5.	DSC analysis .....	179
8.2.6.	ATR FT-IR spectroscopy .....	180
8.3.	RESULTS AND DISCUSSION .....	181
8.3.1.	In-line monitoring of API concentration.....	181
8.3.2.	In-line monitoring of solid state and polymer-drug interactions.....	183
8.3.2.1.	Near-infrared spectroscopy.....	183
8.3.2.2.	Differential scanning calorimetry .....	185
8.3.2.3.	ATR FT-IR spectroscopy .....	188
8.3.2.4.	Raman spectroscopy .....	191
8.4.	CONCLUSION .....	193
8.5.	REFERENCES .....	194
 <b>CHAPTER 9</b>		
<b><i>IN-LINE ULTRASOUND MONITORING OF DRUG CONCENTRATION DURING PHARMACEUTICAL HOT-MELT EXTRUSION .....</i></b>		
<b><i>197</i></b>		
9.1.	INTRODUCTION .....	199
9.2.	MATERIALS AND METHODS .....	201
9.2.1.	Materials.....	201
9.2.2.	Hot-melt extrusion .....	201
9.2.3.	Ultrasound equipment .....	202
9.2.4.	Data analysis.....	203
9.3.	RESULTS.....	204
9.4.	CONCLUSION .....	207
9.5.	REFERENCES .....	208
 <b><i>FUTURE PERSPECTIVES.....</i></b>		
<b><i>209</i></b>		
<b><i>SUMMARY AND GENERAL CONCLUSIONS .....</i></b>		
<b><i>215</i></b>		
<b><i>SAMENVATTING EN ALGEMEEN BESLUIT .....</i></b>		
<b><i>223</i></b>		
<b><i>CURRICULUM VITAE.....</i></b>		
<b><i>233</i></b>		





## LIST OF ABBREVIATIONS

---

<b>API</b>	active pharmaceutical ingredient
<b>ATR</b>	attenuated total reflectance
<b>ATR FT-IR</b>	attenuated total reflectance Fourier transform infrared
<b>BCS</b>	biopharmaceutical classification system
<b>BPP</b>	bis (-pyrene) propane
<b>CA</b>	citric acid
<b>CA MH</b>	citric acid monohydrate
<b>CCD</b>	charge coupled device
<b>CEL</b>	celecoxib
<b>Dcrit</b>	critical distance
<b>DModX</b>	distance to model
<b>DOE</b>	design of experiments
<b>DSC</b>	differential scanning calorimetry
<b>DTGS</b>	deuterated triglycine sulfate
<b>EVA</b>	ethylene vinyl acetate
<b>FA</b>	formaldehyde
<b>FDA</b>	Food and Drug Administration
<b>FT</b>	Fourier transform
<b>FT-IR</b>	Fourier transform infrared
<b>GMP</b>	Good Manufacturing Practice
<b>HDPE</b>	high density polyethylene
<b>HME</b>	hot-melt extrusion
<b>HPLC</b>	high performance liquid chromatography
<b>ICH</b>	International Conference on Harmonization
<b>InGaAs</b>	indium gallium arsenide
<b>IR</b>	infrared
<b>LDPE</b>	low density polyethylene

<b>LLDPE</b>	linear low density polyethylene
<b>MCR</b>	multivariate curve resolution
<b>MgSt</b>	magnesium stearate
<b>MI</b>	melt flow index
<b>MPT</b>	metoprolol tartrate
<b>MSC</b>	multiplicative signal correction
<b>NIR</b>	near infrared
<b>NMR</b>	nuclear magnetic resonance
<b>PA 6</b>	polyamide 6
<b>PAT</b>	process analytical technology
<b>PC</b>	principal component
<b>PCA</b>	principal component analysis
<b>PE</b>	polyethylene
<b>PEO</b>	polyethylene oxide
<b>PLLA</b>	poly-L-lactic acid
<b>PLS</b>	partial least squares
<b>POM</b>	polyoxymethylene
<b>PP</b>	polypropylene
<b>PP-g-MA</b>	polypropylene grafted with maleic anhydride
<b>PS</b>	polystyrene
<b>PVC</b>	polyvinyl chloride
<b>QbD</b>	quality by design
<b>RMSEC</b>	root mean square error of calibration
<b>RMSECV</b>	root mean square error of cross validation
<b>RMSEP</b>	root mean square error of prediction
<b>RTD</b>	residence time distribution
<b>S</b>	section
<b>SEC</b>	standard error of calibration
<b>SEP</b>	standard error of prediction
<b>SFSTP</b>	Société Française des Sciences et Techniques Pharmaceutiques
<b>SIMCA</b>	soft independent modeling of class analogy
<b>SNV</b>	standard normal variate

<b>TCM</b>	thermocouple mesh
<b>T<sub>g</sub></b>	glass transition temperature
<b>THz</b>	terahertz
<b>T<sub>m</sub></b>	melt temperature
<b>TSE</b>	twin-screw extrusion
<b>UV-VIS</b>	ultraviolet – visible
<b>VA</b>	vinyl acetate
<b>XRD</b>	X-ray diffraction



# **CHAPTER 1**

# **INTRODUCTION AND OBJECTIVES**



# CHAPTER 1

## INTRODUCTION AND OBJECTIVES

---

### 1.1. INTRODUCTION AND OBJECTIVES

Hot-melt extrusion is defined as the process of pumping raw materials with one or two rotating screw(s) through a die into a product of uniform shape under controlled conditions, such as temperature, feed rate and pressure [1]. At the end of the eighteenth century, the extrusion technique was originally invented for the manufacturing of lead pipes. Today, it is widely applied in the plastic, rubber and food industry. In pharmaceutical manufacturing, the technique is used to produce molecular dispersions of active pharmaceutical ingredients (APIs) in various polymer and/or lipid matrices. The hot-melt extrusion process has proven to be a viable method for the production of granules, pellets, tablets, suppositories, implants, stents, transdermal systems, transmucosal systems and ophthalmic inserts [2], thereby enhancing the dissolution rate and bioavailability of poorly soluble drugs, enabling controlled or modified release of the drug, masking the bitter taste of several active pharmaceutical ingredients and allowing the formulation of various thin films.

One of the advantages of the hot-melt extrusion technique, compared to the more conventional pharmaceutical manufacturing processes, is its ability to be operated in a continuous mode [3, 4]. The benefits of continuous manufacturing compared to batch production are numerous [5-7]: no scale-up issues resulting in a shorter development time; possible automation of the production line; reduction of production costs; faster product release; less product variability and improved product quality. In contrast with the food and chemical industry where continuous production processes are well established, the pharmaceutical manufacturing industry currently primarily relies on batch wise production [5], where product quality is assessed subsequent to each processing step using off-line,

time-consuming analytical techniques on randomly collected samples to evaluate the end or intermediate product quality.

Pharmaceutical production must be carried out in accordance with the Good Manufacturing Practice (GMP) guidelines, which ensure that products should be consistently produced and controlled to the quality standards appropriate to their intended use and as required by the Marketing Authorization, Clinical Trial Authorization or product specification [8]. Recently, the regulatory authorities began to encourage the transition from batch production to continuous processing. The application of traditional off-line quality control methods would annul the benefits inherent in continuous manufacturing, and therefore real-time, in-process measurements of (intermediate) product quality are essential to sustain a continuous production process. The Process Analytical Technology (PAT) guideline, proposed by the Food and Drug Administration (FDA), presents a framework for the continuous monitoring and control of pharmaceutical production processes [9]. Continuous manufacturing requires a PAT monitoring and control strategy, to allow production according to the Quality by Design (QbD) approach [10]. The ultimate purpose of PAT is to develop manufacturing processes that can compensate for the variability in raw materials and in equipment, to guarantee a consistent end-product quality, as required by the GMP guidelines. Therefore, information on the critical quality attributes is gathered in real-time, to allow process adjustments. PAT ensures that all sources of variability affecting a process are identified, explained and managed.

Despite the increasing popularity of hot-melt extrusion as a pharmaceutical production process, quality control is still performed off-line, and the process is more or less controlled using standard, univariate process monitoring sensors such as temperature and pressure probes. The data generated by these sensors does not suffice to assess the critical quality attributes of the extrudates, and cannot ensure the development of an end product with predefined and consistent quality characteristics. This thesis examines the application of spectroscopic tools as process analytical techniques for the monitoring of critical quality attributes such as API concentration, solid state and occurrence of polymer-drug interactions during hot-melt extrusion, for the visualization of material behaviour in the process environment and to improve the overall process understanding.



In **Chapter 2**, a general overview of the principles of hot-melt extrusion, its advantages and shortcomings for pharmaceutical production and an overview of the extrusion equipment are provided. **Chapter 3** summarizes the concept of PAT, and discusses the various process analytical tools available for observation of critical process and product parameters which are currently being applied in pharmaceutical hot-melt extrusion and in polymer extrusion.

Chapters 4 to 9 provide the results from the conducted experimental work. In **Chapter 4**, the feasibility of Raman spectroscopy as a process analytical tool for in-line monitoring and prediction of the API concentration and for monitoring of the physicochemical state of the extrudates and possible interactions between polymers and drugs during hot-melt extrusion was assessed. Raman spectra were collected in the extrusion die. A predictive PLS model was developed for the in-line determination of the API concentration, and the manifestation of peak broadening and shifts in the in-line collected Raman spectra was correlated to differences in solid state and interactions between the API and the polymer during hot-melt extrusion. Once the suitability of Raman spectroscopy to monitor and predict the API concentration during hot-melt extrusion was verified, an improved API calibration model was developed and a thorough validation method for drug quantification based on Raman spectra collected in the extrusion die was applied (**Chapter 5**). The validation of the developed method was based on the calculation of the accuracy profile, which allowed the determination of the proportion of future measurements that will be found within preset acceptance limits (a preset percentage of the relative bias, here set at 10%). Finally, the uncertainty of the method was determined, and the robustness of the predictive model was assessed via a design of experiments, where possible small fluctuations in process settings were simulated.

In **Chapter 6**, the influence of variations in drug concentration, barrel temperature and screw speed on the polymer-drug solid state and interactions throughout the entire extrusion barrel was examined. A Raman probe was implemented in each section of the extrusion barrel, to visualize and enhance the understanding of material behaviour during hot-melt extrusion.

The aim of the experiments performed in **Chapter 7**, was to create a method for the real-time classification of extrudates according to their solid state, based on Raman spectroscopic measurements collected in the extrusion die of a 12 mm twin-screw extruder. The influence of variations in drug concentration, changes in barrel temperature and three different screw configurations on the physicochemical state of the extrudates was assessed. Soft independent modelling of class analogy was performed to develop a classification model which allowed distinction between glassy solid solutions and crystalline dispersions of a poorly soluble API in a polymer. Additionally, the effects on the Raman measurements of the applied drug concentration, processing temperature and feeder performance, all resulting in fluctuations in die pressure, were evaluated.

In **Chapter 8**, the suitability of NIR spectroscopy for the in-line determination of the drug concentration, the polymer-drug solid state and molecular interactions was evaluated by implementing an NIR probe in the extrusion die. A PLS model was developed for in-line API concentration monitoring. The relationship between peak broadening, peak shifts, and variations in physicochemical state of the extrudates was studied. The manifestation of new peaks in the NIR spectra was used to determine the type of interactions occurring between the selected polymer and API.

The aim of **Chapter 9** was to evaluate the suitability of ultrasonic techniques as process analytical tools for the in-line monitoring of the API concentration. A PLS model for API quantification was developed based on the monitoring of torque, die pressure, ultrasonic transit time and peak height of the ultrasound signal.

## 1.2. REFERENCES

- [1] J.W. McGinity, M.A. Repka, J.J. Koleng Jr., F. Zhang, Hot-Melt Extrusion Technology, In: p. 2004-2020.
- [2] M. Maniruzzaman, J.S. Boateng, M.J. Snowden, D. Douroumis, ISRN Pharm 2012 (2012) 1-9.
- [3] Madan S, Madan S, Asian J Pharm Sci 7 (2012) 123-133.
- [4] M.M. Crowley, F. Zhang, M.A. Repka, S. Thumma, S.B. Upadhye, S. Battu, J.W. McGinity, C. Martin, Drug Dev Ind Pharm 33 (2007) 909-926.
- [5] K. Plumb, Chem Eng Res Des 83 (2005) 730-738.
- [6] C. Vervaet, J.P. Remon, Chem Eng Sci 60 (2005) 3949-3957.
- [7] J.P. Remon, C. Vervaet, Continuous Processing of Pharmaceuticals. In: J. Swarbrick (Ed.), Encyclopedia of Pharmaceutical Technology, third ed., Informa Healthcare USA, Inc., New York, USA, 2007, p. 743-749.
- [8] European Commission, EU Guidelines to Good Manufacturing Practice. Medicinal Products for Human and Veterinary Use, Brussels, Belgium, 2010.
- [9] Food and Drug Administration, Process Analytical Technology Initiative, Guidance for Industry; PAT - A Framework for Innovative Pharmaceutical development, Manufacturing and Quality Assurance, 2004.
- [10] D. Rudd, Pharmacopoeial implications of continuous processes: new concepts compared to batch processes, Presented at Process Analytical Technologies, May 3–4, Cannes, France, 2004.



# CHAPTER 2

## HOT-MELT EXTRUSION AS A PHARMACEUTICAL PRODUCTION PROCESS

Parts of this chapter are published in:

**L. Saerens**, C. Vervaet, J.P. Remon, T. De Beer. Process monitoring and visualization solutions for hot-melt extrusion: A review. *Journal of Pharmacy and Pharmacology*, doi: 10.1111/jphp12123 (2013).



## CHAPTER 2

# HOT-MELT EXTRUSION AS A PHARMACEUTICAL PRODUCTION PROCESS

---

### 2.1. HOT-MELT EXTRUSION

HME is one of the most widely used processing techniques in the plastic and rubber manufacturing industry and is extensively applied in the food processing industry. It is defined as the process of pumping raw materials with a rotating screw through a die into a product of uniform shape under controlled conditions, such as temperature, feed rate and pressure [1, 2]. HME has potential to be applied in continuous manufacturing for a wide variety of dosage forms and formulations, such as granules, pellets, tablets, capsules, implants, suppositories, stents, transdermal and transmucosal systems and ophthalmic inserts [3, 4]. In hot-melt extruded drug delivery systems, active pharmaceutical ingredients (APIs) are embedded in a carrier, containing meltable materials and additional excipients. These materials can be polymeric materials or thermodeformable waxes [5].

HME offers several advantages compared to conventional pharmaceutical production processes [1, 3, 4, 6, 7] of solid dosage forms for certain formulations. Formulations produced with HME often exhibit an enhanced bioavailability of poorly soluble drugs, due to dispersion of the API at molecular level in the final dosage forms [8-10]. The molten polymers can function as thermal binders and act as drug depots or drug release retardants, hence allowing sustained, modified and targeted release. HME also allows masking of the bitter taste of an API [11-13]. An improved content uniformity is obtained by the intense agitation and distributive and dispersive mixing generated by the rotating screw and its selected configuration, resulting in the de-aggregation of suspended particles in the molten

polymer. The process is anhydrous, avoiding potential water-mediated drug degradation. Exclusion of solvents in the production process decreases the number of processing steps and eliminates the need for time-consuming drying steps. The extrudates can be cut into tablets, hence eliminating tableting issues caused by poor compressibility of the formulation. An additional significant advantage is that HME is a continuous process. The advantages of continuous production over traditional batch processes are numerous [14-16]: less scale-up issues resulting in a shorter development time, possible automation of the production line, reduction of production costs and waste, a reduced time-to-market, less product variability and improved product quality.

During extrusion, all components in the formulation must be thermally stable at the selected processing temperatures, which could limit the extrusion of thermosensitive APIs and carriers. However, the residence time in a twin-screw extruder is relatively short, and the temperature of each barrel segment can be controlled accurately. Downstream feeding of thermolabile APIs (behind the kneading zone) can avoid degradation of these compounds due to high temperatures caused by the shear forces generated by the rotating screw and its screw design that are needed to melt the polymers. Hence, the exposure of the API to high temperatures is reduced to a minimum. Another drawback of HME is related to the high energy input from the shear forces in the extrusion barrel, leading to higher, uncontrolled and unknown product temperatures, which could induce drug or polymer degradation, having a significant impact on the product quality. This obstacle can be overcome by adjusting the process parameters as well as the screw and die design [2].



## 2.2. PROCESS AND EQUIPMENT

The equipment for HME comprises an extruder, downstream auxiliary equipment and monitoring tools used for performance and product quality evaluation. The extruder itself (Figure 2.1) consists of a feeding hopper, a temperature controlled barrel with one or two screws, a screw-driving unit, a die to shape the final product and a heating/cooling device [2, 5]. A powder blend, typically containing the API, thermoplastic polymers or waxes as a matrix carrier and other functional excipients (e.g. plasticizers, release modifying agents, superdisintegrants, thickening agents, antioxidants, thermal lubricants, bulking agents and miscellaneous additives [1, 2]), is fed through the feed hopper into the barrel. This barrel usually contains different zones, each with a specific set barrel temperature. The rotating screws within the barrel transport the powder blend towards the extrusion die. The powder blend will melt primarily due to the heat generated by friction as the material is sheared between the rotating screw(s) and the barrel wall, and additional heat is conducted from the barrel [6]. This melt is then pumped through the die located at the end of the extrusion barrel, and subjected to further downstream processing equipment.

The screw design has a significant influence on the efficiency of the HME process and on the quality of the end product. Screw geometry directly affects the throughput, melting rate, mixing, product temperature and homogeneity of the melt. Different screw configurations allow downstream transport of the material in the barrel towards the extrusion die, conveying, melting, mixing, venting or devolatilization, and pumping and compression of the molten powder blend. Several types of screw elements are required to perform these tasks. Conveying elements provide transport of the melt, either forward or backward. Different mixing elements can also be included in the screw design. Their function, distributive or dispersive mixing, is related to their geometry. Furthermore, they also play a key role in transforming the API from its crystalline to its amorphous form [17]. A detailed overview of all possible screw elements can be found in the literature [8, 18, 19].

In pharmaceutical HME, twin-screw extrusion is preferred over single-screw extrusion. In twin-screw extrusion, the screws can rotate in the opposite direction (counter-rotating) or in

the same direction (co-rotating), whichever is most favourable. Counter-rotating designs are used when regions with very high shear are required. These extruder types allow potential air entrapment, high pressure generation and low maximum screw speeds and output [1]. Co-rotating screws are often fully intermeshing, indicating that as the screws rotate, the element on one screw wipes the element on the neighbouring screw, causing material to transfer between both screws [6]. They can be operated at high screw speeds and deliver high outputs, and offer better mixing and conveying of the melt. Other benefits related to co-rotating screws are a shorter residence time, less tendency to overheat the materials, and an easier material feed [6, 20].

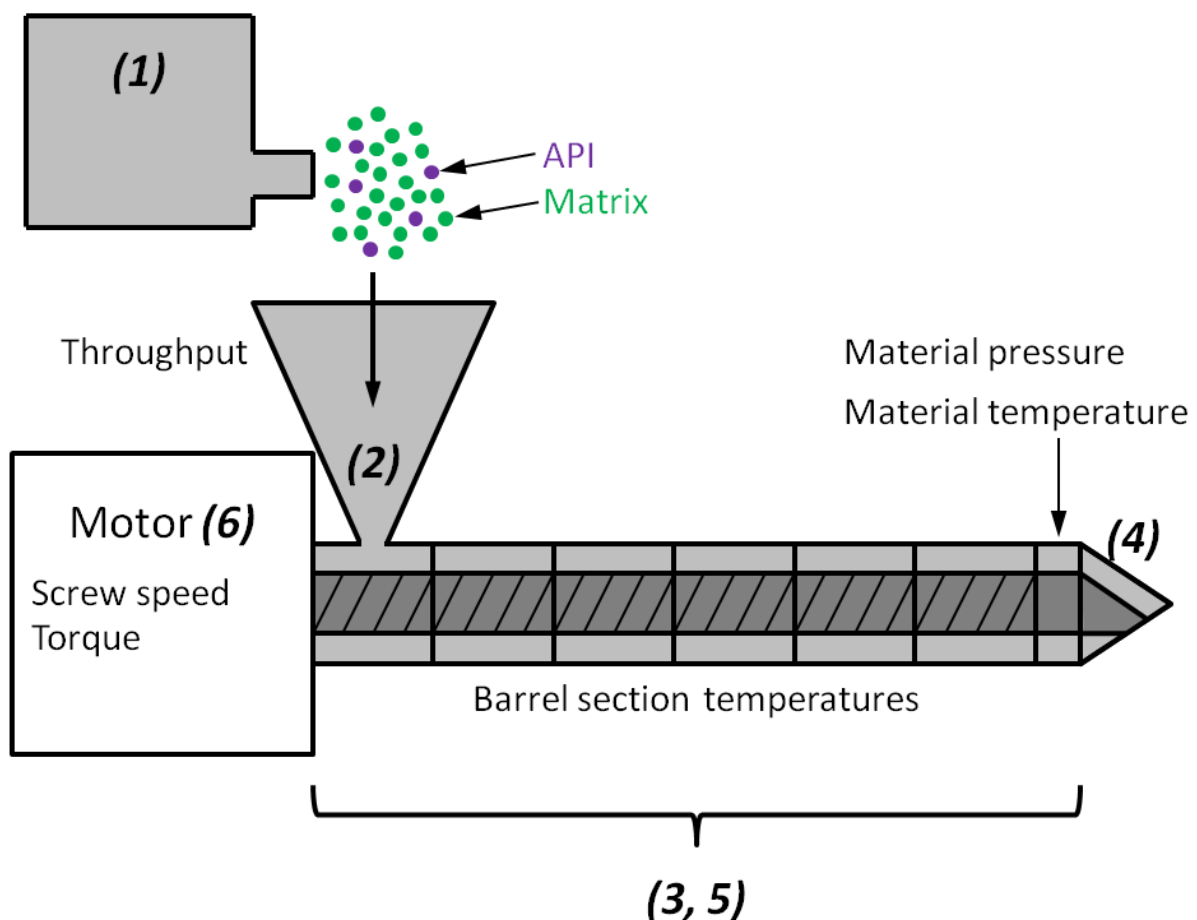


**Figure 2.1.** Hot-melt extrusion equipment and process settings and parameters traditionally monitored during pharmaceutical HME.(1. Feeding system 2. Feeding hopper 3. Temperature controlled barrel with 1 or 2 screws 4. Die 5. Heating and cooling device 6. Screw-driving unit).

Several downstream processing devices are available for further cooling, cutting and shaping of the hot-melt extruded strands. Cooling of the extrudates can be accomplished with air, nitrogen, in water or simply at room temperature on conveyor belts or rolls. Film extrusion on chilled rolls or calenders has been applied for the manufacturing of films for oral administration [21-27] and transdermal drug delivery [28, 29]. Calendering allows continuous shaping of the melt and solidification into tablet- or capsule-like forms [30]. Injection moulding is a downstream process step where the melt is injected into a closed mould under high pressure and temperature conditions after leaving the extrusion die. An overview of the applications of injection moulding for drug delivery is presented in [31]. Another possibility of shaping the extruded strands is by cutting them into small pellets using pelletizers [32-34].

Nowadays, extruders are equipped with standard (univariate) process monitoring sensors. These traditional monitoring options provide information on barrel and die temperatures, feed rate or throughput, screw speed, torque and drive amperage, melt pressure, melt temperature and possibly melt viscosity [1, 35] (Figure 2.1). Classical process control based on measurements of these conventional parameters is in many cases not sufficient to account for process-induced variations in material properties, to guarantee stable processing and to monitor and predict the quality attributes of the extrudates.

## 2.3. REFERENCES

- [1] M.M. Crowley, F. Zhang, M.A. Repka, S. Thumma, S.B. Upadhye, S. Battu, J.W. McGinity, C. Martin, *Drug Dev Ind Pharm* 33 (2007) 909-926.
- [2] Madan S, Madan S, *Asian J Pharm Sci* 7 (2012) 123-133.
- [3] M.A. Repka, S. Battu, S.B. Upadhye, S. Thumma, M.M. Crowley, F. Zhang, C. Martin, J.W. McGinity, *Drug Dev Ind Pharm* 33 (2007) 1043-1057.
- [4] M.A. Repka, S. Majumdar, S. Battu, R. Srirangam, S.B. Upadhye, *Expert Opin Drug Deliv* 5 (2008) 1357-1376.
- [5] J.W. McGinity, M.A. Repka, J.J. Koleng Jr., F. Zhang, *Hot-Melt Extrusion Technology*, In: J. Swarbrick (Ed.), *Encyclopedia of Pharmaceutical Technology*, third ed., Informa Healthcare USA, Inc., New York, USA, 2007, p. 2004-2020.
- [6] J. Breitenbach, *Eur J Pharm Biopharm* 54 (2002) 107-117.
- [7] C. Martin, *Pharm Tech* 32 (2008) 76-86.
- [8] K. Kolter, M. Karl, A. Gryczke, *Hot-Melt Extrusion with BASF Pharma Polymers: Extrusion Compendium*, 2<sup>nd</sup> ed., BASF SE Pharma Ingredients and Services, Ludwigshafen, Germany, 2012.
- [9] K. Dhirendra, S. Lewis, N. Udupa, K. Atin, *Pak J Pharm Sci* 22 (2009) 234-246.
- [10] T. Vasconcelos, B. Sarmiento, P. Costa, *Drug Discov Today* 12 (2007) 1068-1075.
- [11] A. Michalk, V.R. Kanikanti, H.J. Hamann, P. Kleinebudde, *J Control Release* 132 (2008) 35-41.
- [12] R. Witzleb, V.R. Kanikanti, H.J. Hamann, P. Kleinebudde, *Eur J Pharm Biopharm* 77 (2011) 170-177.
- [13] A. Gryczke, S. Schminke, M. Maniruzzaman, J. Beck, D. Douroumis, *Colloids Surf, B* 86 (2011) 275-284.
- [14] K. Plumb, *Chem Eng Res Des* 83 (2005) 730-738.
- [15] C. Vervaet, J.P. Remon, *Chem Eng Sci* 60 (2005) 3949-3957.
- [16] J.P. Remon, C. Vervaet, *Continuous Processing of Pharmaceuticals*. In: J. Swarbrick (Ed.), *Encyclopedia of Pharmaceutical Technology*, third ed., Informa Healthcare USA, Inc., New York, USA, 2007, p. 743-749.

- [17] K. Nakamichi, T. Nakano, H. Yasuura, S. Izumi, Y. Kawashima, *Int J Pharm* 241 (2002) 203-211.
- [18] H.F. Giles Jr., J.R. Wagner Jr., E.M. Mount III, *Extrusion: The Definitive Processing Guide and Handbook*, 1<sup>st</sup> ed., William Andrew, Inc., New York, USA, 2005.
- [19] K. Kohlgrüber, *Co-Rotating Twin-Screw Extruders: Fundamentals: Technology, and Applications*, 1<sup>st</sup> ed., Carl Hanser Verlag, München, Germany, 2008.
- [20] G.P. Andrews, D.S. Jones, O. Abu Diak, D.N. Margetson, *Pharm Tech* 21 (2009) 18-23.
- [21] J.O. Morales, J.T. McConville, *Eur J Pharm Biopharm* 77 (2011) 187-199.
- [22] F. Cilurzo, I.E. Cupone, P. Minghetti, F. Selmin, L. Montanari, *Eur J Pharm Biopharm* 70 (2008) 895-900.
- [23] S.V. Tumuluri, S. Prodduturi, M.M. Crowley, S.P. Stodghill, J.W. McGinity, M.A. Repka, B.A. Avery, *Drug Dev Ind Pharm* 30 (2004) 505-511.
- [24] V.S. Tumuluri, M.S. Kemper, I.R. Lewis, S. Prodduturi, S. Majumdar, B.A. Avery, M.A. Repka, *Int J Pharm* 357 (2008) 77-84.
- [25] P.K. Mididoddi, M.A. Repka, *Eur J Pharm Biopharm* 66 (2007) 95-105.
- [26] S. Prodduturi, R.V. Manek, W.M. Kolling, S.P. Stodghill, M.A. Repka, *J Pharm Sci* 94 (2005) 2232-2245.
- [27] M.A. Repka, K. Gutta, S. Prodduturi, M. Munjal, S.P. Stodghill, *Eur J Pharm Biopharm* 59 (2005) 189-196.
- [28] C. AitkenNichol, F. Zhang, J.W. McGinity, *Pharm Res* 13 (1996) 804-808.
- [29] M.M. Crowley, A. Fredersdorf, B. Schroeder, S. Kucera, S. Prodduturi, M.A. Repka, J.W. McGinity, *Eur J Pharm Sci* 22 (2004) 409-418.
- [30] W. Roth, B. Setnik, M. Zietsch, A. Burst, J. Breitenbach, E. Sellers, D. Brennan, *Int J Pharm* 368 (2009) 72-75.
- [31] L. Zema, G. Loreti, A. Melocchi, A. Maroni, A. Gazzaniga, *J Control Release* 159 (2012) 324-331.
- [32] E. Roblegg, E. Jäger, A. Hodzic, G. Koscher, S. Mohr, A. Zimmer, J. Khinast, *Eur J Pharm Biopharm* 79 (2011) 635-645.
- [33] A. Kalivoda, M. Fischbach, P. Kleinebudde, *Int J Pharm* 439 (2012) 145-156.
- [34] C.R. Young, J.J. Koleng, J.W. McGinity, *Int J Pharm* 242 (2002) 87-92.
- [35] R. Chokshi R, H. Zia, *Iran J Pharm Res* 3 (2004) 3-16.



# CHAPTER 3

## PROCESS MONITORING AND VISUALIZATION SOLUTIONS FOR HOT- MELT EXTRUSION

Parts of this chapter are published in:

**L. Saerens**, C. Vervaet, J.P. Remon, T. De Beer. Process monitoring and visualization solutions for hot-melt extrusion: A review. *Journal of Pharmacy and Pharmacology*, doi: 10.1111/jphp12123 (2013).





# CHAPTER 3

## PROCESS MONITORING AND VISUALIZATION SOLUTIONS FOR HOT-MELT EXTRUSION

---

### 3.1. INTRODUCTION

Process analytical tools for pharmaceutical HME are required for two purposes: (i) improving the understanding of pharmaceutical HME by monitoring and visualizing material behaviour during processing (an enhanced understanding of the process and the material behaviour allows optimization of formulations, process settings such as screw configuration etc.); and (ii) monitoring and analyzing critical product and process parameters for process control, allowing to maintain a desired process state and guaranteeing the quality of the end product.

The implementation of suitable process analytical tools in HME will enable the “Quality by design” (QbD) approach introduced by the Food and Drug Administration (FDA). The Process Analytical Technology (PAT) concept encourages continuous monitoring and control of pharmaceutical production processes based on timely measurements of critical quality and performance attributes of raw and in-process materials and processes [1]. A thorough knowledge of product performance over a range of material attributes, manufacturing process options and process parameters is requested in the ICH Q8 guideline [2], and this understanding can be gained by the application of PAT. Continuous manufacturing cannot rely on the currently applied quality control methods for intermediate or end products which are mainly based on time-consuming and off-line analytical techniques, and annul the advantages of continuous pharmaceutical production. In-process monitoring, analysis and control of the critical process and product parameters are essential to constantly ensure end-product quality during continuous manufacturing. Continuous manufacturing processes,

like HME, are made for continuous process control [3]. They adapt easily to QbD and Design of Experiments (DOE) investigations can be performed by changing process parameters within one experimental run. By implementing process analyzers or PAT tools, real-time information on physical or chemical material properties is obtained, which can be utilized in process control systems to steer the process towards a desired state, to allow real-time release or for scale-up of the production process. The implementation of PAT strategies in HME is valuable both in commercial manufacturing and in the development scale.

### 3.2. PROCESS ANALYTICAL TECHNOLOGY

Conventional pharmaceutical manufacturing is generally accomplished using batch processing followed by time-consuming, expensive and inefficient off-line laboratory testing on randomly collected samples to evaluate the end product quality. The processes themselves are not fully understood and are often inefficient black-boxes. Therefore, the FDA has introduced the concept of PAT [1].

PAT is defined as “a system for designing, analyzing and controlling manufacturing through timely measurements (i.e. during processing) of critical quality and performance attributes of raw and in- process materials and processes, with the goal of ensuring final product quality” [1]. The objective of PAT is to improve process understanding and to control the manufacturing process, and thus to design and develop well understood processes that will compensate for the variability in raw materials and in equipment, thereby consistently ensuring a predefined quality at the end of the manufacturing process. Quality should not be tested into products, it should be built-in, to improve the efficiency of the process, and reduce risks to quality and regulatory concerns. When implementing this QbD paradigm in pharmaceutical manufacturing, PAT strategies are used to reduce identified manufacturing risks associated with product quality. An appropriate combination of several PAT tools provides relevant information concerning the critical sources of variability during manufacturing, allowing real-time, continuous analysis of manufacturing processes and enabling process control and optimization. In the PAT framework, these tools are categorized as followed [1]:

- Multivariate tools for design, data acquisition and analysis

There are many development strategies that can be used to identify optimal formulations and processes. These tools enable the identification and evaluation of product and process variables that may be critical to product quality and performance. Additionally, they allow the identification of potential failure modes and mechanisms and the quantification of their effects on product quality.

- Process analyzers

Process analysis has advanced significantly during the past several decades, from the univariate process measurements (e.g. pressure, temperature, and pH) to analyzers measuring biological, chemical and physical attributes of the materials being processed. The process analyzers applied in hot-melt extrusion should be non-destructive, non-invasive, fast and should require no sample pretreatment. Various measurement setups are possible (Figure 3.1): When the sample is isolated from the process stream and analyzed in close proximity to the process, measurements are performed at-line. At-line monitoring differs from off-line analysis in the reduced time between sampling and analysis results, but still maintains a delay in quality control. On-line measurements involve the diversion of a small part of the product from the process stream which is then presented continuously to an analyzer. The sample is returned to the process stream after analysis. In-line techniques are located directly in the process stream, providing information without removing samples from the process stream.

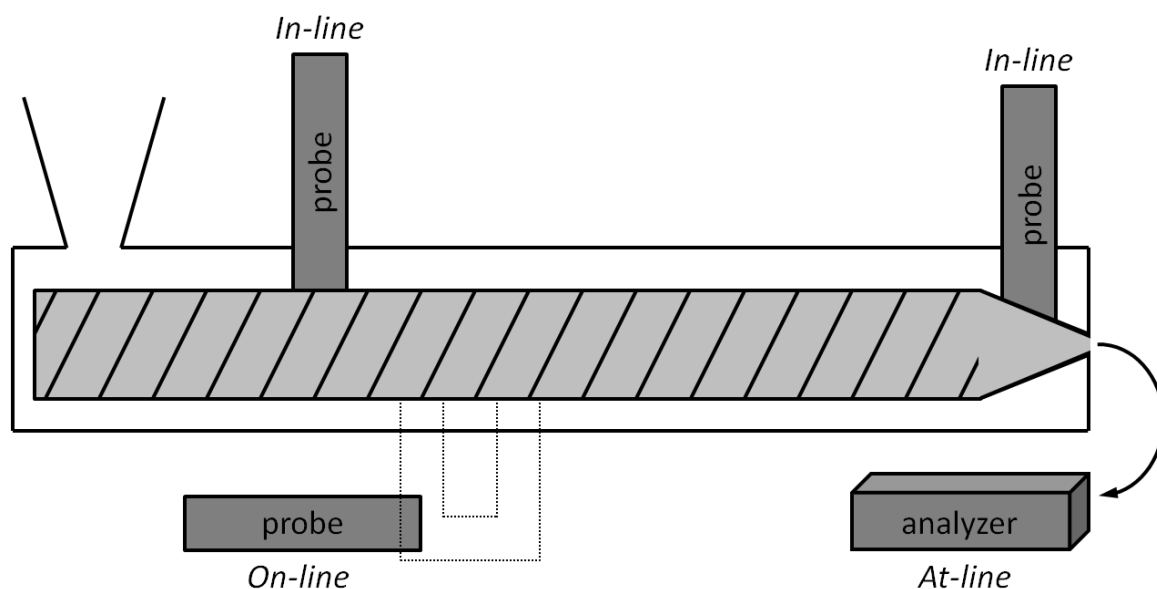


**Figure 3.1.** At-line, on-line and in-line measurement positions for the monitoring of hot-melt extrusion processes.

- Process control tools

The application of process monitoring and control strategies enables monitoring of the state of a process and actively manipulating it to maintain a desired state. Consequently, final product quality can be guaranteed, end product characteristics can be predicted and real-time release can be ensured, hence avoiding batch losses.

- Continuous improvement and knowledge management tools.

Over the life cycle of a product, continuous data collection and analysis are essential to improve understanding of the process and product, and to justify proposals for post-approval changes.

An overview of the applied process analytical tools for pharmaceutical HME discussed in this chapter can be found in Table 3.1, together with their purpose, interfacing possibilities, challenges and disadvantages encountered during implementation. Table 3.2 provides an overview of the reviewed HME process analytical tools used in polymer extrusion with relevant potential for monitoring and control of pharmaceutical HME. Their purpose, possible benefits and shortcomings for pharmaceutical HME and interface positions are also listed in Table 3.2. The reported possible drawbacks of each technique applied in pharmaceutical extrusion and polymer extrusion should be taken into account when considering application of these tools for analysis, understanding and control of pharmaceutical HME processes.

### 3.3. PROCESS ANALYTICAL TECHNIQUES APPLIED FOR PHARMACEUTICAL HOT-MELT EXTRUSION

#### 3.3.1. NIR spectroscopy

Tumuluri et al. [4] applied NIR spectroscopy to predict the clotrimazole quantity in hot-melt extruded polyethylene oxide (PEO) films via a developed partial least squares (PLS) model. A fibre-optic NIR reflectance probe was fixed above the extruded films, behind the extrusion die. Vector normalization of the spectra was performed to reduce the variations in intensity caused by path length variation. Extrusion was performed on a single-screw extruder. The calibration model, containing 9 different PEO films with varying clotrimazole content, regressing the on-line collected NIR spectra versus the actual clotrimazole content as determined with high-performance liquid chromatography (HPLC), yielded a root mean square error of cross validation (RMSECV) of 0.298% (w/w). Four validation samples were predicted within a margin of error of less than 3.5% (w/w). It was shown that the model was more accurate for predictions at higher concentrations.

Saerens et al. [5] implemented a diffuse reflectance NIR probe in the extrusion die of a co-rotating twin-screw extruder (screw diameter = 16 mm) (Figure 3.2) to monitor and predict drug content and to evaluate the physicochemical state of the extrudates before exiting the die. A PLS model was built, regressing the in-line NIR spectra collected during extrusion of physical mixtures containing 20, 30 and 40% (w/w) metoprolol tartrate (MPT) in Kollidon® SR (BASF, Ludwigshafen, Germany) versus the known MPT concentrations. The model was validated with new extrusion experiments, resulting in a root mean square error of prediction (RMSEP) of 1.54% (w/w).

Furthermore, a physical mixture with a drug load of 40% MPT (w/w) in Kollidon® SR was extruded at 135°C and at 105°C. The in-line NIR spectra were compared to the NIR spectrum of the physical mixture. The spectra of both extrudates still contained the MPT peaks, though broader, indicating that not all MPT remained in its crystalline form. This broadening of spectral bands was slightly more pronounced at 135°C than at 105°C. Peak shifts

throughout the entire spectrum were also visible, expressing the extent of molecular interactions between polymer and drug. At 105°C, these shifts were smaller, suggesting stronger interactions between Kollidon® SR and MPT at 135°C. Furthermore, the polymer-drug interactions were confirmed by the manifestation of a new peak, attributed to hydrogen bonded hydroxyl groups. At 135°C, this peak was more intense than at 105°C. Saerens et al. hence demonstrated that NIR spectroscopy can be used in-line during HME to monitor the drug concentration and solid state and hydrogen bonds formed during extrusion. The authors chose a formulation with Kollidon® SR as matrix since this formulation does not produce a transparent extrudate, which could cause detection problems when using reflectance NIR spectroscopy.

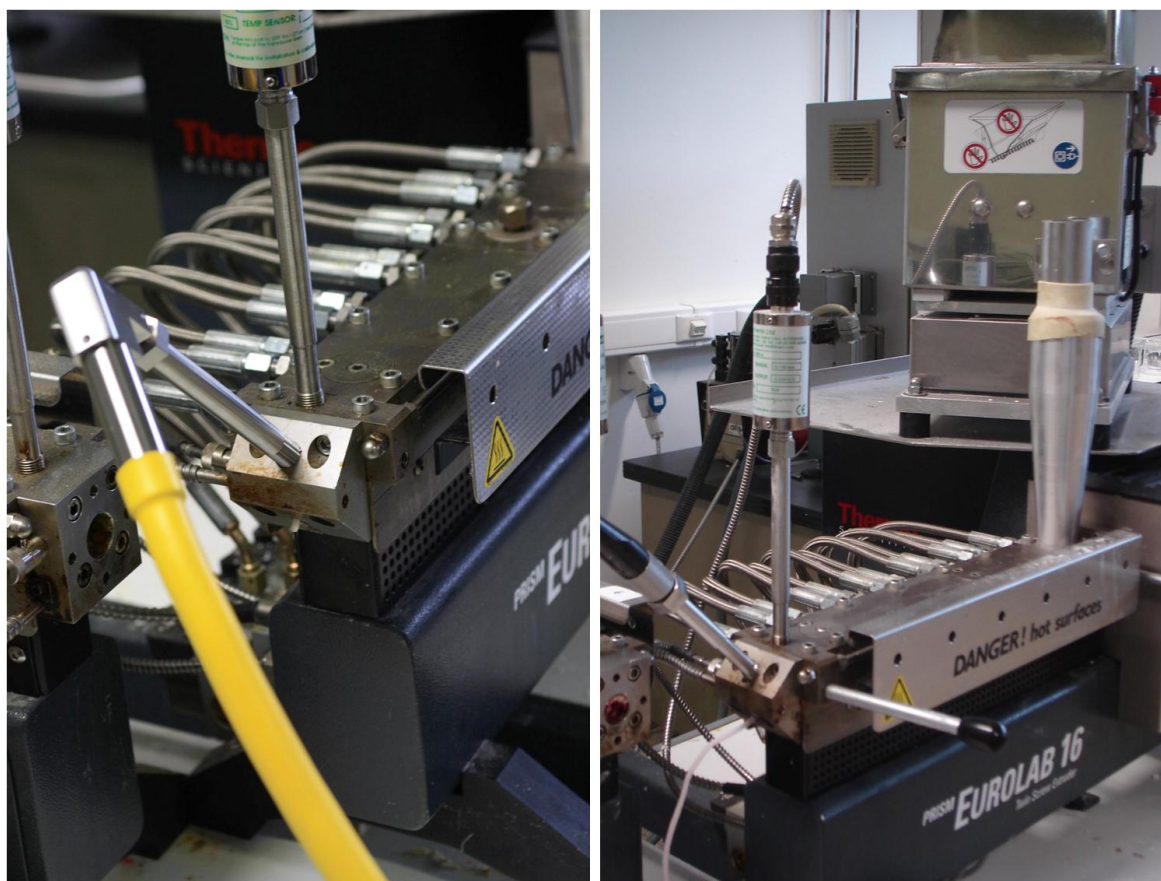


**Figure 3.2.** Implementation of NIR (left) and Raman (right) spectroscopic probes via fibre optic cables in the extrusion die [5, 11].

Smith-Goettler et al. [6] used NIR spectroscopy for real-time predictions of the API loading and surfactant loading (% w/w). Two transmission NIR probes were mounted in a die adapter on a twin-screw extruder with a screw diameter of 27 mm. The first probe is used to

send the light through the melt, and on the opposite side of the melt channel, a second probe captures this signal and sends it to the detector. 20 calibration mixtures for the development of a PLS model and six independent validation mixtures with varying API (0-30.1% w/w) and surfactant (4.8-27.0% w/w) concentrations were extruded with an output varied from 20 kg/h to 35 kg/h. Bands specific for the amorphous API were found in the spectra of the extrudates, indicating that changes in the solid state of the API had occurred. The API loading prediction model yielded an RMSEP of 0.3% w/w. The surfactant loading prediction model yielded an RMSEP of 0.6% w/w. These predictions were then used for fault detection, isolation of suspect material and real-time troubleshooting during HME using the SIPAT software package (Siemens nv/sa, Brussels, Belgium). When a drift in the API loading, due to a change in API lots with different bulk densities, was detected, the molten extrudate stream was diverted to waste. Process parameters regarding the material feeders were investigated, and the material continued to be diverted to waste until the feeder reached steady state. In this research, NIR spectroscopy was hence applied for quantitative monitoring and control of the extrusion process.

McKelvey et al. [7] illustrated the use of transmission NIR spectroscopy to study the impact of process design and scale up on residence time distributions (RTDs) and on composition disturbances caused by feeding issues. RTD measurements as a function of screw speed and feed rate were performed on a co-rotating twin-screw extruder with a screw diameter of 16 mm, by adding a single drop of blue food colouring to the extruder feed inlet and measuring the optical response at the die adapter. This RTD fingerprint was used to assess the ability to scale from the 16 mm to a 27 mm co-rotating twin-screw extruder, using the ratio of free volumes in the extruders (3.63) to adjust the feed rate from 2.75 kg/h to 10 kg/h. In the 27 mm extruder, each component of the mixture (compound 'C', a surfactant and polyvinyl pyrrolidone-polyvinyl acetate copolymer) was fed individually, and NIR spectroscopy was used to monitor the composition of this melt during extrusion. A die block adapter was designed to accommodate the transmission optical probes. A predictive model based on feeder input parameters was used to determine the melt composition and was compared to the real-time concentration measurements with NIR spectroscopy. This model can be used to control the feeding system and to isolate bad product. The transmission NIR spectroscopic tool presented here was successful in measuring RTDs and formulation composition at the



extrusion die, providing possibilities for scale-up of the process and optimization with limited amounts of material and time.

Troup et al. [8] described the development and implementation of an in-line transmission NIR measurement system allowing the determination of the composition of a multi-component melt stream at the exit of a twin-screw extruder. NIR measurements were performed in a custom built die adapter on a 27 mm twin-screw extruder. Two loss-in-weight mass feeders were used to feed the polymer and drug separately into the extruder. A liquid surfactant was fed into the process using a gear pump. Data from the mass feeders and liquid addition system were also logged. Using a PLS model, NIR spectroscopy allowed the simultaneous prediction of the concentration of all three components in the extrudate. The used spectral range was the 1600 – 1800 nm region since all three components have chemical groups with strong absorbance in this region, and since this range is robust to moisture variability. In routine manufacturing, the NIR system demonstrated to be able to detect process upsets and to continuously ensure product uniformity over the entire manufacturing run.

A different application of pharmaceutical HME is the production of cocrystals. Kelly et al. [9] used NIR spectroscopy to monitor the formation of ibuprofen and nicotinamide cocrystals during extrusion based solvent free continuous cocrystallization. The cocrystallization of ibuprofen and nicotinamide in a 1:1 molar ratio was carried out in a co-rotating twin-screw extruder with a screw diameter of 16 mm. A high temperature NIR reflectance probe with a sapphire window was fitted into a threaded port at the end of the extruder barrel. Off-line NIR spectra were taken at several points along the extruder screws to examine the dynamics of the cocrystal formation. The formation of cocrystals occurred mainly in the latter stages of the extruder screw, suggesting that cocrystal formation is highly dependent on the length of the screws, residence time and shear caused by the mixing elements across the length of the screw. The effects of three different screw configurations with different mixing intensities (low, medium and high) dependent on the number and angle of mixing elements, the set temperature profiles and the screw speeds were evaluated. NIR spectra from cocrystals showed significant differences to those from the physical mixture. Once ibuprofen and nicotinamide are bonded together, the vibrations are modified and the peaks shift, giving

rise to the appearance of new peaks in the NIR spectrum. The high mixing intensity screw configuration (the screw design comprising the most mixing elements at an angle of 90°) resulted in the most significant spectral changes compared to the spectrum of the physical mixture. Increasing the set temperature at a screw speed of 30 rpm induced similar spectral changes as increasing the mixing intensity of the screw configuration. Relatively small spectral changes were observed when varying the screw speed (20, 30 and 40 rpm) at 90°C using the high intensity screw configuration. A PLS model, regressing the in-line NIR spectra against cocrystal purity as determined from X-ray diffraction (XRD), was developed using a dataset including only the spectra obtained at a set temperature of 90°C with medium and high screw intensity configurations, since temperature is a well known factor influencing the NIR spectral signals. It was expected that calibrations over multiple temperature configurations would not give accurate results. A correlation coefficient of 0.999 for measured and predicted purity was obtained.

NIR spectroscopy has demonstrated to be a versatile process analysis tool for pharmaceutical HME to monitor several critical product characteristics such as quantitative formulation composition, solid state, polymer-drug interactions and the formation of cocrystals (Table 3.1). Besides the application for monitoring purposes, it was also applied to control API levels adequately. NIR spectroscopy can be applied in both reflectance and transmission mode, depending on the type of formulation used. For transparent formulations, the transmission mode is favoured, since spectra collected in reflection mode contain more noise. Interpretation of the collected NIR spectra can be a challenging task since they contain broad, overlapping overtones and combination bands. However, with the proper chemometric techniques, the relevant information can be extracted from NIR spectra.

**Table 3.1.** Process analytical tools applied in pharmaceutical hot-melt extrusion

<i>Process analytical tool</i>	<i>Interface</i>	<i>In-line or on-line application [1]</i>	<i>Purpose</i>	<i>Reported challenges/disadvantages/shortcomings</i>	<i>References</i>
<b>Near infrared (NIR) spectroscopy: reflection</b>	die	in-line	monitoring of drug concentration	not possible to monitor a transparent formulation (low signal/noise ratio)	[5]
	post die	on-line	monitoring of drug concentration	variations in path length cause variations in signal intensity, normalization is required	[4]
	die	in-line	monitoring of cocrystal production	temperature influence on NIR measurements: the correlation improved when temperature variation was excluded from the dataset	[9]
	die	in-line	monitoring of solid state and polymer-drug interactions	not possible to monitor a transparent formulation (low signal/noise ratio) [5]	[5, 12]
<b>NIR spectroscopy: transmission</b>	die	in-line	monitoring of drug concentration	-	[6-8]
	die	in-line	monitoring of surfactant concentration	-	[6-8]
	die	in-line	monitoring of residence time distribution (RTD)	-	[7]
	die	in-line	identification of feeding disturbances	-	[6-8]

**Table 3.1.** Process analytical tools applied in pharmaceutical hot-melt extrusion (continued)

<i>Process analytical tool</i>	<i>Interface</i>	<i>In-line or on-line application [1]</i>	<i>Purpose</i>	<i>Reported challenges/disadvantages/shortcomings</i>	<i>References</i>
<b>Raman spectroscopy</b>	die	in-line	monitoring of drug concentration	difficulties with collecting spectra from a non-transparent melt [5], resulting in a high background signal	[11]
	post die	on-line	monitoring of drug concentration	film undulation caused differences in path length resulting in variations in signal intensity, normalization is required	[10]
	die	in-line	monitoring of solid state and polymer-drug interactions	difficulties with collecting spectra from a non-transparent melt [5], resulting in a high background signal	[11, 12]
	die	in-line	monitoring of complex formation by an acid-base reaction	-	[14]
	barrel segments	in-line	monitoring of solid state and polymer-drug interactions	sapphire probe window provides peaks in Raman spectrum when window is not completely covered by sample	[13]
<b>Motor load</b>	motor	in-line	monitoring of surfactant concentration	-	[15]

### 3.3.2. Raman spectroscopy

Tumuluri et al. [10] used Raman spectroscopy to quantify the drug load in hot-melt extruded films and to evaluate the physical state of the APIs in the formulations. A fibre optic Raman probe was used for on-line analysis and clamped above the film in a 90° angle behind the extrusion die. Clotrimazole and ketoprofen were used as model APIs and extruded in PEO films on a single-screw extruder. Two PLS models were developed regressing the on-line collected Raman spectra against the known concentration of each API. For both PLS models, normalization to a peak for PEO was performed to allow quantification. A challenge was the undulation of the film, resulting in different path lengths between the extruded film and the Raman probe. This was corrected by using the ratio of the active band to the polymer band.

Saerens et al. [11] used a Raman probe implemented in the extrusion die of a co-rotating twin-screw extruder (screw diameter = 16 mm) (Figure 3.2) to monitor and predict the drug content and to evaluate the physicochemical state of the extrudates before exiting the die. A PLS model was built, regressing in-line Raman spectra collected during extrusion of physical mixtures containing 10, 20, 30 and 40% (w/w) MPT in Eudragit® RL PO (Evonik, Darmstadt, Germany) versus the known MPT concentrations. The model was validated with independent test extrusion runs, and resulted in an RMSEP of 0.59% (w/w). Furthermore, two physical mixtures containing 10% (mixture A) and 40% (mixture B) MPT (w/w) in Eudragit® RS PO (Evonik, Darmstadt, Germany) were extruded at temperatures of 140°C and 105°C, respectively. The in-line Raman spectra were compared to the Raman spectrum of the physical mixtures. In both extrudates, peak shifts occurred, indicating interactions through hydrogen bonds between polymer and drug. The shifts were larger in the extrudates of mixture A, indicating stronger interactions. Evidence was found for the formation of hydrogen bonds between the hydroxyl and/or amino groups from MPT and the carbonyl groups belonging to the polymer. The MPT peaks in the extrudates of mixture B are still well defined, sharp peaks, whereas for mixture A, they have broadened extensively, showing the presence of amorphous MPT. Raman spectroscopy allowed differentiation between solid states of the drug and formulation, and was able to accurately predict drug concentration during HME.

Almeida et al. [12] extruded physical mixtures containing MPT and ethylene vinylacetate (EVA) (50:50) on a co-rotating twin-screw extruder (16 mm). Diffuse reflectance NIR spectroscopy and Raman spectroscopy were implemented in the die to evaluate the material behaviour at a molecular level in-line as a function of the process settings (temperature: 90, 110 and 140°C; screw speed: 90 and 110 rpm). Principal component analysis (PCA) was performed on all in-line collected Raman spectra. The first principal component (PC) captured 60% of the spectral variation, induced by differences in polymer/drug solid state caused by the variation in applied extrusion temperatures. An increased process temperature induced a loss in drug crystallinity. Extrusion of the physical mixtures at 90°C and 110°C provided Raman spectra characterized by sharp MPT bands, indicating that (the majority of) the MPT was crystalline. When the extrusion temperature was increased to 140°C, broadening of the MPT peaks in the spectrum confirmed the melting of the drug. Evidence for interactions (hydrogen bonds) between the drug and polymer, induced by a higher processing temperature, was found. Increasing the screw speed did not result in peak shifts in the Raman spectrum. Besides Raman spectroscopy, diffuse reflectance NIR spectroscopy was also applied for the in-line monitoring of the extrusion process. PCA of the NIR data led to similar conclusions as the Raman spectra. NIR spectroscopy confirmed the formation of hydrogen bonds by the manifestation of an extra peak at  $6500\text{cm}^{-1}$ , attributed to the first overtone of the hydrogen bonded hydroxyl group. NIR and Raman spectroscopy hence provided complementary information concerning the manifestation of hydrogen bonds between polymer and drug in this formulation.

Only one application of spectroscopic in-barrel monitoring has been illustrated [13]. To improve the understanding of material behaviour in the barrel, a Raman probe was implemented in each section of the barrel. MPT concentration (10 and 40% w/w in Eudragit® RS PO), extrusion temperature (100, 120 and 140°C) and screw speed (80 and 160 rpm) were varied to examine their influence on polymer/drug solid state throughout the entire barrel. When extruding the formulation with 40% (w/w) MPT, broadening of MPT peaks indicated melting of MPT between sections 2 and 3, caused by the first kneading zone (Figure 3.3). Decreasing the concentration to 10% w/w showed an additional spectral difference (i.e., peak shifts indicating interactions between MPT and carrier) between sections 5 and 6, due to formation of a solid solution. At a 10% (w/w) MPT load, increasing the extrusion

temperature did not influence the solid state or the barrel section where the final solid state is obtained. At a drug load of 40% (w/w), the solid state of the end product was reached further down the barrel when extrusion was performed at a lower barrel temperature. Doubling the screw speed when processing a 10% MPT formulation (w/w) did not affect the product solid state. In contrast, for a 40% (w/w) drug load, the section where the final product solid state was obtained, was situated earlier in the barrel when applying a higher screw speed. To conclude, the Raman spectra provided real-time information about polymer/drug behaviour throughout the entire extrusion barrel, facilitating process visualisation and understanding. Twin-screw extrusion is a starve-fed process where most screw elements are not completely filled with material. This presents a challenge in positioning the Raman probe, since the distance between probe and measured material varies throughout processing. This variation in distance creates an undesired source of spectral variability which needs to be filtered out.

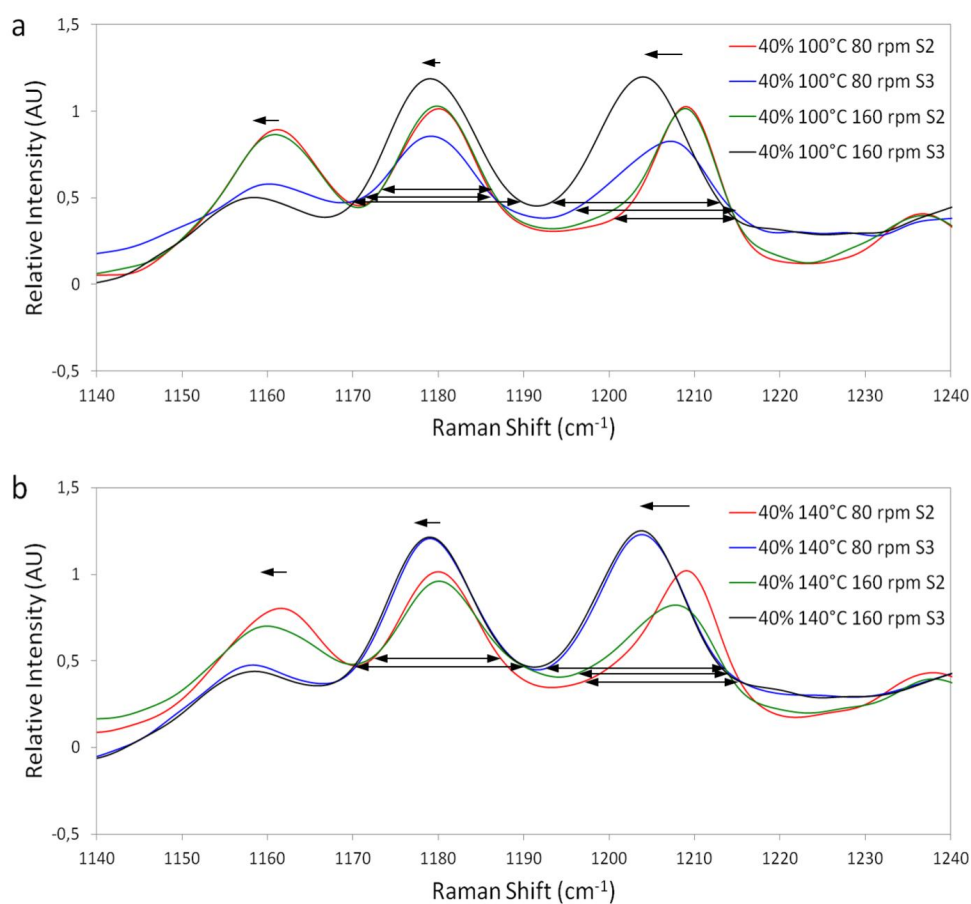


**Figure 3.3.** Detail of the Raman spectra collected in barrel sections 2 and 3 during extrusion of mixtures with 40% MPT (w/w) with all screw speed settings at a) 100°C and b) 140°C [13].

Kindermann et al. [14] used Raman spectroscopy for the monitoring of the formation of polyelectrolyte complexes composed of poorly water-soluble acid drugs (naproxen and furosemide) and basic polymethacrylates (Eudragit® E PO) by an acid base-reaction during HME. Physical mixtures of naproxen and Eudragit® E PO were pre-blended in a mixer and subsequently hot-melt extruded with a co-rotating twin-screw extruder (screw diameter = 27 mm). A Raman spectrometer was equipped with an extruder-compatible probe. The authors do not mention the exact location of implementation of the probe. Raman spectroscopy was used to characterize the drug-polyelectrolyte interaction. The Raman band representing the symmetric stretch vibration of the carbonyl group of naproxen was found in the pure naproxen and in the physical mixture, but disappeared in the spectra of the extrudates, confirming the acid-base-reaction and complex formation in the melt.

Similar to NIR spectroscopy, Raman spectroscopy can be used as a process analytical tool to monitor component concentrations, solid state and intermolecular interactions that might occur during extrusion (Table 3.1). Both techniques are complementary, and depending on the formulation used for extrusion, one technique will be more suitable than the other. Raman spectra are influenced by fluorescence and colour in the formulation, which might cause difficulties due to a high background signal. These can however be (partly) overcome by changing the type of laser.

### **3.3.3. Monitoring of torque and power consumption**

Schilling et al. [15] determined the influence of the plasticizer citric acid on the processability of Eudragit® RS PO during single-screw extrusion. The process parameters screw speed and motor load were monitored as a function of citric acid (CA) content and the preset temperature in the die. The quotient of the maximum applicable screw speed divided by the measured load at a given temperature was calculated for each CA level. This quotient was then interpreted as an index of processability of the formulation at the preset die temperature. Improved processability due to plasticization was reflected by high quotients at lower temperatures. Improved processability of a powder blend by plasticization of the polymer yielded a higher screw speed and a lower motor load at a predefined temperature. A temperature of 140°C was needed to extrude the pure polymer with a screw speed of 20



rpm, while blends containing citric acid monohydrate (CA MH) could be processed at temperatures from 110°C to 130°C. The screw speed/motor load quotient significantly increased when the CA MH concentration was increased from 0 to 10, 15, 20 and 25% (w/w). This indicated a decrease in melt viscosity and enabled extrusion at lower temperatures. The absence of a statistically significant difference between 25 and 30% (w/w) CA MH suggested that the plasticizing effect plateaued at this concentration, coinciding with the solubility limit of CA MH in Eudragit® RS PO. Finally, it was found that CA MH facilitated the extrusion process more efficiently than its anhydrous form.

Torque can be easily measured during HME and is correlated with several important product parameters that cannot straightforwardly be monitored during extrusion, such as the rheological behaviour of the material, plasticizing effects of components in the melt, grinding processes during extrusion and the velocity of material through the extruder. This parameter can easily be monitored during HME without the requirement of barrel and/or die modifications, and without the need for additional sensors.

### 3.4. MONITORING OF POLYMER MELT EXTRUSION

The polymer processing industry has developed and applied numerous process analytical tools to improve HME process understanding, monitoring and control, to enhance product quality and to allow real-time fault detection. In addition to the use of conventional monitoring techniques and spectroscopic techniques such as NIR and Raman spectroscopy, the literature describes applications of ultrasonic techniques, rheological techniques, advanced temperature sensors, dielectric sensors, nuclear magnetic resonance (NMR) spectroscopy, fluorescence spectroscopy, ultraviolet-visible (UV-VIS) spectroscopy and terahertz (THz) spectroscopy. The following section provides an overview of process monitoring techniques that have been applied in polymer extrusion which could be relevant for pharmaceutical HME process monitoring and control. A summarized overview can be found in Table 3.2, together with the analysis possibilities of each technique, the position in the extruder where the technique should be/can be implemented for its purpose and possible challenges, disadvantages and shortcomings of the analytical technique.

#### 3.4.1. Spectroscopic techniques

##### 3.4.1.1. *NIR spectroscopy*

Hansen and Vedula [16] used in-line NIR spectroscopy to monitor the comonomer (vinyl acetate (VA)) concentration in a system of EVA copolymers simultaneously with the polymer melt flow index (MI) for this system. In NIR absorption spectra, variations in chemical composition are dominant effects, whereas the rheological flow effects cause only subtle variations in the NIR spectra. The anisotropic nature of flow depends on the molecular orientation and the orientation distribution of flowing polymer melt, which are related to molecular weight, chain length, entanglement and branching of the polymer chain. Differences in molecular orientation and orientation distribution affect the NIR absorbance spectra and induce spectral shifts, hence providing information about physical properties that directly correlate with molecular weight parameters such as MI. For EVA random copolymers, these rheological properties are not related to the comonomer ratio for VA

concentrations lower than 30%. This indicates that primary effects (composition of the melt) and secondary effects (MI) on the absorbance spectrum are independent. Dual transmission fibre optic probes were mounted in a flow cell attached to a single-screw extruder. The authors developed two PLS models, a first one containing three principal components which is used for MI predictions, and a second PLS model with only one principal component for VA concentration measurements. The standard error of prediction (SEP) values for the two models were 0.46 for MI (ln MI (g/10 min)) predictions and 0.62 wt% for VA predictions. These models were then applied for in-line monitoring of MI and VA concentration. All predicted values for both responses were found between the actual laboratory value  $\pm$  SEP, indicating that NIR spectroscopic measurements can predict the VA content and the MI of the melt during extrusion.

In a second study [17], Vedula and Hansen developed a PLS-1 model to predict the complex viscosity ( $\ln(|\eta^*(\omega)|)$ ) and the VA monomer content of molten EVA copolymers. Dual transmission fibre optic probes were mounted in a flow cell attached to a single-screw extruder. The PLS-1 model, where the NIR spectra were regressed versus the complex viscosities measured with a dynamic stress rheometer at different frequencies, comprised four components. The first PC (explained 31.5% of the variation related to the rheological response) accounted for the spectral variation caused by varying VA content, and a second (63.4%) PC described the spectral variation caused by the rheological response. The standard error of calibration (SEC) and SEP values were 0.38 and 0.8 respectively. Most new predicted measurements are found within the detection limits for predictions as determined by the SEP values. A limitation for this type of measurements is the melt temperature, which has a large effect on rheological properties. These experiments were all performed at the same temperature, assuring only a small variance in melt temperature in the flow cell (1-3°C). A further improvement of the calibration models from both studies might be achieved by including temperature as an independent variable in the X matrix.

Nagata et al. [18] developed an in-line density sensor using NIR spectroscopy. The transmission NIR spectra of molten polyethylene (PE) in flow were collected using a fibre-optic device attached to a single-screw extruder. The PE density depends on the number of polymer chain branches and their length. The degree of branching could be estimated by

measuring the composition ratio of the methyl group (-CH<sub>3</sub>, at the ends of branches and main chains) to the methylene (-CH<sub>2</sub>-, in polymer chains) group. In attempts to correlate the density with the NIR spectra, the correlation coefficient  $R^2$  between polymer densities and scaled absorbances of 14 polymer grades was calculated, and the highest  $R^2$  (0.9853) was found at 1170 nm. Using this model, it was hence possible to monitor the PE density in-line in the extrusion die.

Witschnigg et al. [19] developed an NIR method where the results of on-line extensional rheometry (on-line measurements of drawing force performed by on-line Rheotens equipment), Young's modulus (calculated out of tensile tests) and interlayer distance (determined by small angle X-ray scattering) are correlated with in-line collected NIR spectra. A mixture of 90% polypropylene (PP), 5% organoclay and 5% compatibilizer (w/w) was extruded in a co-rotating twin-screw extruder, which had a bypass system to create a melt string for on-line Rheotens measurements. The NIR probe was implemented in front of the extrusion die. Two different screw geometries (1 and 2) were applied during experiments. Screw geometry 1 contained three kneading zones, whereas only 1 kneading zone was present in geometry 2. For geometry 1, a PLS model with 5 components regressing the NIR spectra versus the Young's modulus was developed resulting in an RMSECV of 30 MPa. For geometry 2, a four component PLS model was built resulting in an RMSECV of 94 MPa. For the correlation with drawing force, 2 component PLS models were developed resulting in an RMSECV of 2.64 mN for geometry 1 and an RMSECV of 1.98 mN for geometry 2. Concerning the correlation of NIR spectra with the interlayer distance, a PLS model with 1 component and an RMSECV of 0.013 nm was developed for geometry 1 and for geometry 2, a PLS model with 2 components resulted in an RMSECV of 0.019 nm. The measurements were not performed at different aggregate states (melt state vs. semicrystalline solid state), since this creates differences in NIR spectra that would affect the chemometric models. Variations in NIR spectra caused by changing the physicochemical state of the extrudates might interfere with the variations attributed to Young's modulus, drawing force and interlayer distance. Nevertheless, the authors demonstrated that NIR spectra can be used with sufficient precision for in-line quality monitoring. However, in this publication it is not mentioned how changes in Young's modulus, interlayer distance and drawing force affect the in-line collected NIR spectra.

In pharmaceutical HME, NIR spectroscopy is mainly applied to monitor the concentration of melt components, and in some cases to determine the solid state and occurring intermolecular interactions within the melt. In polymer extrusion applications however, NIR spectra showed to correlate well with Young's modulus, interlayer distance, drawing force, melt flow index, complex viscosity and density.

#### 3.4.1.2. *UV-VIS spectroscopy*

Wang et al. [20] applied the UV-VIS spectroscopy technique to monitor the process induced degradation of poly-L-lactic acid (PLLA) during extrusion. Extrusion was performed on a co-rotating twin-screw extruder, equipped with a special measurement slit die that contained the UV-VIS transmission probes. The influence of the processing parameters barrel temperature, screw speed and throughput on the degradation of PLLA was investigated. Samples were also collected for off-line analysis (molar mass, melt viscosity and in vitro biodegradation). The residence time distribution was determined by adding a red coloured pellet to the feeding during stationary state. A reference spectrum was taken, and subtracted from all the UV-VIS spectra collected during experiments. These difference spectra ( $\Delta A$ ) exhibited a maximum at 310 nm for all processing conditions, indicating the wavelength range of the most significant spectral changes due to degradation.  $\Delta A$  increased with increasing processing temperature and screw speed as well as with decreasing throughput. This means that an increase in  $\Delta A$  is accompanied by decrease in average molar mass and an increase in specific mechanical energy. UV-VIS absorption of the melt can be used to get an estimate of the molar mass of the extrudates of dry PLLA, regardless of variations in extrusion parameters. To evaluate the effects of processing parameters on the biodegradation rate of the extrudates, an in vitro biodegradation experiment at elevated temperature was performed for selected extrudates. Higher in vitro weight loss was related to higher UV-VIS absorption of the extruded materials, which is correlated with lower molar mass of the extruded materials. The authors demonstrated that UV-VIS is very sensitive to colour changes of the PLLA melt, and a clear correlation between increasing absorption and a decrease in molar mass of the extrudates was found, which can be used as a measure of polymer degradation.

**Table 3.2.** Process analytical tools applied in polymer extrusion

<i>Process analytical tool</i>	<i>Interface</i>	<i>In-line or on-line application [1]</i>	<i>Purpose</i>	<i>Reported challenges/disadvantages/shortcomings</i>	<i>References</i>
<b>Near infrared (NIR) spectroscopy: transmission</b>	die	in-line	monomer concentration	-	[16]
	die	in-line	complex viscosity	-	[17]
	die	in-line	density by monitoring polymer chain branches	-	[18]
<b>NIR spectroscopy: reflection</b>	die	in-line	drawing force and Young's modulus	Different aggregate states will affect the chemometric models negatively.	[19]
<b>Ultraviolet/visible (UV-VIS) spectroscopy: transmission</b>	die	in-line	polymer degradation	The low count rate of the UV-VIS diode array detector leads to a large error, since this area is the wavelength range where the absorption of the optical fibres connecting the probe with the spectrometer becomes dominant.	[20]
<b>UV-VIS spectroscopy: reflectance</b>	die	in-line	residence time distribution (RTD)	-	[21]

**Table 3.2.** Process analytical tools applied in polymer extrusion (continued)

<b>Fluorescence spectroscopy</b>	die	in-line	melt temperature measurements, temperature gradient measurements	<ul style="list-style-type: none"> <li>- Can only be used in development phase with inert fluorescent dyes.</li> <li>- Effect of pressure on calibration curve must be considered, accurate temperature measurements require simultaneous acquisition of pressure (temperature results need to be compensated).</li> <li>- Only a small sample volume is allowed (specific probe and lens design).</li> <li>- Radial measurements need to be possible (specific probe and lens design).</li> <li>- Selection of fluorescent dyes: dyes need to be stable at high temperatures, spectra should show significant changes with varying temperature, dyes should be soluble in polymer resin and should be chemically inert.</li> <li>- Effect of shear on temperature measurements: sensor needs to be located beyond the end of screw (low shear rate flow region).</li> </ul>	[22, 23, 25]
	die	in-line	RTD	Global RTD measurements in single-screw extrusion are delicate, as the tracer must be incorporated at the feed opening under very specific conditions (to avoid material accumulation, starve feed conditions and the distribution of the dye in different screw turns, a minimal concentration though easily detectable should be used) [25].	[25-27]
	barrel	in-line	RTD	-	[25]
	mixing zone	in-line	melt temperature measurements, temperature gradient measurements	<ul style="list-style-type: none"> <li>- Calibration should involve pressure data.</li> <li>- Temperature spikes in data are associated with shear heating, these spikes need to be filtered out to calculate average temperatures.</li> </ul>	[25]
	kneading block	in-line	RTD	Video images revealed that, in contrast with the kneading block, the conveying elements upstream of the kneading block were only partially filled, causing unstable and weak signals. Therefore, measurements were performed exclusively on the kneading block.	[25]

**Table 3.2.** Process analytical tools applied in polymer extrusion (continued)

<b>Terahertz spectroscopy</b>	die	in-line	refractive index measurements related to additive compound content	<ul style="list-style-type: none"> <li>- Complexity of the system, high costs, very sensitive to vibration → a new, partially fibre coupled terahertz spectrometer was developed.</li> <li>- Die adaptations were required: silica plates that can withstand pressures only up to 26 bar and temperatures only up to 260°C.</li> <li>- The recording time needs to be reduced: only the amplitude value at a fixed time position is used as an indicator.</li> <li>- The pressure and temperature of the melt need to be observed in order to correct the experimental data.</li> </ul>	[28]
<b>Dielectric spectroscopy</b>	die	in-line	comonomer concentration, sidechain composition	At higher temperatures, the analysis becomes more difficult since ions, permanent dipoles and induced dipoles may all have a significant influence at an elevated temperature.	[29]
	die	in-line	filler concentrations	Measuring cells are not sensitive for the melt in the centre of the ring, cells should therefore be as narrow as possible.	[30]
	die	in-line	melt viscosity	The sensor utilizes a fringe field to monitor the polymer melt, so the field of the measurement is limited to the depth of penetration of the fringe field. Therefore, the dielectric parameters are measured at the surface of the melt stream.	[51]
<b>Optical probes</b>	die	in-line	particle size and concentration of dispersed phase	-	[31]
	die	in-line	melting behaviour	-	[34]
	mixing zone	in-line	RTD	Dependent on the optical characteristics of the extruded polymer and tracer, the optical probe measured the RTD of either the entire channel volume or that of a surface layer of the volume.	[36]
<b>Nuclear magnetic resonance (NMR) spectroscopy</b>	die	on-line	temperature, composition, homogeneity	<ul style="list-style-type: none"> <li>- Increasing temperature decreases the magnetic field strength.</li> <li>- Ferromagnetic materials in the extruder might deform the static field.</li> <li>- Low sensitivity, but this can be overcome by increasing the experiment time for signal accumulation.</li> </ul>	[35]



**Table 3.2.** Process analytical tools applied in polymer extrusion (continued)

<b>Ultrasonic techniques: longitudinal waves</b>	melting, mixing, pumping zones	-	barrel integrity at melting, mixing and pumping zones, screw and barrel wear	-	[41]
	melting, mixing, pumping zones	in-line	RTD	-	[36]
	die	in-line	RTD	-	[36, 37]
	barrel	in-line	melting phenomena dependent on screw configurations	The channel should be completely filled at measurement position: adaptations in screw configuration/probe location are required.	[38]
<b>Ultrasonic techniques: shear waves</b>	die	in-line	melt density	<ul style="list-style-type: none"> <li>- Assumption: a change in melt density will be directly manifested by a change in extrudate density (accurate for most polymer extrusion applications).</li> <li>- The accuracy of the measurements is highly dependent on the condition of the ultrasound transducer and stability of the process: constant cooling of the transducer was necessary.</li> <li>- It is essential to keep the melt temperature and pressure within a narrow range during extrusion: a change in either will affect the acoustic properties of the melt and will interfere with the accuracy of the intended measurements: normalisation procedures should be applied.</li> </ul>	[39]
<b>Ultrasonic techniques: undefined wave type</b>	die	in-line	melt density	-	[51]

**Table 3.2.** Process analytical tools applied in polymer extrusion (continued)

<b>Rheological techniques:</b>					
<b>Stress and shear rate sensor</b>	die	in-line	melt viscosity as a function of shear rate	-	[42]
<b>Capillary rheometer</b>	barrel	on-line	torque, shear stress, shear rate, melt flow index, linear viscoelastic behaviour	Large deformations and relatively high shear rates associated with the flow in a capillary rheometer may affect the morphology of the material and consequently its rheological response.	[43]
<b>Oscillatory rheometer</b>	barrel	on-line	linear visco-elastic behaviour	-	[43]
<b>Rotational rheometer</b>	barrel	on-line	morphology development, reaction kinetics, linear viscoelastic behaviour	-	[44]
	barrel	on-line	storage and loss modulus of polymer melts	-	[45]
<b>Extensional rheometer</b>	die	on-line	melt strength	-	[47]
<b>Slit die</b>	die	in-line	thermal degradation of polymer	-	[46]

**Table 3.2.** Process analytical tools applied in polymer extrusion (continued)

<b>Perturbation method</b>	barrel sections	in-line	melting behaviour of polymer blends	-	[48]
<b>Temperature measurements:</b>					
<b>Thermocouple</b>	die	in-line	melt temperature	<ul style="list-style-type: none"> <li>- Slow response time.</li> <li>- Measurements are highly dominated by barrel/die wall metal temperature.</li> </ul>	[49]
<b>Infrared (IR) sensor</b>	die	in-line	melt temperature	<ul style="list-style-type: none"> <li>- Temperature information is limited to a small volume of the melt flow.</li> <li>- IR measurements may be affected by polymer type and sensor calibration accuracy.</li> </ul>	[49]
<b>Thermocouple mesh (TCM)</b>	die	in-line	melt temperature	<ul style="list-style-type: none"> <li>- Melt flow may be slightly disturbed by the TCM.</li> <li>- TCM measurements are slightly influenced by shear heating depending on the size of the mesh wires and junctions.</li> <li>- Mesh wires may be damaged under poor melting conditions (e.g. highly viscous or un-melted materials).</li> </ul>	[49]
<b>Monitoring of motor current</b>	motor	in-line	friction, torque, identification of conveying issues	Since the screw load torque signal is dominated by the solids conveying torque, it is not sensitive enough to identify unstable melting issues.	[50]

Gilmor et al. [21] developed an in-line colour monitoring system: the colour of the melt during changeover from one pigmented PE to another was continuously measured directly in an extruder using a fibre-optic assisted charge coupled device spectrometer. The fibre-optic reflection probe was inserted into the die of a single-screw extruder. Residence time distributions were calculated from the in-line reflectance data, without requiring knowledge of the absolute concentration values in the melt.

UV-VIS spectroscopy is a process analytical technique that can be applied in pharmaceutical HME to monitor residence time distributions of the melt, to detect polymer and/or drug degradation, to detect impurities in the melt and to quantitatively analyse the melt compounds. It is a simple, straightforward technique, which can be implemented through the use of fibre optic cables. The most important advantage of UV-VIS spectroscopy compared to NIR and Raman spectroscopy is its much lower detection limit. UV-VIS spectral bands are highly overlapping, therefore chemometric analysis and proper pre-processing of the obtained spectra is required.

#### 3.4.1.3. ***Fluorescence spectroscopy***

Migler and Bur [22] incorporated bis(-pyrene) propane (BPP), a temperature-sensitive fluorescent dye in the polymer resin at dopant levels. By monitoring relevant spectral features of this dye, its temperature can be measured. And through a focusing technique (confocal fluorescent optics), the temperature can be measured as a function of distance into the resin. Temperature profiles were measured in a circular die at the exit of a twin-screw extruder. These measurements are based on the dependence of  $I_e/I_m$  (e = eximer, m = monomer) with temperature for BPP in polyethylene. In a succeeding study, Bur et al. [23] added different temperature sensitive fluorescent dyes to the polymer melt during single-screw extrusion processing to overcome the inadequacies of thermocouple and infrared radiometer transducers. The fluorescence spectrum, collected in a slit die rheometer attached to the extruder, reflects the resin temperature in its neighbourhood. The temperature measurement is based on the calibration curve where the ratio  $I_{464}/I_{473}$  is plotted versus temperature for atmospheric pressure. A pressure compensation factor was added later on. Additionally, Bur et al. [24] relocated the fluorescent confocal sensor and

positioned it over the top of the mixing section of a 63.5 mm diameter single-screw extruder to monitor the temperature gradient in the channel, as a function of screw speed, screw design and melt flow rate. Temperatures were found to be lowest in the centre of the channel and increased at the barrel wall and at the root of the screw for the conventional screw with only transporting elements. As expected, the channel temperatures increased with increasing screw speed. For the mixing screw, the temperature was lowest at the barrel wall and highest at the root of the screw. In summary, this sensor is capable of measuring melt temperatures and temperature gradients within the melt.

Carneiro et al. [25] determined the RTD along a kneading block via in-line monitoring of the light emission of a fluorescent tracer (perylene) in a slit die attached to a single-screw extruder and at several locations along a co-rotating twin-screw extruder. RTD measurements are often used to monitor and control process attributes such as consistency, extent of polymer degradation and degree of mixing. Three devices were developed to accommodate the probe: a slit die for single-screw extrusion, a sampling device with rotating valve for partial measurements within twin-screw extrusion which can be inserted between any 2 consecutive barrel sections and a transparent barrel modified to accommodate the probe (Figure 3.4). First, the probe position (horizontal or vertical) and the influence of screw speed were evaluated on a single-screw extruder. The authors found that increasing screw speed reduced the RTD and by changing the probe position, different fractions of the melt stream are monitored. Secondly, concentration versus time curves were generated to characterize the RTD at several locations along the barrel of a twin-screw extruder, and direct comparison with off-line data using a silica tracer produced good results. Finally, experiments were performed on a co-rotating twin-screw extruder with a transparent barrel to visualize the flow within a mixing block with staggered kneading disks. Video images revealed that, in contrast with the kneading block, the conveying elements upstream of the kneading block were only partially filled, causing unstable and weak signals. Therefore, measurements were performed exclusively on the kneading block. The determination of partial RTD is particularly relevant in compounding operations, or when processing thermally sensitive materials, since it provides information that can be used to optimize the operating window or to improve the screw configuration. In this work, an in-line technique, based on the light emission of a perylene fluorescent tracer, was developed for the measurement of

RTD along the extruder axis. In-line readings were compared with off-line measurements, and a good agreement was found. Two other examples of RTD monitoring with fluorescence spectroscopy are presented by Barnes et al. [26] and Fang et al. [27].

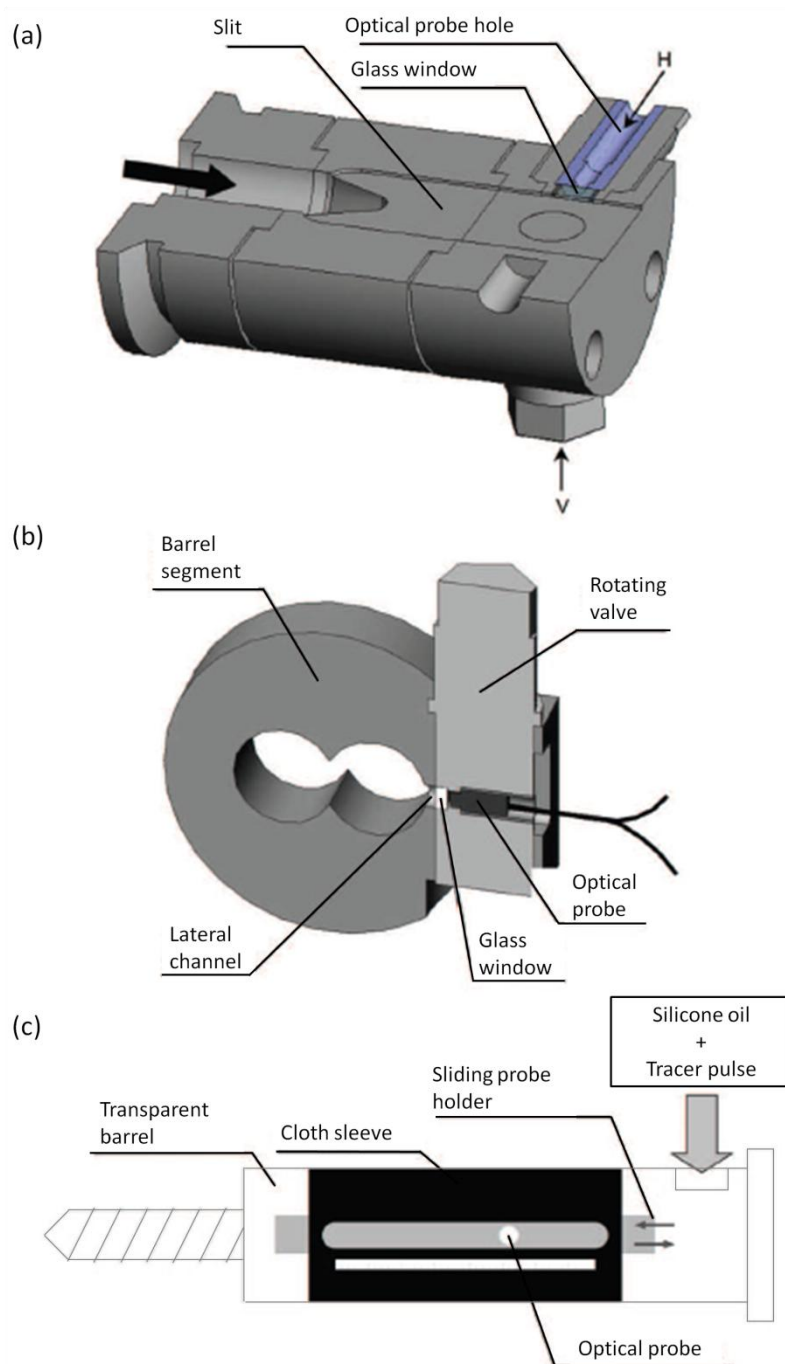


**Figure 3.4.** Solutions to accommodate the optical probe: (a) slit die used for measurements in a single-screw extruder; (b) modified sampling device for partial measurements in a twin-screw extruder; (c) device for partial measurement along a transparent barrel [25].

Fluorescence spectroscopy has been mainly applied to monitor residence times via the use of fluorescent tracers in the melt. The RTD of a formulation provides information on the mixing history of the melt. A lower RTD indicates a decrease in degree of mixing in the extrusion barrel. In addition, fluorescent tracers allow more accurate melt temperature measurements. These applications might be of interest in pharmaceutical HME, especially for monitoring of extrusion processes during formulation development. The addition of fluorescent tracers will provide insight in residence times and temperature gradients throughout the melt, and the exposure time of an API to high temperatures can be estimated. This will enhance the understanding of material behaviour within the barrel, and will allow the optimization of screw designs.

#### 3.4.1.4. ***Terahertz (THz) spectroscopy***

Krumbholz et al. [28] demonstrated the potential of an in-line monitoring method using a fibre-coupled THz spectrometer, to study the influence of temperature and pressure on molten PP. Measurements were performed in a custom-made die at the end of a planetary gear extruder. The temperature and pressure of a PP melt were varied independently. No influence of melt pressure on the terahertz parameters (absorption coefficient and refractive index) was found. Also, no effect on the absorption coefficient was obtained when changing the melt temperature. However, when the temperature was increased, the refractive index decreased. The refractive index of a melt can be calculated from the time delay of the THz pulse propagating through the melt. It is directly related to the additive content of a compound. When extruding polymer-filler compounds, a linear relation between the refractive index of the compound and its volumetric additive content was established. Though a THz spectrometer is a very complex and expensive system, these first measurements with a newly developed probe supply promising results for refractive index measurements. The refractive index of a melt depends on the melt composition, but is also related to the melt density, allowing the monitoring of melt density as well.

#### 3.4.1.5. *Dielectric spectroscopy*

Perusich and McBrearty [29] applied dielectric spectroscopy to make composition measurements of the comonomer concentration along polymer chains. Dielectric spectroscopy imposes an electric field across the flowing polymer and measures the resultant alternating current produced from the movement and energy associated with dipole orientation and ionic conduction. These measurements are related to the physical and chemical structure of the polymer. The dielectric permittivity or capacitance was found to be proportional to the polymer sidechain composition. A short sidechain required a high measurement frequency (short relaxation time), whereas a longer sidechain, needed a much lower frequency (longer relaxation time) to orient the sidechain to a measurable extent. Two types of extruders were used. First, a 22 mm single-screw extruder where the sensor assembly was positioned at the exit of a static mixer section downstream from the screw. And second, a twin-screw extruder without static mixer, and with the sensor positioned downstream from the screw directly upstream from the die. The melt composition of a variety of polymer melt systems was measured with an in-line dielectric sensor. In-line measurements were performed on Elvax<sup>®</sup> (DuPont, Wilmington, Delaware, USA), an EVA copolymer. Once the polymer reached the die, the measured capacitance increased dramatically, and after 10 min a plateau was achieved. The absolute plateau value was a direct function of the applied frequency. The measured capacitance was found to be proportional to the VA content of Elvax<sup>®</sup>. Bur et al. [78] used the same setup on a twin-screw extruder to perform permittivity and conductivity measurements of resin melts to quantify filler concentrations. Sensitivity to polymer/filler composition can arise because of permittivity contrast between polymer and filler or because of changes in conductivity caused by variations in filler concentration. The authors found that the interelectrode separation distance was crucial for the measurement quality. By increasing the separation, the fringe field will extend beyond the surface, and the capacitance of the cell will decrease and affect the sensitivity of the measurements.

Dielectric measurements are used to analyze the physical/chemical structure of organic materials through the measurement of their dielectric properties. Since the dielectric loss factor is affected by dipolar alignment and by ionic mobility, it provides information on



changes in viscosity in a material. Thus, in addition to the monitoring of comonomer content and filler concentrations, dielectric spectroscopy could also be applied to perform rheological measurements in the melt [30]. For example, wall slip may be preceded by extensional stress, orienting the material and producing anisotropic dielectric properties. Migration of polymer additives at high shear stress can be detected as well. These measurements can easily be performed in-line, and therefore present an interesting addition to the existing analytical techniques applied in pharmaceutical HME.

#### 3.4.1.6. **Optical detectors**

Pinheiro et al. [31] measured the morphology of immiscible blends containing PP and polyamide 6 (PA 6) in a co-rotating twin-screw extruder. The disperse phase particle size and concentration were determined in-line with an optical device developed by Mélo and Canevarolo [32, 33], placed at a slit die with transparent windows at the extruder exit. A polychromatic, visible light source illuminates the entire surface of the glass window and a photocell. The detector's signal depends on the volume concentration and size of the disperse phase. The normalized detector's signal follows a linear correlation with particle concentration of four calibration standards ( $\text{Al}_2\text{O}_3$  0.5 and 2.0  $\mu\text{m}$  and  $\text{TiO}_2$  0.5 and 2.0  $\mu\text{m}$ ). Mixtures of  $\text{Al}_2\text{O}_3$  with different particle sizes (0.5 and 2.0  $\mu\text{m}$ ) at different ratios showed that the signal increases linearly with an increase in the concentration of 0.5  $\mu\text{m}$ . The detector captures the average value of a set of particles once the signal is linear with the weight average particle size. The signal also increased with increasing PA 6 content (disperse phase) because of the higher light scattering. The results showed that this detector is an accurate device for the assessment of parameters such as particle size and concentration.

The same device was applied by Canevarolo et al. [34] to assess the melting behaviour during polymer extrusion in a co-rotating twin-screw extruder. Melting of two polyamide tracers was studied by changing the barrel temperature and keeping all other operating conditions constant. Increasing the barrel temperature led to a fast growth of the normalized intensity due to melting of the tracer, eventually saturating once all tracer was molten. This type of detector can be applied in pharmaceutical HME during both the formulation development stage and during pharmaceutical production. It can be applied as a

monitoring device, to determine the optimal process settings to obtain a completely molten or dissolved API with minimal energy input but it is also relevant for process control during manufacturing, to monitor and control the state of the melt.

#### 3.4.1.7. *Nuclear magnetic resonance (NMR) spectroscopy*

Gottwald and Scheler [35] designed a surface NMR probe to monitor extrusion processes. Surface NMR gives access to molecular mobility, correlated to temperature, composition and homogeneity. Two main obstacles are the temperature, which decreases the magnetic field strength and the ferromagnetic materials in the extruder which deform the static field. The device was located next to the die of a single-screw extruder (30 mm diameter) and measurements were performed on a sheet of soft polyvinyl chloride (PVC). The probe withstood the harsh conditions although the melt was in direct contact with its surface. The detected signal of the PVC melt could be clearly distinguished from the background signal. Based on these results, the authors plan to modify an extruder element to fit the NMR probe, allowing the in-line monitoring of any NMR-detectable parameter, rheological information and component composition. In pharmaceutical processes, NMR is used to monitor interactions between drugs and excipients during production, to characterize the different polymorphic forms of an API, and for the identification and characterization of APIs. It is sensitive for small amounts of API in the formulation.

#### 3.4.2. Ultrasonic techniques

Sun et al. [36] monitored the RTD at the melting, mixing and pumping zones as well as at the die exit of a twin-screw extruder (30 mm diameter) by mounting the ultrasonic probes on the extruder barrel over the screw elements and at the die. In order to relate the measured ultrasonic signal to the RTD, the relationship between the signal strength and the  $\text{CaCO}_3$  concentration (the ultrasonic tracer) was calibrated, which was linear in the tested concentration range. Secondly, the RTD was measured by injecting a pulse of tracer and monitoring the ultrasonic signal strength. The change of the strength of the ultrasonic signal reflected from the rotating screw was caused by a change in acoustic impedance of the filled

material, the scattering loss by the filler and the change in the absorption of acoustic energy due to the presence of the filler.

Lee et al. [37] also performed RTD measurements based on the ultrasonic response of  $\text{CaCO}_3$  in PE. Measurements were performed at the die exit (slit die) of a co-rotating twin-screw extruder. The RTD was also evaluated at different filler concentrations, screw speeds, feeding rates and screw configurations. Increasing the screw speed or feed rate reduced the mean residence time and the variance of the residence time, whereas increasing  $\text{CaCO}_3$  concentration increased the mean residence time and variance of residence time. Both were also increased by the presence of reverse screw elements in the configuration. The in-line determination of RTD by ultrasound during extrusion was successfully realized.

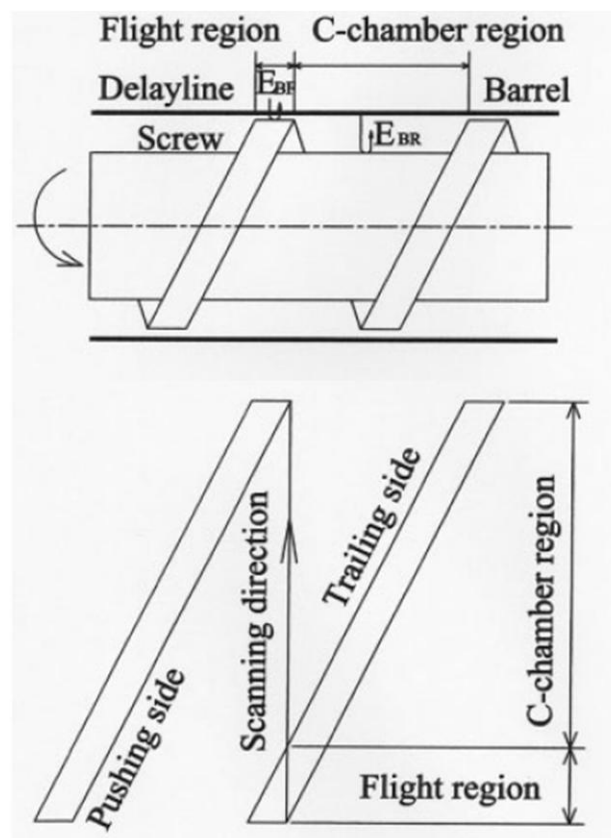


**Figure 3.5.** Ultrasound scanning regions: flight region and C-chamber [38].

Wang and Min [38] developed an ultrasound in-line monitoring system to investigate the melting behaviour of linear low density PE (LLDPE) and PVC compounds in the barrel of an intermeshing counter-rotating twin-screw extruder (30 mm diameter). Monitoring of the

ultrasound wave attenuation allowed the characterization of the melting process and uniformity across the screw channels. Various melting phenomena were described depending on the selected materials, processing conditions and screw configurations. Materials are periodically scanned by ultrasound in the flight region and in a C-chamber (Figure 3.5). Melting in the flight region finishes much faster than in the C-chamber for both LLDPE and PVC, due to the combination of heat conduction and viscous energy dissipation. The melting in the C-chamber always starts at the pushing side of the flight and then spreads to the trailing side. Melting level and uniformity increase with the increase of pressure in the material. During the extrusion of LLDPE and PVC compounds, dispersed or dissipation melting phenomena are dominant under most processing conditions. The ultrasound in-line monitoring method efficiently investigated the melting phenomena of various polymer systems fed in powder form or pellet form.

Abu-Zahra [39] measured the density of a polymer melt using ultrasound shear waves propagating at a frequency of 2.25 MHz. At a solid-liquid interface, the amount of ultrasonic shear wave energy reflected back into the solid is dependent on the operating frequency and properties of the fluid (viscosity and density) and of the solid (density and shear modulus). The acoustic impedance of the polymer melt is calculated using the measured reflection coefficient of the polymer melt interface boundary. This ultrasound measurement is independent of the attenuation in the polymer melt and the thickness of the melt stream. A special die adapter was mounted between the extruder barrel and the die of a 19 mm single-screw extruder, containing a shear ultrasound sensor. Different mixtures of PVC with varying levels of blowing agent and acrylic processing aid were extruded. Statistical correlation between the density measured by energy ration of shear ultrasound waves and the laboratory density measurements was 96% at constant processing conditions. The main assumption was that a change in the melt density will be directly manifested by a change in the extrudate density, which is accurate for most polymer extrusion applications. The difference between this application of ultrasound monitoring and the three previous examples is the use of ultrasound shear waves instead of longitudinal waves. In longitudinal waves, the oscillations occur in the direction of wave propagation, whereas the particles in shear waves oscillate at a right angle to the direction of wave propagation. At a solid-liquid interface, the amount of shear wave energy reflected back into the solid depends on the

operating frequency and on properties of the fluid (viscosity and density) and the solid (density, shear modulus). A relation between the melt density and the energy ratio of shear ultrasound waves can be established. The longitudinal wave reflection method is used to measure the time of flight of ultrasonic waves and the ultrasound velocity in polymer melt. These data are then used to calculate the density. Longitudinal waves can be generated in liquids, as well as solids because the energy travels through the atomic structure by a series of compressions and expansion movements, whereas shear waves require an acoustically solid material for effective propagation, and therefore, are not effectively propagated in liquids.

In polymer extrusion, ultrasound techniques have been used to monitor melt temperature and pressure, changes in material type, effects of process settings on rheological characteristics of the melt and filler concentration [40]. Besides qualitative and quantitative monitoring of the polymer melt, ultrasonic sensors can be used to monitor the barrel and screw integrity at the melting, mixing and pumping zones of the extruder via barrel or flange. This application was discussed by Jen et al [41]. Extrusion of low density PE (LDPE) was performed on a 30 mm co-rotating twin-screw extruder and on a 50 mm counter-rotating twin-screw extruder. Four types of high pressure ultrasound transducers were developed and used at the melting, mixing and pumping zones of the extruder to monitor the screw and barrel wear.

### **3.4.3. Rheological techniques**

Chiu et al. [42] developed a new in-line viscometer that can directly test melt viscosity as a function of shear rate. The viscometer contains a stress sensor and a shear rate sensor which were installed between the screw and the die of a single-screw extruder. During extrusion of LDPE, different temperatures and screw speeds were applied, and a decreasing viscosity with increasing temperature was detected, due to the shear thinning behaviour of LDPE. The in-line results were compared to measurements with an off-line capillary rheometer, where the viscosity results were lower when the shear rate was lower than  $600 \text{ s}^{-1}$ , and higher when the shear rate was higher than  $600 \text{ s}^{-1}$ , possibly due to the instability of both the flow

meter and the stress sensor. Further research and adaptations are required to improve the accuracy of this device.

Covas et al. [43] presented new equipment to monitor the evolution of relevant characteristics of polymer systems along the screw axis. A sampling device was constructed, allowing the extraction of material from the screw channel. First, an on-line capillary rheometer was connected to the sampling device. When the material extracted from the barrel is pushed through the die, the torque is recorded, wall shear stress is determined and wall shear rate is calculated. The tool can also be applied for the on-line measurement of melt flow index/melt volume flow rate. This equipment was used to measure the rheological response of a 12% (w/w) PP-based carbon fibre composite after melting in an intermeshing co-rotating twin-screw extruder. The coherence between on-line and off-line shear data was clear. Large deformations and relatively high shear rates associated with the flow in a capillary rheometer may affect the morphology of the material and consequently its rheological response. Therefore, an on-line oscillatory rheometer was manufactured to determine the linear viscoelastic behaviour and the non-linear properties of the melt extracted from the screw channel. On-line monitoring along the axis of an extruder can provide a wealth of data, contributing to the understanding of the physical and chemical phenomena occurring inside the barrel.

In a subsequent study, Covas et al. [44] also developed an on-line rotational rheometer, enabling the determination of morphology development and reaction kinetics along the screw axis (Figure 3.6). The rheometer is very accurate when compared to commercial laboratorial instruments, an average deviation in linear viscoelasticity results between the new device and two off-line rheometers varied between 3 and 8% for various melts and blends. Results also showed that the on-line rheometer was more accurate in capturing structural evolutions of the materials along the extruder than analysis performed off-line on samples collected on-line for complex multiphase systems.

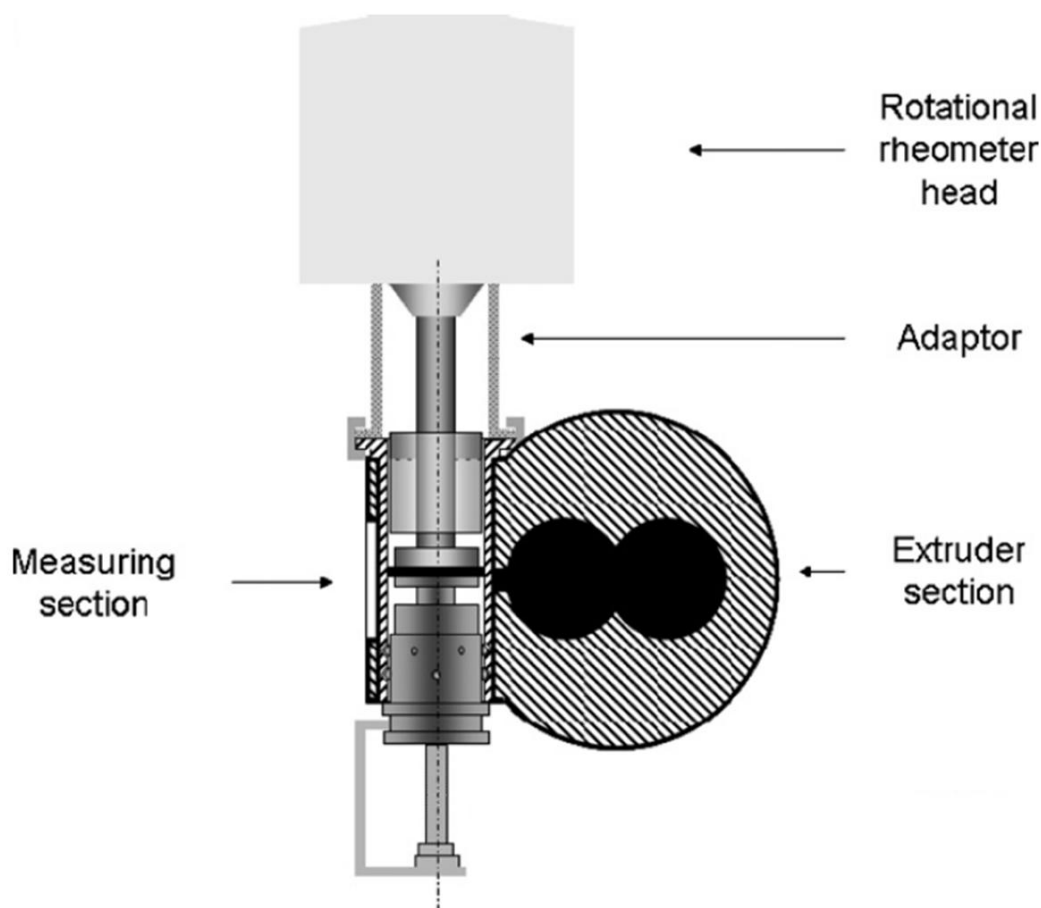


**Figure 3.6.** General overview of the on-line rotational rheometer (O2R) [44].

Mould et al. [45] monitored the dynamic rheological response of PP in a co-rotating twin-screw extruder using a new version of the on-line rotational rheometer developed by Covas et al. [44]. The technique was validated with off-line measurements at room temperature and at high temperatures, and on-line, and the validation step was considered successful. The usefulness of the instrument was first demonstrated with PP, and  $G'$  (storage modulus) and  $G''$  (loss modulus) decreased along the extruder. Then, PP grafted with maleic anhydride (PP-g-MA) was extruded, and a decrease of the rheological moduli was anticipated, due to chain scission during grafting. The on-line rheometer confirmed the shift of the moduli to lower values. Next, a PP/PP-g-MA system was extruded with 8.8% (w/w) montmorillonite organoclay, to produce a nanocomposite. As expected,  $G'$  and  $G''$  shifted to higher moduli values, the elasticity increased and evolution along the barrel was clearly observed. The results were in line with observations reported in literature, and evidenced the sensitivity and reliability of the apparatus.

Rajan et al. [46] monitored the thermal degradation of polyoxymethylene (POM) during extrusion on a co-rotating twin-screw extruder. The degradation is indicated by the emission of formaldehyde (FA) gas, which was monitored off-line with acetyl acetone colour measurements and by a reduction of viscosity. The on-line viscosity of the melt was measured by the difference in melt pressure when the melt was forced through a slit die at constant volume flow rate. When the throughput decreased and the screw speed increased, an enhanced thermal degradation was found. A good correlation between the viscosity measured in the slit die and the off-line FA measurements was observed. The thermal degradation of POM is successfully monitored by means of on-line viscosity measurements. With the use of on-line extensional rheometry on a co-rotating twin-screw extruder and off-line rotational rheometry, Kracalik et al. [47] tested different nanocomposites and investigated the effect of screw speed and geometry on the elongational and viscoelastic properties. In extensional rheometry, the extruded strand is elongated by rotating wheels. The rotation speed is increased to the time when the molten string breaks, to measure the melt strength level. The fast assessment of the melt strength measured by extensional rheometry correlates with a high accuracy with dynamic rheological data measured by rotational rheometry.  $\cot \delta$  ( $G'/G''$  ratio), which reflects the rigidity of the melt can be correlated with the melt strength level. The main benefit of extensional rheometry is the simplicity without the need for expensive equipment.

During extrusion, the raw materials are subjected to shear, increased temperatures and pressure conditions resulting in physicochemical changes within the mixture. The rheological response of a material to an imposed stress depends on the composition, morphology, degree of mixing and temperature. For process control purposes, it is important to obtain rheological properties of the melt that has experienced the complete history within the extruder, since these physicochemical changes are highly sensitive to the processing history. However, monitoring the rheological characteristics of the melt at several locations throughout the barrel will improve understanding of the process, and will provide useful information for optimization of the screw configuration and the operating conditions.



#### 3.4.4. Other process analytical techniques

Chen et al. [48] determined the differences in melting behaviour between a PP/polystyrene (PS) 80:20 and a PP/PS 20:80 blend in a twin-screw extruder under identical operating conditions. Therefore, a perturbation method was used together with temperature and pressure measurements along the channel of a co-rotating twin-screw extruder. A glass window was fitted in one of the nine barrel segments of the extruder, and a spacer plate was installed upstream of the segment with the glass window. Three pressure transducers, one RTD probe and three thermocouples were mounted in the spacer plate. In the perturbation method, a material mass pulse is added to the extruder feed to generate a disturbance to the steady-state operation. The pressure, temperature, residence time and drive motor power are monitored. The time history of the pulse material in the channel can be tracked with the RTD data, and can be combined with information from the motor power signals to detect the location of reactions in the extrusion channel. The melting process was visualized through the glass window using a high-speed video recording device. Once measurements at one position were completed, the barrel was moved to the next position. Three distinct regions for the melting of the PP/PS blends were determined: the partially filled region, the transition region and the fully filled region. The location of the transition region was determined from visualization results, temperature and pressure information and the pulse signals. Solid polymer pellets melted through an erosion mechanism in all three regions. The end of the melting process was identified using the visualization results, and the pressure profile. With these techniques, the melting profile of several materials in the barrel can be visualized using dyes. In pharmaceutical HME, the glass window in the barrel might also be applied to visualize other phenomena such as dispersion and distribution of API within the melt, given that the API has a different colour than the other components in the formulation.

Abeykoon et al. [49] evaluated five different melt temperature measurement techniques on a single-screw extruder. The point/bulk temperature of the die melt was measured with a 1 mm diameter non-insulated wall mounted thermocouple, a 3 mm diameter semi-insulated wall mounted thermocouple, a 0.5 mm diameter insulated wall mounted thermocouple and a Methotrexate infrared (IR) sensor. Melt temperatures at different radial locations of the

die were measured using a thermocouple mesh (TCM) with seven junctions placed between the adapter and die. LDPE was selected for the experiments. The three wall mounted thermocouples provided poor results in capturing variations in temperature. The IR sensor showed a better performance in detecting thermal variations, but even here the information is limited to a small volume of the melt flow. The TCM demonstrated that the thermal fluctuations varied significantly across the melt flow cross-section, and these variations increased with screw speed. However, the TCM does interfere with the melt flow, and is difficult to implement. Accurately monitoring the melt temperature remains one of the main challenges in HME. When only the surface temperature is monitored, information on the melt temperature at the screws is not known. A too high temperature in the melt can cause API and excipient degradation and affects the rheological properties of the melt. These consequences can be monitored separately with other process analytical tools described in this review, such as UV-VIS spectroscopy, ultrasonic techniques and rheometers. However, knowing the true temperature of the melt at any point within the barrel will eliminate the need to use several complementary techniques providing the same information.

Commonly used process monitoring devices, such as temperature and pressure sensors, provide limited information on process dynamics inside the extruder barrel. Therefore, Abeykoon et al. [50] performed inferential monitoring of the screw load torque signal by monitoring the motor current. The torque signal was dominated by the solid friction in the barrel and did not correlate well with melting fluctuations. However, torque measurements were proven useful for on-line identification of solids conveying issues. This technique to monitor polymer behaviour can be adapted in pharmaceutical HME without the requirement of barrel and/or die modifications and without the need for additional sensors.

#### **3.4.5. Combinations and comparison of complementary process analytical techniques**

Sun et al. [36] compared RTD measurements with an ultrasound probe and a reflective optical probe. Both probes were implemented at the mixing zone of the screws of a twin-screw extruder, in the same cross section of the barrel. A tracer was added to the polymer melt to monitor the RTD. Dependent on the optical characteristics of the extruded polymer

and tracer, the optical probe measured the RTD of either the entire channel volume or that of a surface layer of the volume, whereas the ultrasonic measurements always determined the RTD of the entire channel volume. For certain polymer systems, the ultrasound generated by the probe has a larger penetration depth than the light. The ultrasonic technology uses signals reflected from the screw, whereas the optical probe detects signals scattered by the tracer in the surface layer of the screw channel. The ultrasonic probe was proven to be more appropriate for measuring the RTD of the entire channel volume, and both techniques could provide complementary information to improve understanding of the extrusion process.

Abu-Zahra [51] attached a special die adapter to a 19 mm diameter single-screw extruder. An ultrasound transducer and a dielectric sensor were mounted in this die. PVC was extruded with varying levels of chemical blowing agent (AZO)4 and processing aid (K400). Ultrasound measurements are correlated to the melt density and the dielectric properties of the melt provide information on the mechanical viscosity. Both complementary techniques allow the simultaneous monitoring of the rheological properties density and viscosity of the melt.

### **3.5. CONCLUSION**

So far, monitoring of pharmaceutical HME processes remains limited to conventional monitoring of the process settings and parameters (barrel and die temperatures, feed rate or throughput, screw speed, torque and drive amperage, melt pressure and melt temperature) and the application of NIR and Raman spectroscopy to monitor the API concentration and the physicochemical state of the melt. However, the quality of an extrudate cannot simply be assessed by monitoring its drug load and solid state. Promising steps towards a thorough process understanding have been taken recently, but further monitoring of component degradation, rheological properties of the melt and their effect on processing efficiency and accurate melt temperature measurements are required to guarantee the quality of the extrudates and to predict the physical and chemical characteristics of the extrudates before starting the downstream processing.

Various sensors are available for observation of critical process and product parameters during extrusion, as reported in literature related to polymer extrusion. The implementation of the different process analytical techniques evaluated in this chapter will lead to a thorough process understanding and will allow monitoring of the critical process and product parameters. This monitoring will eventually lead to optimization of the HME process and the formulations, and provide the possibility for improved process control in routine manufacturing.

### 3.6. REFERENCES

- [1] Food and Drug Administration, Process Analytical Technology Initiative, Guidance for Industry; PAT - A Framework for Innovative Pharmaceutical development, Manufacturing and Quality Assurance, 2004.
- [2] International Conference on Harmonisation of Technical Requirements for Registration of Pharmaceuticals for Human Use, Pharmaceutical Development Q8 (R2), 2009.
- [3] I.M. Ziegler, Bulletin Technique Gattefossé 105 (2012) 44-67.
- [4] S.V. Tumuluri, S. Prodduturi, M.M. Crowley, S.P. Stodghill, J.W. McGinity, M.A. Repka, B.A. Avery, Drug Dev Ind Pharm 30 (2004) 505-511.
- [5] L. Saerens, L. Dierickx, T. Quinten, P. Adriaensens, R. Carleer, C. Vervaet, J. P. Remon, T. De Beer, Eur J Pharm Biopharm 81 (2012) 230-237.
- [6] B. Smith-Goettler, C.M. Gendron, N. MacPhail, R.F. Meyer, J.X. Phillips, Spectroscopy (2011).
- [7] C. Mckelvey, L. Schenck, M. Lowinger, G. Troup, Soc Plast Eng 54 (2008).
- [8] G.M. Troup, C.A. Mckelvey, L. Schenck, M. Lowinger, B. rudeen, A. Sinha, J.P. Higgins, Soc Plast Eng 56 (2009).
- [9] A.L. Kelly, T. Gough, R.S. Dhumal, S.A. Halsey, A. Paradkar, Int J Pharm 426 (2012) 15-20.
- [10] V.S. Tumuluri, M.S. Kemper, I.R. Lewis, S. Prodduturi, S. Majumdar, B.A. Avery, M.A. Repka, Int J Pharm 357 (2008) 77-84.
- [11] L. Saerens, L. Dierickx, B. Lenain, C. Vervaet, J.P. Remon, T. De Beer, Eur J Pharm Biopharm 77 (2011) 158-163.
- [12] A. Almeida, L. Saerens, T. De Beer, J.P. Remon, C. Vervaet, Int J Pharm 439 (2012) 223-229.
- [13] L. Saerens, C. Vervaet, J.P. Remon, T. De Beer, Anal Chem 85 (2013) 5420-5429.
- [14] C. Kindermann, K. Matthée, J. Strohmeyer, F. Sievert, J. Breitzkreutz, Eur J Pharm Biopharm 79 (2011) 372-381.
- [15] S.U. Schilling, N.H. Shah, A.W. Malick, M.H. Infeld, J.W. McGinity, J Pharm Pharmacol 59 (2007) 1493-1500.
- [16] M.G. Hansen, S. Vedula, J Appl Polym Sci 68 (1998) 859-872.

- [17] S. Vedula, M.G. Hansen, *J Appl Polym Sci* 68 (1998) 873-889.
- [18] T. Nagata, M. Ohshima, M. Tanigaki, *Polym Eng Sci* 40 (2000) 1107-1113.
- [19] A. Witschnigg, S. Laske, M. Kracalik, M. Feuchter, G. Pinter, G. Maier, W. Märzinger, M Haberkorn, G. Rüdiger Langecker, C. Holzer, *J App Polym Sci* 117 (2010) 3047-3053.
- [20] Y.M. Wang, B. Steinhoff, C. Brinkmann, I. Alig, *Polymer* 49 (2008) 1257-1265.
- [21] C. Gilmor, S.T. Balke, F. Calidonio, A. Rom-Roginski, *Polym Eng Sci* 43 (2003) 356-368.
- [22] K.B. Migler A.J. Bur, *Polym Eng Sci* 38 (1998) 213-221.
- [23] A.J. Bur, M.G. Vangel, S.C. Roth, *Polym Eng Sci* 41 (2001) 1380-1389.
- [24] A.J. Bur, S.C. Roth, M.A. Spalding, D.W. Baugh, K.A. Koppi, W.C. Buzanowski, *Polym Eng Sci* 44 (2004) 2148-2157.
- [25] O.S. Carneiro, J.A. Covas, J.A. Ferreira, M.F. Cerqueira, *Polym Test* 23 (2004) 925-937.
- [26] S.E. Barnes, M.G. Sibley, H.G.M. Edwards, P.D. Coates, *Trans Inst Meas Control* 29 (2007) 453-465.
- [27] H.X. Fang, F. Mighri, A. Ajji, P. Cassagnau, S. Elkoun, *J Appl Polym Sci* 120 (2011) 2304-2312.
- [28] N. Krumbholz, T. Hochrein, N. Vieweg, T. Hasek, K. Kretschmer, M. Bastian, M. Mikulics, M. Koch, *Polym Test* 28 (2009) 30-35.
- [29] S. Perusich, M. McBrearty, *Polym Eng Sci* 40 (2000) 214-226.
- [30] A.J. Bur, S.C. Roth, M. McBrearty, *Rev Sci Instrum* 73 (2002) 2097-2102.
- [31] L.A. Pinheiro, G.H. Hu, L.A. Pessan, S.V. Canevarolo, *Polym Eng Sci* 48 (2008) 806-814.
- [32] T.J.A. Melo, S.V. Canevarolo, *Polym Eng Sci* 42 (2002) 170-181.
- [33] T.J.A. Melo, S.V. Canevarolo, *Polym Eng Sci* 45 (2005) 11-19.
- [34] S.V. Canevarolo, M.K. Bertoline, L.A. Pinheiro, V. Palermo, S. Piccarolo, *Macromol Symp* 279 (2009) 191-200.
- [35] A. Gottwald, U. Scheler, *Macromol Mater Eng* 290 (2005) 438-442.
- [36] Z. Sun, C.K. Jen, C.K. Shih, D.A. Denelsbeck, *Polym Eng Sci* 43 (2003) 102-111.
- [37] S.M. Lee, J.C. Park, S.M. Lee, Y.J. Ahn, J.W. Lee, *Korea-Aust Rheol J* 17 (2005) 87-95.
- [38] D.B. Wang, K. Min, *Polym Eng Sci* 45 (2005) 998-1010.
- [39] N.H. Abu-Zahra, *Int J Adv Manuf Tech* 24 (2004) 661-666.
- [40] Brown EC. *Ultrasonic monitoring of polymer melt extrusion*, Bradford, UK: University of Bradford, 1998.
- [41] C.K. Jen, Z. Zun, M. Kobayashi, *Meas Sci Technol* 16 (2005) 842-850.

- [42] S.H. Chiu, H.C. Yiu, S.H. Pong, *J Appl Polym Sci* 63 (1997) 919-924.
- [43] J.A. Covas, O. S. Carneiro, P. Costa, A.V. Machado, J.M. Maia, *Plast Rubber Compos* 33 (2004) 55-61.
- [44] J.A. Covas, J.M. Maia, A.V. Machado, P. Costa, *J Non-Newton Fluid* 148 (2008) 88-96.
- [45] S. Mould, J. Barbas, A.V. Machado, J.M. Nóbrega, J.A. Covas, *Polym Test* 30 (2011) 602-610.
- [46] V.V. Rajan, R. Wäber, J. Wieser, *J Appl Polym Sci* 115 (2010) 2394-2401.
- [47] M. Kracalik, S. Laske, A. Witschnigg, C. Holzer, *Rheol Acta* 2011; 50: 937-944.
- [48] H.B. Chen, U. Sundararaj, K. Nandakumar, M.D. Wetzel, *Ind Eng Chem Res* 43 (2004) 6822-6831.
- [49] C. Abeykoon, P.J. Martin, A.L. Kelly, E.C. Brown, *Sensor Actuat a-Phys* 182 (2012) 16-27.
- [50] C. Abeykoon, M. McAfee, K. Li, P.J. Martin, A.L. Kelly, *J Mater Process Tech* 211 (2011) 1907-1918.
- [51] N.H. Abu-Zahra, *Mechatronics* 14 (2004) 789-803.





# CHAPTER 4

## RAMAN SPECTROSCOPY FOR THE IN-LINE POLYMER-DRUG QUANTIFICATION AND SOLID STATE CHARACTERIZATION DURING A PHARMACEUTICAL HOT-MELT EXTRUSION PROCESS

Parts of this chapter are published in:

**L. Saerens**, L. Dierickx, B. Lenain, C. Vervaet, J.P. Remon, T. De Beer. Raman spectroscopy for the in-line polymer–drug quantification and solid state characterization during a pharmaceutical hot-melt extrusion process. *European Journal of Pharmaceutics and Biopharmaceutics*, 77 (2011) 158-163.

## ABSTRACT

Chapter 4 evaluates the suitability of Raman spectroscopy as a Process Analytical Technology (PAT) tool for the in-line determination of the active pharmaceutical ingredient (API) concentration and the polymer-drug solid state during a pharmaceutical hot-melt extrusion process.

For in-line API quantification, different metoprolol tartrate (MPT) - Eudragit<sup>®</sup> RL PO mixtures, containing 10, 20, 30, and 40% MPT (w/w), were extruded and monitored in-line in the die using Raman spectroscopy. A PLS model, regressing the MPT concentrations versus the in-line collected Raman spectra, was developed and validated, allowing real-time API concentration determination. The correlation between the predicted and real MPT concentrations of the validation samples is acceptable ( $R^2=0.997$ ). The predictive performance of the calibration model is evaluated by the root mean square error of prediction (RMSEP), which is 0.59% (w/w).

Two different polymer-drug mixtures were prepared to evaluate the suitability of Raman spectroscopy for in-line polymer-drug solid state characterization. Mixture 1 contained 90% Eudragit<sup>®</sup> RS PO and 10% MPT (w/w), and was extruded at 140°C, hence producing a solid solution. Mixture 2 contained 60% Eudragit<sup>®</sup> RS PO and 40% MPT (w/w), and was extruded at 105°C, producing a solid dispersion. The Raman spectra collected during these extrusion processes provided two main observations. First, the MPT Raman peaks in the solid solution broadened compared to the corresponding solid dispersion peaks, indicating the presence of amorphous MPT. Secondly, peak shifts appeared in the spectra of the solid dispersion and solid solution compared to the physical mixtures, suggesting interactions between Eudragit<sup>®</sup> RS PO and MPT, most likely hydrogen bonds. These shifts were larger in the spectra of the solid solution. DSC analysis and ATR FT-IR confirmed these Raman solid state observations and the interactions seen in the spectra. Raman spectroscopy is a potential PAT-tool for the in-line determination of the API-concentration and the polymer-drug solid state during pharmaceutical hot-melt extrusion.

# CHAPTER 4

## RAMAN SPECTROSCOPY FOR THE IN-LINE POLYMER-DRUG QUANTIFICATION AND SOLID STATE CHARACTERIZATION DURING PHARMACEUTICAL HOT-MELT EXTRUSION

---

### 4.1. INTRODUCTION

Hot-melt extrusion (HME) is one of the most widely used processing technologies in the plastic, food and rubber industry [1]. Recently, it also found its application in pharmaceutical manufacturing operations, offering many advantages compared to traditional pharmaceutical processing techniques [1-5]. Nowadays, extruders allow in-line monitoring and control of the process parameters barrel and die temperature, feed rate and screw speed, and in-line monitoring of the motor load and the melt pressure in the extruder and die. The in-line monitoring and control of quality parameters corresponding to the extruded product itself, such as drug load and solid state, will allow real-time product quality evaluation and an increased understanding of the product behaviour during extrusion.

Recently, there is a tendency within the pharmaceutical industry to move from traditional batch processes towards continuous processing, hereby increasing process efficiency and production. Continuous processes offer many advantages: there is no difficult scale-up necessary, resulting in a shorter development time, an automatic production line would be possible, production costs can be reduced, it ensures faster product release and improved product quality [6]. Hot-melt extrusion can be operated as a continuous process, capable of

consistent product flow at relatively high throughput rates [1], making it a suitable technique for large scale production.

The FDA has introduced the concept of PAT in 2004 [7]. Pharmaceutical products must meet very strict specifications. Conventional pharmaceutical manufacturing is generally accomplished using batch processing followed by time-consuming, expensive and less efficient off-line laboratory testing on randomly collected samples to evaluate the end product quality, with an increased risk of batch rejection after manufacturing. The processes themselves are not fully understood and are often inefficient black-boxes. The general principle of PAT is to build quality into products rather than testing it into products. PAT-tools such as Raman spectroscopy provide in-line and real-time process information concerning critical formulation parameters, which allows the steering of processes towards their desired state through adaptations of process settings. Consequently, final product quality is guaranteed, end product characteristics can be predicted and real-time release can be ensured, hence avoiding batch losses.

Raman spectroscopy enables rapid, non-destructive and in-line measurements, and has previously been used during hot-melt extrusion (single-screw extrusion) to monitor EVA copolymer melt composition [8, 9], to analyze film formulations [10], and to monitor the composition of a series of high-density polyethylene (HDPE)/polypropylene (PP) blends [11, 12]. It has also been implemented in a twin-screw extrusion process to determine the concentration of Irganox additive in PP [13]. Raman spectroscopy has also been applied for off-line confirmation of drug dispersion within PEO and interaction with PEO in extrudates [14], for characterization of the hydrogen bonding nature in  $\alpha$ - and amorphous indomethacin [15], and for comparison of the solid state properties of solid dispersions prepared by HME and solvent co-precipitation processes [16].

## 4.2. MATERIALS AND METHODS

### 4.2.1. Materials and hot-melt extrusion

Hot-melt extrusion was performed using a Prism Eurolab 16 co-rotating, fully intermeshing twin-screw extruder (Thermo Fisher Scientific, Germany). The hot-melt extruder was equipped with a DD Flexwall® 18 gravimetric feeder (Brabender® Technologie, Germany), which was set in its gravimetric feeding mode.

For the development of a calibration model allowing in-line API quantification, 4 different polymer-drug mixtures, containing 10, 20, 30 and 40% (w/w) API respectively, were extruded. Eudragit® RL PO (Evonik Röhm, Germany) was used as polymer and metoprolol tartrate (MPT) was used (Esteve Quimica, Spain) as API. Before extrusion, the polymer and drug were mixed in a mortar. Each mixture was hot-melt extruded with a feeder speed of 0.3 kg/h and a screw speed of 50 rpm. The barrel temperature profile was set at 90-140-140-140-140-140°C (from hopper to die). The torque dropped from 70% motor capacity for the 10% MPT mixture, over 35% for the 20% MPT mixture and 20% for the 30% MPT mixture to 15% for the mixture containing 40% MPT (w/w). The die pressure, measured with a pressure probe, decreased with increasing MPT content, from 2 bar in the 10% MPT mixture to 0 bar in the 40% (w/w) mixture.

Two different polymer-drug mixtures were prepared to evaluate the suitability of Raman spectroscopy for in-line polymer-drug solid state characterization. Mixture A contained 10% MPT and 90% Eudragit® RS PO (w/w) (Evonik Röhm, Germany), which has an identical molecular structure as the RL PO form, but contains fewer ammonium groups. It was extruded with a barrel temperature profile of 90-140-140-140-140-140°C, which is above the melting temperature of pure MPT, 120°C, to produce a solid solution. This resulted in a torque of 50% of the motor capacity and a die pressure of 1 bar. Mixture B consisted of 60% Eudragit® RS PO and 40% MPT (w/w), and was extruded with a barrel temperature profile of 90-105-105-105-105-105°C, resulting in a solid dispersion. The torque was 65% and the die pressure 0 bar. For both mixtures, the feeder speed rate was set at 0.4 kg/h and the screw

speed at 80 rpm. The minimum batch size used was 700g of mixture. The Hansen solubility parameters of all polymers and MPT were calculated using SPWin version 2.1 [17].

#### **4.2.2. Raman spectroscopy**

Raman spectra were collected with a Raman Rxn1 spectrometer (Kaiser Optical Systems, Ann Arbor, MI, USA), equipped with an air-cooled CCD detector. A fibre-optic Raman Dynisco probe was built into the extrusion die, behind the pressure probe, to monitor the process stream before the melt is forced through the die. The laser wavelength was the 785 nm line from a 785 nm Invictus NIR diode laser. All spectra were recorded with a resolution of  $4\text{ cm}^{-1}$  and an exposure time of 1 second, using a laser power of 400 mW. Spectra were collected every 5 seconds. Data collection and data transfer were automated using the HoloGRAMS™ data collection software, the HoloREACT™ reaction analysis and profiling software and the Matlab software (version 7.1, The MathWorks Inc., Natick, MA). The analyzed spectral region was  $50 - 1800\text{ cm}^{-1}$ , since this region contained all useful drug and polymer information.

Data analysis was performed using SIMCA P+ (Version 12.0.1.0, Umetrics, Umeå, Sweden). Mean centering, Savitzky-Golay and SNV pre-processing were applied on the in-line collected spectra before principal components analysis (PCA) and partial least squares analysis (PLS), to exclude inter-batch variation and variation caused by baseline-shifts, respectively. For PCA and PLS, 20 spectra of each polymer-drug mixture were used to develop the models. A PLS model was developed, regressing the MPT-concentrations (Y) versus the corresponding in-line collected Raman spectra (X). This model was validated with 20 other spectra from each polymer-drug mixture, which were not used to develop the PLS model.

#### **4.2.3. Differential scanning calorimetry (DSC)**

Differential scanning calorimetry with a DSC Q 2000 (TA Instruments, Belgium) was used to confirm the Raman findings. Thermograms were produced with the Thermal Advantage Release 5.1.2 software and analysed with TA Instruments Universal Analysis 2000 4.7A (TA Instruments, Belgium). Aluminium hermetic pans (TA Instruments, Belgium) were used to

contain the samples. Measurements were carried out in a nitrogen atmosphere, with a heating/cooling rate of 10°C/min.

#### **4.2.4. Attenuated total reflectance Fourier transform infrared (ATR FT-IR)**

Besides DSC analysis, attenuated total reflectance (ATR) Fourier transform (FT) infrared (IR) spectroscopy was used to confirm the observations in the Raman spectra. Spectra were collected from the pure components, MPT and Eudragit® RS PO, from the physical mixtures A and B and from the extrudates of physical mixture A at 140°C and B at 105°C. The ATR FT-IR spectra were measured with a Bruker Vertex 70 FT-IR spectrometer, equipped with a DTCS detector and a PIKE accessory, equipped with a diamond ATR crystal.

## 4.3. RESULTS AND DISCUSSION

### 4.3.1. In-line API concentration monitoring

10, 20, 30 and 40% MPT - Eudragit® RL PO (w/w) mixtures were extruded. The concentration variations were visible in the in-line collected Raman spectra (Figure 4.1). PCA on all in-line collected spectra showed that two principle components covered nearly all spectral variation. The PC 1 versus PC 2 scores plot (Figure 4.2) shows a clear distinction between the spectra of the different mixtures and confirms that the first principal component captures the variation caused by differences in API-polymer concentration.

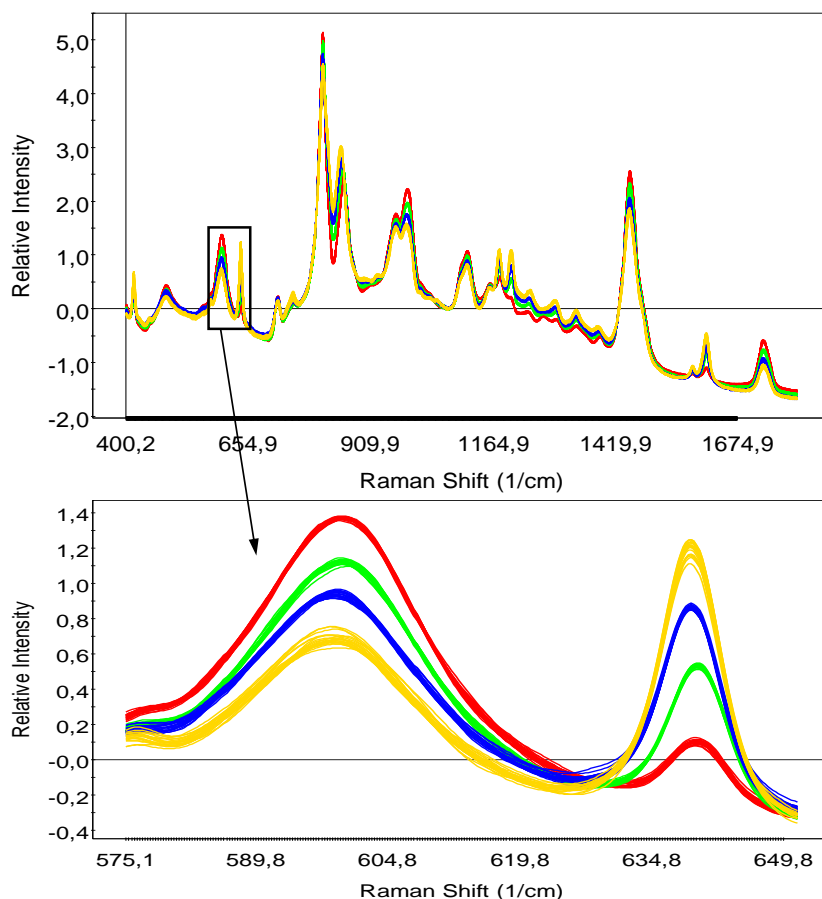


**Figure 4.1.** In-line collected Raman spectra of different MPT – Eudragit® RL PO mixtures. Red = 10% MPT, green = 20% MPT, blue = 30% MPT, yellow = 40% MPT (w/w).

For the development of the PLS model, allowing prediction of the MPT concentration in unknown samples during hot-melt extrusion processes, the in-line Raman collected spectra



(X) were regressed versus the known MPT concentrations (Y). Two PLS components were chosen, since the goodness of prediction of the model ( $Q^2 = 0.997$ ) did not increase significantly after adding extra components [18]. To evaluate the predictive performance of this model, 20 test spectra of each mixture were used (i.e., other spectra than used for composing the PLS model) and were projected onto the model to predict the corresponding MPT concentrations. Figure 4.3 shows the predicted versus the observed MPT concentration values for these validation spectra ( $R^2 = 0.997$ ). The resulting root mean square error of prediction (RMSEP) is 0.59% (w/w).

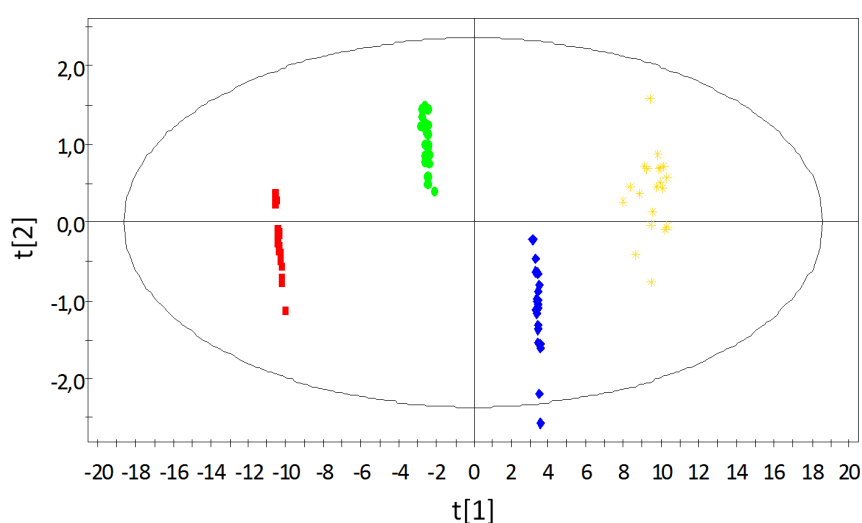


**Figure 4.2.** PC 1 vs. PC 2 scores plot of the in-line collected Raman spectra. Red = 10% MPT, green = 20% MPT, blue = 30% MPT, yellow = 40% MPT (w/w).

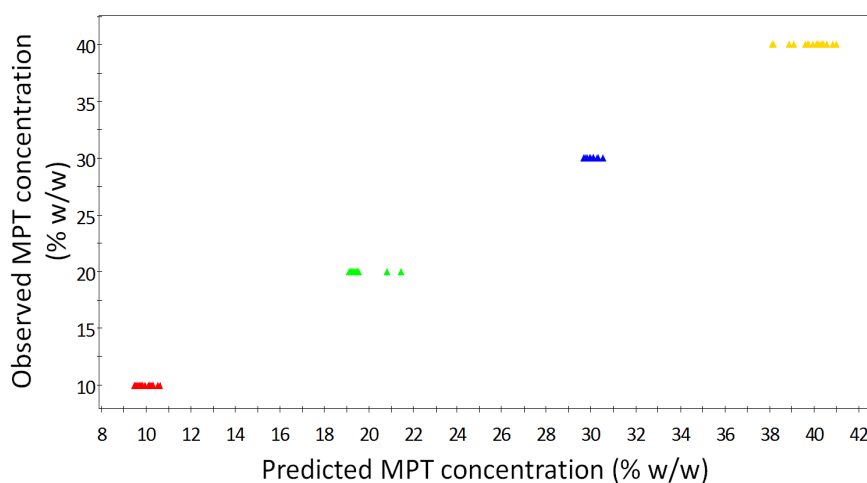


**Figure 4.3.** Predicted vs. observed MPT concentrations for the validation spectra. Red = 10% MPT, green = 20% MPT, blue = 30% MPT, yellow = 40% MPT (w/w).

### 4.3.2. In-line solid state monitoring

To obtain a good compatibility between polymer and drug, the difference in solubility parameters ( $\delta$ ) of polymer and drug should not be more than  $7.0 \text{ MPa}^{1/2}$  [19]. When this is achieved, miscibility is significant and, therefore, glass solution formation during melt extrusion can possibly be obtained. The Hansen solubility parameter for MPT is  $23.6 \text{ MPa}^{1/2}$ ,  $19.7 \text{ MPa}^{1/2}$  for Eudragit® RS PO and  $19.6 \text{ MPa}^{1/2}$  for Eudragit® RL PO. The smaller the difference in solubility parameters, the greater the miscibility between two compounds. Hence, a good miscibility and possible formation of a solid solution between Eudragit® RS PO and MPT was expected.

Two mixtures (A and B) were extruded at two different extrusion temperatures ( $140^\circ\text{C}$  and  $105^\circ\text{C}$  respectively). Mixture A was expected to result in a solid solution where the MPT has transferred from the crystalline to the amorphous state. This would be the result of a high processing temperature (above the melting temperature of pure MPT) and a good miscibility between both components. Mixture B was expected to result in a solid dispersion, since the extrusion temperature is lower than the melting temperature of MPT, which will prevent the transfer of all MPT in the melt into the amorphous state. Hence, a fraction of the MPT will remain crystalline and the extrudate of mixture B will exist of at least 2 phases.

Figure 4.4a shows a detail of the in-line collected Raman spectra for the extruded mixtures A and B and the Raman spectra of the physical mixtures before extrusion. Comparison of these spectra resulted into two major observations. First, throughout the entire Raman spectrum, the extrudates show peak shifts compared to the spectra of the pure components and the spectra of the physical mixtures. These peak shifts in the spectra of the extrudates indicate interactions between MPT and Eudragit® RS PO. These interactions are stronger for extruded mixture A, as the shifts are larger. All MPT in extruded mixture A was amorphous, which enhances interaction with the polymer. In extruded mixture B, some MPT has transferred to the amorphous state, but the largest fraction remained crystalline, explaining the smaller peak shifts for this mixture. The occurring interactions are most likely hydrogen bonds between MPT and Eudragit® RS PO, which can take place between the hydroxyl functions or amino functions from MPT and the carbonyl groups from the polymer (Figure 4.5). Shifts of

the corresponding Raman peaks from these groups are indeed visible (Figure 4.4b). Hydrogen bonding in Raman and IR spectra can be mainly observed as a broadening of the spectral bands and a shift of these bands to lower frequencies [19]. The peak of  $\nu(\text{C}=\text{O})$  stretch vibration[20] of Eudragit® RS PO has shifted from  $1729.5 \text{ cm}^{-1}$  in pure Eudragit to  $1729.2 \text{ cm}^{-1}$  in extruded mixture B and  $1729.2 \text{ cm}^{-1}$  in extruded mixture A. The shift of the vibration of this bond is much smaller than that of the O-H or N-H stretch [19]. The peak of  $\nu(\text{C}-\text{N})$  in pure MPT can be found at  $1181 \text{ cm}^{-1}$  [21], and shifts over  $1179.6 \text{ cm}^{-1}$  in extruded mixture B to  $1178.7 \text{ cm}^{-1}$  in extruded mixture A. The  $\nu(\text{C}-\text{O})$  peak of pure MPT [21] is located at  $1109.7 \text{ cm}^{-1}$ , but shifts cannot be seen in the in-line collected spectra, since Eudragit® RS PO also has a  $\nu(\text{C}-\text{O})$  peak, appearing at  $1116.3 \text{ cm}^{-1}$ . These peaks overlap in the spectra of the extruded mixtures, causing difficulties to see the peak shifts. The decrease in vibration frequency of  $\nu(\text{C}-\text{N})$  adjacent to the hydrogen bond is due to weakening of these bonds, caused by the hydrogen bond formation.

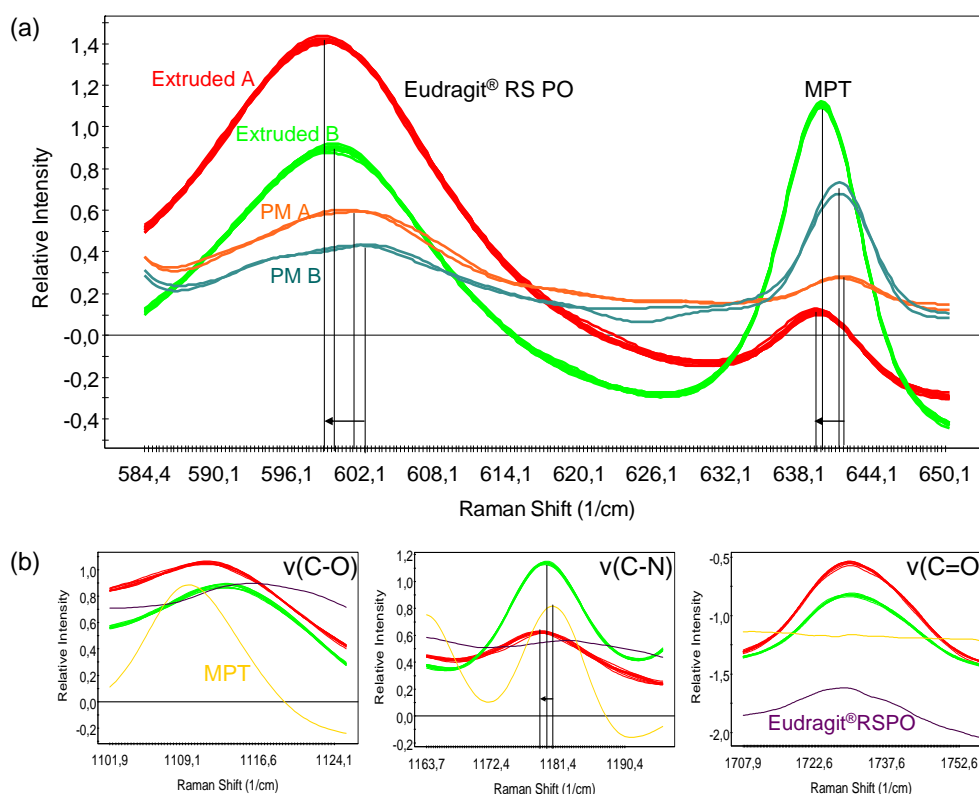


**Figure 4.4.** a) Raman spectra of the physical mixtures of 10% MPT in Eudragit® RS PO (w/w) (PM A, orange) and 40% MPT in Eudragit® RS PO (w/w) (PM B, blue) and the in-line collected Raman spectra of extruded mixture A (red) and extruded mixture B (green). b) Raman spectra of pure MPT (yellow) and pure Eudragit® RS PO (purple) and the in-line collected Raman spectra of extruded mixture A (red) and extruded mixture B (green).

A second observation of interest lies in the peaks of MPT. Since pure MPT is crystalline, its Raman spectrum contains narrow, well defined peaks. Extruded mixture B still contains a fraction of MPT in the crystalline state. The peaks of MPT have slightly broadened, but are still well defined. In extruded mixture A, the MPT peaks have broadened or even disappeared, indicating the presence of amorphous MPT. In the physical mixtures, the peaks of MPT remain as sharp as the original peaks. Interactions or transitions have not taken place in these physical mixtures.

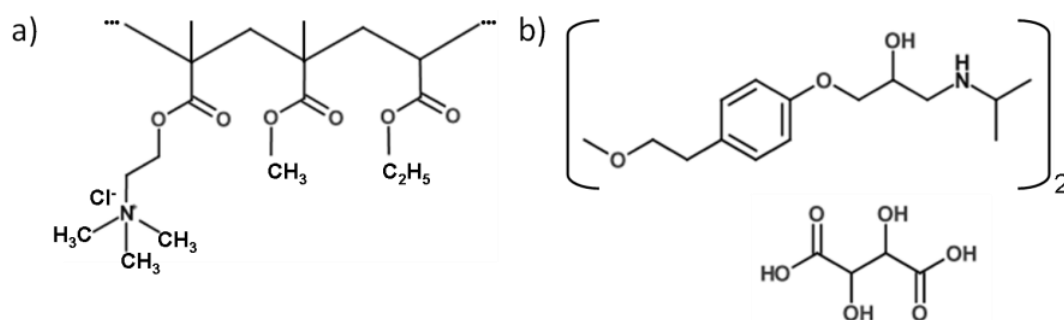


**Figure 4.5.** Molecular structures of a) Eudragit® RL/RS PO and b) Metoprolol tartrate.

The spectra in the  $50 - 150 \text{ cm}^{-1}$  region of the Raman spectrum contain information about lattice vibrations corresponding to vibrations and translations of the entire molecule in the lattice [15]. These vibrations are characteristic for the crystal structure and sensitive to local order or disorder. For the spectrum of pure MPT, this region has sharp, well defined peaks, which are still present in the spectra of extruded mixture B, but which have nearly disappeared in the spectra of extruded mixture A. In extruded mixture A, broad bands are visible, indicating a more disordered structure (Figure 4.6).

DSC analysis (Figure 4.7) was performed to confirm these interpretations from the Raman spectra. For the samples containing Eudragit® RS PO, the maximum heating temperature was restricted to  $140^\circ\text{C}$ , to avoid degradation of the polymer, which can occur above  $150^\circ\text{C}$ . The glass transition temperature ( $T_g$ ) of Eudragit® RS PO reaches a lower temperature in the extrudates, due to the plasticizing effect of MPT on the polymer, and due to the extrusion process, which slightly lowers the  $T_g$  of a polymer [22]. A lower  $T_g$  indicates a molecular dispersion of the drug in the polymer, whereas an unchanged  $T_g$  implies separation of the polymer- and drug phase [23]. The  $T_g$  of Eudragit® RS PO in the extrudates of 10% and 40%

MPT (w/w) is 46.6°C and 46.5°C, respectively, whereas the  $T_g$  of Eudragit® RS PO of the physical mixtures A and B used to prepare these extrudates is 55.1°C and 58.1°C, respectively, which is higher than the  $T_g$  after extrusion. This decrease in  $T_g$  after extrusion is caused by the interaction between Eudragit® RS PO and MPT during hot-melt extrusion. The chain mobility of the polymer increases due to incorporation of MPT in the polymer matrices, which translates into a decrease in  $T_g$ .

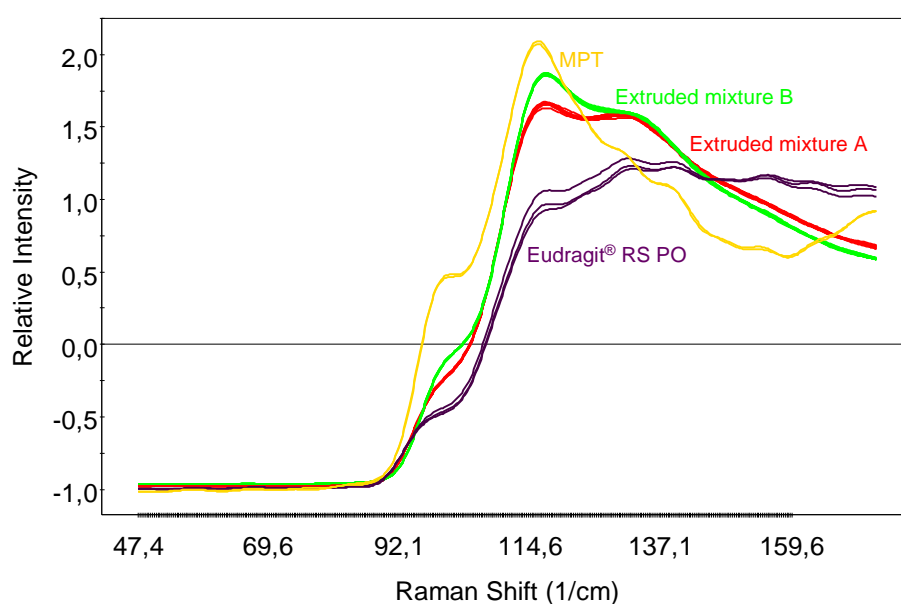


**Figure 4.6.** Detail of the Raman spectra for the  $50\text{ cm}^{-1}$  to  $150\text{ cm}^{-1}$  spectral region. Yellow = pure MPT; Purple = pure Eudragit® RS PO; red = extruded mixture A; green = extruded mixture B.

A similar shift in the endothermic melting peak of the crystalline MPT appears. The melting temperature of pure MPT is measured at  $124^\circ\text{C}$ , and its onset temperature at  $122.3^\circ\text{C}$ . In the physical mixtures A and B, this melting temperature has shifted to  $110^\circ\text{C}$  and  $122.3^\circ\text{C}$ , respectively, and the onset temperature to  $103.3^\circ\text{C}$  and  $117.3^\circ\text{C}$  respectively. An even larger shift occurs in the thermogram of extrudate B, where the  $T_m$  of MPT is  $105.6^\circ\text{C}$  and its onset temperature  $102.5^\circ\text{C}$ . This shift again implies interactions between the polymer and the drug. These interactions are more explicit in extrudate B, but also appear in the physical mixtures. This endothermic peak has disappeared in the thermogram of extrudate A, indicating that all of the MPT has become amorphous during processing. Since there is only one  $T_g$  present, MPT and Eudragit® RS PO have interacted to form one single phase. Hence, the extrudate of mixture A is a solid solution.

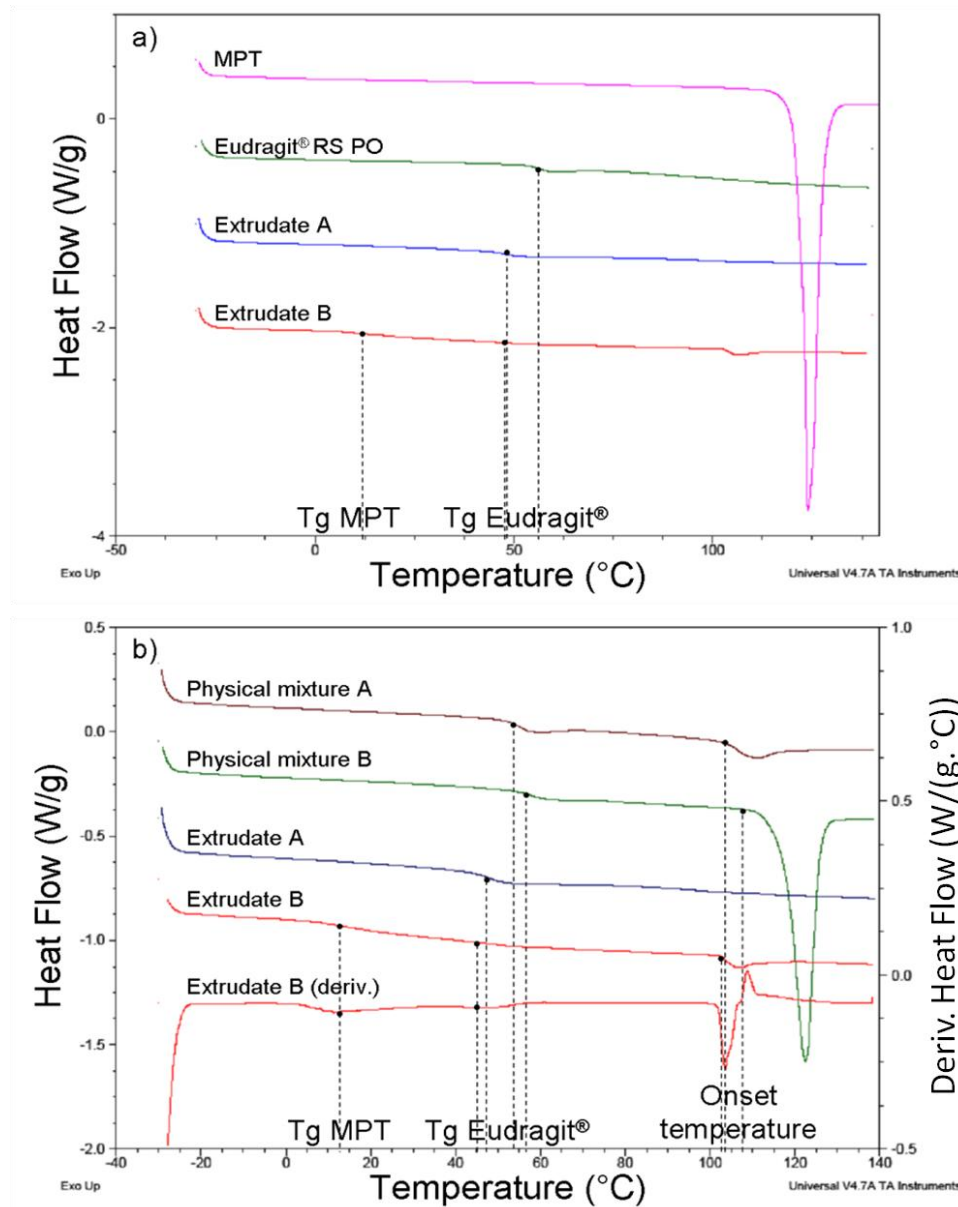


**Figure 4.7.** a) Thermograms of pure MPT and Eudragit® RS PO and of mixture A and B after hot-melt extrusion. b) Thermograms of physical mixtures A and B before hot-melt extrusion and of mixture A and B after hot-melt extrusion.

The first derivative of the thermogram of extrudate B shows 2  $T_g$ 's, one for Eudragit® RS PO (46.5°C) and one for MPT (12°C,  $T_g$  of pure MPT = 14.2°C). A fraction of the MPT in this mixture has become amorphous during processing, but has not interacted with the polymer phase. Hence, this extrudate exists of three phases: an amorphous polymer phase, an amorphous drug phase and a crystalline drug phase. This extrudate is in fact a solid dispersion which is partially crystalline and partially amorphous. Therefore, the DSC thermograms confirm the observations from the in-line Raman spectra.

Figures 4.8a and 4.8b represent the ATR FT-IR spectra of metoprolol tartrate and Eudragit® RS PO, respectively. The IR spectra of the physical mixtures of metoprolol tartrate and Eudragit® RS PO (Figure 4.8c and 4.8d) can be seen as the combinations of the IR spectra of the independent products in their respective ratios. The MPT signals are sharp and the fingerprint area ( $1500\text{ cm}^{-1} - 600\text{ cm}^{-1}$ ) shows an explicit pattern. The position of the bands in the IR spectra of the physical mixtures remains unchanged compared to the corresponding bands in the spectra of the pure components. No new bands or band shifts occur.

The IR spectrum of mixture B, which was extruded at a temperature of  $105^{\circ}\text{C}$ , results in a significantly changed IR pattern (Figure 4.8f). In the spectral area of  $3800\text{ cm}^{-1} - 2800\text{ cm}^{-1}$ , the C-H stretch vibrations of the acrylate polymer are dominantly present. The pattern of the different OH and NH vibrations of the API has disappeared. They are replaced by a broad band between  $3700\text{ cm}^{-1}$  and  $2300\text{ cm}^{-1}$ , which can be assigned to associated hydroxyl groups due to hydrogen bonding with the carbonyl functions of the polymer. The band representing the ester group of the acrylate polymer is dominantly present compared to the corresponding physical mixture (Figure 4.8f vs. 4.8d). The bands in the  $1610\text{ cm}^{-1} - 1585\text{ cm}^{-1}$  area, belonging to the metoprolol carboxylate groups, have shifted. In the fingerprint area ( $1500\text{ cm}^{-1} - 600\text{ cm}^{-1}$ ), the pattern has disappeared and the bonds arising from the polymer are explicitly present compared to the physical mixture. This indicates a strong association of the API with the polymer, forming coupled vibrations of MPT with the polymer.

In the IR spectrum of mixture A, which was extruded at a temperature of  $140^{\circ}\text{C}$ , this effect is even more distinct (Figure 4.8e), showing only the vibrational state (and thus spectrum) of the polymer. Due to the formation of strong hydrogen bonds between the hydroxyl groups of MPT and the ester carbonyl groups of the polymer, a macromolecular structure with its own vibrations is generated, where the MPT is no longer present as an independent molecule. With exception of very weak IR absorption bands at  $1612\text{ cm}^{-1}$  and  $1513\text{ cm}^{-1}$ , no typical absorption bands of MPT can be detected in the IR spectrum. The spectral area of  $3500\text{ cm}^{-1} - 2800\text{ cm}^{-1}$  also shows only 1 weak and broadened band of the associated hydroxyl groups of the drug.

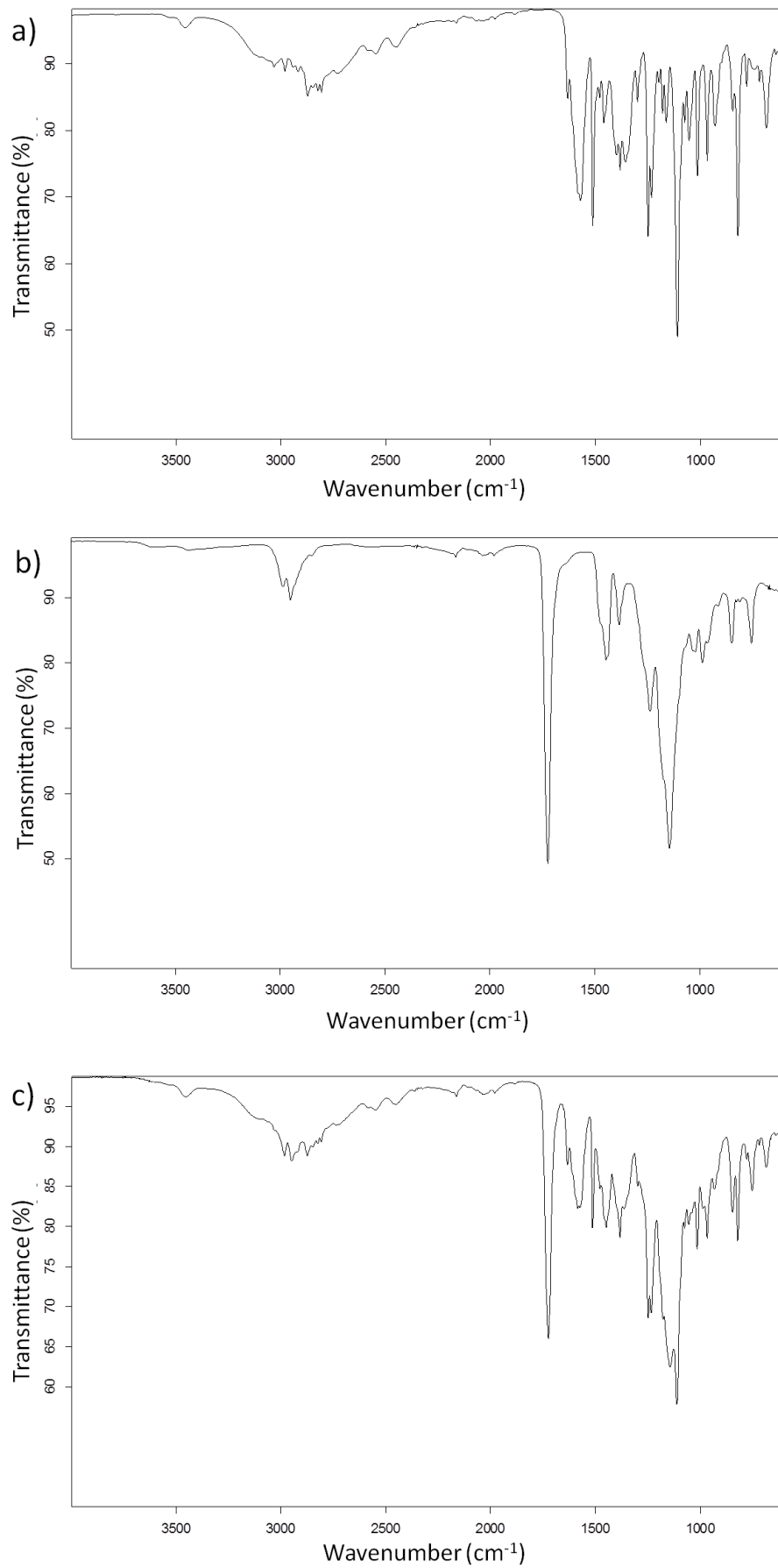


**Figure 4.8.** ATR FT-IR spectra of a) MPT, b) Eudragit® RS PO, c) physical mixture A



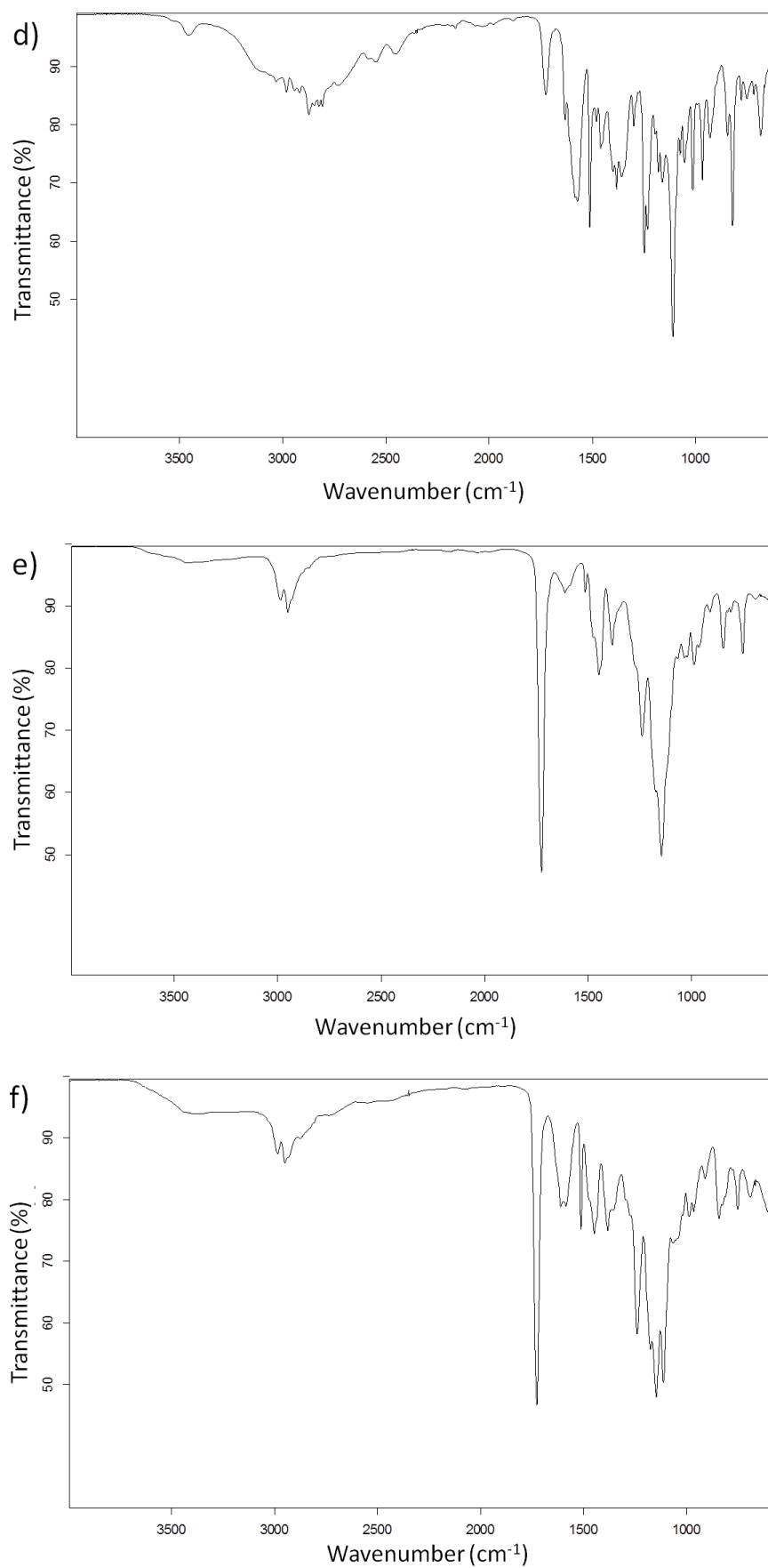


**Figure 4.8.** ATR FT-IR spectra of d) physical mixture B, e) extrudate of mixture A at 140°C, f) extrudate of mixture B at 105°C.

To demonstrate that the broadening of peaks and the peak shifts occurring in the in-line collected spectra are not an effect of the measurement environment (i.e. caused by the effect of temperature changes on the Raman measurements), samples were collected during extrusion of a mixture containing 40% MPT and 60% Eudragit® RS PO (w/w), and cooling at room temperature was monitored with Raman spectroscopy immediately after sample collection. After one day of storage at room temperature, Raman spectra of the samples were collected again. All of these spectra were compared to the spectra of the physical mixtures and the spectra gathered in-line during extrusion. During extrusion, a throughput of 0.3 kg/h, a screw speed of 80 rpm and a barrel temperature of 140°C were applied.

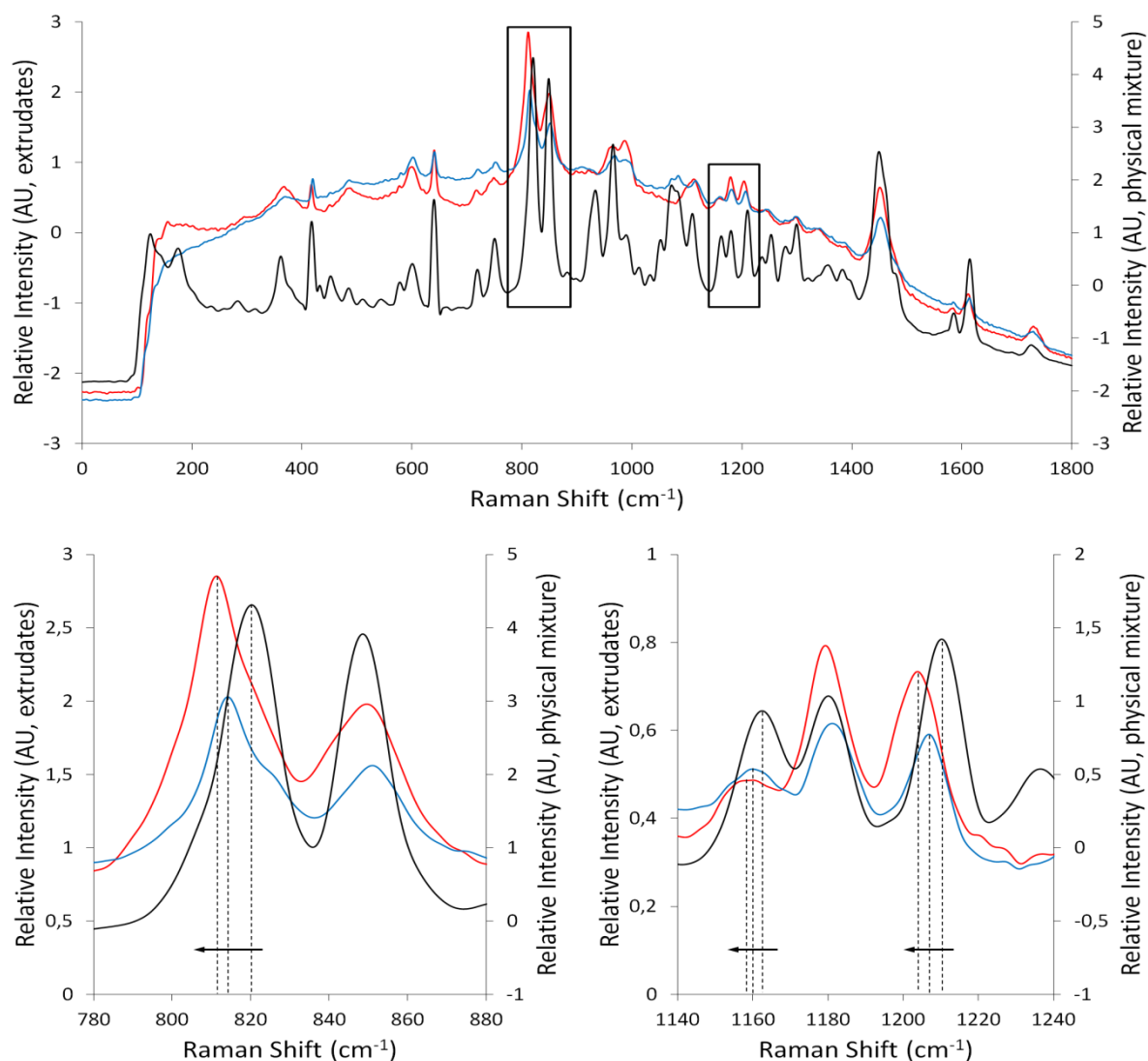


**Figure 4.9.** Raman spectra from the physical mixture (MPT – Eudragit® RS PO 40-60) (black), the extrudates during extrusion (red) and the extrudates after cooling at room temperature (blue).

As demonstrated in Figure 4.9, the spectral difference between the physical mixture and the in-line measurements is manifested as peak broadening, due to a transition from crystalline to amorphous MPT, and as peak shifts, caused by the interaction of MPT with Eudragit® RS PO. After cooling the extrudates at room temperature, the broadening of the peaks remained visible, as well as the peak shifts, indicating that this is an actual physicochemical difference between sample and physical mixture, rather than an effect of measurement environment.

#### 4.4. CONCLUSION

In this chapter, Raman spectroscopy was evaluated as a PAT tool to monitor the API concentration and polymer-drug melt solid state during pharmaceutical hot-melt extrusion processes. Comparison between the in-line collected Raman spectra and the off-line obtained DSC thermograms and ATR FT-IR spectra demonstrated that information about the physicochemical state of a polymer-drug melt can be obtained from the Raman spectra, allowing monitoring and prediction of the polymer-drug solid state throughout the extrusion process. With Raman spectroscopy, it was possible to detect differences between amorphous and crystalline polymer drug melts. The in-line collected Raman spectra also gave an indication of the occurring interactions during the hot-melt extrusion process, which leads to a better understanding of the process.

A PLS model was developed and validated, allowing drug concentration monitoring of unknown samples during hot-melt extrusion. Raman spectroscopy was able to detect variations in drug concentration and to predict drug concentrations with an RMSEP of 0.59% (w/w).

## 4.5. REFERENCES

- [1] R. Chokshi, H. Zia, *Iranian J Pharm Res* 3 (2004) 3-16.
- [2] J. Breitenbach, *Eur J Pharm Biopharm* 54 (2002) 107-117.
- [3] M.M. Crowley, F. Zhang, M.A. Repka, S. Thumma, S.B. Upadhye, S. Battu, J.W. McGinity, C. Martin, *Drug Dev Ind Pharm* 33 (2007) 909-926.
- [4] M.A. Repka, S. Battu, S.B. Upadhye, S. Thumma, M.M. Crowley, F. Zhang, C. Martin, J.W. McGinity, *Drug Dev Ind Pharm* 33 (2007) 1043-1057.
- [5] M.A. Repka, S. Majumdar, S. Battu, R. Srirangam, S.B. Upadhye, *Expert Opin Drug Deliv* 5 (2008) 1357-1376.
- [6] E.I. Keleb, A. Vermeire, C. Vervaet, J.P. Remon, *Int J Pharm* 273 (2004) 183–194.
- [7] Food and Drug Administration, Process Analytical Technology Initiative, Guidance for Industry; PAT - A Framework for Innovative Pharmaceutical development, Manufacturing and Quality Assurance, 2004.
- [8] S.E. Barnes, M.G. Sibley, H.G.M. Edwards, P.D. Coates, *Trans Inst Meas Control*, 29 (2007) 453-465.
- [9] S.E. Barnes, E.C. Brown, M.G. Sibley, H.G.M. Edwards, P.D. Coates, *Analyst* 130 (2005) 286-292.
- [10] V.S. Tumuluri, M.S. Kemper, I.R. Lewis, S. Prodduturi, S. Majumdar, B.A. Avery, M.A. Repka, *Int J Pharm* 357 (2008) 77-84.
- [11] S.E. Barnes, E.C. Brown, M.G. Sibley, H.G.M. Edwards, I.J. Scowen, P.D. Coates, *Appl Spectrosc* 59 (2005) 611-619.
- [12] P.D. Coates, S.E. Barnes, M.G. Sibley, E.C. Brown, H.G.M. Edwards, I.J. Scowen, *Polymer* 44 (2003) 5937-5949.
- [13] I. Alig, D. Fischer, D. Lellinger, B. Steinhoff, *Macromol Symp* 230 (2005) 51-58.
- [14] L. Li, O. AbuBaker, Z.J. Shao, *Drug Dev Ind Pharm* 32 (2006) 991-1002.
- [15] L.S. Taylor, G. Zografi, *Pharm Res* 14 (1997) 1691-1698.
- [16] Z. Dong, A. Chatterji, H. Sandhu, D.S. Choi, H. Chokshi, N. Shah, *Int J Pharm* 355 (2007) 141-149.
- [17] J. Breitreutz, *Pharm Res* 15 (1998) 1370-1375.

- [18] L. Eriksson, E. Johansson, N. Kettaneh-Wold, J. Trygg, C. Wikström, S. Wold, Multi- and Megavariate Data Analysis Part I: Basic Principles and Applications, 2<sup>nd</sup> ed., Umetrics Academy, Umeå, Sweden, 2006.
- [19] Y. He, B. Zhu, Y. Inoue, Prog Polym Sci 29 (2004) 1021-1051.
- [20] M. De Veij, P. Vandenabeele, T. De Beer, J.-P. Remon, L. Moens, J Raman spectrosc 40 (2008) 297-30.
- [21] G. Socrates, Infrared and Raman Characteristic Group Frequencies: Tables and Charts, 3<sup>rd</sup> ed., John Wiley & Sons Ltd., Chichester, UK, 2004.
- [22] V.B. Mathot, Calorimetry and Thermal Analysis of Polymers, 1<sup>st</sup> ed., Hanser Publishers, New York, USA, 1994.
- [23] S. Qi, A. Gryczke, P. Belton, D.Q.M. Craig, Int J Pharm 354 (2008) 158-167.

# CHAPTER 5

## VALIDATION OF AN IN-LINE RAMAN SPECTROSCOPIC METHOD FOR CONTINUOUS API QUANTIFICATION DURING PHARMACEUTICAL HOT-MELT EXTRUSION

Parts of this chapter are published in:

**L. Saerens**, N. Segher, C. Vervaet, J.P. Remon, T. De Beer. Validation of an in-line Raman spectroscopic method for continuous API quantification during pharmaceutical hot-melt extrusion. Accepted for publication in *Analytica Chimica Acta* (2013).

## ABSTRACT

A calibration model for in-line API determination was developed based on Raman spectra collected during hot-melt extrusion. This predictive model was validated by calculating the accuracy profile based on the analysis results of validation experiments. Furthermore, based on the data of the accuracy profile, the measurement uncertainty was determined. Finally, the robustness of the model was evaluated.

A Raman probe was implemented in the die of a twin-screw extruder, to monitor the drug concentration during extrusion of physical mixtures containing 15, 20, 25, 30 and 35% (w/w) metoprolol tartrate (MPT) in Eudragit® RS PO. Different calibration models for the prediction of the MPT content were developed, based on the use of single spectra or averaged spectra, and using partial least squares (PLS) regression or multivariate curve resolution (MCR). These predictive models were validated by extruding and monitoring mixtures containing 17.5, 22.5, 25.0, 27.5 and 32.5% (w/w) MPT. Each validated concentration was monitored on three different days, by two different operators. The  $\beta$ -expectation tolerance intervals were calculated for each model and for each of the validated MPT concentration levels ( $\beta$  was set at 95%), and acceptance limits were set at 10% (relative bias), indicating that at least 95% of future measurements should not deviate more than 10% from the true value. The only model where these acceptance limits were not exceeded, was the MCR model based on averaged Raman spectra. The uncertainty measurements for this model showed that the unknown true value can be found at a maximum of  $\pm 7.00\%$  around the measured result, with a confidence level of 95%. The robustness of this model was evaluated via an experimental design varying throughput, screw speed and barrel temperature. The robustness designs showed no significant influence of any of the fluctuating process settings on the predicted concentration values.

Raman spectroscopy proved to be a fast, non-destructive and reliable method for the quantification of MPT during hot-melt extrusion. From the accuracy profile of the MCR model based on averaged spectra, it was concluded that for each MPT concentration in the validated concentration range, 95 out of 100 future routine measurements will be included within the acceptance limits (10%).



# CHAPTER 5

## VALIDATION OF AN IN-LINE RAMAN SPECTROSCOPIC METHOD FOR CONTINUOUS API QUANTIFICATION DURING PHARMACEUTICAL HOT-MELT EXTRUSION

---

### 5.1. INTRODUCTION

Raman spectroscopy is a molecular vibrational spectroscopic technique, allowing fast and non-destructive measurements which do not require any sample pretreatment. The use of custom made fibre optic probes connected to the spectrometers allows the implementation into the process stream [1]. A Raman spectrum is an overlay of the fingerprints (i.e., a combination of spectral bands) of the individual components in a mixture, making Raman spectroscopy a suitable tool for quantification purposes. Hence, Raman spectroscopy can be applied as a process analytical tool to monitor and predict the concentration of an active pharmaceutical ingredient (API) during hot-melt extrusion.

So far, only two quantitative applications of Raman spectroscopy during hot-melt extrusion have been reported. In a first application [2] the API concentration was monitored behind the extrusion die, where a Raman probe was clamped above an extruded film. In the second application [3], the Raman probe was implemented in the extrusion die to monitor the API content of the extrudates. In both applications, a partial least squares (PLS) regression model was developed for the prediction of the API concentration, and a traditional chemometric validation approach [4] was used to validate the predictive models. First, the

root mean square error of calibration (RMSEC) and the root mean square error of the cross validation (RMSECV) are calculated, and then an external validation dataset is used to validate the predictive model. The quantitative performance of the Raman spectroscopic models is evaluated by calculating the root mean square error of prediction (RMSEP) based on the prediction results of the validation experiments. Small values of RMSEC, RMSECV and RMSEP indicate a good quantitative performance of the models. However, this validation approach does not fulfil the regulatory requirements in the ICH Q2 [5] and FDA [6] guidelines for validation of analytical procedures.

Many official documents [5, 6] describe the validation criteria which should be assessed, but no experimental protocols are provided. The ICH Q2 guideline [5] requires the assessment of accuracy, precision (repeatability and intermediate precision), specificity, linearity and range to validate an analytical quantification method for the active pharmaceutical ingredient in a drug product. The same validation characteristics are entailed by the FDA guidelines for validation [6], with addition of the robustness of the method. However, these guidelines are most often limited to these general concepts [7]. The determination of the validation parameters and the chemometric values (RMSEC, RMSECV, and RMSEP) does not suffice to evaluate the risk that every future measurement will be close enough to the unknown true value of the sample. These statistics only provide information concerning previously performed experiments. Statistics allowing to make a decision related to the validity of a method for future analyses are necessary.

The Société Française des Sciences et Techniques Pharmaceutiques (SFSTP) has developed a validation strategy based on the total error of the procedure (bias + standard deviation). Each analytical measurement reflects its true value, the bias of the method and its precision [8]. This approach minimizes the risk to accept an inaccurate calibration method or to reject a capable method. The objective of validation is to guarantee that every measurement performed in future analysis is close enough to the unknown true value [7], and that the difference will be lower than a preset acceptance limit. In this chapter, a Raman spectroscopic method for the quantification of metoprolol tartrate (MPT) in a polymer matrix during a hot-melt extrusion process was developed and validated by calculating the accuracy profile based on the analysis results of validation experiments.

## 5.2. MATERIALS AND METHODS

### 5.2.1. Materials

Physical mixtures containing MPT (Esteve Quimica, Spain), Eudragit® RS PO (Evonik, Germany) and magnesium stearate (Mg St) (Fagron, Belgium) were blended in a Turbula mixer before extrusion. The Mg St was added to the formulation to improve feeding behaviour of the mixtures in the extruder. Preparation of the validation mixtures was performed in triplicate, to allow extrusion on three different days, by two different operators.

### 5.2.2. Hot-melt extrusion

All physical mixtures were extruded on a 16 mm twin-screw extruder (Prism Eurolab 16, Thermo Fisher Scientific, Germany). The hot-melt extruder was equipped with a DD Flexwall® 18 gravimetric feeder (Brabender® Technologie, Germany), which was set in its gravimetric feeding mode and supplied the physical mixtures with a throughput of 0.3 kg/h. The applied screw speed was 80 rpm for all experiments, and the barrel temperature from feeding area to die was set at 70-142-142-142-142-120°C.

### 5.2.3. Raman spectroscopy

In-line Raman spectra were collected with a Raman Rxn1 spectrometer (Kaiser Optical Systems, Ann Arbor, MI, USA). A fibre-optic Raman Dynisco probe was implemented into the die head (Figure 5.1) [3], to monitor the MPT concentration of the melt before it is forced through the die. The laser wavelength was the 785 nm line from a 785 nm Invictus NIR diode laser. All in-line collected spectra were recorded with a resolution of 4 cm<sup>-1</sup> and an exposure time of three seconds, using a laser power of 400 mW. Spectra were collected every 15 seconds. Data collection and data transfer were automated using the HoloGRAMS™ data collection software, and the Matlab software (version 7.1, The MathWorks Inc., Natick, MA). Once an experiment was started, 15 minutes stabilization time was applied before starting

the collection of the spectra. After this, the experiments were continued for another 15 minutes, during which 60 in-line spectra were collected.

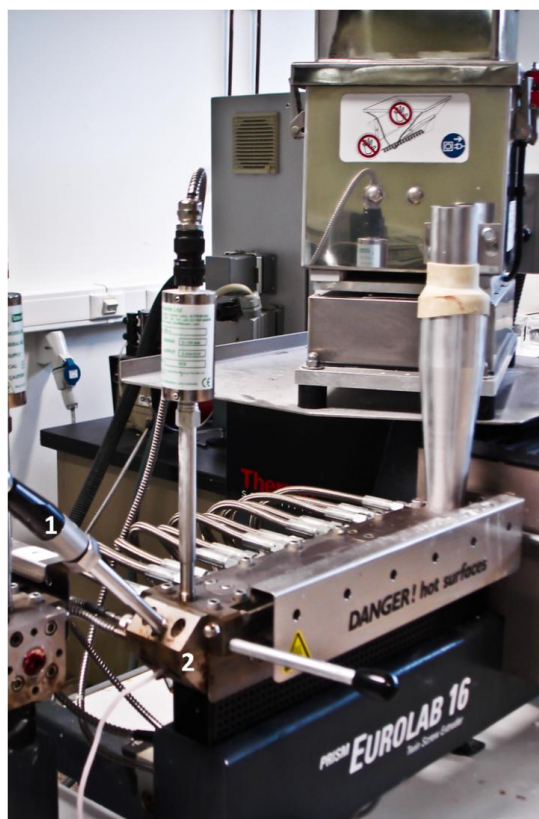


**Figure 5.1.** Experimental setup: Raman Dynisco probe (1) implemented in the die (2) of a 16 mm twin-screw extruder.

#### 5.2.4. Development of the Raman calibration models

Four different calibration models based on the Raman spectra collected during extrusion of the calibration mixtures (Table 5.1) were developed and evaluated. First, a PLS model was developed using the SIMCA P+ software (Version 12.0.1.0, Umetrics, Umeå, Sweden) (Model 1). Prior to modelling, SNV pre-processing and Savitzky-Golay smoothing were applied on the spectral range of  $0 - 1800 \text{ cm}^{-1}$  to eliminate the additive baseline offset variations and to allow noise reduction in the spectra. The PLS model was built by regressing the 300 in-line collected and preprocessed spectra (5 concentration levels x 60 spectra/concentration level) versus the actual MPT concentration values (Table 5.1).

**Table 5.1.** Composition of the calibration and validation mixtures.

<b>Calibration mixtures</b>	Metoprolol tartrate (MPT) (% w/w, theoretical)	Eudragit® RS PO (% w/w)	Magnesium stearate (% w/w)	Actual MPT concentration (% w/w)		
1	15,0	84,5	0,5	15,0141		
2	20,0	79,5	0,5	20,0090		
3	25,0	74,5	0,5	25,0072		
4	30,0	69,5	0,5	30,0077		
5	35,0	64,5	0,5	35,0025		
<b>Validation mixtures</b>	MPT (% w/w, theoretical)	Eudragit® RS PO (% w/w)	Magnesium stearate (% w/w)	Actual MPT concentration (% w/w) day 1	Actual MPT concentration (% w/w) day 2	Actual MPT concentration (% w/w) day 3
1	17,5	82,0	0,5	17,5056	17,4989	17,5078
2	22,5	77,0	0,5	22,5049	22,5049	22,5032
3	25,0	74,5	0,5	25,0037	25,0012	24,9993
4	27,5	72,0	0,5	27,4995	27,4995	27,5071
5	32,5	67,0	0,5	32,4979	32,5012	32,5023

Model 2, a PLS model as well, was not based on the original spectra collected during extrusion of the calibration mixtures, but on the averaged spectra of ten successively collected spectra. Therefore, this model was developed using 30 spectra (5 concentration levels x 6 averaged spectra/concentration level). No official regulations on sample size for extrusion processes exist, but the FDA guidance on content uniformity [9] states that sample quantities larger than three times the dosage unit range can only be used with an adequate scientific justification. The amount of MPT passing the probe window during one measurement (three seconds) in the mixture with the highest MPT concentration (i.e. 35% w/w), at a throughput of 0.3 kg/h is 87.5 mg. Since the unit dosage is 200 mg, and the Raman signal does not penetrate the entire melt volume, the combination of ten spectra does not exceed this limit.

For a third predictive model (Model 3), multivariate curve resolution (MCR) was applied, using the HoloREACT<sup>TM</sup> reaction analysis and profiling software (Kaiser Optical Systems, Ann Arbor, MI, USA). In MCR, a two-way data matrix  $D$  ( $m \times n$ ) is decomposed into two matrices  $C$  ( $m \times k$ ) and  $S^T$  ( $k \times n$ ), containing the pure concentration profiles for each modelled component in the system and the corresponding pure spectra of the  $k$  species of the unknown mixture, respectively [10]. This decomposition is performed according to Eq. (5.1):

$$D = C S^T + E \quad (5.1)$$

Where  $E$  ( $m \times n$ ) is the error matrix containing the residual variation. Before analysis, a baseline correction and normalization were applied on two spectral ranges. The first range, 1600 -1630  $\text{cm}^{-1}$ , represents a peak specific for MPT, and the second range from 1710 – 1750  $\text{cm}^{-1}$  contains a peak for Eudragit<sup>®</sup> RS PO. Next, a model based on the MCR scores of the MPT peak from 300 spectra (5 concentration levels x 60 spectra/ concentration level) versus the actual MPT concentration, was developed. The same approach was used to develop Model 4, but using the average spectra of ten successively collected spectra.

### 5.2.5. Validation of the Raman method and estimation of its uncertainty

The strategy suggested by the SFSTP [7, 8, 11, 12] was applied for validation of the developed calibration models. The main objective of this commission was the harmonization of approaches for the validation of quantitative analytical procedures. The objective of validation is to guarantee that the difference between every single measurement ( $x_i$ ), which will be performed in routine analysis, and the unknown true value of the sample ( $\mu_T$ ) will be lower than an acceptable limit ( $\lambda$ ) [7] (Eq. (5.2)):

$$|x_i - \mu_T| < \lambda \quad (5.2)$$

For this particular analytical procedure,  $\lambda$  was set at 10%. A procedure is qualified as acceptable when it can assure that the probability (Eq. (5.3)) that measurements will fall outside the preset acceptance limits is less or equal to the risk that the analyst is able to take during routine use:

$$P(|x_i - \mu_T| < \lambda) \geq \beta \quad (5.3)$$

with  $\beta$  being the proportion of measurements inside the acceptance limits. The expected proportion of measurements falling outside the acceptance limits evaluates the risk of an analytical procedure. In this study, the desired proportion of measurements found within the acceptance limits was set at 95%.

The MPT concentration levels of the validation samples are overviewed in Table 5.1, and the mean concentrations as calculated by the four different models are shown in Table 5.2. Each validation mixture was extruded on three different days by two operators, accounting for the inter-day and operator variation. Problems occurred during extrusion of the validation mixture with a 32.5% (w/w) MPT concentration on the third day, caused by a defect in the temperature monitoring device. Therefore, these spectral data were excluded from the data analysis.

**Table 5.2.** Mean predicted MPT concentrations (% w/w).

MPT concentration (% w/w)	Actual MPT concentration (% w/w)	Mean predicted MPT concentration (% w/w) Model 1	Mean predicted MPT concentration (% w/w) Model 2	Mean predicted MPT concentration (% w/w) Model 3	Mean predicted MPT concentration (% w/w) Model 4
17,5 - day 1	17,5056	13,6026	13,7674	16,2110	17,0442
17,5 - day 2	17,4989	14,8947	14,8176	18,0945	17,6324
17,5 - day 3	17,5078	15,0605	15,2321	17,9913	17,7284
22,5 - day 1	22,5049	20,7349	21,0132	20,9911	22,0764
22,5 - day 2	22,5049	21,6028	21,7217	21,3559	21,7461
22,5 - day 3	22,5032	19,5813	19,8187	22,3763	21,4988
25,0 - day 1	25,0037	21,7440	22,0244	23,3160	23,4095
25,0 - day 2	25,0012	23,1770	23,4599	23,8353	24,2815
25,0 - day 3	24,9993	22,9997	23,2904	24,0506	24,0160
27,5 - day 1	27,4995	25,0717	25,3138	25,0914	25,3532
27,5 - day 2	27,4995	27,7401	27,7172	27,8007	26,8305
27,5 - day 3	27,5071	27,5212	27,6717	27,1136	27,0039
32,5 - day 1	32,4979	31,4534	31,6651	31,7784	32,1468
32,5 - day 2	32,5012	33,1504	33,3448	33,8719	32,9962



The objective of validation is to evaluate the risks or confidences that every single measurement that will be performed, will be close enough to the unknown true value of the sample. Therefore, the determination of trueness, precision, linearity and other validation criteria is not sufficient to provide these guarantees. The adapted decision tool was the accuracy profile of the analytical procedure based on the  $\beta$ -expectation tolerance interval and the concept of total error (bias + standard deviation). Every analytical method is characterized by a systematic error or true bias and a random error or true variance (measured by a standard deviation) [7]. Both these parameters are inherent of the analytical method and always unknown as well as the true value. The accuracy profile of a method is acquired by calculating the  $\beta$ -expectation tolerance interval at every concentration level [13], and is used to decide whether the analytical procedure is considered as valid or not [8].

The variance used to estimate the  $\beta$ -expectation tolerance interval is equal to the sum of the total variance of the method plus the variance of the bias. The standard deviation of the  $\beta$ -expectation tolerance interval can be used as an estimate of the standard uncertainty in the measurements. Using the data collected for the development of the accuracy profile, the measurement uncertainty was estimated [14]. The uncertainty is defined as a parameter associated with the result of a measurement, which characterizes the dispersion of the values that could reasonably be attributed to the measurand [15].

#### **5.2.6. Evaluation of the robustness of the Raman calibration models**

Finally, a robustness testing design was created with the MODDE software (version 9.1.0.0, Umetrics, Umeå, Sweden) to evaluate whether the performance of the quantification method is sensitive to small fluctuations in process settings. The factors throughput, screw speed and barrel temperature were varied during extrusion of a physical mixture containing 25% MPT, 74.5% Eudragit® RS PO and 0.5% Mg St (w/w). The robustness testing design used was a linear  $2^{3-1}+3$  fractional factorial design (resolution III) (Table 5.3). The factor levels were chosen by considering which changes may occur in the laboratory. The responses used in these designs were the MPT concentrations predicted by the developed models. The ideal result in a robustness testing study is identical response values for each trial [16]. The significance and lack of fit of the robustness design models were assessed via an F-test, to

evaluate the robustness of the responses. The robustness testing design was performed for Model 4, which delivered the best accuracy profile.

**Table 5.3.** Robustness design.

Experiment number	Run Order	Throughput (kg/h)	Screw speed (rpm)	Temperature (°C)
1	7	0,275	70	70-144-144-144-144-120
2	4	0,325	70	70-140-140-140-140-120
3	5	0,275	90	70-140-140-140-140-120
4	1	0,325	90	70-144-144-144-144-120
5	3	0,3	80	70-142-142-142-142-120
6	6	0,3	80	70-142-142-142-142-120
7	2	0,3	80	70-142-142-142-142-120

## 5.3. RESULTS AND DISCUSSION

### 5.3.1. Development of the Raman calibration models

For the development of Model 1, the first predictive model for MPT concentration monitoring, all in-line collected preprocessed Raman spectra (300 spectra in total) (X) were regressed versus the actual MPT concentrations (Y). Two principal components were chosen, since the goodness of prediction of the model ( $Q^2 = 0.993$ ) did not improve significantly when adding extra components. The scores and loading plot for the first principal component ( $R^2 = 0.937$ ) confirm that this component represents the variation in the Raman spectra caused by the difference in MPT concentration level in the calibration mixtures (Figure 5.2). Positive peaks in the loading of the first component correspond to MPT-peaks, whereas the negative peaks belong to the polymer. A higher PC 1 score value therefore indicates a higher MPT concentration. The RMSECV of this two-component PLS model is 0.61% (w/w). The predictive performance of this model was evaluated by calculating the MPT concentrations for the spectra collected during extrusion of all validation mixtures. This resulted in an RMSEP value of 2.28% (w/w).

A second PLS model, referred to as Model 2 in section 5.2.4., was developed using the averaged spectra collected during extrusion of the calibration mixtures. A two-component model was developed ( $Q^2 = 0.994$ ), and the first principal component ( $R^2 = 0.941$ ) captured the variation in the Raman spectra originating from concentration level differences in the calibration mixtures. The RMSECV of this two-component PLS model was 0.57% (w/w). The predictive performance of the model was evaluated by calculating the MPT concentrations for the averaged spectra collected during extrusion of all validation mixtures. This resulted in an RMSEP value of 2.09% (w/w).

Models 3 and 4 are calibration models based on the MCR scores for one MPT peak ( $1600 - 1630 \text{ cm}^{-1}$ ) from the original (300) and averaged (30) spectra, respectively. Linear regression of these MPT scores resulted in an  $R^2$  of 0.95 and 0.99, and an RMSEP of 1.57% and 1.09% (w/w) for Models 3 and 4, respectively.

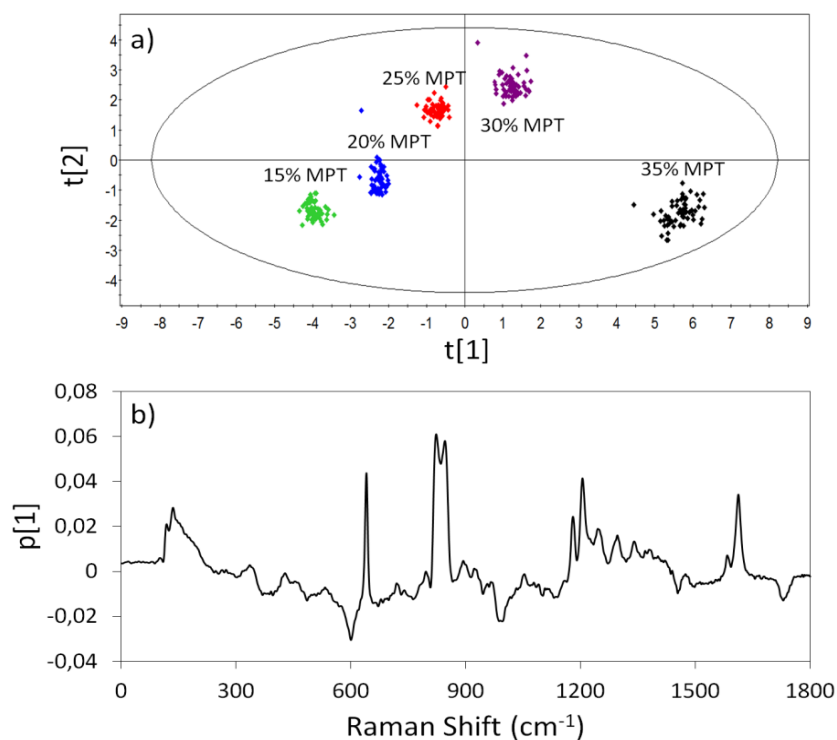


**Figure 5.2.** a) PC 1 versus PC 2 scores scatterplots of in-line collected Raman spectra during extrusion of the calibration mixtures and b) loading plot of the first principal component.

### 5.3.2. Validation of the Raman method and estimation of its uncertainty

The MPT concentration of the validation mixtures was predicted during extrusion, using the four developed calibration models. The mean calculated concentrations for each model are presented in Table 5.2. Since the introduced MPT concentrations for each concentration level differed slightly, an alignment on the concentration level was performed prior to data analysis. For each validation concentration level, trueness, precision, and  $\beta$ -expectation tolerance intervals were calculated (Table 5.4) and the linearity was assessed (Table 5.4 and Figure 5.3). The specificity of the method was demonstrated by the loadings of PC 1 (Figure 5.2b), which clearly showed that the largest source of variation (93.7%) in the in-line collected Raman spectra is related to changes in MPT concentration. For all four models, a linear relation between the introduced MPT concentration and the MPT concentration as calculated by the model was found, and the  $R^2$  values (Figure 5.3) all approach 1. The calculated values for precision (Table 5.4) show that the results for intermediate precision are equal to or worse than the repeatability results for all MPT concentration levels in all applied calibration models. The intermediate precision comprises both the variability caused

by the extrusion of the validation mixtures on different days, and the fact that the experiments were performed by two different operators. This difference between repeatability and intermediate precision indicates that the inter-day variability in the dataset is larger than the within-day variability, which is caused by an operator or day effect. Regarding the operator effect, each operator might for instance fixate the Raman probe more tightly or loosely in the extrusion die, also causing variations in the in-line collected Raman spectra.

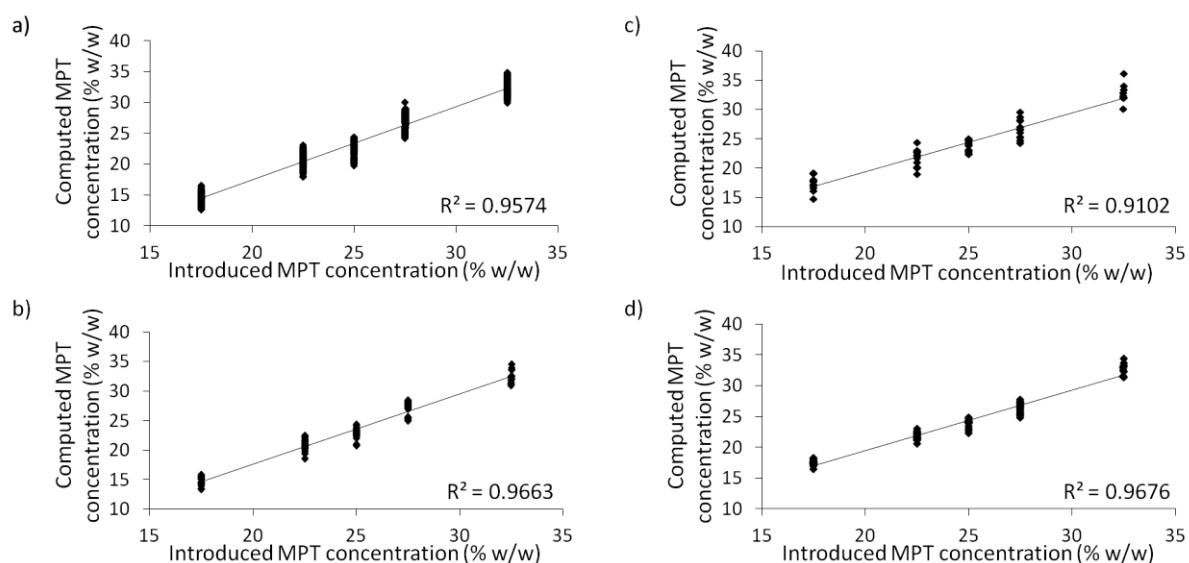


**Figure 5.3.** Assessment of linearity (computed concentration =  $f(\text{introduced concentration})$ ) for a) Model 1, b) Model 2, c) Model 3, d) Model 4.

For models 1, 2 and 3, the  $\beta$ -expectation tolerance intervals exceeded the preset acceptance limits (10% relative bias) for each of the validated concentration levels (Figure 5.4). In model 4, the only validated concentration of which the acceptance limits were exceeded by the  $\beta$ -expectation tolerance interval, is the mixture with 27.5% MPT (w/w). Table 5.2 shows that for this concentration level, the mean predicted concentration for Model 4 is much lower on day 1, 25.3532% MPT, than on day 2 and 3, 26.8305% MPT and 27.0039% MPT (w/w) respectively. The Raman spectra collected on this day showed larger background signal variations than on day 2 and 3, which might cause the larger error in prediction of the MPT concentration. However, a clear cause for these background variations was not found. When the data from day 1 were excluded from the accuracy profile calculations, the  $\beta$ -expectation tolerance intervals for all validated concentrations remained within the

acceptance limits of 10% (Figure 5.5). Thus the entire accuracy profile, created after connecting the upper and lower tolerance limits for the validated concentration levels in order to interpolate the behaviour of the limits for the entire method range, was found within the preset acceptance limit. This indicates that, for at least 95 out of 100 future routine measurements, the predicted concentrations will be included within the acceptance limits.

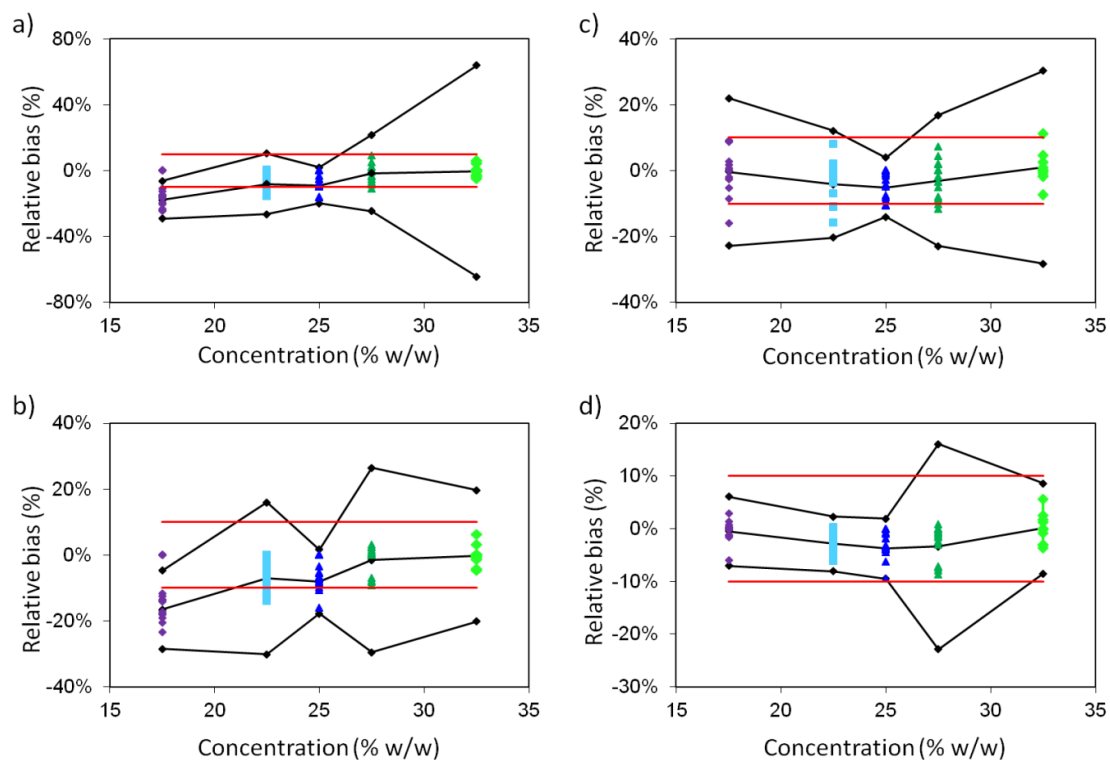


**Figure 5.4.** Accuracy profiles for a) Model 1, b) Model 2, c) Model 3, d) Model 4. The red lines represent the acceptance limits which were set at 10% relative bias.

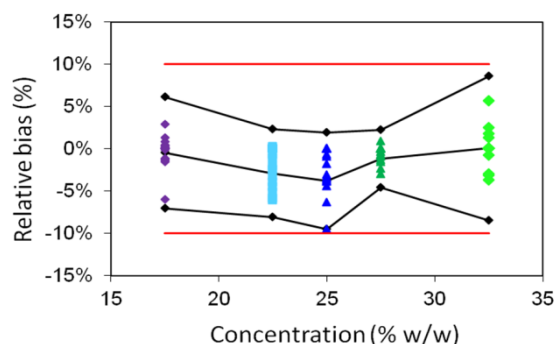


**Figure 5.5.** Accuracy profile for Model 4, with exclusion of the spectra collected during extrusion of the validation mixture with 27.5% MPT (w/w) on day 1. The red lines represent the acceptance limits which were set at 10% relative bias.

**Table 5.4.** Validation parameters for each calibration model: trueness, precision, accuracy and linearity.

<b>Trueness</b>	<b>Model 1</b>		<b>Model 2</b>		<b>Model 3</b>		<b>Model 4</b>	
MPT concentration (% w/w)	Relative bias (%)	Recovery (%)	Relative bias (%)	Recovery (%)	Relative bias (%)	Recovery (%)	Relative bias (%)	Recovery (%)
17,50	-17,05	82,95	-16,56	83,44	-0,41	99,59	-0,20	99,80
22,50	-8,29	91,71	-7,35	92,65	-4,13	95,87	-3,18	96,82
25,00	-9,45	90,55	-8,31	91,69	-5,07	94,93	-4,40	95,60
27,50	-2,63	97,37	-2,19	97,81	-3,03	96,97	-4,02	95,98
32,50	-0,61	99,39	0,02	100,02	1,00	101,00	0,22	100,22
<b>Precision</b>	<b>Model 1</b>		<b>Model 2</b>		<b>Model 3</b>		<b>Model 4</b>	
MPT concentration (% w/w)	Repeatability standard deviation (%)	Intermediate precision standard deviation (%)	Repeatability standard deviation (%)	Intermediate precision standard deviation (%)	Repeatability standard deviation (%)	Intermediate precision standard deviation (%)	Repeatability standard deviation (%)	Intermediate precision standard deviation (%)
17,50	4,98	5,64	3,04	4,63	6,03	8,02	1,71	2,34
22,50	3,41	5,66	2,47	5,11	7,30	7,30	2,31	2,31
25,00	3,63	4,55	2,72	3,74	4,09	4,09	2,37	2,49
27,50	3,97	6,64	1,06	5,74	4,78	6,71	1,08	4,09
32,50	2,56	4,32	2,96	4,07	4,48	5,94	3,29	3,29

**Table 5.4.** Validation parameters for each calibration model: trueness, precision, accuracy and linearity (continued).

<b>Accuracy</b>	<b>Model 1</b>	<b>Model 2</b>	<b>Model 3</b>	<b>Model 4</b>
MPT concentration (% w/w)	$\beta$ -expectation tolerance limits (%)	$\beta$ -expectation tolerance limits (%)	$\beta$ -expectation tolerance limits (%)	$\beta$ -expectation tolerance limits (%)
17,50	[-29,19; -6,38]	[-28,46; -4,72]	[-22,82; 22,00]	[-7,04; 6,10]
22,50	[-26,54; 10,39]	[-30,13; 15,97]	[-20,35; 12,09]	[-8,08; 2,31]
25,00	[-19,95; 2,02]	[-17,71; 1,65]	[-14,07; 3,93]	[-9,47; 1,94]
27,50	[-24,69; 21,77]	[-29,50; 26,47]	[-22,86; 16,80]	[-22,857; 16,10]
32,50	[-64,34; 63,85]	[-20,17; 19,47]	[-28,30; 30,30]	[-8,49; 8,62]
<b>Linearity</b>	<b>Model 1</b>	<b>Model 2</b>	<b>Model 3</b>	<b>Model 4</b>
R <sup>2</sup>	0,9574	0,9663	0,9102	0,9676
Intercept	-6,4101	-6,3373	-0,8193	-0,1888
Slope	1,1914	1,1957	1,0082	0,9821



**Table 5.5.** Estimates of the different uncertainties for each level of the accuracy profile in each calibration model.

	MPT concentration level (% w/w)	Uncertainty of the bias (% w/w)	Uncertainty (% w/w)	Expanded uncertainty (% w/w)	Relative expanded uncertainty (%)
<b>Model 1</b>	17,5	0,30	0,87	1,79	9,89
	22,5	0,58	1,31	2,61	11,60
	25,0	0,43	1,12	2,25	8,98
	27,5	0,89	2,01	4,01	14,60
	32,5	0,85	1,64	3,28	10,10
<b>Model 2</b>	17,5	0,32	0,75	1,50	8,55
	22,5	0,56	1,21	2,41	10,72
	25,0	0,38	0,94	1,88	7,53
	27,5	0,89	1,79	3,58	13,00
	32,5	0,73	1,51	3,01	9,30
<b>Model 3</b>	17,5	0,61	15,30	3,05	17,44
	22,5	0,45	1,64	3,28	14,56
	25,0	0,28	1,01	2,02	8,08
	27,5	0,81	1,96	3,93	14,30
	32,5	1,05	2,21	4,43	13,60
<b>Model 4</b>	17,5	0,18	0,45	0,89	5,11
	22,5	0,15	0,52	1,05	4,66
	25,0	0,20	0,63	1,26	5,05
	27,5	0,14	0,37	0,74	2,70
	32,5	0,38	1,14	2,27	7,00

According to a recent draft of guide ISO/DTS 21748 [14, 17], the measurement uncertainty can be estimated from trueness and precision (repeatability and reproducibility). Table 5.5 shows the estimates for the uncertainty of bias, the uncertainty which combines the uncertainty of bias with the intermediate precision standard deviation, the expanded uncertainty and the relative expanded uncertainty for each level of the accuracy profile in each calibration model. The expanded uncertainty defines a 95% probability interval around the mean value in which the unknown true value is found. The relative expanded uncertainty is the expanded uncertainty divided with the corresponding introduced concentration [15]. For Model 4, the relative expanded uncertainty was not higher than 7.00% (after exclusion of the data generated during extrusion of the validation mixture containing 32.5% MPT (w/w) on day 1). This demonstrates that with a confidence level of 95%, the unknown true value is found at a maximum of  $\pm 7.00\%$  around the measured result.

### 5.3.3. Evaluation of the robustness of the Raman calibration models

Since Model 4, based on the averaged Raman spectra and developed with MCR resulted in the best accuracy profile, the robustness was only assessed for this model. During robustness testing, the sensitivity of the responses to small changes in the factors was determined. A physical mixture containing 25% MPT, 74.5% Eudragit<sup>®</sup> RS PO and 0.5% Mg St (w/w) was extruded according to a linear  $2^{3-1}+3$  fractional factorial design, where the effects of small changes in barrel temperature (140 – 144°C), throughput (0.275 – 0.325 kg/h) and screw speed (70 – 90 rpm) on the predicted MPT concentration (response) were evaluated (Table 5.3).

The model parameters of interest for robustness evaluation are listed in Table 5.6. An ideal result is a  $Q^2$  near zero, indicating a weak relationship between the factors and the response. Model 4 resulted in a  $Q^2$  of -0.2, demonstrating that the response, i.e. the predicted MPT concentration, was robust. A negative  $Q^2$  suggests a very poor model. Besides the calculation of  $Q^2$ , two F-tests were performed. The first F-test, the regression model significance test, was used to determine whether the modellable variation in the dataset is larger than the residual variation. When  $p_1$  is smaller than 0.05, the variance

explained by the model is larger than the unexplained variance, and the model is significant [18]. For Model 4, the  $p_1$  value exceeded the 0.05 reference value, indicating that the model was insignificant. A second F-test, the lack of fit test, compared the model error (the fact that the model is imperfect) to the replicate error (presence of variation when performing replicate experiments) [18]. A  $p_2$  value higher than the reference value of 0.05, indicates that both errors are small and of the same magnitude.  $p_2$  is 0.050 for model 4, demonstrating that it showed (or bordered on) lack of fit. From these parameters, it can be concluded that there was no significant relationship between the predicted MPT concentrations and the small factor changes. Therefore, the response is robust to the applied variations in process settings.

**Table 5.6.** Model parameters of interest for robustness evaluation.

	$Q^2$	$p_1$ (Regression model significance test)	$p_2$ (Lack of fit test)
<b>Model 4</b>	-0,2	0,19	0,05

## 5.4. CONCLUSION

An in-line Raman spectroscopic method was developed and validated for the determination of the active content during pharmaceutical hot-melt extrusion, based on multivariate curve resolution modelling of the averaged in-line collected Raman spectra. The method was thoroughly validated, and showed good precision, trueness, linearity, specificity and accuracy over the applied concentration range. The accuracy profile guaranteed that 95 out of 100 future routine measurements will be included within the preset acceptance limits of 10%. The uncertainty of the measurements was assessed via the uncertainty of bias and the expanded uncertainty at each concentration level. The robustness of the response was also evaluated, and demonstrated that the determined MPT concentration was insensitive to the applied fluctuations in process settings.

## 5.5. REFERENCES

- [1] T. De Beer, A. Burggraeve, M. Fonteyne, L. Saerens, J.P. Remon, C. Vervaet, *Int J Pharm* 417 (2011) 32-47.
- [2] V.S. Tumuluri, M.S. Kemper, I.R. Lewis, S. Prodduturi, S. Majumdar, B.A. Avery, M.A. Repka, *Int J Pharm* 357 (2008) 77-84.
- [3] L. Saerens, L. Dierickx, B. Lenain, C. Vervaet, J.P. Remon, T. De Beer, *Eur J Pharm Biopharm* 77 (2011) 158-163.
- [4] C. De Bleye, P.F. Chavez, J. Mantanus, R. Marini, P. Hubert, E. Rozet, E. Ziemons, *J Pharm Biomed Anal* 60 (2012) 125-132.
- [5] International Conference on Harmonisation of Technical Requirements for Registration of Pharmaceuticals for Human Use, *Validation of Analytical Procedures: Text and Methodology Q2 (R1)*, 2005.
- [6] Food and drug administration, *Guidance for Industry (draft), Analytical Procedures and Methods Validation*, 2000.
- [7] P. Hubert, J.J. Nguyen-Huu, B. Boulanger, E. Chapuzet, P. Chiap, N. Cohen, P.A. Compagnon, W. Dewé, M. Feinberg, M. Lallier, M. Laurentie, N. Mercier, G. Muzard, C. Nivet, L. Valat, *J Pharm Biomed Anal* 32 (2004) 579-586.
- [8] P. Hubert, J.J. Nguyen-Huu, B. Boulanger, E. Chapuzet, N. Cohen, P.A. Compagnon, W. Dewé, M. Feinberg, M. Laurentie, N. Mercier, G. Muzard, L. Valat, E. Rozet, *J Pharm Biomed Anal* 45 (2007) 82-96.
- [9] Food and Drug Administration, *Guidance for Industry, Powder Blends and Finished Dosage Units - Stratified In-Process Dosage Unit Sampling and Assessment*, 2003.
- [10] C. Ruckebusch, L. Blanchet, *Anal Chim Acta* 765 (2013) 28-36.
- [11] P. Hubert, J.J. Nguyen-Huu, B. Boulanger, E. Chapuzet, P. Chiap, N. Cohen, P.A. Compagnon, W. Dewé, M. Feinberg, M. Lallier, M. Laurentie, N. Mercier, G. Muzard, C. Nivet, L. Valat, E. Rozet, *J Pharm Biomed Anal* 45 (2007) 70-81.
- [12] P. Hubert, J.J. Nguyen-Huu, B. Boulanger, E. Chapuzet, N. Cohen, P.A. Compagnon, W. Dewé, M. Feinberg, M. Laurentie, N. Mercier, G. Muzard, L. Valat, E. Rozet, *J Pharm Biomed Anal* 48 (2008) 760-771.
- [13] R.W. Mee, *Technometrics* 26 (1984) 251-253.

- [14] M. Feinberg, B. Boulanger, W. Dewé, P. Hubert, *Anal Bioanal Chem* 380 (2004) 502-514.
- [15] Eurachem/CITAC Guide CG4. Quantifying Uncertainty in Analytical Measurement, 3<sup>rd</sup> ed., 2012.
- [16] L. Eriksson, E. Johansson, N. Kettaneh-Wold, Wikström, S. Wold, Experimental objective: Robustness testing, In: *Design of Experiments: Principles and Applications*, 3<sup>rd</sup> ed., Umetrics Academy, Umeå, Sweden, 2008, p. 169-181.
- [17] ISO/DTS 21748 Guide to the use of repeatability, reproducibility and trueness estimates in measurement uncertainty estimation, ISO, Geneva, Switzerland, 2003.
- [18] L. Eriksson, E. Johansson, N. Kettaneh-Wold, Wikström, S. Wold, Analysis of Variance: ANOVA, In: *Design of Experiments: Principles and Applications*, 3<sup>rd</sup> ed., Umetrics Academy, Umeå, Sweden, 2008, p. 317-322.

# CHAPTER 6

## VISUALIZATION AND PROCESS UNDERSTANDING OF MATERIAL BEHAVIOUR IN THE EXTRUSION BARREL DURING A HOT-MELT EXTRUSION PROCESS USING RAMAN SPECTROSCOPY

Parts of this chapter are published in:

**L. Saerens**, C. Vervaet, J.P. Remon, T. De Beer. Visualization and process understanding of material behavior in the extrusion barrel during a hot-melt extrusion process using Raman spectroscopy. *Analytical Chemistry*, 85 (2013) 5420-5429.

## ABSTRACT

The aim of Chapter 6 was to improve the understanding of material behaviour in pharmaceutical hot-melt extrusion by implementing a Raman probe in each section of the barrel. FT-IR measurements were performed to confirm the Raman observations. Metoprolol tartrate (MPT) concentration (10 and 40% in Eudragit® RS PO (w/w)), extrusion temperature (100, 120 and 140°C) and screw speed (80 and 160 rpm) were varied to examine their influence on polymer/drug solid state throughout the barrel. When extruding a formulation with a 40 (w/w) MPT concentration, broadening of MPT peaks indicates melting of MPT between sections 2 and 3 of the extrusion barrel, caused by the presence of a first kneading zone. Decreasing the concentration to 10% (w/w) shows an additional spectral difference (i.e. peak shifts indicating interactions between MPT and carrier) between sections 5 and 6, due to formation of a solid solution. At a 10% MPT load (w/w), increasing the extrusion temperature does not influence the solid state or the barrel section where the final solid state is obtained. At a drug load of 40% (w/w), the solid state of the end product is reached further down the barrel when the temperature decreases. Doubling the screw speed when processing a 10% MPT (w/w) formulation does not affect the solid state of the product or the location where it is obtained. In contrast, at 40% drug load (w/w), the section where the final product is produced, is situated earlier in the barrel when a higher speed was applied. The Raman spectra provide real-time information about polymer/drug behaviour throughout the barrel, facilitating process understanding and optimisation.



# CHAPTER 6

## VISUALIZATION AND PROCESS UNDERSTANDING OF MATERIAL BEHAVIOUR IN THE EXTRUSION BARREL DURING A HOT-MELT EXTRUSION PROCESS USING RAMAN SPECTROSCOPY

---

### 6.1. INTRODUCTION

Hot-melt extrusion (HME) is one of the most widely applied processing technologies in the plastic, food and rubber industry [1]. In pharmaceutical manufacturing, HME is used to obtain formulations where (poorly soluble) drugs are embedded in polymer matrices, offering many advantages compared to conventional pharmaceutical processing techniques. This processing technique does not require water or solvents; products have a short residence time; bioavailability of poorly soluble drugs can be improved; production of formulations with controlled, sustained or targeted release is possible and HME is a continuous production process [1, 2].

Today, the pharmaceutical industry intends to move from the traditional batch processes towards continuous processes, hereby increasing process efficiency and production. Continuous processes are based on the 'one-in-one-out' principle and offer many advantages: no scale-up issues resulting in a shorter development time; possible automation of the production line; reduction of production costs; faster product release; less product variability and improved product quality [3, 4]. The currently applied quality

control methods for intermediate or end products are mainly based on time-consuming and off-line analytical techniques, and annul the advantages of continuous pharmaceutical production. Evidently, continuous in-process measurements are required to obtain a continuous production process. The ICH Q8 guideline on pharmaceutical development states that real-time control of drug product quality is recommended rather than end-product testing on limited samples of the final product [5]. Understanding the sources of variability and their impact on drug product quality provides an opportunity to minimize the need for end product testing.

Thermal stability of the individual compounds is a requirement for hot-melt extrusion, although not all thermolabile compounds are excluded because of the short residence times in the extrusion barrel. Another drawback of the hot-melt extrusion technology is related to the high energy input from the shear forces in the extrusion barrel, leading to higher, uncontrolled product temperatures, which could induce drug or polymer degradation, having a significant impact on the product quality [1, 2]. This setback can be overcome by adjusting the process parameters as well as the screw design and die, which requires a thorough process understanding. Sufficient process understanding can be generated by implementing PAT tools such as Raman spectroscopy, allowing the visualization of the materials in the process environment and linking these observations to applied process and formulation parameters. Appropriate custom made fibre optic probes connected to the spectrometer can be implemented into the HME equipment [6]. In-die monitoring of formulation parameters such as drug load and solid state during a pharmaceutical hot-melt extrusion process, has already been demonstrated using Raman spectroscopy [7] and NIR spectroscopy [8]. By using Raman spectroscopy along the extruder barrel, physical and chemical properties of the melt throughout the entire barrel can be examined. This will be demonstrated in this chapter.

The in-barrel monitoring of melt characteristics and behaviour during twin-screw extrusion (TSE) has not yet been reported for pharmaceutical hot-melt extrusion processes, but has been investigated in the field of polymer extrusion. An ultrasound in-line monitoring system was used to investigate the melting behaviour of linear low density polyethylene and polyvinyl chloride compounds in an intermeshing counter-rotating twin-screw extruder [9].

Monitoring of the ultrasound wave attenuation allowed characterization of the melting process and uniformity across the screw channels. Various melting phenomena were described depending on the selected materials, processing conditions and screw configurations. An on-line capillary rheometer was used to measure the rheological response of a 12 wt-% polypropylene-based carbon fibre composite after melting in an intermeshing co-rotating twin-screw extruder [10]. The recorded torque was used to determine the apparent wall shear stress, which is used to calculate the true values for wall shear rate and stress. The linear viscoelastic behaviour of linear low-density polyethylene (LLDPE) was measured on-line with an oscillatory rheometer [11]. Rheological measurements are sensitive to composition, morphology, degree of mixing and temperature. Finally, determination of the residence time distribution along a kneading block has been performed by on-line monitoring of the light emission of a fluorescent tracer at several locations along the extruder [12]. Concentration versus time curves were generated to characterize the residence time distribution along a mixing block with staggered kneading disks in a twin-screw extruder.

To allow the optimization and to improve the understanding of a pharmaceutical hot-melt extrusion process, all process and formulation variables must be considered in combination with the behaviour of the melt in the different extruder sections. So far, the majority of the PAT tools used in hot-melt extrusion has been inserted between the extruder barrel and the die, whereas the major material changes occur within the extruder barrel [11]. The aim of this chapter was to improve the understanding of the material behaviour in a pharmaceutical hot-melt extrusion process environment by monitoring and visualizing the polymer-drug processing throughout the entire extrusion barrel using Raman spectroscopy. Additionally, the in-line collected Raman spectra allow to assess the impact of process settings such as barrel temperature and screw speed on the interactions between polymer and drug. The spectroscopic measurements throughout the barrel might therefore help to optimize the process settings, the screw design and the barrel length required to obtain extrudates with predefined solid state properties.

## 6.2. MATERIALS AND METHODS

### 6.2.1. Materials

Metoprolol tartrate (MPT) (Esteve Quimica, Barcelona, Spain) was chosen as model drug. It has a melting temperature ( $T_m$ ) of 120°C. Eudragit® RS PO (Evonik Rohm, Germany) was used as polymer to form the matrix systems. Eudragit® RS PO is an amorphous copolymer of acrylic and methacrylic acid esters with a low content of quaternary ammonium groups, which are present as salts. It has a glass transition temperature ( $T_g$ ) of approximately 65°C. The solubility parameters of both components are 23.6 MPa<sup>½</sup> and 19.7 MPa<sup>½</sup> for MPT and Eudragit® RS PO, respectively [13]. Components with similar solubility parameters are likely to be miscible ( $\Delta\delta_t < 7$  MPa<sup>½</sup>) and components with  $\Delta\delta_t > 10$  MPa<sup>½</sup> are likely to be immiscible. As the difference in total solubility parameter is less than 4 MPa<sup>½</sup>, a good miscibility and possible formation of a solid solution can be expected [14].

### 6.2.2. Hot-melt extrusion

Hot-melt extrusion was performed with a Prism Eurolab 16 co-rotating, fully intermeshing twin-screw extruder (Thermo Fisher Scientific, Germany). The hot-melt extruder was equipped with a DD Flexwall® 18 gravimetric feeder (Brabender® Technologie, Germany), which was set in its gravimetric feeding mode and supplied the physical mixtures with a throughput of 0.3 kg/h. The applied screw configuration is shown in Figure 6.1. The screws consist of three kneading blocks, surrounded by transport zones. The kneading elements are required for intensive mixing [15], both distributive and dispersive, since they retain the melt in the extruder for a longer period under intense shear. Furthermore, they also play a key role in transforming the drug from its crystalline to its amorphous form [16]. The first kneading block, located in sections 2 and 3, contains five kneading elements at a 30° angle towards each other, three elements at a 60° angle and finally four elements at a 90° angle. The second, smaller kneading block, in section 4 has only three elements at a 30° angle followed by one element at a 60° angle. The final, third kneading element, situated in

sections 5 and 6, consists of three kneading elements at a 30° angle, three elements at a 60° angle and finally 6 elements at a 90° angle.

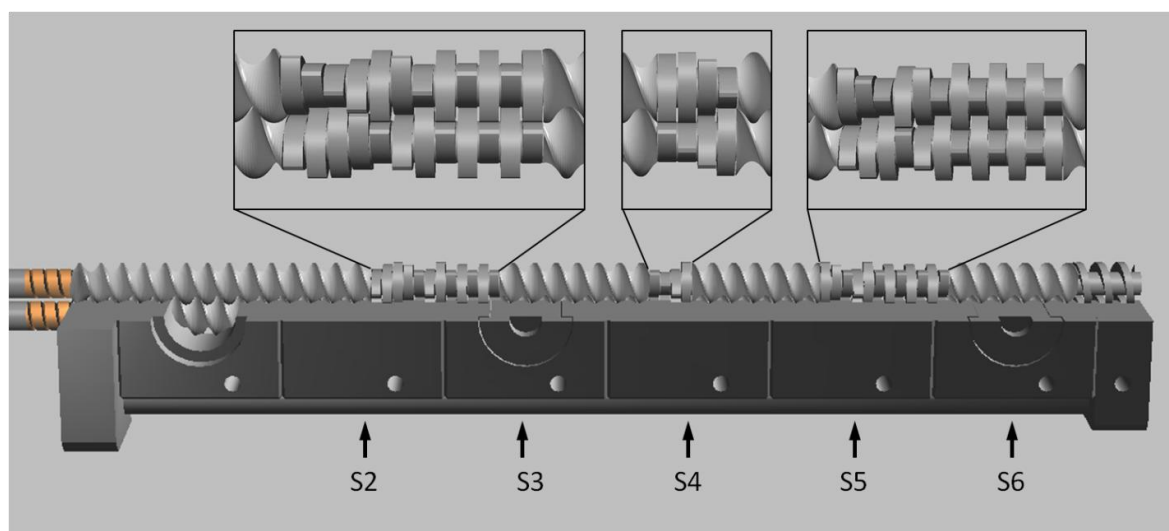


**Figure 6.1.** Applied screw configuration. The arrows indicate the insert positions of the Raman probe.

The extruder has a modular design with 6 sections (S) (one feeding zone and 5 barrel sections, Figure 6.1) and a die. The temperature of each section can be controlled separately, with exception of the feeding zone. MPT concentration (10 and 40% w/w), barrel temperature (120 and 140°C, and 100 and 140°C for 10% and 40% MPT (w/w), respectively) and screw speed (80 and 160 rpm) were varied during hot-melt extrusion (Table 6.1). The temperature of barrel section 2 was kept constant at 70°C to prevent sticking of the physical mixture in the feed zone. Each physical mixture was extruded for 25 minutes, where the first 10 min were process stabilization time, followed by 15 minutes of in-line Raman monitoring.

### 6.2.3. Raman spectroscopy

Raman spectra were collected with a Raman Rxn1 spectrometer (Kaiser Optical Systems, Ann Arbor, MI, USA). A fibre-optic Raman Dynisco probe was built into each of the 5 free barrel sections (Figure 6.2), to monitor the physicochemical state of the melt and to understand the polymer-drug behaviour throughout the entire extruder barrel during extrusion. The diameter of this probe at interface point is 7.7 mm, and the diameter of the laser beam on the sample surface is approximately 100 micron. The laser wavelength was

the 785 nm line from a 785 nm Invictus NIR diode laser. All spectra were recorded with a resolution of  $4\text{ cm}^{-1}$  and an exposure time of two seconds, using a laser power of 400 mW. The Raman spectra were acquired in dynamic mode. When determining the acquisition time of one spectrum, the signal intensity (and noise) of the sample and the amount of material passing by the probe window during this exposure time should be considered. At two seconds, the acquisition time is long enough to obtain sufficient signal intensity and at the same time short enough to avoid large amounts of material passing by the probe window. Spectra were collected every 20 seconds. The analyzed spectral region was  $100 - 1800\text{ cm}^{-1}$ , since this region contains all useful drug and polymer information. Data collection and data transfer were automated using the HoloGRAMS<sup>TM</sup> data collection software, the HoloREACT<sup>TM</sup> reaction analysis and profiling software and the Matlab software (version 7.1, The MathWorks Inc., Natick, MA).

**Table 6.1.** Extrusion experiments.

Experiment number	Metoprolol tartrate (% w/w)	Eudragit <sup>®</sup> RS PO (% w/w)	Barrel temperature profile S2-S3-S4-S5-S6-Die (°C)	Screw speed (rpm)
1	10	90	70-120-120-120-120-120	80
2	10	90	70-140-140-140-140-140	80
3	10	90	70-120-120-120-120-120	160
4	10	90	70-140-140-140-140-140	160
5	40	60	70-100-100-100-100-100	80
6	40	60	70-140-140-140-140-140	80
7	40	60	70-100-100-100-100-100	160
8	40	60	70-140-140-140-140-140	160

Data analysis was performed using SIMCA P+ (Version 12.0.1.0, Umetrics, Umeå, Sweden). Standard normal variate (SNV) pre-processing was applied on the in-line collected spectra before principal components analysis (PCA), to remove undesirable scatter effects which could be caused by the variation in the angle of incidence from the laser light, and the varying probe-sample distance due to the rotating screws. Twenty subsequent spectra of

each extrusion experiment (Table 6.1) were selected for PCA. Once an experiment was started, a period of 15 minutes was allowed for stabilization of the process. The residence time of this formulation is shorter than ten minutes, indicating that the 20 succeeding spectra were collected when the process was stable.

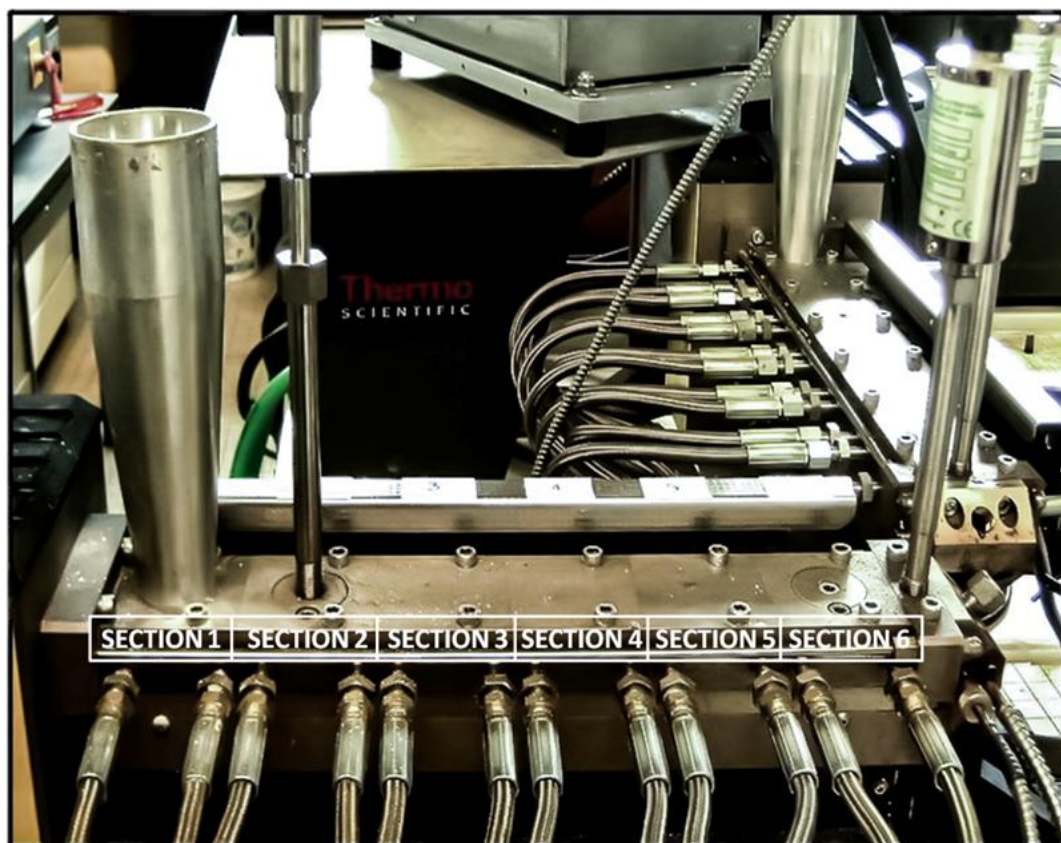


Figure 6.2. Experimental setup with Raman Dynisco probe mounted in section 2.

#### 6.2.4. Fourier transform infrared spectroscopy (FT-IR)

To confirm the in-line Raman observations, samples were collected for off-line analysis by pausing the extrusion operation, opening the extrusion barrel and collecting the samples from the screws at the position where the Raman probe is inserted in the barrel. FT-IR was selected to confirm the crystallinity of the collected samples. FT-IR measurements were performed with a Bruker Vertex 70 FT-IR spectrometer, equipped with a DTGS detector and a PIKE accessory, equipped with a diamond ATR crystal.

### **6.2.5. Differential scanning calorimetry (DSC)**

Differential scanning calorimetry was performed with a DSC Q 2000 (TA Instruments, Belgium). The thermograms were produced with the Thermal Advantage Release 5.1.2 software and analysed with TA Instruments Universal Analysis 2000 4.7A (TA Instruments, Belgium). Hermetically sealed aluminium pans (TA Instruments, Belgium) were filled with the samples collected from every barrel section. Measurements were carried out in a nitrogen atmosphere. The flow rate of dry nitrogen gas was 50 mL/min. Temperature and enthalpic calibration was performed using indium as standard. Samples were subjected to three cycles. First, the pans were heated with a heating rate of 10,0°C/min from -30°C up to 140°C in the first heating cycle. After heating, a cooling cycle was started with a cooling rate of -10,0°C/min to -30°C, followed by a second and final heating cycle which was identical to the first.



### 6.3. RESULTS AND DISCUSSION

Raman spectra collected during extrusion provide information regarding the physicochemical state of the polymer-drug melt and the interactions that occur during processing [7]. Broadening of the spectral MPT bands indicates the transition from its crystalline state, usually represented by sharp and well defined peaks in the Raman spectrum, to its amorphous form. Peak shifts in Raman spectra collected during extrusion compared to the spectrum of the physical mixture, are indicative of interactions between MPT and Eudragit® RS PO.

#### 6.3.1. Influence of MPT concentration on the solid state of the extrudates

Principal component analysis was applied on the dataset containing the in-line collected Raman spectra from all extrusion experiments (800 spectra: 20 spectra per experiment per section, 8 experiments, Table 6.1). The loadings of principal component 1 (PC 1) show that PC 1 distinguishes between the background signals from the probe itself and the signals from the formulation (65% of the total spectral variation) (Figure 6.3a). In TSE, most screw elements are not completely filled with material, since TSE is a starve-fed process. The background signal from the probe itself contains three peaks, at  $418\text{ cm}^{-1}$ ,  $577\text{ cm}^{-1}$  and  $750\text{ cm}^{-1}$ , with a rather low intensity. These three peaks will be overwhelmed by the spectrum of the formulation when the sapphire window of the probe is completely covered by material. However, when parts of the sapphire window do not contain material or when the distance between this window and the sample increases, these three peaks appear in the collected Raman spectra with varying intensity dependent on the percentage of fill of the screw element where measurements were performed. In Figure 6.3b, the average spectra of the Raman spectra collected during extrusion of mixtures with 40% MPT (w/w) at  $140^{\circ}\text{C}$  with a screw speed of 160 rpm in S2 and S6 are shown. The increased level of filling in S6 can be distinguished from the loss of intensity of the peaks specific for the Raman probe (indicated by the arrows), whereas the intensity of the peaks representing Eudragit® RS PO and MPT at  $600\text{ cm}^{-1}$  and  $640\text{ cm}^{-1}$  respectively, remains constant.

The second principal component (PC 2, capturing 16% of the total variation) describes the spectral variation originating from the different applied MPT concentrations during the experiments (Figure 6.4). In the loading of PC 2, all positive peaks represent Raman peaks originating from MPT, and the negative bands can be found as peaks in the Raman spectrum of Eudragit® RS PO. The higher the score value in PC 2, the more MPT is present in the extruded mixtures. To eliminate this overwhelming concentration-dependent spectral variation when examining differences in polymer/drug solid state, the spectra collected during the experiments with different concentration levels are analyzed separately.

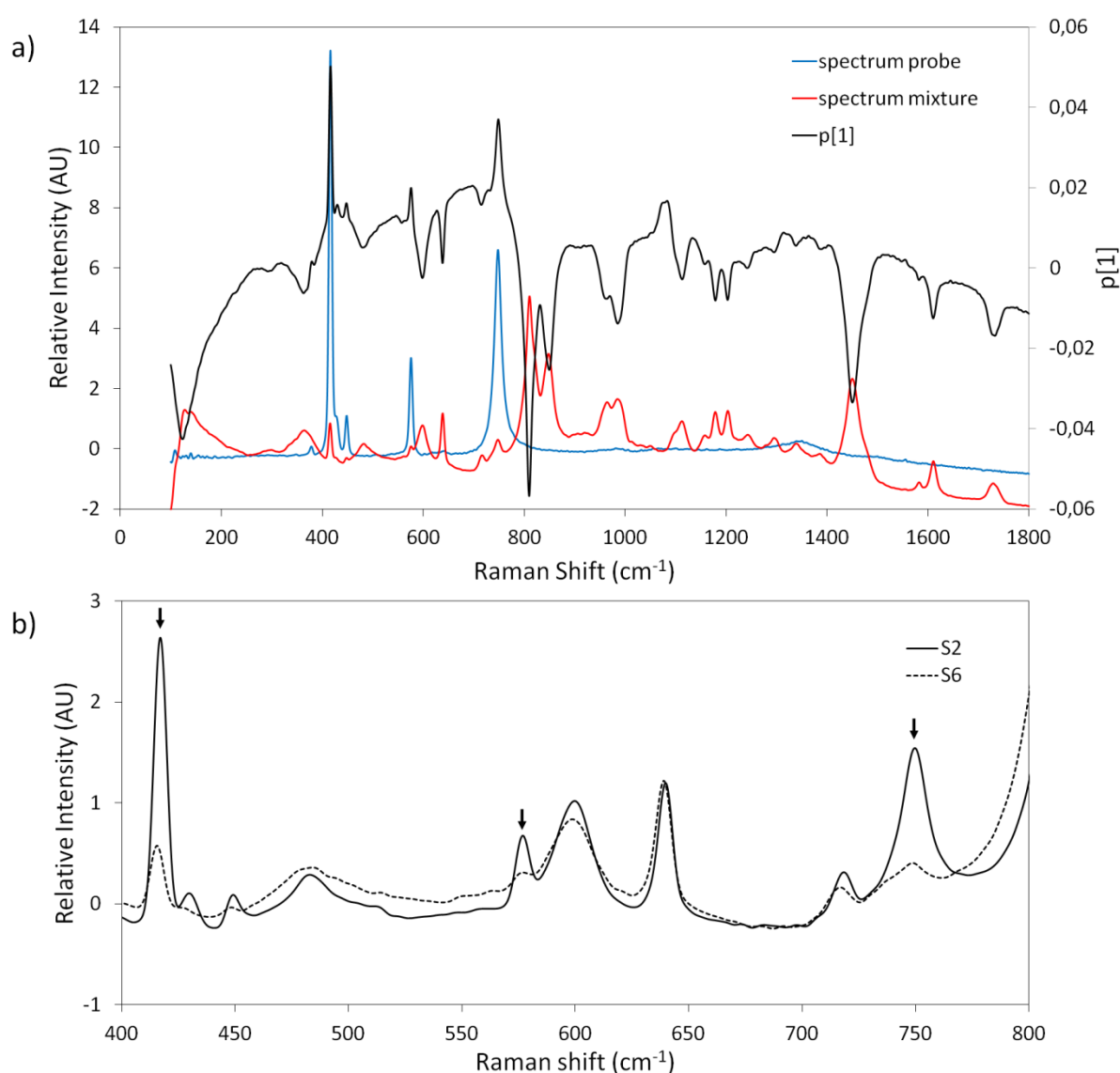


**Figure 6.3.** a) Comparison of the PC 1 loading, the spectrum inherent to the probe and the spectrum of the Eudragit® RS PO – MPT mixture. b) mean Raman spectra collected during extrusion of a mixture with 40% MPT (w/w) at 140°C and with 160 rpm in segments 2 and 6.

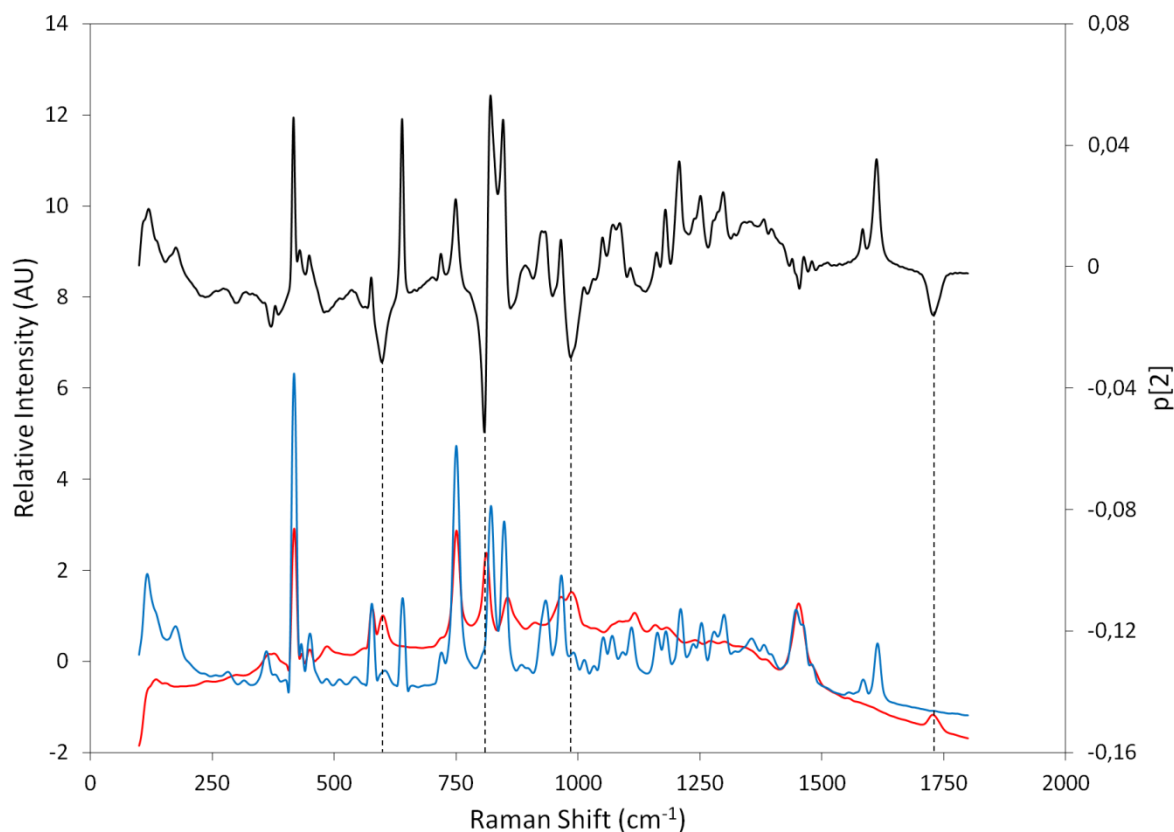


**Figure 6.4.** Comparison of the loading from the second principal component (black) and the spectra of pure Eudragit® RS PO (red) and MPT (blue).

Figures 6.5a and 6.5b show the PC 1 versus PC 2 scores scatterplot of the Raman spectra collected during the extrusion experiments with a drug load of 10% (w/w) (experiments 1 to 4, Table 6.1) and 40% MPT (w/w) (experiments 5 to 8, Table 6.1), respectively. PC 1 captures the variation in the Raman spectra caused by differences in degree of filling in the screw elements. This component describes 76% of the total spectral variation of the 40% MPT (w/w) spectra and 78% of the total variation of the 10% MPT (w/w) spectra. PC 2, representing 13% of the variation of both the 40% MPT (w/w) spectra and 10% MPT (w/w) spectra, explains the spectral differences in the solid state of MPT (Figure 6.6). In this figure, the PC 2 loading is compared to the mean spectra collected in sections 2 and 6 during an extrusion experiment of a mixture with a drug load of 40% (w/w), at a temperature of 100°C and with a screw speed of 160 rpm (Table 6.1, experiment 7). Positive peaks in this loading represent MPT in its crystalline form, and can be found in the spectra gathered in section 2, where the Raman probe is still collecting spectra of the physical mixture. The sharp negative

peaks represent the amorphous MPT that has interacted with the polymer, causing peak shifts in the spectra of section 6 compared to section 2.

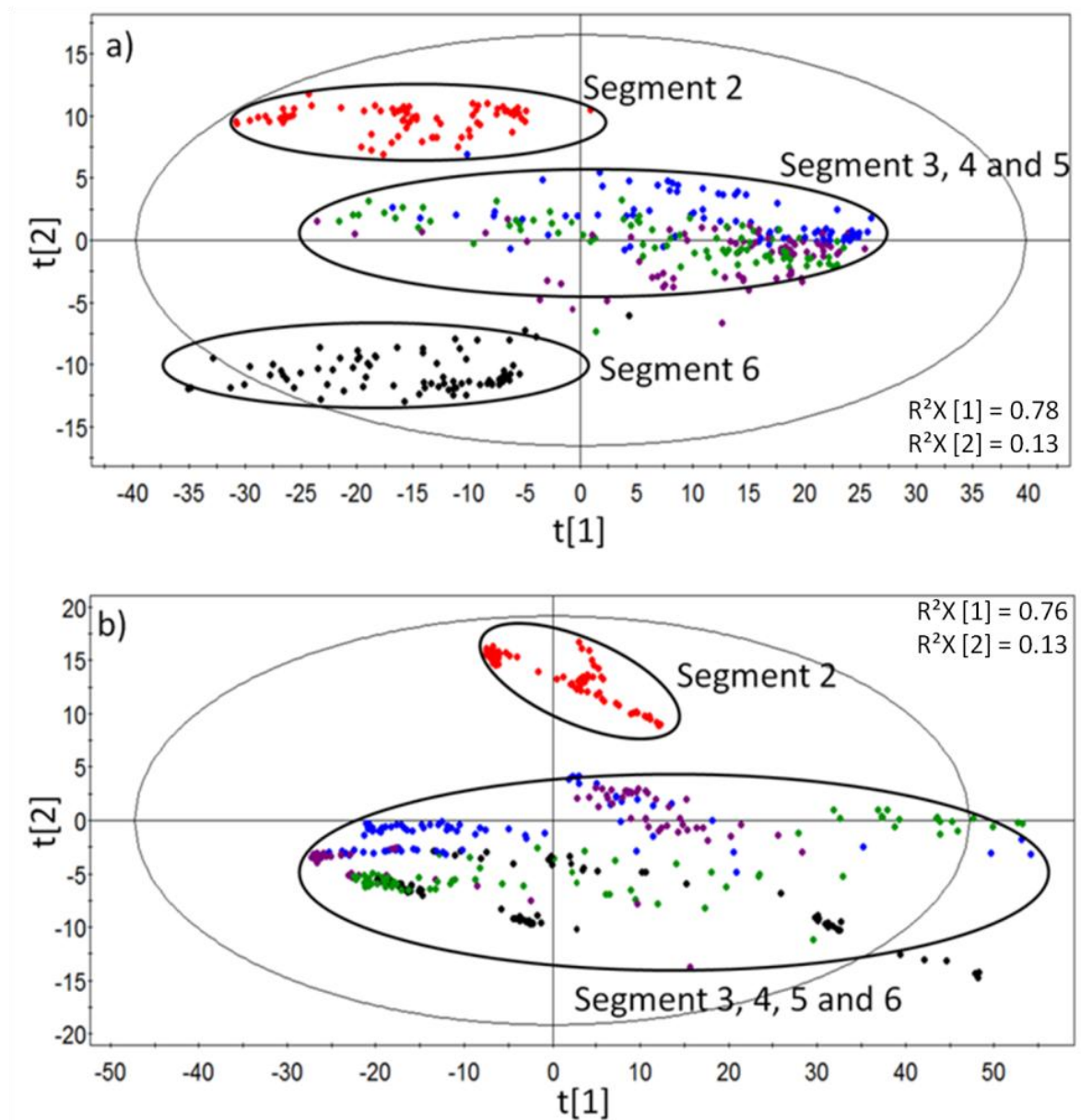


**Figure 6.5.** PC 1 versus PC 2 scores scatterplots of in-line collected Raman spectra of all extrusion runs with mixtures containing a) 10% MPT, and b) 40% MPT (w/w). (red = spectra collected in S2, blue = S3, purple = S4, green = S5, black = S6).

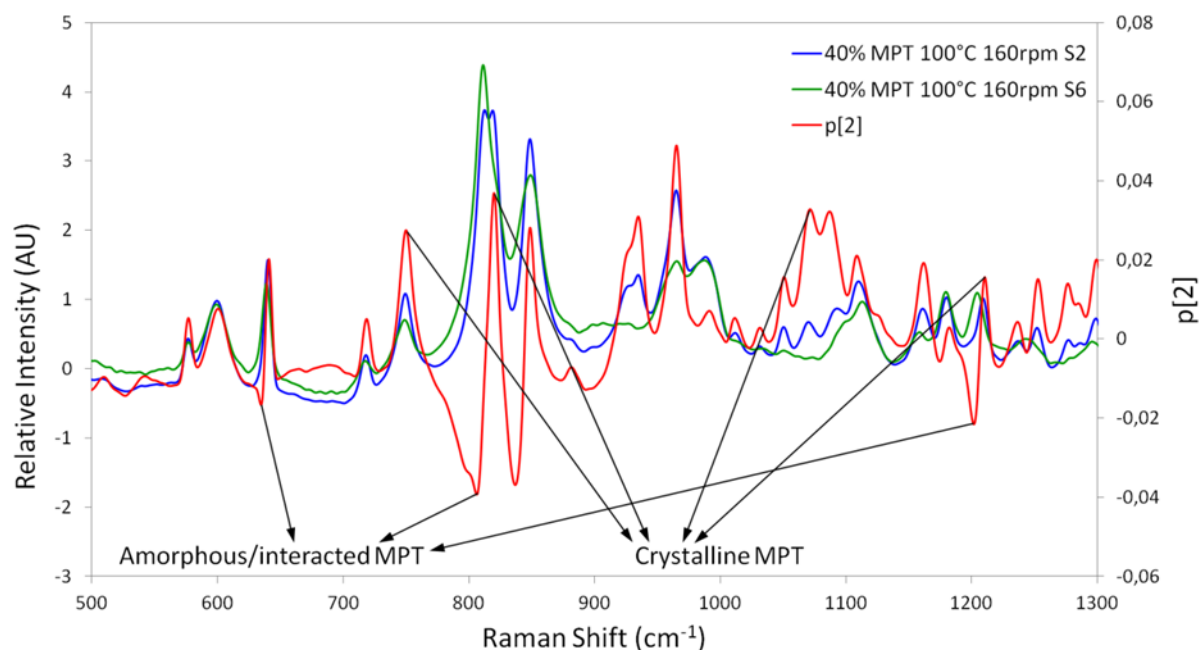


**Figure 6.6.** Comparison of the PC 2 loading (red) with the spectra collected in sections 2 (blue) and 6 (green) during extrusion of a mixture containing 40% MPT (w/w) with a screw speed of 160 rpm and at a temperature of 100°C.

At a high drug load (40% MPT (w/w), Figure 6.5.b), the variation between the Raman spectra collected in section 2 and section 3 is larger compared to the variation between other neighbouring sections (i.e. sections 3 and 4, sections 4 and 5, sections 5 and 6) according to PC 2. This indicates that the main changes in solid state, caused by the melting of MPT, occur at this position in the extrusion barrel. The Raman spectra (Figure 6.7) illustrate peak broadening in the absorption bands of MPT and peak shifts when the melt arrives in section 3, compared to the material in section 2. This is primarily caused by the retention of the melt between both sections, due to the presence of the first kneading block. The melt is subjected for a longer time to the higher temperature and shear forces between section 2 and 3, causing MPT to melt. Although extrusion at 100°C is performed at a set temperature 20°C below the melting temperature of the drug, the addition of kneading zones allows melting of MPT due to input of mechanical energy generated by the high shear forces applied on the mixture. When looking more in detail at Figure 6.5.b, an additional difference between sections 5 and 6 is present in the PC 1 versus PC 2 scores scatterplot of the mixture containing 40% MPT (w/w) which was extruded at 140°C with a screw speed of 160 rpm (black data points outside the ellipse) (Table 6.1, experiment 8). The high temperature and

high shear forces originating from the increased screw speed allow the formation of a solid solution in section 6, which was not stable due to the high drug load of the extrudate.

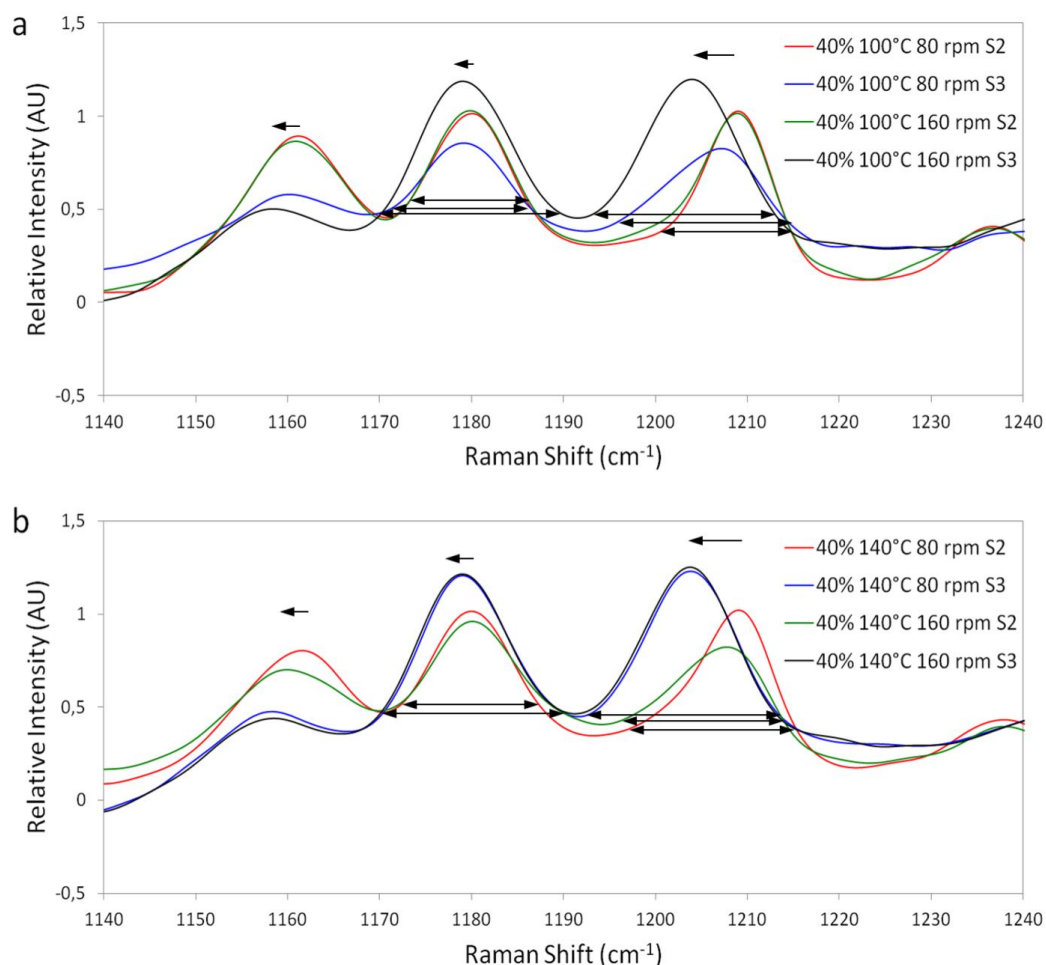


**Figure 6.7.** Detail of the Raman spectra collected in barrel sections 2 and 3 during extrusion of mixtures containing 40% MPT (w/w) at all screw speed settings at a) 100°C and b) 140°C.

When extruding a mixture with a low drug load (10% MPT (w/w), Figure 6.5.a), a similar variation between section 2 and section 3 is observed. However, in contrast to the experiments at higher drug load, an additional difference can also be noticed between the last two sections of the barrel. At a 40% drug load (w/w), MPT melt when passing through the first kneading zone due to the higher temperature and shear forces in section 3 and a solid glassy suspension is produced, but a solid solution is not formed, due to the high drug load. In the extrudates with a 10% drug load (w/w), the final kneading zone, located in section 5 facilitates the dissolution of the drug into the polymer matrix and a complete solid solution is created due to shear forces. The formation of a solid solution was confirmed by the DSC thermograms from the samples collected in section 6 (Figure 6.8). All thermograms

exhibit only one  $T_g$ , and no melting peaks for MPT are visible. This indicates that MPT is dissolved into the polymer and that a one phase system is created when the melt passes through the final kneading zone in section 5. The extrudates created with a 10% MPT concentration (w/w) are all transparent, in contrast with the opaque end products containing 40% MPT (w/w).

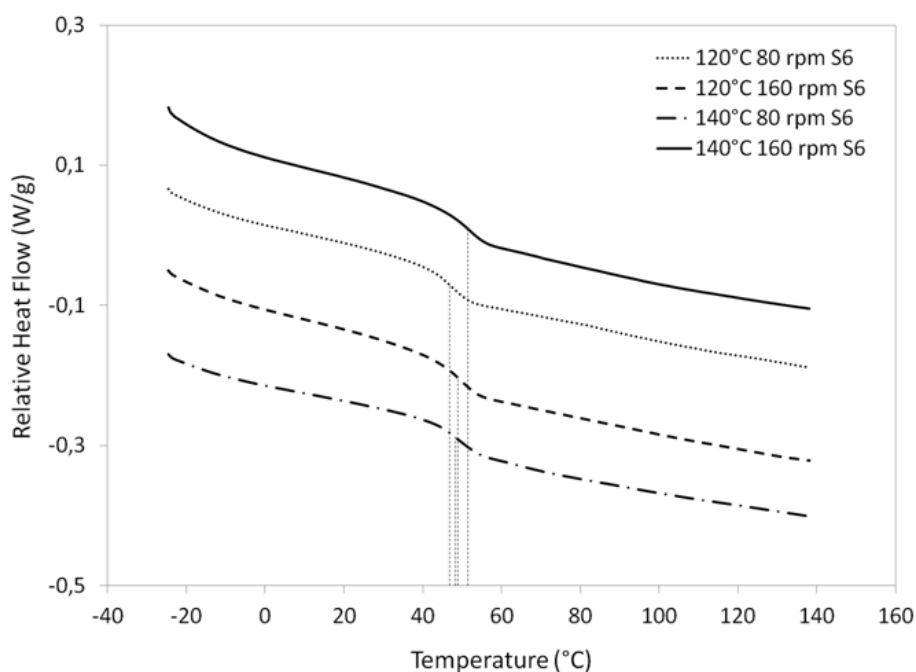


**Figure 6.8.** DSC thermograms of samples collected in barrel section 6 from all extrusion runs with mixtures containing 10% MPT (w/w).

The off-line FT-IR measurements of the samples collected in the barrel confirm that extrusion of physical mixtures containing 10% MPT (w/w) results in the formation of a solid solution for all experimental runs. The IR spectra from the samples collected in section 6 during all 10% MPT (w/w) experiments (Table 6.1, experiments 1-4) show that the IR absorption bands of the polymer are more explicitly present in both the fingerprint area and the X-H region, indicating the dissolution of MPT into the polymer (data not shown). In the spectral region of  $3000\text{ cm}^{-1} - 3100\text{ cm}^{-1}$  [17], the absence of OH stretch vibrations of alcohol groups in the spectra collected in section 6 shows that all MPT molecules have interacted with the polymer through the formation of hydrogen bonds, and that there are no independent MPT molecules present. In sections 2 to 5, peaks representing these vibrations can still be detected. The hydrogen bond formation is thus facilitated by the

kneading zone located in section 5. These OH stretch vibrations and other absorption bands specific for MPT are still present in spectra obtained in section 6 from all extrusion runs with mixtures of 40% MPT (w/w). However, in-line Raman spectra indicated an additional difference when extrusion was performed at a temperature of 140°C and with a screw speed of 160 rpm (Table 6.1, experiment 8). This difference between in-line collected Raman spectra and off-line gathered FT-IR spectra can be explained by the instability of this solid solution, containing a high drug load. The time delay between extrusion and collection of the FT-IR spectrum was sufficient for MPT to recrystallize. This recrystallization is caused by the decrease in temperature when the samples are taken from the screws and barrel.

### **6.3.2. Influence of the barrel temperature on the solid state of the extrudates**

Since the extruder barrel is modular, the temperature can be set for each section individually. A straight temperature profile [18] was used, where the temperature of section 2 was kept at 70°C throughout all experiments, and the temperatures of sections 3 to 6 were set according to Table 6.1. Physical mixtures with a drug load of 10% (w/w) could not be extruded at temperatures below 120°C, as the extrusion torque exceeded its limits. MPT has a plasticizing effect on Eudragit® RS PO [7], allowing extrusion of the physical mixture containing 40% (w/w) MPT at a barrel temperature of 100°C.

During extrusion of the physical mixtures containing 10% MPT (w/w), there is no noticeable spectral variation related to solid state caused by varying the barrel temperature, since the actual product temperature exceeds the melt temperature of the drug in all cases.

The PC 1 versus PC 2 scores scatterplot of the spectra collected during extrusion of a mixture containing 40% MPT (w/w) applying a screw speed of 80 rpm (Fig 6.9.a) (Table 6.1, experiments 5 and 6) shows clustering into three different groups (along PC 2) at both temperatures. A first group represents the physical mixture as measured in section 2, followed by a second cluster where MPT is molten. In the third group, some of the MPT has interacted with the polymer, inducing spectral shifts, but there still are molten MPT molecules that did not interact with the polymer present in the mixture. An increase of 40°C in temperature does not affect the solid state of the end product, but it does determine



how fast the solid state of the final product is reached. When extruding at 100°C, this end state is reached in section 6, with the help of the kneading zone located ahead of this section. This kneading zone is not required at a barrel temperature of 140°C, since the final solid state is attained in section 4. These observations can be found in the Raman spectra collected during extrusion as well (Figure 6.9.b). The peak situated at 812 cm<sup>-1</sup> represents the C-C stretching vibration of Eudragit® RS PO [19], and the peak located at 819 cm<sup>-1</sup> corresponds to the out-of-plane vibration of the COOH groups of MPT [17]. This peak becomes wider when the mixture reaches a temperature higher than 120°C, due to the melting of MPT.

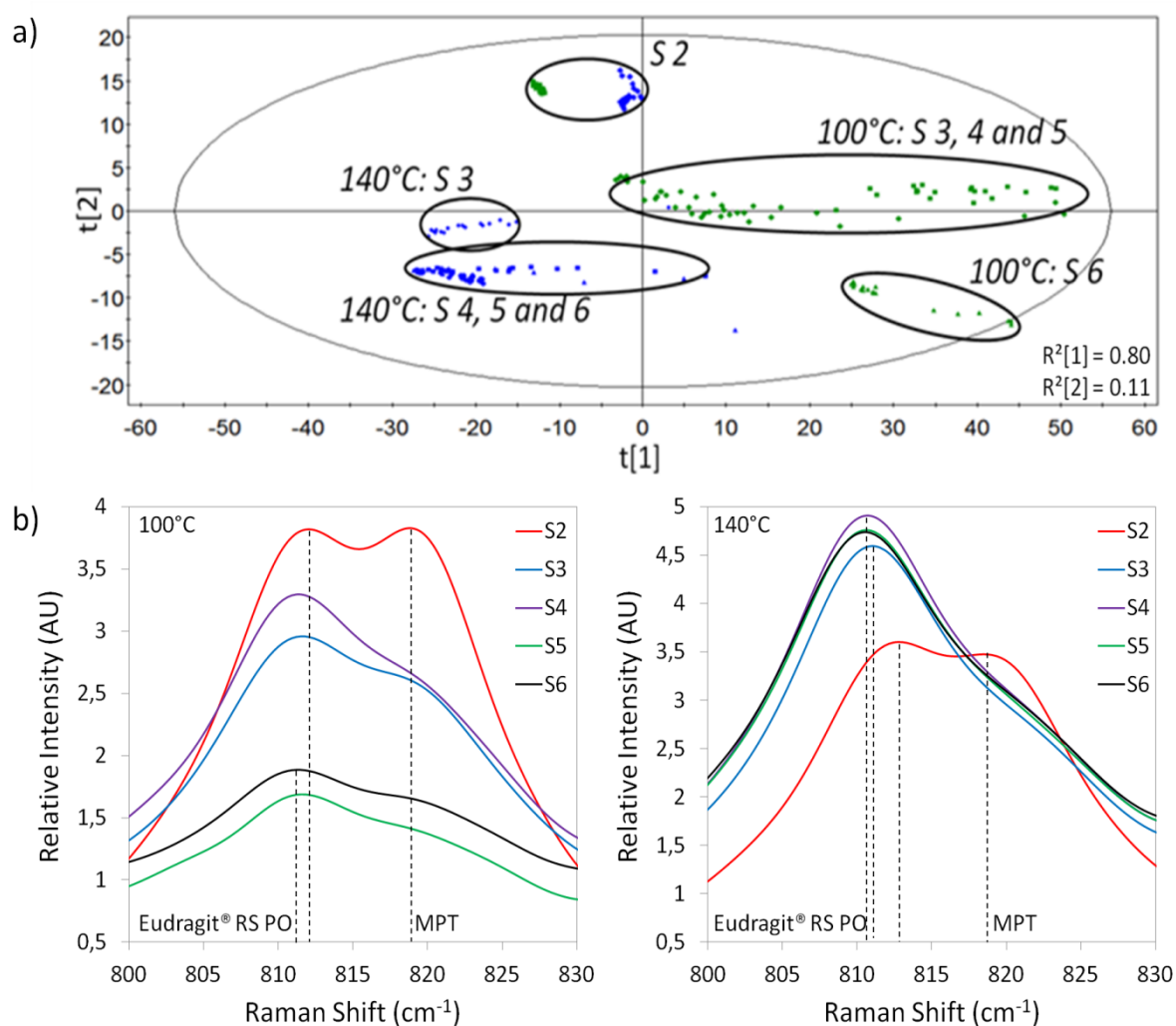


**Figure 6.9.** a) PC 1 versus PC 2 scores scatterplot of the in-line collected Raman spectra during extrusion of mixtures containing 40% MPT (w/w) with a screw speed of 80 rpm at 100°C and 140°C and b) mean Raman spectra collected in all different sections during extrusion of mixtures containing 40% MPT (w/w) with a screw speed of 80 rpm at 100°C and 140°C.

When extruding the 40% MPT (w/w) mixture with a screw speed of 160 rpm (Table 6.1, experiments 7 and 8), an increase in barrel temperature from 100°C to 140°C enables the formation of an instable solid solution, as previously mentioned. Since a high screw speed is applied, shear forces on the material are much higher, and the additional energy input due to the higher barrel temperature allows the molecular dispersion of MPT into the polymer.

### **6.3.3. Influence of the rotational screw speed on the solid state of the extrudates**

The second process parameter which was varied throughout the experiments, was the rotational screw speed (80 - 160rpm). In a twin-screw extruder, the screw speed is a critical parameter in controlling mixing of polymer, drug and excipients; melting behaviour; pressure and melt temperature [18]. The selected screw speed determines the percentage of fill of the screws, the residence time of materials in the extruder and the torque level. An increase in screw speed (for a constant barrel temperature profile and throughput) will result in a higher shear rate [20] which reduces the viscosity of the melt due to the shear thinning effect, resulting in a lower torque. Moreover, higher screw speeds raise the melt temperature, reducing the torque level as well. Additionally, a higher screw speed results in improved mixing, a shorter residence time and a lower percentage of screw fill [18].

The PC 1 versus PC 2 scores scatterplot of the in-line collected Raman spectra during extrusion of a mixture containing 10% MPT (w/w) at 120°C (Figure 6.10.a) (Table 6.1, experiments 1 and 3) demonstrates that at both screw speeds, three different groups can be distinguished regarding solid state (PC 2). A first group includes the spectra collected in section 2, which show sharp peaks for MPT. This mixture still contains crystalline MPT. A second cluster displays the spectra obtained in sections 3, 4 and 5, where MPT is molten. The third and final group shows the Raman spectra from section 6 where MPT molecules have interacted with the polymer and a solid solution is produced. In this figure, it can be seen that doubling the screw speed does not have an impact on the solid state of the final product, since the spectra in section 6 show a similar solid state for both 80 and 160 rpm. However, a small difference caused by changes in screw speed can be noticed in-line, more specific in sections 3, 4 and 5. The higher screw speed increases the shear rate and the melt temperature, which results in a solid state that leans more towards the solid state of the

end product than when using a low screw speed. This small difference in solid state can be distinguished in the Raman spectra collected in sections 3, 4 and 5 during extrusion (Figure 6.11a). The spectra display larger peak shifts at a screw speed of 160 rpm compared to 80 rpm, indicating stronger interactions between the polymer and the drug. The same results can be observed during extrusion of a mixture with 10% MPT (w/w) at 140°C (Table 6.1, experiments 2 and 4).

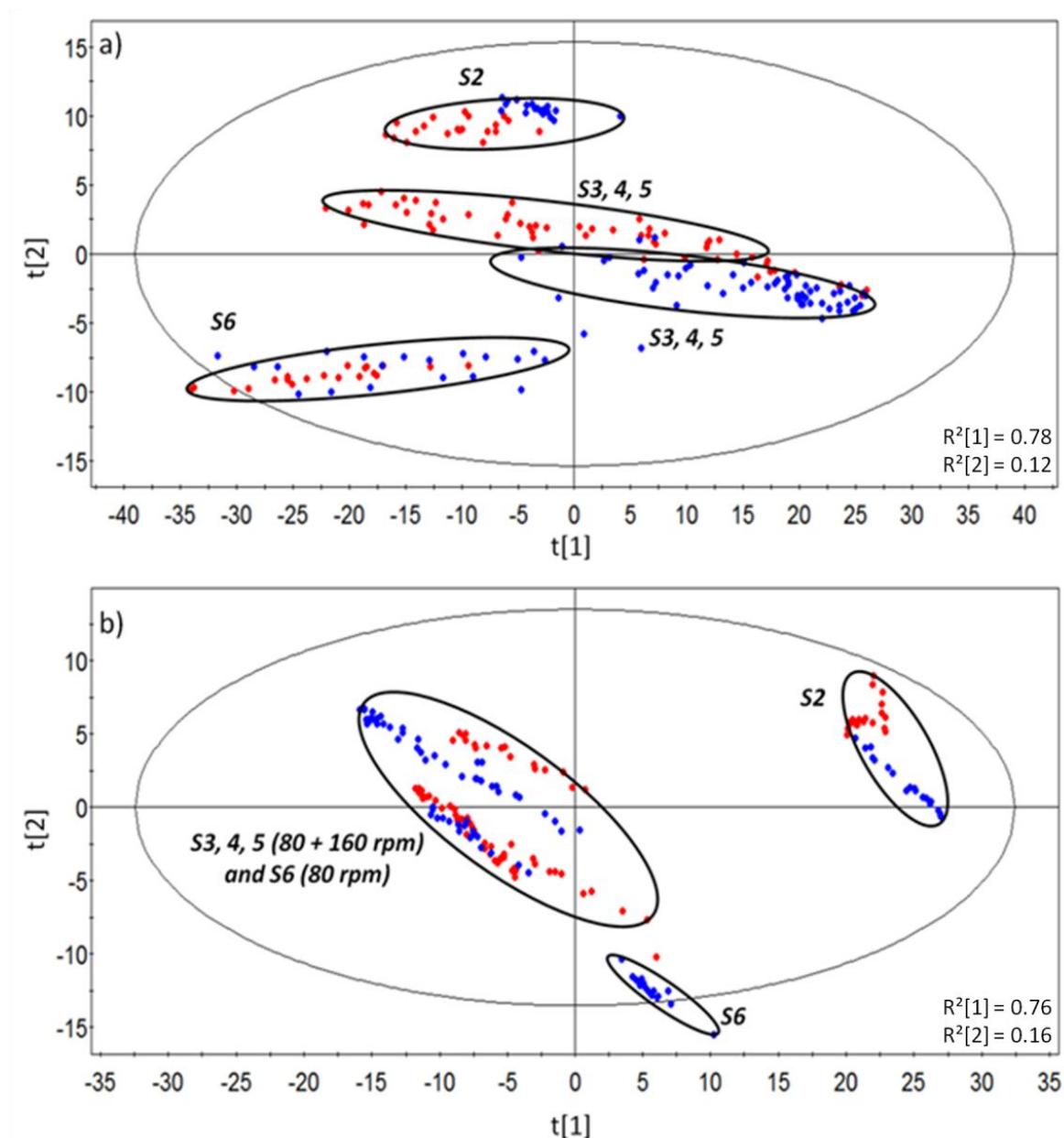


**Figure 6.10.** PC 1 versus PC 2 scores scatterplots of the in-line collected Raman spectra during extrusion of mixtures containing 10% MPT (w/w) at a temperature of 120°C and with screw speeds of 80 and 160 rpm (a), and mixtures containing 40% MPT (w/w) at a temperature of 140°C and with screw speeds of 80 and 160 rpm (b). (red = 80 rpm, blue = 160 rpm).

During extrusion of a mixture containing 40% MPT (w/w) at 140°C (Table 6.1, experiments 6 and 8), changes in screw speed have a significant impact on the solid state of the end product (Figure 6.10.b). In this case, an increase of the screw speed from 80 rpm to 160 rpm enables the formation of a solid solution with a drug load of 40% (w/w), as shown in the difference in solid state (PC 2) in section 6 for both screw speeds. Even though a higher screw speed reduces the residence time, the higher shear forces and temperature induce interactions between polymer and drug, which can be noticed in the spectra obtained in section 6 (Figure 6.11b). The kneading zone located between sections 5 and 6 facilitates the formation of a solid solution in this extrusion run. However, due to the high MPT concentration, the produced solid solution is instable and recrystallizes during cooling at room temperature. It can also be noticed that the PC 2 scores for section 2 and 3 of the extrusion run at 140°C and 160 rpm (Table 6.1, experiment 8) have almost identical values for PC 2. This could be due to conduction of heat in the mixture that is retained in front of the kneading zone between these sections of the barrel, which initiates MPT melting even before it reaches the kneading zone.

At 100°C (Table 6.1, experiments 5 and 7), doubling of the screw speed does not influence the solid state of the end product (data not shown). However, it does change the location in the barrel where this solid state is reached. When extruding at a screw speed of 80 rpm, the solid state corresponding to the final product is obtained in section 6, as a result of the kneading element located between sections 5 and 6 which increases the shear forces on the melt. At higher screw speed, the solid state of the end product is already obtained in section 5, without the requirement of additional kneading elements, since the higher screw speed induces higher shear forces earlier in the barrel. Consequently, increasing the screw speed during extrusion of mixtures with a high drug load reduces the number of barrel sections required to obtain the end product. By reducing the barrel length, the mean residence time and therefore the time in which the mixture is in contact with a high temperature can be decreased, avoiding degradation problems.

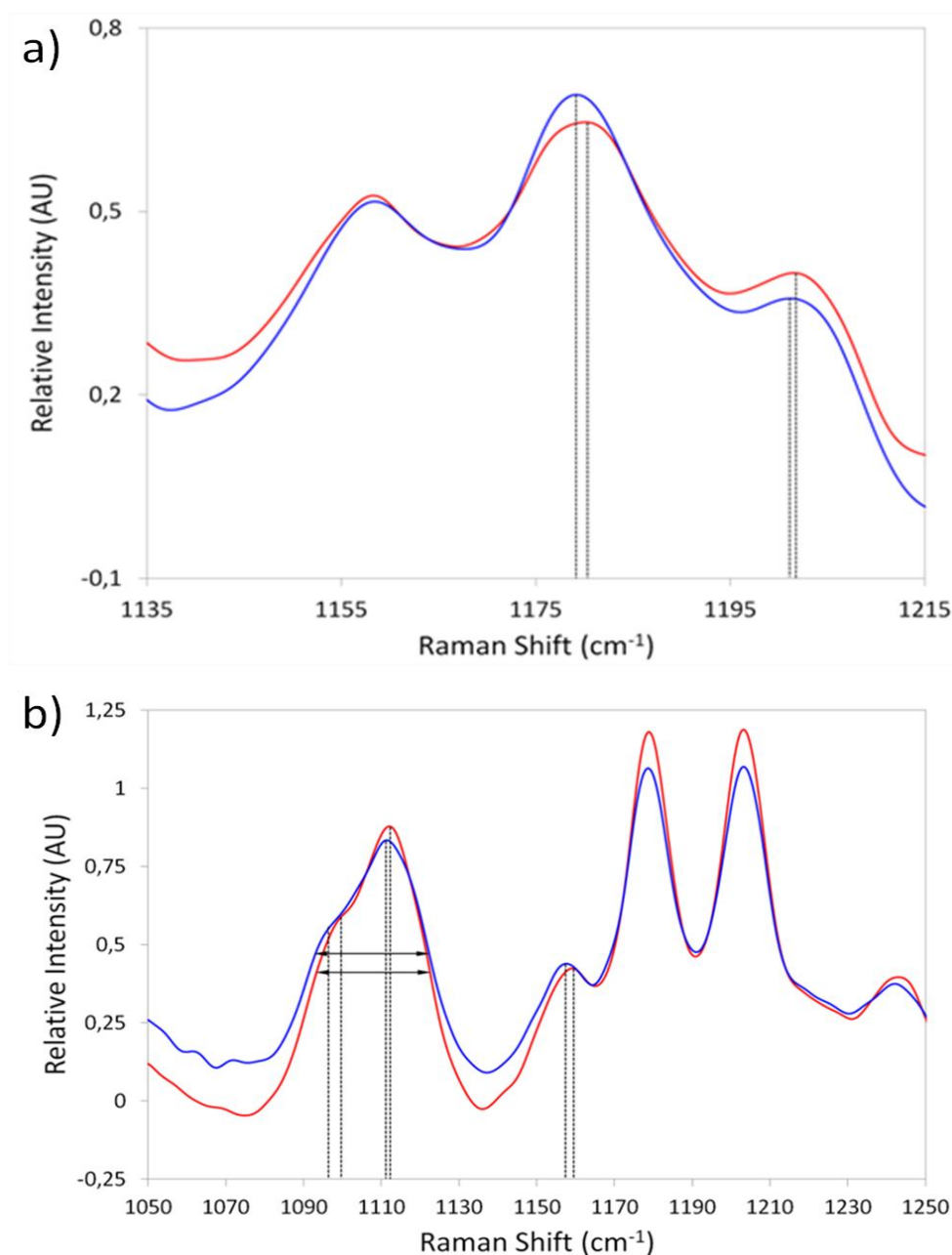


**Figure 6.11.** Detail of the mean Raman spectrum collected in barrel sections 3, 4 and 5 during extrusion of mixtures containing 10% MPT (w/w) at 120°C, with a screw speed of 80 rpm (red) and 160 rpm (blue). b) Detail of the mean Raman spectrum collected in barrel sections 3, 4 and 5 during extrusion of mixtures containing 40% MPT (w/w) at 140°C, with a screw speed of 80 rpm (red) and 160 rpm (blue).

Throughout the experiments it has also been demonstrated that the second kneading zone, located in section 4, does not have a relevant influence on the solid state of this formulation. Almost no differentiation can be detected between spectra collected in sections 3, 4 and 5. This second, smaller kneading zone does not affect the extrusion process for this formulation.

## 6.4. CONCLUSION

Raman spectroscopy is a suitable PAT-tool for the monitoring of the polymer-drug solid state during hot-melt extrusion. By implementing the probe in the different sections of the extruder barrel, a complete visualization and improved understanding of the polymer-drug behaviour throughout the entire extrusion barrel is gained, leading to a more profound understanding of the hot-melt extrusion process. The impact of variations in process and formulation parameters on the physicochemical state of the extrudates was evaluated in the different barrel sections, allowing the optimization of barrel and screw design depending on the selected settings and formulation. The spectroscopic visualisation of the entire extrusion barrel might therefore be helpful to optimize the process settings, the screw design and the barrel length required to obtain extrudates with predefined solid state properties.

## 6.5. REFERENCES

- [1] J. Breitenbach, J. Eur J Pharm Biopharm 54 (2002) 107-1171.
- [2] M.M. Crowley, F. Zhang, M.A. Repka, S. Thumma, S.B. Upadhye, S.K. Battu, J.W. McGinity, C. Martin, Drug Dev Ind Pharm 33 (2007) 909-926.
- [3] C. Vervaet, J.P. Remon, Chem Eng Sci 60 (2005) 3949-3957.
- [4] K. Plumb, Chem Eng Res Des 83 (2005) 730-738.
- [5] International Conference on Harmonisation of Technical Requirements for Registration of Pharmaceuticals for Human Use, Pharmaceutical Development Q8 (R2), 2009.
- [6] T. De Beer, A. Burggraeve, M. Fonteyne, L. Saerens, J.P. Remon, C. Vervaet, Int J Pharm 417 (2011) 32-47.
- [7] L. Saerens, L. Dierickx, B. Lenain, C. Vervaet, J.P. Remon, T. De Beer, Eur J Pharm Biopharm 77 (2011) 158-163.
- [8] L. Saerens, L. Dierickx, T. Quinten, P. Adriaensens, R. Carleer, C. Vervaet, J.P. Remon, T. De Beer, Eur J Pharm Biopharm 81 (2012) 230-237.
- [9] D. Wang, K. Min, Polym Eng Sci 45 (2005) 998-1010.
- [10] C.W. Macosko, Rheology: Principles, Measurements and Applications, 1<sup>st</sup> ed., Wiley-VCH, New York, USA, 1994.
- [11] J.A. Covas, O.S. Carneiro, P. Costa, P.; A.V. Machado, J.M. Maia, Plast Rubber Compos 33 (2004) 55-61.
- [12] O.S. Carneiro, J.A. Covas, J.A. Ferreira, M.F. Cerqueira, Polym Test 23 (2004) 925-937.
- [13] J. Breitzkreutz, Pharm Res 15 (1998) 1370-137.
- [14] A. Forster, J. Hempenstall, I. Tucker, T. Rades, Int J Pharm 226 (2001) 147-161.
- [15] E. Verhoeven, T.R.M. De Beer, G. Van den Mooter, J.P. Remon, C. Vervaet, Eur J Pharm Biopharm 69 (2008) 312-319.
- [16] K. Nakamichi, T. Nakano, H. Yasuura, S. Izumi, Y. Kawashima, Int J Pharm 241 (2002) 203-211.
- [17] A. Bright, T.S. Renuga Devi, S. Gunasekaran, ChemTech 2 (2010) 379-388.
- [18] H.F. Giles Jr., J.R. Wagner Jr., E.M. Mount III, Extrusion: The Definitive Processing Guide and Handbook, 1<sup>st</sup> ed., William Andrew, Inc., New York, USA, 2005.

- [19] M. De Veij, P. Vandenabeele, T. Beer, J.P. Remon, L.J. Moens, Raman spectrosc 40 (2008) 297-307.
- [20] H. Liu, P. Wang, X. Zhang, F. Shen, C.G. Gogos, Int J Pharm 383 (2010) 161-169.



# CHAPTER 7

## IN-LINE SOLID STATE PREDICTION DURING PHARMACEUTICAL HOT-MELT EXTRUSION IN A 12 MM TWIN SCREW EXTRUDER USING RAMAN SPECTROSCOPY

Parts of this chapter are published in:

**L. Saerens**, D. Ghanam, C. Raemdonck, K. Francois, J. Manz, R. Krüger, S. Krüger, C. Vervaet, J.P. Remon, T. De Beer. In-line solid state prediction during pharmaceutical hot-melt extrusion in a 12 mm twin-screw extruder using Raman spectroscopy. Submitted to European Journal of Pharmaceutics and Biopharmaceutics (2013).

## **ABSTRACT**

In Chapter 7, Raman spectroscopy was used for the in-line monitoring of the solid state of materials during pharmaceutical hot-melt extrusion in the die head of a 12 mm (development scale) twin-screw extruder during formulation development.

A full factorial (mixed) design was generated to determine the influence of variations in concentration of Celecoxib (CEL) in Eudragit® E PO, three different screw configurations and

varying barrel temperature profiles on the solid state, melt temperature and die pressure of continuously produced extrudates in real-time. Off-line XRD and DSC analysis were used to evaluate the suitability of Raman spectroscopy for solid state predictions. First, principal component analysis (PCA) was performed on all in-line collected Raman spectra from the experimental design. The resulting PC 1 versus PC 2 scores plot showed clustering according to physicochemical state of the extrudates, and two classes, one class where crystalline CEL is still present and a second class where no crystalline CEL was detected, were found. Then, a soft independent modelling of class analogy (SIMCA) model was developed, by modelling these two classes separately by disjoint PCA models. These two separate PCA models were then used for the classification of new produced extrudates and allowed distinction between glassy solid solutions of CEL and crystalline dispersions of CEL. All extrudates were classified similarly by Raman spectroscopy, XRD and DSC measurements, with exception of the extrudates with a 30% CEL concentration (w/w) extruded at 130°C. The Raman spectra of these experiments showed bands which were sharper than the amorphous spectra, but broader than the crystalline spectra, indicating the presence of CEL that has dissolved into the matrix and CEL in its crystalline state. XRD and DSC measurements did not detect this. Modifications in the screw configuration did not affect the solid state and did not have an effect on the solid state prediction of new produced extrudates.

Secondly, the influence of variations in die pressure on the Raman spectra was examined. The applied drug concentration, processing temperature and feeder performance influence the die pressure, which was reflected in the Raman spectra as a change in spectral intensity. When applying PCA on the raw spectra from the experimental design, the first principal component described the influence of die pressure on the spectra, which was seen as a decrease in Raman intensity of the whole spectrum when the pressure in the sample increased. Clustering according to processing temperature was found, although the temperature in the die remained constant, indicating that a difference in viscosity, resulting in a changed die pressure, was detected. When the feeder was stopped, the score values of the first principal component almost simultaneously decreased, and only stabilized once the die pressure became stable. Since Raman spectra collected in the extrusion die are influenced by changes in die pressure, disturbances upstream of the extrusion process can be observed and identified in the Raman measurements.

## CHAPTER 7

# IN-LINE SOLID STATE PREDICTION DURING PHARMACEUTICAL HOT-MELT EXTRUSION IN A 12 MM TWIN SCREW EXTRUDER USING RAMAN SPECTROSCOPY

---

### 7.1. INTRODUCTION

The high throughput screening of potential therapeutic agents has increased the amount of poorly soluble drug candidates. In the Biopharmaceutical Classification System (BCS), many active pharmaceutical ingredients (APIs) such as Celecoxib (CEL) have been categorized as Class II, implying that they have a high permeability, but a low aqueous solubility. The bioavailability of this type of compounds is limited by their dissolution rate. The low water solubility of these compounds makes it challenging to formulate them for oral delivery. Several manners of improving the dissolution of the drug have been proposed [1], but the preferred option to enhance the solubility and therefore the bioavailability of the drug is through formulation approaches. Presenting the compound as a solid dispersion will reduce the particle size of the API, improve the wettability, increase the porosity, and allow the formulation of drugs in their amorphous state [2]. The current method of choice for the manufacturing of solid dispersions is hot-melt extrusion (HME) [1]. Melt extrusion has several advantages over solvent based methods for the formation of glass solid solutions (solid dispersions where the API is completely dissolved in an amorphous carrier). When applying solvent evaporation methods, the first challenge is to find a solvent in which both API and carrier are soluble [3]. Other disadvantages of solvent methods include difficulties of removing the residual (organic) solvent, toxicity issues due to residual solvent, the

requirement of a secondary drying step and possible ecological problems [1, 2, 4]. Using hot-melt extrusion to produce solid dispersions requires high processing temperatures, but avoids the need for solvents. Furthermore, HME is a one step continuous process with decreased ecological implications. It has been shown that glassy solid solutions of CEL can be produced via hot-melt extrusion using several polymer carriers, each increasing the dissolution rate of the drug [5, 6].

Process analytical tools such as Raman spectroscopy can provide in-line and real-time information about critical process and formulation parameters. Raman spectroscopy has been used off-line in previous studies for the physical characterization of solid dispersions. It can be applied to determine the type of solid dispersion (solid solution, glass suspension, etc.), the solid state of the API and polymers and the occurring molecular interactions between polymer and drug [6-9]. Custom made fibre optic probes connected to the spectrometer can be implemented into the HME equipment [10]. In-die monitoring of solid state and molecular interactions during a pharmaceutical hot-melt extrusion process has already been demonstrated using Raman spectroscopy [9] and NIR spectroscopy [11]. In this chapter, the application of Raman spectroscopy as a PAT tool during formulation development and to determine the influence of varying process settings on the material properties was demonstrated. Therefore, the physicochemical properties of the melt were determined in-line during hot-melt extrusion on a 12 mm development scale twin-screw extruder with low material need, avoiding the dissipation of materials and making off-line analysis redundant.

## 7.2. MATERIALS AND METHODS

### 7.2.1. Materials

Celecoxib (CEL) (Selectchemie, Zürich, Switzerland) was selected as a model drug. CEL is an example of a poorly soluble (BCS Class II) drug with a water solubility of 3-7 mg/L and a melting temperature ( $T_m$ ) of 163°C. The polymer Eudragit® E PO (Evonik®, Weiterstadt, Germany) was used to form the matrix system. It is a cationic copolymer based on dimethylaminoethyl methacrylate, butyl methacrylate, and methyl methacrylate. Eudragit® E PO is an amorphous polymer, used to create the matrix in which CEL is dissolved.

The solubility parameters of both components were calculated with SPWin, version 2.11 [12], to give an indication of miscibility of polymer and drug. The calculated values were 26.7 MPa<sup>1/2</sup> and 19.7 MPa<sup>1/2</sup> for CEL and Eudragit® E PO respectively. For components with a difference in solubility parameters ( $\Delta\delta_t$ ) smaller than 7.0 MPa<sup>1/2</sup>, miscibility is likely, whereas components with  $\Delta\delta_t > 10$  MPa<sup>1/2</sup> are expected to be immiscible [13]. When  $\Delta\delta_t$  lays between 5 MPa<sup>1/2</sup> and 10 MPa<sup>1/2</sup>, prediction of glass solution formation requires further investigation with thermal analysis. As the difference in total solubility parameters is 7.0 MPa<sup>1/2</sup>, further DSC measurements were performed to assess the solubility of CEL in Eudragit® E PO.

Physical mixtures of both components were prepared with a Turbula® T2F mixer (Willy A. Bachofen GmbH, Muttenz, Switzerland). The concentration of CEL was varied between 30% and 50% (w/w) in Eudragit® E PO throughout the experiments (Table 7.1).

### 7.2.2. Hot-melt extrusion

Hot-melt extrusion was performed with a development scale co-rotating twin-screw extruder with a screw diameter of 12mm (PTSE 12/36, Brabender® Pharma, Duisburg, Germany). The extruder was equipped with a loss in weight feeder (Brabender® Technologie, Duisburg, Germany), which was used in its gravimetric feeding mode and supplied the

**Table 7.1.** Performed extrusion experiments (full factorial (mixed) screening design).

<i>Process and formulation settings</i>				<i>Responses</i>		
Experiment number	Drug load (% w/w)	Screw Configuration	Barrel temperature profile (feeding zone → die) (°C)	Melt temperature in die (°C)	Die pressure (bar)	PC 1 Score values
1	30	FF	20-70-130-130-130-110	110,90	13,77	4,5461
2	30	FF	20-70-150-150-150-110	113,58	11,22	-3,4645
3	30	FB	20-70-130-130-130-110	111,31	18,28	2,6151
4	30	FB	20-70-150-150-150-110	114,20	16,36	-4,1576
5	30	2F	20-70-130-130-130-110	111,11	16,65	1,9484
6	30	2F	20-70-150-150-150-110	113,70	15,67	-3,1045
7	50	FF	20-70-130-130-130-110	111,35	16,89	8,7996
8	50	FF	20-70-150-150-150-110	114,06	7,75	-4,8359
9	50	FB	20-70-130-130-130-110	111,00	11,93	11,5758
10	50	FB	20-70-150-150-150-110	113,35	5,81	-5,7765
11	50	2F	20-70-130-130-130-110	111,18	14,45	8,0646
12	50	2F	20-70-150-150-150-110	113,55	7,11	-4,5921
13	40	FB	20-70-140-140-140-110	112,20	10,63	-2,3848
14	40	FB	20-70-140-140-140-110	112,01	10,77	-5,5010
15	40	FB	20-70-140-140-140-110	112,11	11,27	-3,7324

physical mixtures with a throughput of 1.5 g/min. Three different screw configurations were applied during experiments (Table 7.1): the first configuration included 2 consecutive forward kneading elements (FF), a second configuration contained a forward kneading element followed by a backward kneading element (FB), and the third screw setup comprised 2x2 consecutive forward kneading elements (2F) (Figure 7.1). The FF configuration will induce the lowest amount of shear on the mixture and will result in the shortest residence time. When the shear forces on the mixture increase, and the time of exposure to a high temperature becomes longer, the formation of a glass solution will be facilitated. Shear forces and residence time values will increase when two more forward kneading elements are added to the design, or when a forward kneading element is replaced by a backward kneading element. The impact of these design alterations is expected to be more distinct at lower processing temperatures than at the higher barrel temperatures. The processing temperature was varied from 130°C to 150°C throughout the experiments, and the die temperature was kept constant (110°C) for each experiment to guarantee a solid end product (Table 7.1). Logging of the extrusion settings (throughput, screw speed, barrel and die temperature) and parameters (actual barrel, die and product temperature, actual throughput, actual screw speed, die pressure, motor load) was performed with the WinExtXT® software (Brabender® Pharma, Duisburg, Germany). Extrudate samples were collected during the experiments and stored at room temperature.

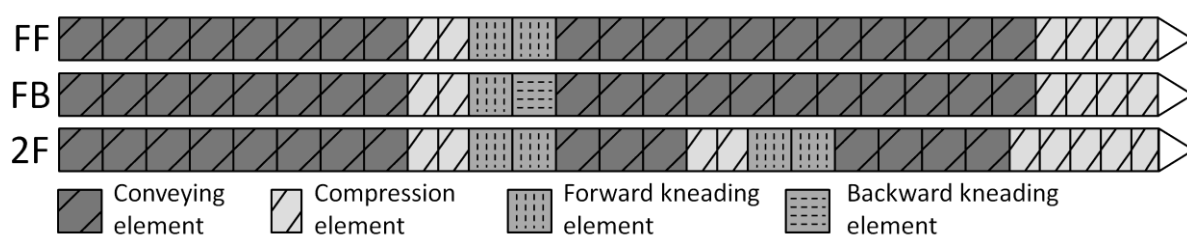


Figure 7.1. Applied screw configurations: FF, FB and 2F.

### 7.2.3. Raman spectroscopy

Both in-line and off-line Raman spectra were collected with a Raman Rxn1 spectrometer (Kaiser Optical Systems, Ann Arbor, MI, USA). For in-line measurements, a fibre-optic Raman Dynisco probe was built into the die head (Figure 7.2), to monitor the physicochemical state



of the extrudate before it is forced through the die. The laser wavelength was the 785 nm line from a 785 nm Invictus NIR diode laser. All in-line collected spectra were recorded with a resolution of  $4\text{ cm}^{-1}$  and an exposure time of one second, using a laser power of 400 mW. Spectra were collected every 20 seconds. The analyzed spectral region was  $100 - 1800\text{ cm}^{-1}$ , since this region contains all envisaged drug and polymer information. Prior to data analysis, SNV pre-processing was applied on the in-line collected spectra to eliminate the additive baseline offset variations and multiplicative scaling effects in the spectra, induced by pressure variations at the measurement point.



**Figure 7.2.** Experimental setup. 1) Extruder control panel, 2) Feeder control panel, 3) Feeder unit, 4) Extrusion barrel, 5) Extrusion die with implemented Raman probe.

After storage of the samples collected during extrusion at room temperature for one year, off-line Raman spectra of the extrudates were collected to verify the stability of the end products. These spectra were recorded with a resolution of  $4\text{ cm}^{-1}$  and an exposure time of five seconds, using a laser power of 400 mW.

#### 7.2.4. Data collection, alignment and analysis

An experimental design (Table 7.1) was created using the MODDE software (version 9.1.0.0, Umetrics, Umeå, Sweden) to study the influence of the above described factors (drug load, screw configuration and processing temperature) on extrusion. The applied design was a full factorial (mixed) screening design with two quantitative factors, CEL concentration and processing temperature, and screw configuration as a qualitative factor with three levels (FF, FB and 2F, Figure 7.1). The monitored responses in the design were the melt temperature as measured by the temperature probe in the die head, die pressure and the physicochemical state of the extrudates, which was monitored with Raman spectroscopy. Data collection during each design experiment (Raman spectral data + logged data) and data alignment were automated using the SIPAT software (Siemens NV, Brussels, Belgium) and SIMCA Q (Umetrics, Umeå, Sweden). Raman spectral data analysis was performed using SIMCA P+ (version 12.0.1.0, Umetrics, Umeå, Sweden).

The analysed spectral region was the region from 0 to 1800  $\text{cm}^{-1}$ . Since the formulation coloured slightly yellow (due to the use of Eudragit® E PO) during extrusion, the background signal of all Raman spectra gained intensity. Coloured substances will absorb laser beam energy, and generate fluorescence which contaminates the Raman spectrum. However, the peaks of CEL were still detectable in the in-line collected spectra. Soft independent modelling of class analogy (SIMCA) was used to distinguish between extrudates containing crystalline CEL, and extrudates where a glassy solid solution was formed, where CEL is molecularly dissolved into the polymer matrix. Therefore, principal component analysis (PCA) was in first instance performed on all spectra collected during the design experiments (Table 7.1), hence providing a general overview of the data and giving an indication of present class separation (i.e., glassy solid solution versus crystalline suspension), trends and outliers [14]. Subsequent to this initial overview, each class of observations determined from this PCA was modelled separately by disjoint PCA models. These two separate PCA models were then used to predict a likely class membership for new observations. Based on the residual variation of each class, the distance to the model (DModX) for each (new) observation can be calculated [14]. DModX values are calculated by Eq. (7.1):

$$DModX = \sqrt{\frac{\sum e_{ik}^2}{(K-A)}} \quad (7.1)$$

Where  $e_{ik}$  are the sum-squared residuals after projection of the observation on the PCA model of a certain class, A is the number of principal components retained to model this class and K is the number of variables. A critical distance (Dcrit) to the model is calculated (from the F-distributed values of the residual standard deviation of each observation divided by the pooled residual standard deviation of the model) and is set at the 0.05 probability level. When the probability of belonging to the model is higher than 95%, the observation is considered as a member of that particular class. Observations that do not fit any class, i.e. observations found outside Dcrit are considered as either outliers or members of a new, unseen class. In a Coomans' plot, DModX values for two classes are plotted against each other in a scatter plot. By plotting the class membership limits (Dcrit) as well, four areas of diagnostic interest are created. The upper left-hand and lower right-hand area contain observations belonging to one of both classes can be found. In the lower left-hand area of the plot, there is a region where prediction set samples that fit both models are found, and in the upper right-hand area the observations that do not conform with either of the models are found.

The ability of a class model to classify observations correctly cannot be realistically assessed if only training set samples are considered. It is recommended that an independent prediction set of observations that has not influenced the model calculations is employed. This will enable a more realistic assessment of the classification performance of each model [14]. The classification model developed for classification of new samples was implemented in the SIPAT software, and applied for real-time data analysis and solid state predictions of new runs.

### **7.2.5. Differential scanning calorimetry**

From each experiment (Table 7.1), samples were collected after extrusion. Differential scanning calorimetry was performed with a DSC Q 2000 (TA Instruments, Belgium). The thermograms were produced with the Thermal Advantage Release 5.1.2 software and

analysed with TA Instruments Universal Analysis 2000 4.7A (TA Instruments, Belgium). Hermetically sealed aluminium hermetic pans (TA Instruments, Belgium) were used to contain the samples. Measurements were carried out in a nitrogen atmosphere. The flow rate of dry nitrogen gas was 50 mL/min. Samples were subjected to three cycles. First, the pans were heated with a heating rate of 10,0 °C/min from 0°C up to 200°C in the first heating cycle. Then, a cooling cycle was started with a cooling rate of -10,0 °C/min to 0°C, followed by a second and final heating cycle which was identical to the first. The results from the first heating cycle reflect the influences of the hot-melt extrusion processing on the mixture, whereas the second heating cycle provides insight in the possible interactions between both pure components.

#### **7.2.6. X-ray powder diffraction**

The crystallinity of CEL was assessed using X-ray diffraction on the pure compounds, the physical mixtures and the produced extrudates. X-ray diffraction was performed with a D2 Phaser (Bruker) in the angular range of  $5^\circ < 2\theta < 70^\circ$  using a step scan mode (step size =  $0.020^\circ$ , step time = 1s).

## 7.3. RESULTS AND DISCUSSION

### 7.3.1. In-line monitoring of solid state

DSC measurements were performed on the pure components CEL and Eudragit® E PO and on a physical mixture (50:50) of both to assess the solubility of CEL in Eudragit® E PO (Figure 7.3). To determine the  $T_m$  for CEL and the  $T_g$  for Eudragit®, the first heating cycle was used. The  $T_m$  of CEL was found at 164.1°C with an onset temperature of 162.9°C, and the  $T_g$  of Eudragit® E PO was located at 55.6°C with an onset temperature at 54.8°C. To determine whether CEL is soluble in the Eudragit® E PO matrix, a physical mixture containing 50% of each component (w/w) was first heated, then cooled and reheated to verify the absence of crystalline CEL. No endothermic melting peak for CEL was detected in the thermogram of the second heating cycle, and only one  $T_g$  is visible at 62.5°C with an onset temperature of 57.1°C. This indicates that, in this 50:50 (% w/w) mixture, all CEL has interacted with the polymer on a molecular level, resulting in a glassy solution. Since CEL is soluble in the Eudragit® E PO matrix, it was not required to perform hot-melt extrusion at or above the  $T_m$  of CEL, hence lowering the processing temperatures required during the experiments.

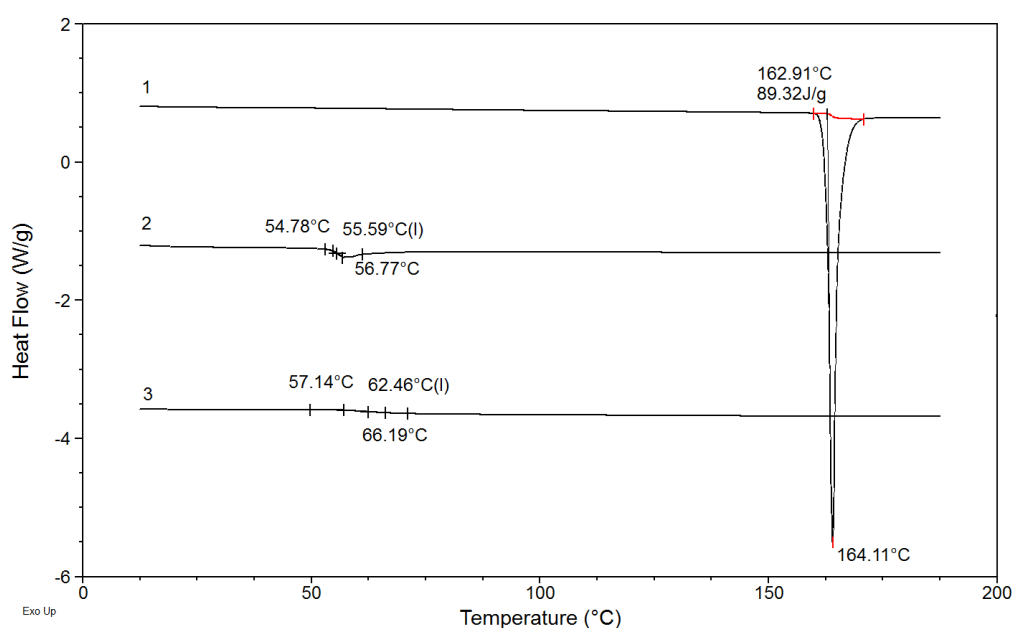


**Figure 7.3.** DSC thermograms of 1) pure CEL, first heating cycle, 2) pure Eudragit® E PO, first heating cycle and 3) a physical mixture of both (50:50), second heating cycle.

PCA was performed on the off-line obtained XRD and DSC data from the extrudate samples collected after each design experiment (Table 7.1). The resulting principal component (PC) 1 versus PC 2 scores plot and corresponding PC 2 loadings plot for the XRD data are shown in Figure 7.4a and 7.4b. PC 1 captures the variation in the XRD diffraction pattern caused by differences in baseline intensities between the extrudates of the different experiments.

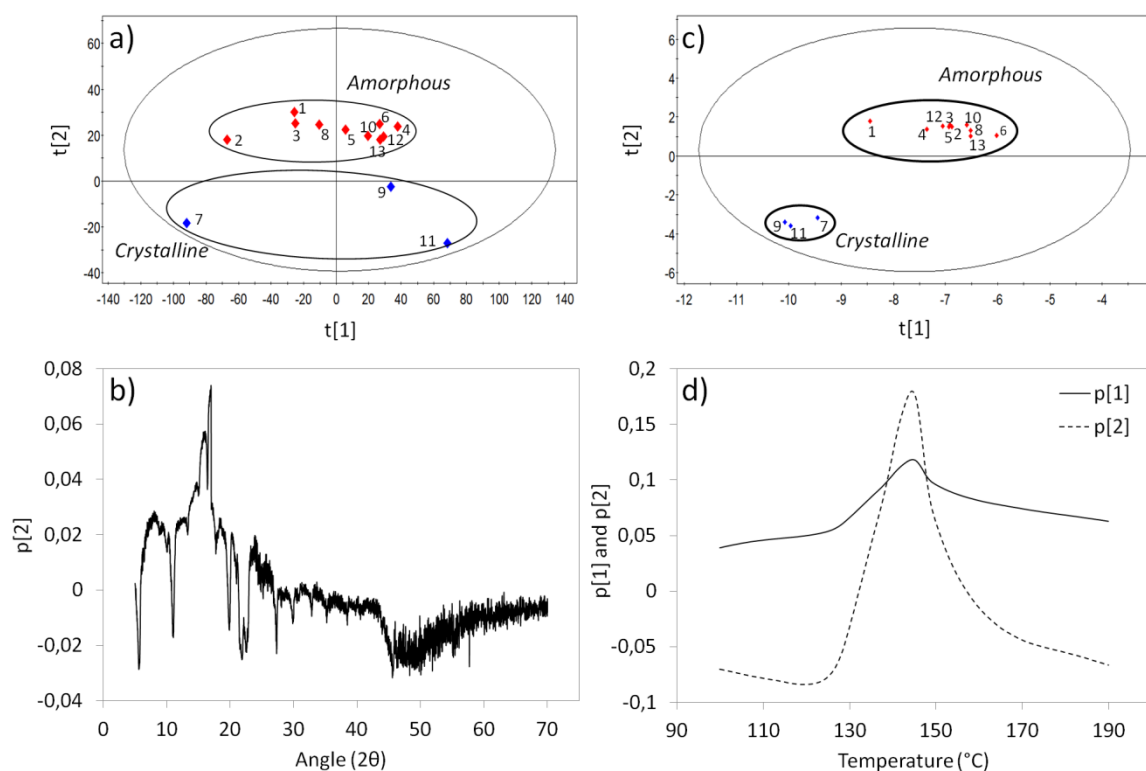


**Figure 7.4.** PC 1 versus PC 2 scores plots and loadings obtained after principal component analysis of the XRD diffraction patterns (a and b) and of the DSC thermograms (c and d) from the end products of each design experiment (experiment numbers according to Table 7.1).

The second principal component ( $R^2=0.15$ ) distinguishes between the extrudates still containing crystalline CEL and the samples where no crystalline peaks were visible in the XRD patterns. The PC 2 loadings have very sharp, negative peaks. These peaks correspond to the signals of crystalline CEL that were found in the diffraction pattern of pure CEL, indicating that the observations with a low score value for PC 2 will contain the most CEL in its crystalline form. All design experiments resulted in amorphous extrudates, except for three experiments where physical mixtures containing 50% CEL (w/w) were extruded at 130°C (experiments 7, 9 and 11, Table 7.1). In these three extrudates, crystalline CEL can be seen in the XRD patterns, resulting in low PC 2 score values (Figure 7.4a, blue observations). These

extrudates were also opaque, whereas all other formulations resulted in transparent end products.

PCA was also performed on all thermograms (first heating cycle) collected after each design experiment. Only a small region of the thermograms was used for analysis, from 100°C to 190°C, since this region captures information related to the presence of a melt peak for CEL. The PC 1 ( $R^2=0.93$ ) versus PC 2 ( $R^2=0.06$ ) scores plot and the loadings plots for both components are shown in Figure 7.4c and 7.4d, respectively. The loadings for both PC 1 and PC 2 show a peak at the position where crystalline CEL displays a melting peak in the thermogram. This indicates that measurements with low score values in both components will contain crystalline CEL. Hence, DSC analysis of the extrudates clustered the end products in an identical manner as the XRD analysis. In the three experiments with a concentration of 50% CEL (w/w) at a temperature of 130°C (blue observations in Figure 7.4c), an endothermic melting peak was visible at 143.3°C, 143.7°C and 145.3°C when using the FF, FB and 2F screw configurations, respectively.

During each extrusion experiment (15 experiments, Table 7.1), 15 in-line Raman spectra were collected resulting in a data set of 225 spectra. In first instance, a general overview of the data was envisaged by applying PCA on this training set. The resulting PC 1 versus PC 2 scores plot (Figure 7.5a) shows three clusters of spectra oriented along PC 1 ( $R^2=0.96$ ). The spectra having the highest PC 1 score values correspond to the extrudates containing 50% CEL (w/w) extruded at 130°C. The loadings of this component (Figure 7.5b) indeed represent the sharp peaks of crystalline CEL, indicating that the spectra having a high PC 1 score value correspond to extrudates containing crystalline CEL. This was confirmed by the off-line XRD and DSC analysis. However, Raman spectroscopy seems to distinguish two groups within the spectra collected during all other experiments of the design. The spectra obtained during extrusion of 30% CEL (w/w) mixtures at 130°C (experiments 1, 3 and 5, Table 7.1) have lower PC 1 score values than the spectra collected during extrusion of 50% CEL (w/w) mixtures at 130°C, but these score values are remarkably higher than those for all other experiments of the design. Raman spectroscopy apparently detects an additional difference between the spectra collected during extrusion of 30% CEL (w/w) at 130°C and the other experiments, which was not found in XRD and DSC analysis. According to the latter two, these extrudates

did not contain any crystalline CEL. Nevertheless, the Raman spectra suggest that there is some crystalline CEL present when extruding a 30% CEL (w/w) mixture at 130°C.

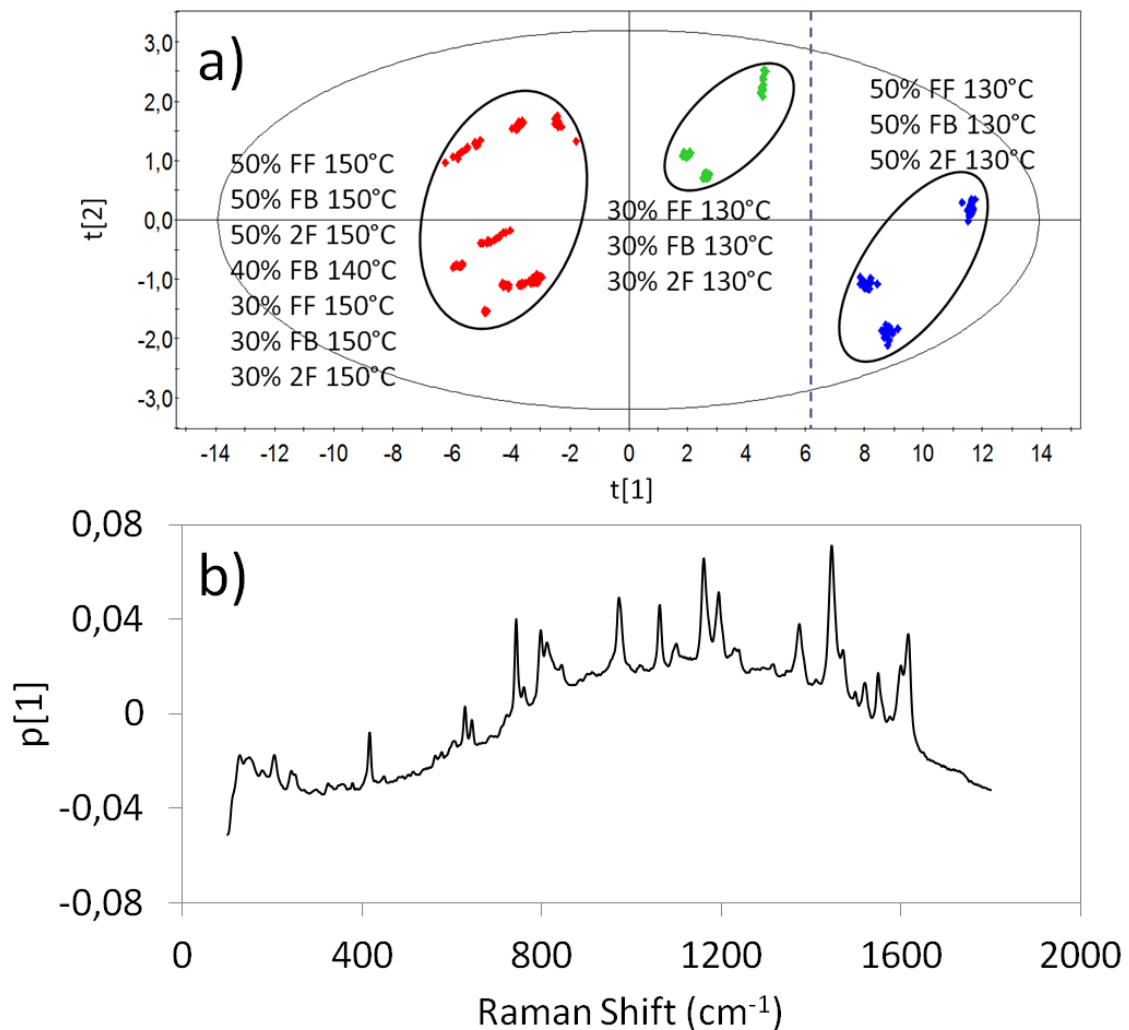


**Figure 7.5.** a) PC 1 versus PC 2 scores scatterplot obtained after PCA of the in-line collected Raman spectra and b) PC 1 loadings plot.

When the scores of PC 1 are used as responses in the experimental design (Table 7.1), only the factor temperature has a significant (negative) effect on the scores of PC 1, which captures the spectral variation related to physicochemical state of the extrudates. It is possible to create glassy solutions with 30%, 40% and 50% CEL (w/w), as long as the selected processing temperature is high enough. A negative effect of temperature on the score values for PC 1 was registered, indicating that the lower the processing temperature is, the higher the score values in PC 1 will be and thus the more crystalline CEL will be. The tested



modifications in the screw configuration did not affect the physicochemical state of the extrudates for this formulation.

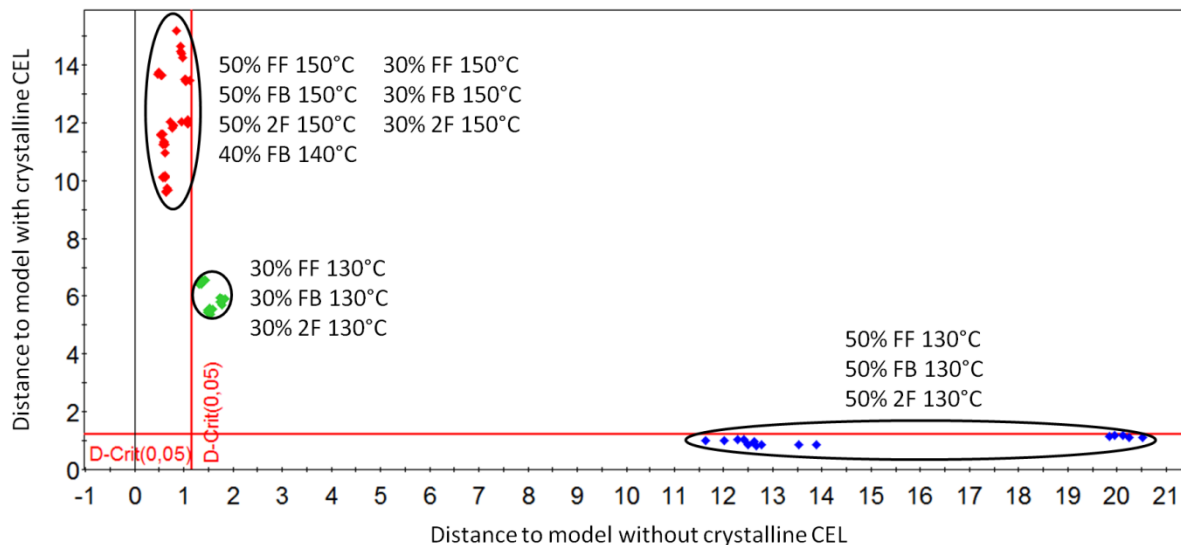


**Figure 7.6.** Coomans' plot for the validation set: Distances of the new Raman observations to the models with (y-axis) and without crystalline CEL (x-axis).

In a next step, a classification model was developed allowing the classification according to solid state of new extruded physical mixtures. Therefore, SIMCA modelling was applied. The dataset used for PCA with Raman spectra was split into two separate groups (classes) according to the off-line DSC and XRD measurements (one class where crystalline CEL is still present and a second class where no crystalline CEL was detected) and a separate PCA model was fit for each class. The class where crystalline CEL was detected in the off-line measurements contained 45 spectra (experiments 7, 9 and 11, Table 7.1) and the class where no crystalline CEL was found comprised 180 spectra (all other experiments). The class membership of a validation set containing 75 in-line collected Raman spectra (5 non subsequent spectra from each experiment) which were not used to build the model was estimated by calculating the distance to the model of these new spectra (observations). A Coomans' plot was used as a diagnostic tool to interpret the classification results of this validation set (Figure 7.6). The experiments at 130°C with 50% CEL (w/w) (experiments 7, 9 and 11, Table 7.1) are assigned to the group containing crystalline CEL, and all other experiments, with exception of the spectra collected during extrusion of 30% CEL (w/w) at 130°C (experiments 1, 3 and 5, Table 7.1), belong to the group where no crystalline CEL is detected. In-line Raman measurements do not classify the spectra of the latter as completely crystalline or without any crystallinity, since the critical distance (Dcrit, red lines)

is exceeded for both models. The Raman spectra of these three experiments showed bands which were sharper than the amorphous spectra, but broader than the crystalline spectra (Figure 7.7), indicating the presence of CEL that has dissolved into the matrix and CEL in its crystalline state. This indicates a possible higher sensitivity of in-line Raman spectroscopy to determine the physicochemical state of the extrudates compared to the off-line XRD and DSC results. This developed classification model was added to the measuring method in the SIPAT software, allowing real-time determination of the solid state in the continuously produced extrudates.

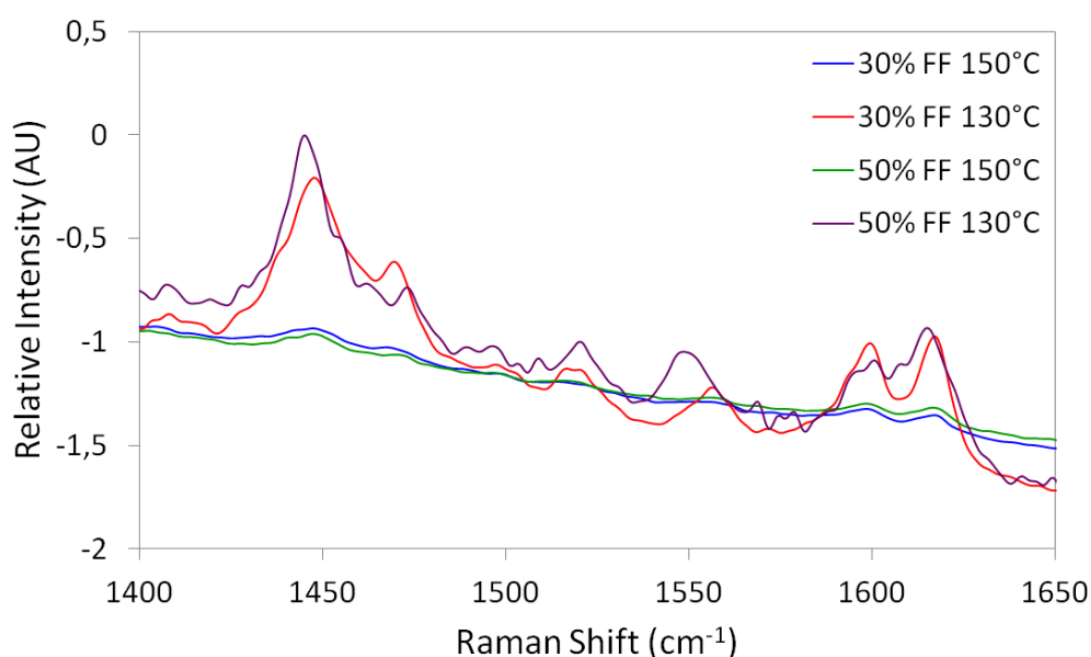


**Figure 7.7.** In-line collected Raman spectra during extrusion of 50% CEL (w/w) at 130°C (purple) and 150°C (green) and of 30% CEL (w/w) at 130°C (red) and 150°C (blue).

A Coomans' plot was calculated for the off-line XRD and DSC measurements as well (Figure 7.8a and 7.8b, respectively). Two separate PCA models were fit for each class observed in the original PCA models, i.e. a class where crystalline CEL was detected, and a class where no crystalline CEL was found. The class with crystalline CEL contained the off-line data from experiments 7, 9 and 11 (Table 7.1), and all other off-line measurements were assigned to the class without crystalline CEL. The distance to these two new PCA models for new off-line measurements performed on extrudate samples collected after each experiment was calculated and plotted. The XRD diffraction patterns show that all measurements with

exception of the three experiments with physical mixtures containing a 50% CEL concentration (w/w) that were extruded at 130°C, have a DModX lower than Dcrit for the PCA model without the crystalline data. In the Coomans' plot based on the DSC measurements, four datapoints exceed the critical distance to the model without crystalline CEL. Three of these points are the measurements conducted on extrudates containing 50% CEL (w/w) and extruded at 130°C, and the other datapoint, only slightly exceeding the limit, is the extrudate with 40% CEL (w/w).

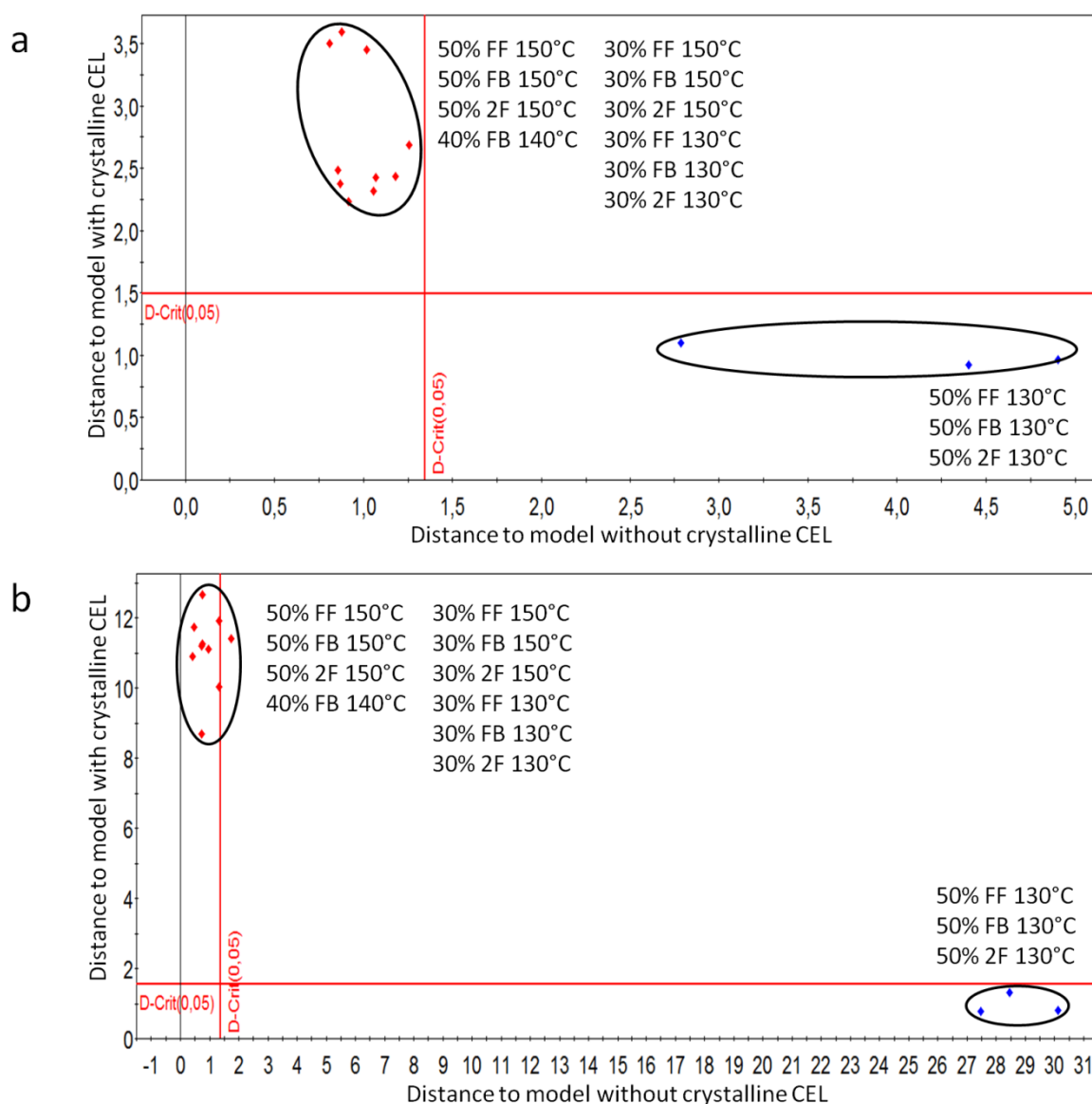


**Figure 7.8.** a) Coomans' plot for the prediction of off-line measurements: distance of the new observations in XRD (a) and DSC (b) measurements to the models with (y-axis) and without crystalline CEL (x-axis)

From each run of the experimental design, extrudate samples were collected and stored at room temperature for one year. Then, off-line Raman spectra were collected from these samples, to verify the stability of the extrudates. Principal component analysis was applied to these measurements, and the resulting PC 1 ( $R^2=0.81$ ) versus PC 2 ( $R^2=0.15$ ) scores plot (Figure 7.9a) demonstrates that the spectra collected from extrudates with 30% CEL (w/w) extruded at 130°C (experiments 1, 3 and 5, Table 7.1) and with 50% CEL (w/w) extruded at 130°C (experiments 7, 9 and 11, Table 7.1) have higher PC 1 score values than the spectra collected from all other extrudate samples. The loadings of this component (Figure 7.9b) again represent crystalline CEL. This indicates that recrystallization has occurred in the extrudates containing 30% CEL (w/w) which were extruded at 130°C. The Raman spectra for these samples show sharp bands for CEL. Therefore, the developed classification model for solid state also provides an indication of the storage stability of the extrudates.

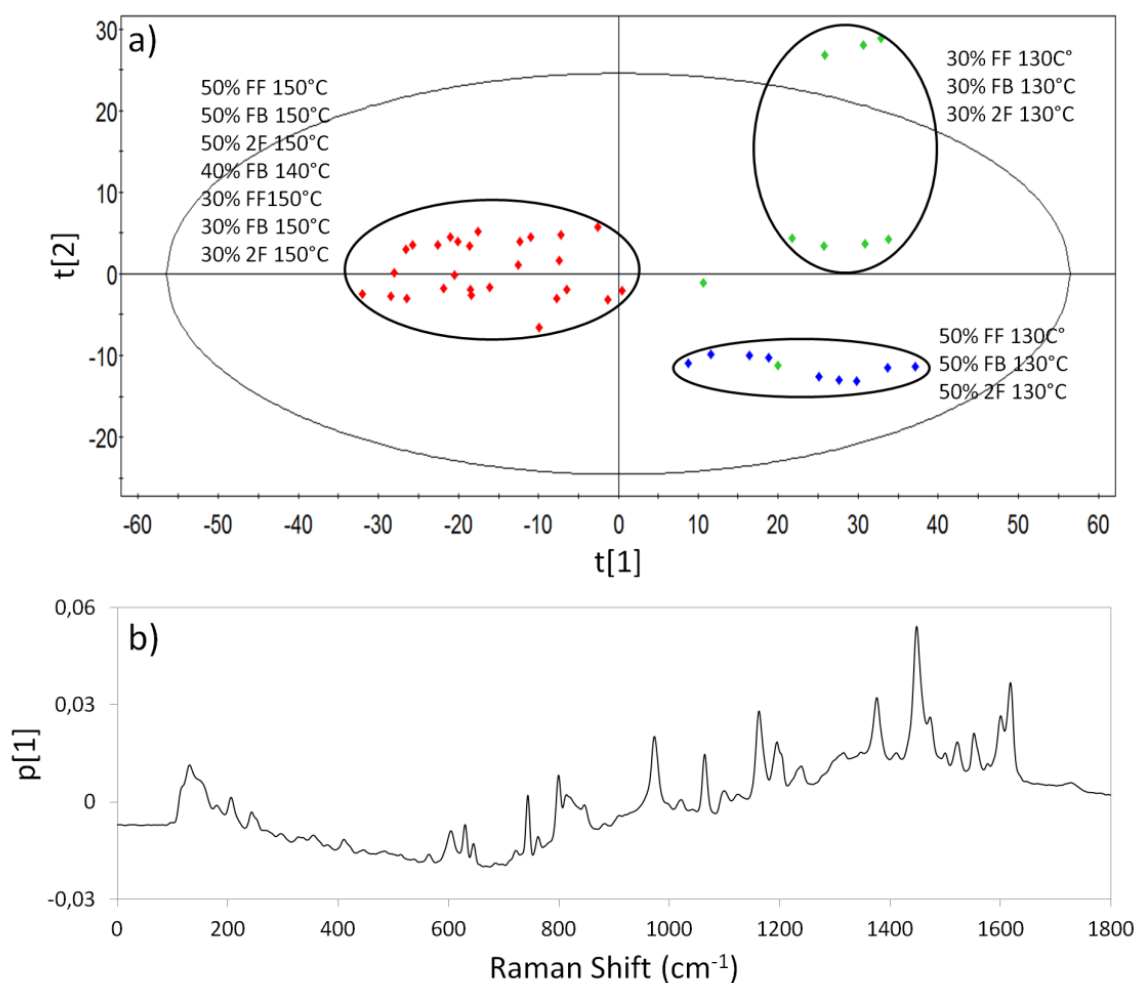


**Figure 7.9.** a) PC 1 versus PC 2 scores scatterplot obtained after PCA of the off-line collected Raman spectra after storage at room temperature for 1 year and b) PC 1 loadings plot.

### 7.3.2. Influence of die pressure on in-line collected Raman spectra

In addition to solid state properties, Raman spectra collected during extrusion in the die head also provide information on processing history. When PCA is applied on the raw spectra of all experiments in Table 7.1 (without any pre-processing), clustering in the PC 1 versus PC 2 scores plot along PC 1 according to processing temperature can be observed (Figure 7.10a). This is expressed in the Raman spectra as differences in background signal (Figure 7.10b). However, the temperature at the Raman measurement point, the die, was kept constant at 110°C, and the average monitored melt temperature in the die did not vary more than  $\pm 3^\circ\text{C}$  between all the experiments from the design (Table 7.1). On the other hand, a large variation in average die pressure can be noticed between the different experiments (Table 7.1 and Figure 7.10b). This variation is caused by two factors. First, a higher processing temperature reduces the viscosity of the melt, and lowers the die pressure. Secondly, CEL has a plasticizing effect on Eudragit® E PO [5]. The CEL molecules settle between the polymer chains and decrease the interaction between the polymer molecules. The more CEL interacts with the matrix, the lower the viscosity of the melt, resulting in the lowest die pressures when 50% CEL (w/w) is extruded at a temperature of 150°C and the highest pressures when 30% and 50% CEL (w/w) are processed at 130°C. A higher pressure at the measurement point results in a decrease in Raman intensity [15]. Possible causes for this intensity decrease are the scattering losses due to heterogeneities induced by pressure gradients, and a change of absorption coefficient with pressure. This is a general observation, and is manifested as an intensity decrease in the whole spectrum (Figure 7.10b).

Die pressure changes during hot-melt extrusion are not only related to drug concentration or processing temperatures, but can also be caused by changes in feeder performance. Since the in-line collected Raman spectra are influenced by the relative pressure in the die, Raman spectroscopy also reflects the performance of the feeding equipment during processing. PCA was applied on all Raman spectra collected during experiment number 10 from the design (Table 7.1) with a physical mixture containing 50% CEL (w/w), at a temperature of 150°C and with the FB screw configuration. The scores from the first principal component were plotted together with the feed rate and the die pressure versus process time (Figure 7.11). The

product temperature remained constant throughout the experiment and therefore did not influence the die pressure. During this extrusion experiment, Raman spectra were collected every 20 seconds. At timepoint 161 (53 minutes and 40 seconds after the start of the experiment), the feeder stopped due to insufficient filling volume. A refill was required, and the feeding unit was restarted at timepoint 168 (140 seconds later). This drop in feed rate induced almost immediately (at timepoint 162) a decrease in die pressure. This decrease in die pressure simultaneously causes a drop in the score values of PC 1 at time point 162. The Raman signal did not immediately return to its steady state value when the feed rate was increased again, but stabilized only when the die pressure stabilized. As a result, it can be concluded that pressure fluctuations in the die are reflected in the Raman spectra which are collected in the die. Hence, disturbances upstream of the extrusion process can be observed and identified in the Raman measurements.

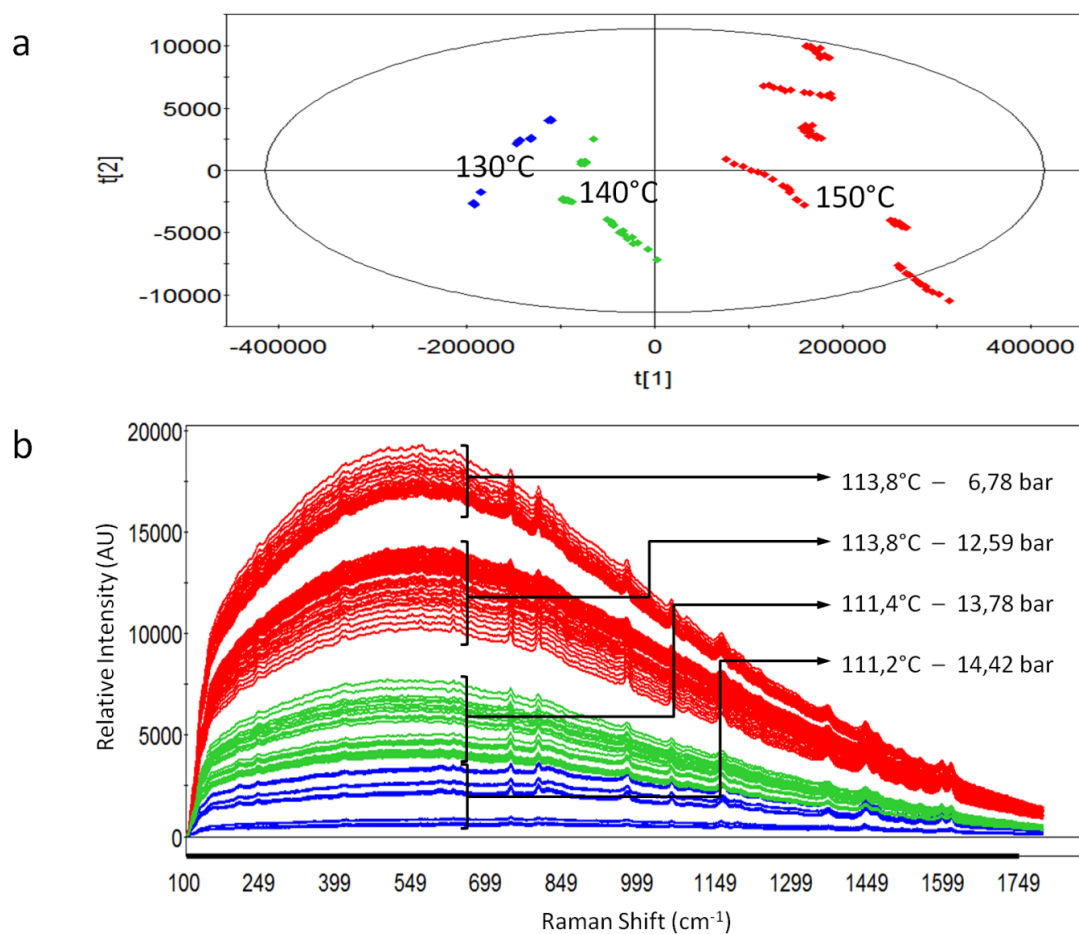


**Figure 7.10.** a) PC 1 versus PC 2 scores scatterplot obtained after PCA of the in-line collected raw Raman spectra. b) In-line collected raw Raman spectra with mean melt temperatures and die pressures.

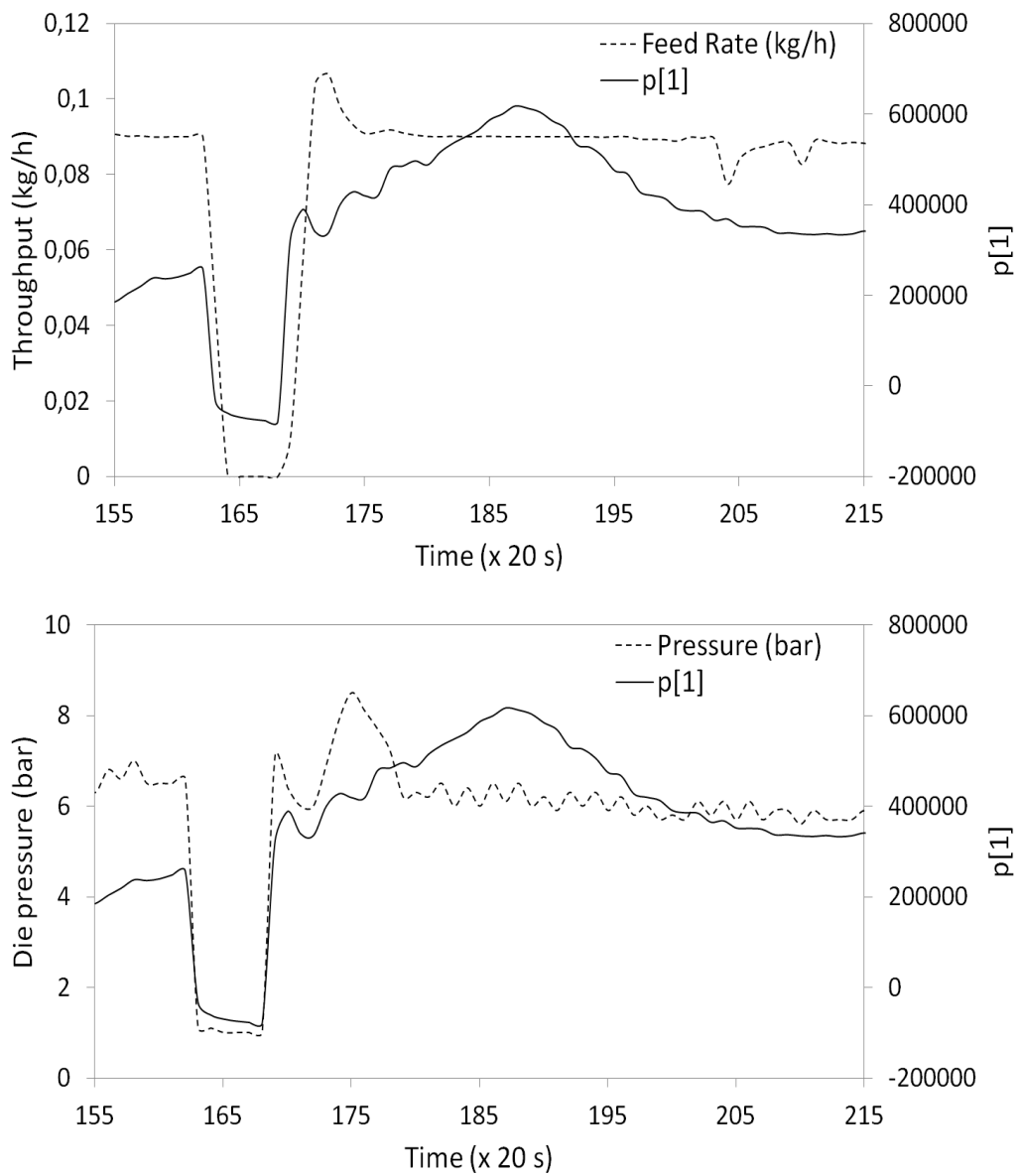


**Figure 7.11.** PC 1 score values for the Raman spectra from the first principal component plotted with the feed rate (kg/h) and the measured die pressure (bar).

## **7.4. CONCLUSION**

The results in chapter 7 demonstrate that Raman spectroscopic measurements allowed the differentiation between glassy solid solutions and crystalline dispersions. A classification model was developed to classify continuously produced extrudates according to solid state in real-time. Off-line analysis with DSC and XRD appeared not to be sensitive enough to detect small fractions of crystalline CEL that later on induced recrystallization of CEL in the extrudates during storage. This small fraction was noticed in the Raman spectra, which therefore also provided information on the stability of the extrudates. Consequently, Raman spectroscopy can be used for the monitoring of product quality during hot-melt extrusion on the development scale. Additionally, die pressure fluctuations caused by feeding disturbances upstream the extrusion process are reflected in the Raman spectra.



## 7.5. REFERENCES

- [1] C. Leuner, J. Dressman, *Eur J Pharm Biopharm* 50 (2000) 47-60.
- [2] T. Vasconcelos, B. Sarmiento, P. Costa, *Drug Discovery Today* 12 (2007) 1068-1075.
- [3] K. Dhirendra, S. Lewis, N. Udupa, K. Atin, *Pak J Pharm Sci* 22 (2009) 234-246.
- [4] S. Janssens, G. Van den Mooter, *J Pharm Pharmacol* 61 (2009) 1571-1586.
- [5] J. Albers, Hot-melt extrusion with poorly soluble drugs, Institut für Pharmazeutische Technologie und Biopharmazie, Heinrich-Heine Universität, Düsseldorf, Germany, 2008.
- [6] G.P. Andrews, O. Abu-Diak, F. Kusmanto, P. Hornsby, Z. Hui, D.S. Jones, *J Pharm Pharmacol* 62 (2010) 1580-1590.
- [7] G.P. Andrews, O.A. Abu-Diak, D.S. Jones, *J Pharm Sci* 99 (2010) 1322-1335.
- [8] L.S. Taylor, G. Zografi, *Pharm Res* 14 (1997) 1691-1698.
- [9] L. Saerens, L. Dierickx, B. Lenain, C. Vervaet, J.P. Remon, T. De Beer, *Eur J Pharm Biopharm* 77 (2011) 158-163.
- [10] T. De Beer, A. Burggraeve, M. Fonteyne, L. Saerens, J.P. Remon, C. Vervaet, *Int J Pharm* 417 (2011) 32-47.
- [11] L. Saerens, L. Dierickx, T. Quinten, P. Adriaensens, R. Carleer, C. Vervaet, J. P. Remon, T. De Beer, *Eur J Pharm Biopharm* 81 (2012) 230-237.
- [12] J. Breitzkreutz, *Pharm Res* 15 (1998) 1370-1375.
- [13] A. Forster, J. Hemenstall, I. Tucker, T. Rades, *Int J Pharm* 226 (2001) 147-161.
- [14] L. Eriksson, E. Johansson, N. Kettaneh-Wold, J. Trygg, C. Wikström, S. Wold, PLS, In: *Multi- and Megavariate Data Analysis Part I: Basic Principles and Applications*, 3<sup>rd</sup> ed., Umetrics Academy, Umeå, Sweden, 2006, p. 63-101.
- [15] G. Lucazeau, *J Raman Spectrosc* 34 (2003) 478-496.



# CHAPTER 8

## IN-LINE NIR SPECTROSCOPY FOR THE UNDERSTANDING OF POLYMER-DRUG INTERACTION DURING PHARMACEUTICAL HOT-MELT EXTRUSION

Parts of this chapter are published in:

**L. Saerens**, L. Dierickx, T. Quinten, P. Adriaensens, R. Carleer, C. Vervaet, J.P. Remon, T. De Beer. In-line spectroscopy for the understanding of polymer-drug interaction during pharmaceutical hot-melt extrusion. *European Journal of Pharmaceutics and Biopharmaceutics*, 81 (2012) 230-237.

## **ABSTRACT**

Chapter 8 evaluates the use of near-infrared spectroscopy for the in-line determination of the drug concentration, the polymer-drug solid state behaviour and molecular interactions during hot-melt extrusion.

Kollidon<sup>®</sup> SR was extruded with varying metoprolol tartrate (MPT) concentrations (20, 30, and 40% w/w) and monitored using NIR spectroscopy. A PLS model allowed drug concentration determination. The correlation between predicted and real MPT concentrations was good ( $R^2=0.97$ ). The predictive performance of the model was evaluated by the root mean square error of prediction, which was 1.54%. Kollidon<sup>®</sup>SR with 40% MPT (w/w) was extruded at 105°C and 135°C to evaluate the suitability of NIR spectroscopy for in-line polymer-drug solid state characterization.

NIR spectra indicated the presence of amorphous MPT and hydrogen bonds between drug and polymer in the extrudates. More amorphous MPT and interactions could be found in the extrudates produced at 135°C than at 105°C. Raman spectroscopy, DSC and ATR FT-IR were used to confirm the NIR observations. Due to the instability of the formulation, only in-line Raman spectroscopy was an adequate confirmation tool. NIR spectroscopy is a potential PAT-tool for the in-line determination of API-concentration and for the polymer-drug solid state behaviour monitoring during pharmaceutical hot-melt extrusion.

# CHAPTER 8

## IN-LINE NIR SPECTROSCOPY FOR THE UNDERSTANDING OF POLYMER-DRUG INTERACTION DURING PHARMACEUTICAL HOT-MELT EXTRUSION

---

### 8.1. INTRODUCTION

Hot-melt extrusion (HME) is one of the most widely used processing technologies in the plastic, food and rubber industry [1]. Recently, it also found its application in pharmaceutical manufacturing operations, offering many advantages compared to traditional pharmaceutical processing techniques [1-5] for solids: the process is anhydrous; poorly compactable materials can be incorporated into tablets; the materials have a short residence time in the extruder during processing; HME enables superior mixing (both distributive and dispersive); it allows the production of formulations with modified release; it allows masking of the bitter taste of several active pharmaceutical ingredients (API's) and in addition it improves the dissolution rate and the bioavailability of poorly water soluble drugs by the formation of solid solutions or solid dispersions [6]. A solid dispersion consists of at least two different components, generally a hydrophilic matrix and a hydrophobic drug [7]. The polymer matrix can be either crystalline or amorphous, and the drug can be dispersed molecularly, in amorphous clusters or in crystalline particles. Each of these solid states has its own properties such as storage stability, dissolution rate, etc. The degree of crystallinity or amorphism in pharmaceutical materials is recognized as a critical factor that will affect drug stability and dosage form performance [8].

Nowadays, extruders already allow in-line monitoring and control of process parameters (e.g. barrel and die temperature, powder feed rate and screw speed, torque and melt pressure in the extruder and die). In-line monitoring and control of quality parameters corresponding to the extruded product itself, such as drug load and solid state, has been performed recently with Raman spectroscopy [9], but not yet with NIR spectroscopy. Besides real-time assessment of product characteristics, in-line spectroscopic monitoring helps to increase the understanding of the product behaviour during extrusion.

Today, the intention within the pharmaceutical industry is to move from traditional batch processing towards continuous processing, hereby increasing process efficiency and production. Continuous processes are based on the one-in-one-out principle and offer many advantages: no scale-up issues resulting in a shorter development time, possible automation of the production line, reduction of production costs, faster product release, less product variability and improved product quality [10,11]. Hot-melt extrusion can be operated as a continuous process, capable of consistent product flow at relatively high throughput rates [1], making it suitable for large scale production.

The FDA has introduced the concept of Process Analytical Technology (PAT) in 2004 [12]. Pharmaceutical products must meet very strict specifications. However, conventional pharmaceutical manufacturing is generally accomplished using batch processing followed by time-consuming, expensive and less efficient off-line laboratory testing on randomly collected samples to evaluate the intermediate or end product quality. The processes themselves are not fully understood and are often inefficient black-boxes. PAT-tools such as near-infrared (NIR) spectroscopy provide in-line and real-time process information concerning critical formulation parameters, which might contribute to steering processes towards their desired state through adaptations of process settings. It is evident that continuous manufacturing needs continuous process monitoring and control.

Near-infrared spectroscopy is a fast, non-destructive analytical technique, which requires (nearly) no sample pre-treatments [13]. In the near infrared area (800-2500 nm or 12500-4000  $\text{cm}^{-1}$ ), mainly vibrations of CH, OH, NH and SH bonds are observed as overtones or combinations of the fundamental IR bands, resulting in overlapping absorption bands in the

spectra. Hence, NIR spectra are more complex and difficult to interpret compared to IR spectra. Therefore, chemometrics are often required to extract the useful information from the NIR spectra [14]. Because of its unique properties [14], like high analysis speed, no need for sample preparations, its non-destructive and non-invasive nature of analysis and the use of fibre optical probes, NIR spectroscopy is an ideal process analyzer for hot-melt extrusion. Furthermore, due to the fact that NIR spectra are sensitive to changes in hydrogen bonding and packing in the crystal lattice, NIR can be applied for solid state analysis and the understanding of molecular interactions [15].

NIR spectroscopy has been applied in-line and in the transmission mode during single-screw hot-melt extrusion to monitor the HDPE/PP [16, 17] and LDPE/PP [18] polymer melt composition in the extrusion die. Furthermore, NIR spectroscopy has been used to monitor the ethylene vinylacetate copolymer composition in the extrusion die during single-screw extrusion [19-21], and for the quantification of the copolymer composition in a polypropylene and ethylene vinyl acetate blend [22] during twin-screw extrusion. NIR has also been applied to measure the polymer melt flow index [21] in single-screw extrusion and to detect and quantify small amounts of Irganox in polypropylene [23] and  $Mg(OH)_2$  in LDPE [20] and HDPE [24] during twin-screw extrusion. In another application, NIR spectroscopy was used to monitor the content of pulverised chalk in polypropylene [22], to quantify the melamin cyanurate concentration in polyamid 12 [25] and to quantify the composition of a PE/PS blend [25] during twin-screw extrusion.

In this chapter, the suitability of NIR spectroscopy in its reflectance mode for the in-line monitoring of pharmaceutical HME processes was evaluated. Via fibre optic cables, an NIR probe was implemented in the HME equipment, to monitor the API content and the polymer-drug behaviour (solid state and molecular interactions) during hot-melt extrusion.

## 8.2. MATERIALS AND METHODS

### 8.2.1. Materials

Metoprolol tartrate (MPT) (Esteve Quimica, Barcelona, Spain) (Figure 8.1a) was chosen as a model drug. It has a melting temperature ( $T_m$ ) around 120°C. Kollidon® SR (Figure 8.1b) was kindly donated by BASF (Ludwigshafen, Germany). This amorphous polymer consists of 8 parts polyvinyl acetate (w/w) and 2 parts polyvinyl pyrrolidone (w/w). The solubility parameters of both components were calculated by SPWin, version 2.11 [26] to predict the solid state miscibility.

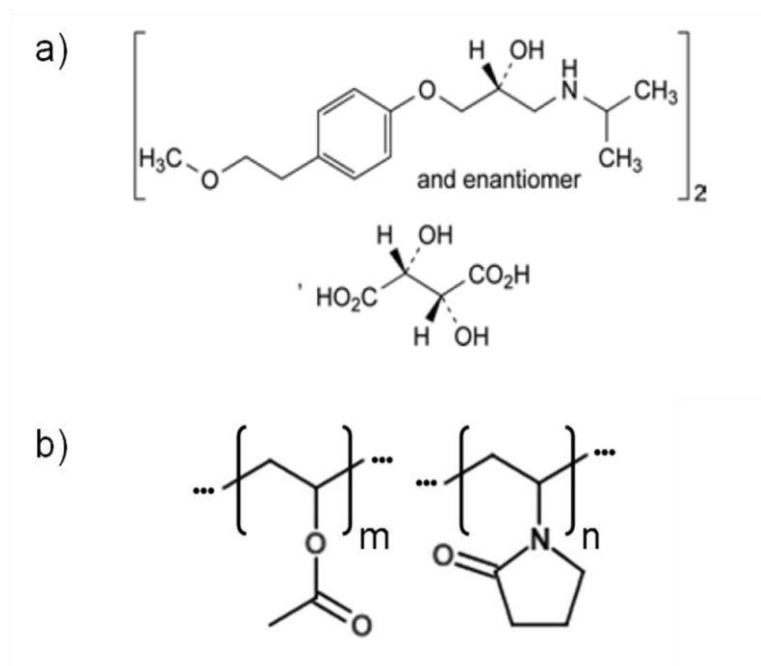


**Figure 8.1.** Molecular structures of a) Metoprolol tartrate (Ph. Eur. 7.0) and b) Kollidon® SR.

### 8.2.2. Hot-melt extrusion

Hot-melt extrusion was performed with a Prism Eurolab 16 co-rotating, fully intermeshing twin-screw extruder (Thermo Fisher Scientific, Germany). The temperature of each segment of the extruder and of the die can be controlled separately. The hot-melt extruder was equipped with a DD Flexwall® 18 feeder (Brabender® Technologie, Germany), which was set in its gravimetric feeding mode.



For the development of a calibration model allowing in-line API quantification, 3 different polymer-drug mixtures, consisting of Kollidon® SR and 20%, 30% and 40% (w/w) MPT respectively, were extruded. Prior to hot-melt extrusion, the polymer and drug were blended in a mortar. Each mixture was hot-melt extruded with a feeder speed of 0.5 kg/h and a screw speed of 80 rpm. The barrel temperature profile was set at 90-135-135-135-135-135°C (from hopper to die) for all mixtures. The minimum batch size used was 700g of polymer-drug mixture.

In a second part of the study, two identical polymer drug-mixtures were prepared to evaluate the suitability of NIR spectroscopy for in-line polymer-drug solid state characterization. Both physical mixtures contained 40% MPT and 60% Kollidon® SR (w/w), and were extruded with a powder feed rate of 0.5 kg/h and a screw speed of 80 rpm. The first mixture was extruded using a barrel temperature profile of 90-135-135-135-135-135°C, which is above the melting temperature of pure MPT. The other mixture was extruded using a barrel temperature profile of 90-105-105-105-105-105°C.

### **8.2.3. NIR spectroscopy**

Diffuse reflectance NIR spectra were continuously collected in-line and noninvasively during hot-melt extrusion using a Fourier-Transform NIR spectrometer (Thermo Fisher Scientific, Zellik, Belgium, Nicolet Antaris II near-IR analyzer) equipped with an InGaAs detector, a quartz halogen lamp, and a fibre-optic probe which was mounted in the extrusion die (Figure 8.2). Spectra were collected every 30 seconds in the 9000 – 4500  $\text{cm}^{-1}$  region with a resolution of 16  $\text{cm}^{-1}$  and averaged over 32 scans. For the monitoring of the stability of the extruded end products, spectra of the extrudates were continuously collected off-line for 20 minutes immediately after extrusion at room temperature. Here, spectra were collected every 13 seconds with a resolution of 16  $\text{cm}^{-1}$  and averaged over 32 scans.

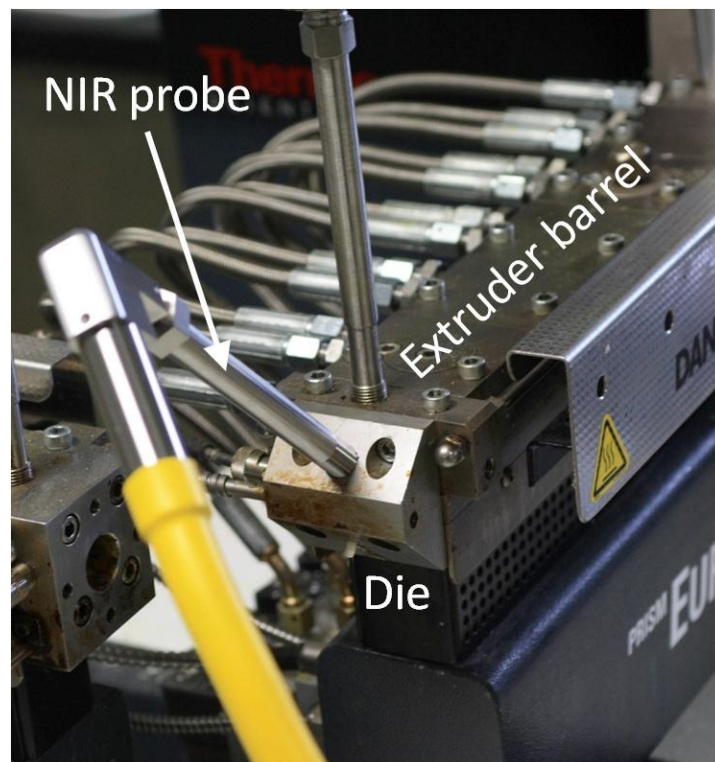


**Figure 8.2.** In-line NIR spectroscopic monitoring setup.

Data analysis was performed using the Result software (Version 3.0, Thermo Fisher Scientific, Zellik, Belgium) and SIMCA-P+ (version 12.0.1.0, Umetrics, Umeå, Sweden). Spectra collected in the diffuse reflectance mode often require spectral pre-treatment before analysis. The degree of scattering depends on the wavelength of the light and the refractive index of the sample, which causes a non-equal scatter over the whole spectrum. This can result in a baseline shift [22]. Therefore, multiplicative signal correction (MSC) was used before chemometric analysis of the spectra. Using MSC, undesired scatter is removed from the raw spectra to prevent it from dominating over the chemical information within the spectra. The result of MSC pre-processing is that each corrected spectrum has the same offset and amplitude, eliminating the difference in light scatter in the spectra from the different samples, before developing the calibration model [27]. Furthermore, second derivative pre-processing was performed after MSC correction. Second derivatives of NIR spectra magnify differences in spectral features, provide baseline normalization and remove data offsets due to scattering effects and path length variation [28]. For principal component analysis (PCA) and for the development of the partial least squares (PLS) regression model, 20 spectra of each polymer-drug mixture (20%, 30% and 40% MPT w/w) were used. Prior to PCA and PLS, spectra were mean centred. The PLS model was developed by regressing the

MPT-concentrations (Y) versus the corresponding in-line collected NIR spectra (X). This model was validated using 5 new NIR spectra collected during new extrusion runs of each polymer-drug mixture. These validation spectra were used to evaluate the predictive performance of the PLS model.

#### **8.2.4. Raman spectroscopy**

To confirm the in-line NIR polymer-drug solid state observations, Raman spectra were collected using a Raman Rxn1 spectrometer (Kaiser Optical Systems, Ann Arbor, MI, USA), equipped with an air-cooled CCD detector. A fibre-optic Raman Dynisco probe was used to monitor the extrusion process in-line. The Raman Dynisco probe was implemented into the extrusion die [9], in an identical manner as the NIR probe (see Figure 8.2). The laser wavelength was the 785 nm line from a 785 nm Invictus NIR diode laser. All spectra were recorded with a resolution of  $4\text{ cm}^{-1}$  and an exposure time of 2 seconds, using a laser power of 400 mW. Spectra were collected every 15 seconds. Data collection and data transfer were automated using the HoloGRAMS™ data collection software, the HoloREACT™ reaction analysis and profiling software, the Matlab software (version 7.1, The MathWorks Inc., Natick, MA) and SIMCA-P+ (version 12.0.1.0, Umetrics, Umeå, Sweden) was used for data analysis. The analyzed spectral region was  $0 - 1800\text{ cm}^{-1}$ , since this region contained all useful drug and polymer information. Savitzky-Golay and SNV pre-processing were applied on the in-line collected spectra to exclude inter-batch variation and variation caused by baseline-shifts, respectively.

#### **8.2.5. DSC analysis**

Differential scanning calorimetry was performed with a DSC Q 2000 (TA Instruments, Belgium). The thermograms were produced with the Thermal Advantage Release 5.1.2 software and analysed with TA Instruments Universal Analysis 2000 4.7A (TA Instruments, Belgium). Hermetically sealed aluminium pans (TA Instruments, Belgium) were used containing the samples of approximately 5 mg. Measurements were carried out in a nitrogen atmosphere. The flow rate of dry nitrogen gas was 50 mL/min. Temperature and enthalpic calibration was performed using indium as standard. Samples were subjected to three

cycles. First, the pans were heated with a heating rate of 10,0°C/min from -30°C up to 180°C in the first heating cycle. Then, a cooling cycle was started with a cooling rate of -10,0°C/min to -30°C, followed by a second and final heating cycle which was identical to the first.

#### **8.2.6. ATR FT-IR spectroscopy**

In addition to DSC analysis and Raman spectroscopy, attenuated total reflectance (ATR) Fourier transform (FT) infrared (IR) spectroscopy was also used to confirm the solid state observations in the NIR spectra. Spectra were collected from MPT and Kollidon® SR, from the physical mixture containing 40% MPT in Kollidon® SR (w/w) and from the extrudates of this physical mixture extruded at 135°C and 105°C. The ATR FT-IR spectra were collected with a Bruker Vertex 70 FT-IR spectrometer, equipped with a DTGS detector and a PIKE accessory, equipped with a diamond ATR crystal.

## 8.3. RESULTS AND DISCUSSION

### 8.3.1. In-line monitoring of API concentration

Mixtures of 20, 30 and 40% (w/w) MPT in Kollidon® SR were hot-melt extruded. Figure 8.3 shows the differences in the pre-processed in-line collected NIR spectra (6150 - 4500  $\text{cm}^{-1}$ ). PCA was applied on 60 NIR spectra (20 spectra per extruded MPT concentration level) leading to a model with two principal components covering nearly all spectral variation. The first principal component (PC 1) captures 99.0% of the variation; the second component (PC 2) covers 0.4% of extra variation. The variation captured by the first component is caused by differences in API concentration, as confirmed by the PC 1 versus PC 2 scores plot (Figure 8.4). The variation captured by the second principal component, contains only a minor part of the total spectral variation, which is not caused by differences in drug loading.

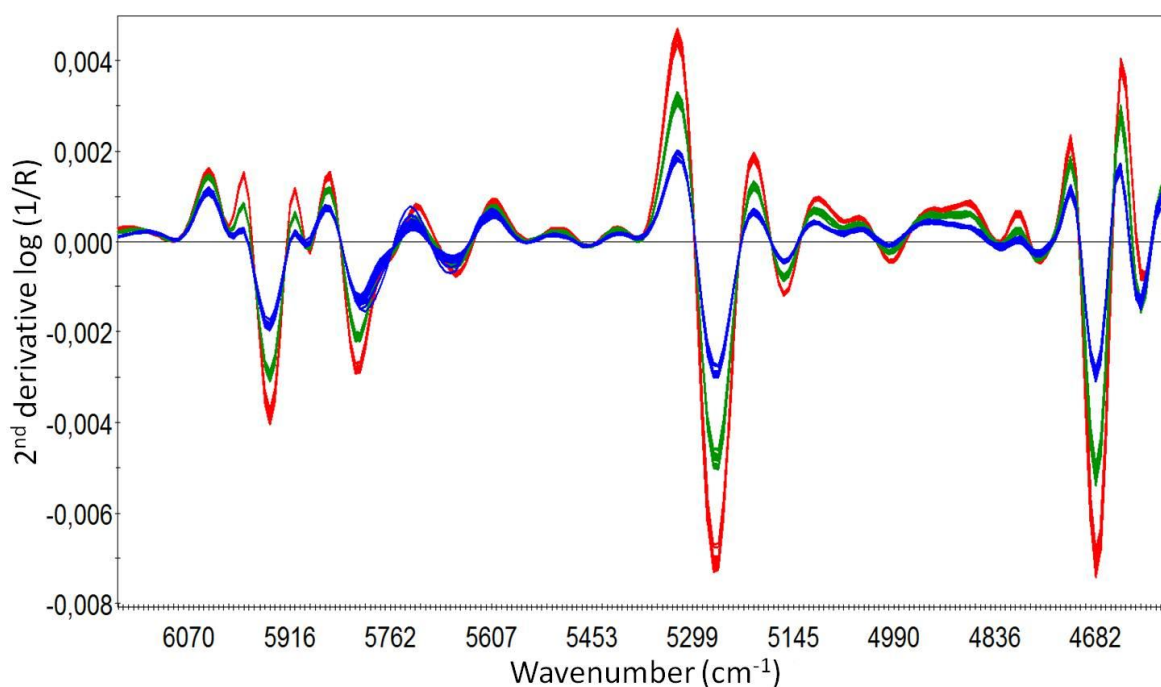


**Figure 8.3.** Pre-processed in-line collected NIR spectra of different MPT – Kollidon® SR mixtures. Red = 20% MPT, green = 30% MPT, blue = 40% MPT (w/w).

A PLS model, allowing prediction of the MPT concentration in unknown samples during hot-melt extrusion processes was developed. The in-line collected NIR spectra (X) were regressed versus the known MPT concentrations (Y). A model with two PLS components was

chosen, since the goodness of prediction of the model ( $Q^2$ ) did not increase significantly after adding extra components [27]. The predictive performance of this PLS model was evaluated using five test spectra collected during new hot-melt extrusion runs of three mixtures, also containing 20%, 30% and 40% (w/w) MPT in Kollidon® SR. The PLS model was used to predict the corresponding MPT concentrations of these 15 NIR test spectra. When plotting the predicted versus the observed MPT concentration values an  $R^2$  of 0.97 was obtained. The resulting root mean square error of prediction (RMSEP) was 1.54%. The spread in predicted concentration values was larger for mixtures containing a drug load of 20% compared to the 30% and 40% MPT mixtures (w/w). NIR absorption bands are typically broad, and due to overlapping of peaks, it is more difficult to accurately predict small drug concentrations, since the peaks of MPT are masked by larger peaks of Kollidon® SR.

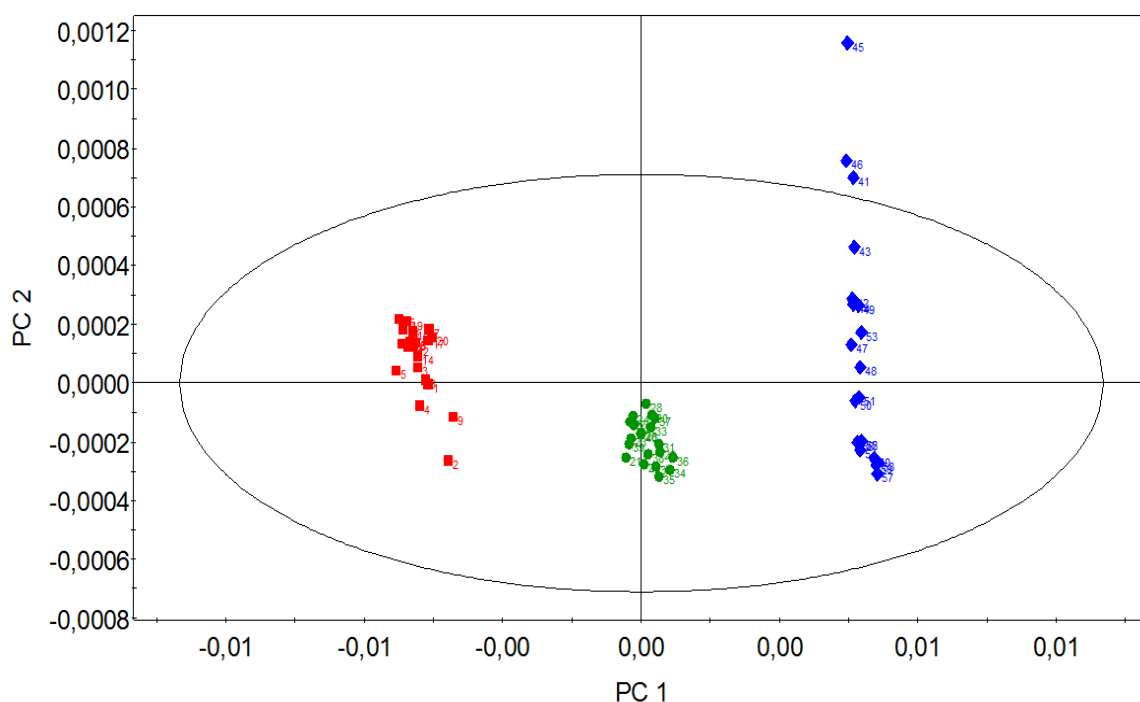


**Figure 8.4.** PC 1 (99%) versus PC 2 (0.2%) scores plot obtained after PCA on the pre-processed in-line collected NIR spectra during extrusion of mixtures containing Kollidon® SR and 20% (red), 30% (green) and 40% (blue) MPT (w/w).

### 8.3.2. In-line monitoring of solid state and polymer-drug interactions

#### 8.3.2.1. Near-infrared spectroscopy

To obtain a good compatibility between polymer and drug, the difference between solubility parameters ( $\delta$ ) of polymer and drug should be less than  $7.0 \text{ MPa}^{1/2}$  [29]. When this is achieved, miscibility is likely and, therefore, a glass solution could be formed during melt extrusion. Components with a difference in solubility parameters higher than  $10 \text{ MPa}^{1/2}$  are likely to be immiscible. The solubility parameter for MPT is  $23.6 \text{ MPa}^{1/2}$  and  $20.9 \text{ MPa}^{1/2}$  for Kollidon® SR. As the difference between these solubility parameters is  $2.7 \text{ MPa}^{1/2}$ , sufficient miscibility between Kollidon® SR and MPT may be expected.

Two mixtures containing both 40% MPT and 60% Kollidon® SR (w/w) were extruded at  $105^\circ\text{C}$  and  $135^\circ\text{C}$ , respectively. It was expected that the fraction of crystalline MPT would be larger when extrusion was performed at  $105^\circ\text{C}$ , since this temperature is below the melting temperature of MPT ( $\pm 120^\circ\text{C}$ ). At  $135^\circ\text{C}$ , more MPT was expected to transform to the amorphous state. It is evident that formulations containing a mixture of crystalline and amorphous API are not stable and therefore not desired in pharmaceutical dosage forms. However, the aim of the experiments described in this chapter was not to develop a stable pharmaceutical formulation, but to demonstrate the potential of NIR spectroscopy to monitor different states of a drug within a formulation and to detect undesired changes in the solid state of the drug during the hot-melt extrusion process.

Figure 8.5 shows the NIR spectra of the physical mixture (Kollidon® SR with a drug load of 40% MPT (w/w)) and the in-line collected spectra during extrusion of this physical mixture at  $105^\circ\text{C}$  and  $135^\circ\text{C}$ . When comparing the spectra of the extrudates to those of the physical mixture, peak shifts throughout the entire spectrum are visible (Figure 8.5a). These shifts indicate molecular interactions between polymer and drug. The shifts are smaller for the extrudate produced at  $105^\circ\text{C}$  compared to the extrudate processed at  $135^\circ\text{C}$ , suggesting more interaction between Kollidon® SR and MPT in the latter. Some of the MPT in the extrudates produced at  $135^\circ\text{C}$  (above  $T_m$  of MPT) is amorphous, which enhances interaction

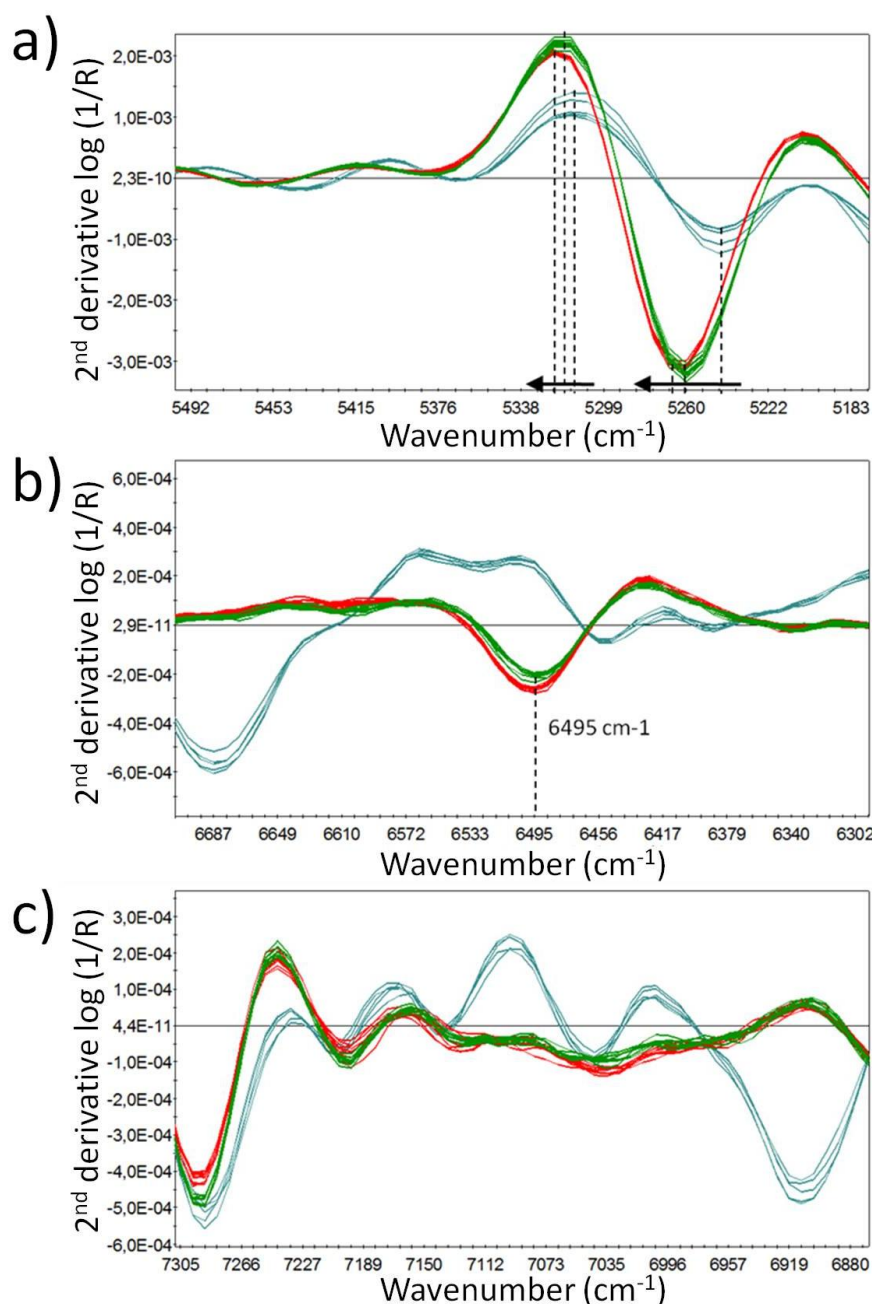


**Figure 8.5.** Pre-processed NIR spectra of the physical mixture containing 60% Kollidon® SR and 40% MPT (w/w) (blue) and of the in-line collected spectra during hot-melt extrusion at 105°C (green) and 135°C (red).

with the polymer. At 105°C (below  $T_m$  of MPT), a larger fraction of MPT remains crystalline, explaining the smaller peak shifts in the spectra of this extrudate. Polymers can improve the physical stability of drugs in solid dispersions, due to specific interactions such as ion-dipole interactions and intermolecular hydrogen bonding with functional groups of the drug [6, 30]. These interactions are confirmed by the appearance of a peak at 6495 cm<sup>-1</sup> (1540 nm) in the spectra of the extrudates (Figure 8.5b), which is absent in the spectrum of the physical



mixture. This peak indicates the formation of hydrogen bonds in which the hydroxyl groups of MPT act as proton donors. In hydrogen bonded alcohols, a broad peak manifests in the 6850 – 6240  $\text{cm}^{-1}$  region, which is attributed to the first overtone of the bonded hydroxyl [31]. At 135°C, more MPT is present in the amorphous state, which means that more MPT is free to interact with the polymer, leading to the formation of more hydrogen bonds. This explains why the peak at 6495  $\text{cm}^{-1}$  is slightly more intense in the spectra of the extrudates produced at 135°C than at 105°C.

The NIR spectra of pure MPT contain well defined, rather narrow bands. Both extrudates still contain the MPT peaks (Figure 8.5c), though they are broader, indicating that not all MPT remained in its crystalline form and that some MPT became amorphous. Broad bands indicate a lack of long-range three-dimensional order of the molecules [32]. The peaks in the extrudate at 135°C are slightly broader and less defined than at 105°C, indicating the presence of more amorphous MPT in the extrudate at 135°C. Since Kollidon® SR is an amorphous polymer, this broadening does not occur in polymer peaks. In the physical mixture, no interactions have occurred. Consequently, the peaks of MPT in the spectrum of the physical mixture remain as sharp as the original MPT peaks.

### **8.3.2.2. Differential scanning calorimetry**

DSC analysis, ATR FT-IR spectroscopy and Raman spectroscopy were used to confirm the interpretation of solid state and drug-polymer interaction from the NIR spectra. Figure 8.6a details the thermograms of the physical mixture and the extrudates of the physical mixture extruded at 105°C and 135°C. In the extrudates, the glass transition temperature ( $T_g$ ) of Kollidon® SR decreased due to the extrusion process itself, which slightly lowers the  $T_g$  of a polymer [33], and due to the plasticizing effect of MPT on the polymer, shown in Figure 8.6b. For confirmation of the NIR spectral information, data from the first heating cycle were used, whereas the data from the second heating cycle were used to confirm the plasticizing effect of MPT on Kollidon® SR. The higher the drug loading in a physical Kollidon® SR – MPT mixture, the lower the  $T_g$  in the second heating cycle of the DSC experiment. A lower  $T_g$  indicates a molecular dispersion and thus miscibility of the drug in the polymer, whereas an unchanged  $T_g$  implies separation of the polymer- and drug phase [34]. The thermogram of

the physical mixture shows a  $T_g$  at 45.4°C for Kollidon® SR (Figure 8.6a). The  $T_g$  of Kollidon® SR in the extrudates containing 40% MPT (w/w) at 105°C and 135°C is 40.2°C and 40.7°C, respectively. The chain mobility of the polymer has increased due to incorporation of MPT in the polymer matrix, which results into a decrease in glass transition temperature. However, the decrease in  $T_g$  is identical for both extrudates, suggesting that an equal level of interactions has occurred in both extrudates, which is in contrast with the NIR measurements, where a stronger peak shift in the extrudate produced at 135°C was observed.

A similar shift in the endothermal melting peak of the crystalline MPT appears (Figure 8.6a). The melting temperature of MPT in the physical mixture is measured at 120.7°C, with an onset temperature of the endothermal peak at 113.7°C. This melting peak is also present in both thermograms of the extrudates. However, the melting enthalpy for MPT in the extrudate at 135°C is much smaller than the one in the extrudate at 105°C, even though both extrudates contain 40% MPT (w/w). In the extrudate at 135°C, more MPT has transformed to the amorphous state, leaving a smaller fraction of crystalline MPT and thus a smaller area under the curve of the melting peak. The melt enthalpy for MPT in the physical mixture is 37.2 J/g. In the extrudate at 105°C, this enthalpy has reduced to 6.7 J/g, meaning that only 18.0% of the MPT is crystalline in this extrudate, assumed that MPT in the physical mixture is 100% crystalline. For the extrudate at 135°C, the amount of crystalline MPT is even lower, 9.1%, since the melt enthalpy is only 3.4 J/g. The melting points ( $T_m$ ) for the extrudates produced at 105°C and 135°C can be found at 115.7°C and 117.1°C, with onset melting temperatures of the corresponding endotherms at 109.7°C and 110.0°C respectively. Compared to the physical mixture, this shift again implies interactions between the polymer and the drug, but no variations can be seen in interaction strength between both extrudates.

The extrudates show a second  $T_g$ , at a lower temperature than the  $T_g$  of Kollidon® SR. This is the glass transition temperature of amorphous MPT, at 16.9°C and 17.0°C in the extrudates processed at 105°C and 135°C, respectively. A fraction of the MPT in both mixtures has become amorphous during processing, but has not been dispersed at a molecular level in the polymer matrix as there are 2  $T_g$ 's visible in the thermograms. Hence, the extrudates

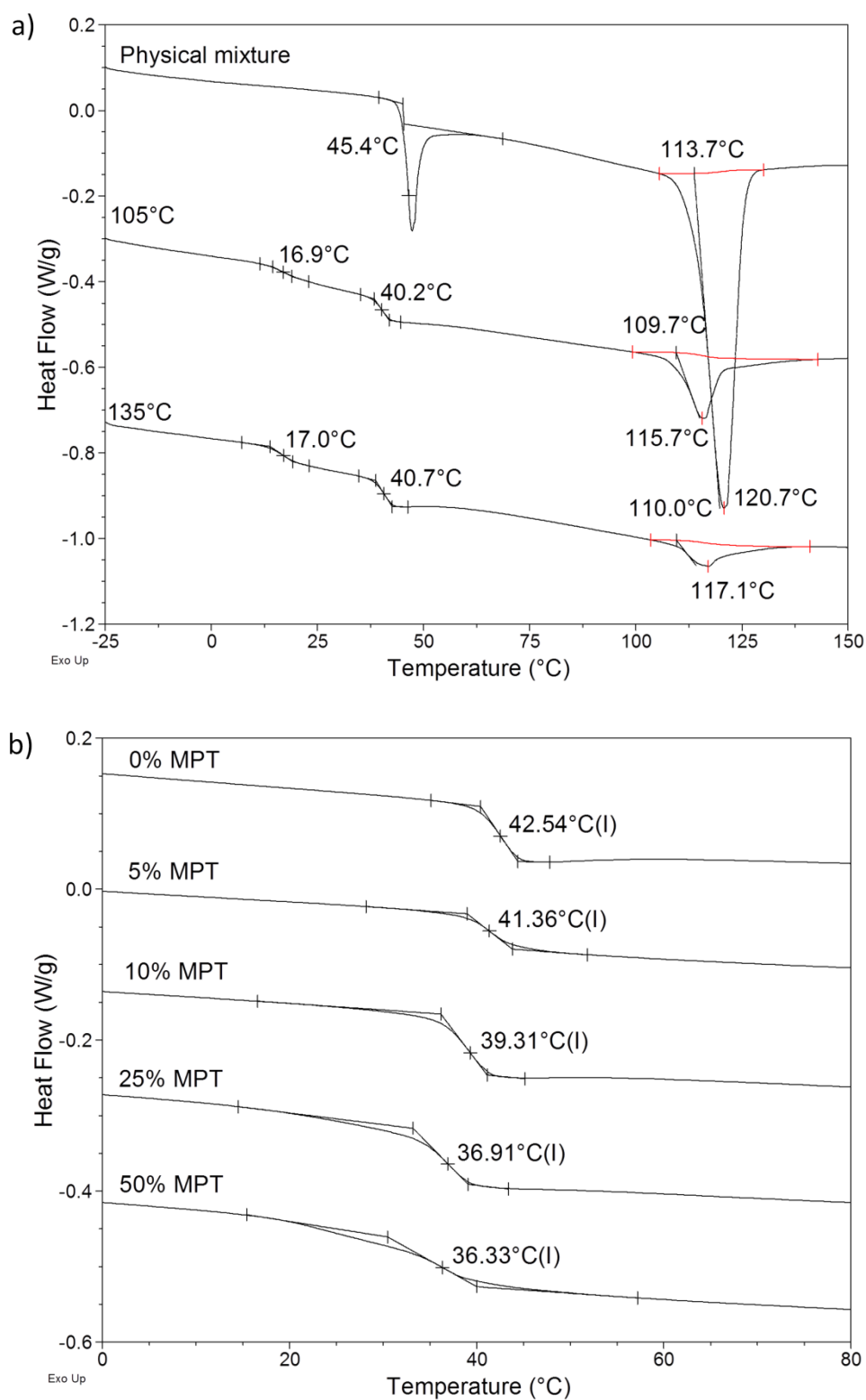


**Figure 8.6.** a) Thermograms of the physical mixture containing 60% Kollidon® SR and 40% MPT (w/w) and the extrudates produced at 135°C and 105°C. b) Effects of MPT loading (% w/w) on glass transition temperature ( $T_g$ ) of Kollidon® SR in physical mixtures.

consist of three phases: an amorphous polymer phase, an amorphous drug phase and a crystalline drug phase. These extrudates are in fact solid dispersions which are partially crystalline and partially amorphous. The free amorphous drug fraction has the tendency to recrystallize due to the poor physical stability of formulations in the amorphous state. These results do not completely confirm the in-line NIR observations. The NIR spectra suggest that more and stronger interactions occur in the extrudate at 135°C than at 105°C. However, in the DSC thermograms, no differences were obtained between both extrudates, with exception of the difference in amount of amorphous MPT.

### **8.3.2.3. ATR FT-IR spectroscopy**

Figures 8.7a and 8.7b represent the FT-IR spectra of metoprolol tartrate and Kollidon® SR respectively. The FT-IR spectrum of the physical mixture of 40% metoprolol tartrate and 60% Kollidon® SR (w/w) (Figure 8.7c) is a combination of the FT-IR spectra of the individual components (Figs. 8.7a and 8.7b). The MPT signals are sharp and the fingerprint area, 1500  $\text{cm}^{-1}$  – 600  $\text{cm}^{-1}$  shows an explicit pattern. The position of the bands in the IR spectra of the physical mixture remains unchanged compared to the corresponding bands in the spectra of the pure components. No new bands or band shifts can be seen.

The FT-IR spectra of the mixtures containing Kollidon® SR and MPT (60:40, w/w), which were extruded at a temperature of 105°C and 135°C (Figure 8.7d), result in a significantly changed FT-IR pattern compared to the spectrum of the physical mixture. The FT-IR spectrum of the extrudate produced at 105°C shows that the IR absorption bands of the polymer are more explicitly present (Figure 8.7). This indicates an association of the API with the polymer, forming coupled vibrations of MPT with the polymer. In the spectral region of 2800  $\text{cm}^{-1}$  – 3800  $\text{cm}^{-1}$ , the presence of OH stretch vibrations of alcohol groups indicates that some independent MPT molecules are still present and that not all drug molecules have interacted with the polymer. The infrared spectrum of the extrudate produced at 135°C is similar to the IR spectrum of the extrudate produced at 105°C (data not shown), showing no difference in interactions between the extrudates produced at different temperatures.

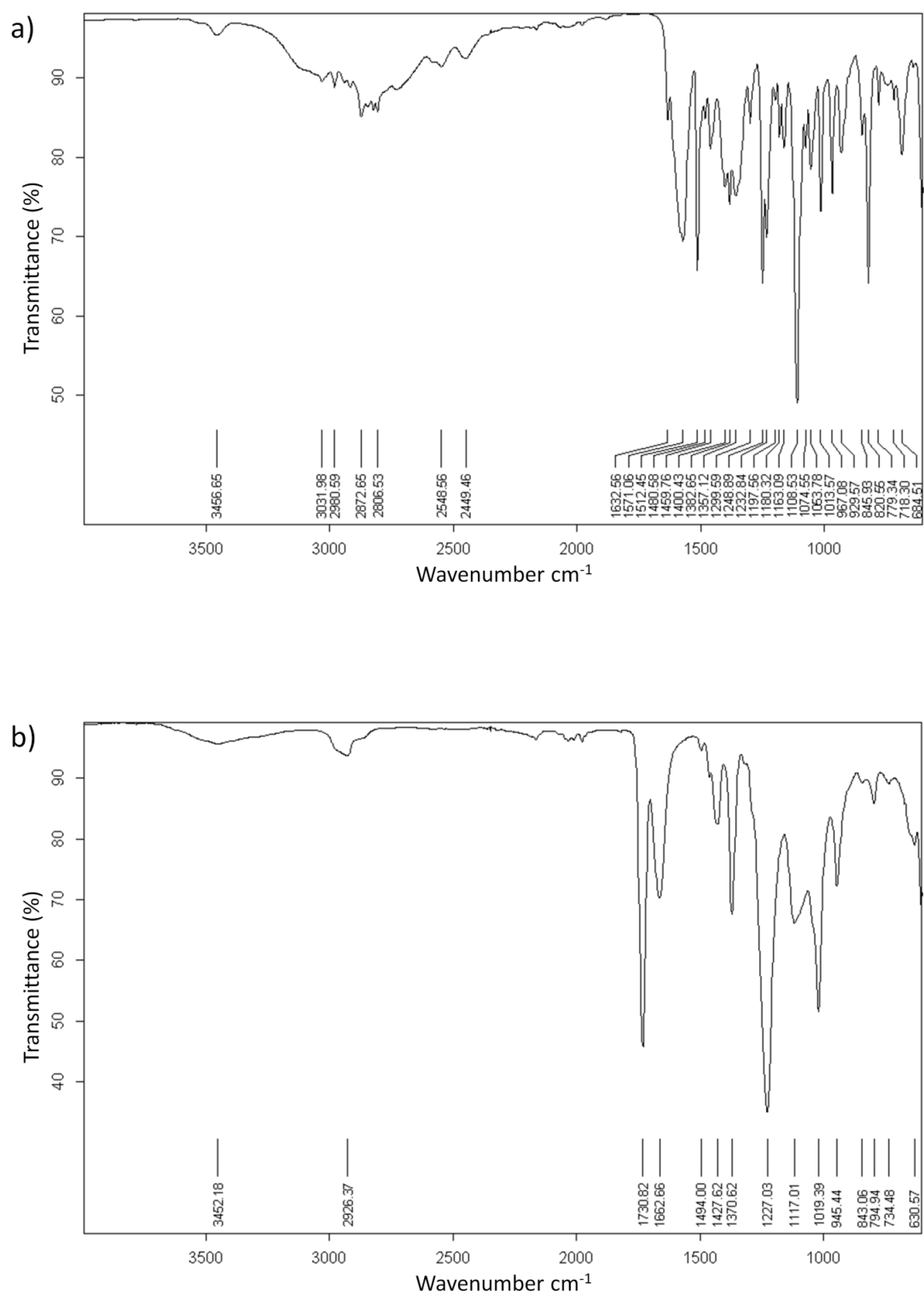
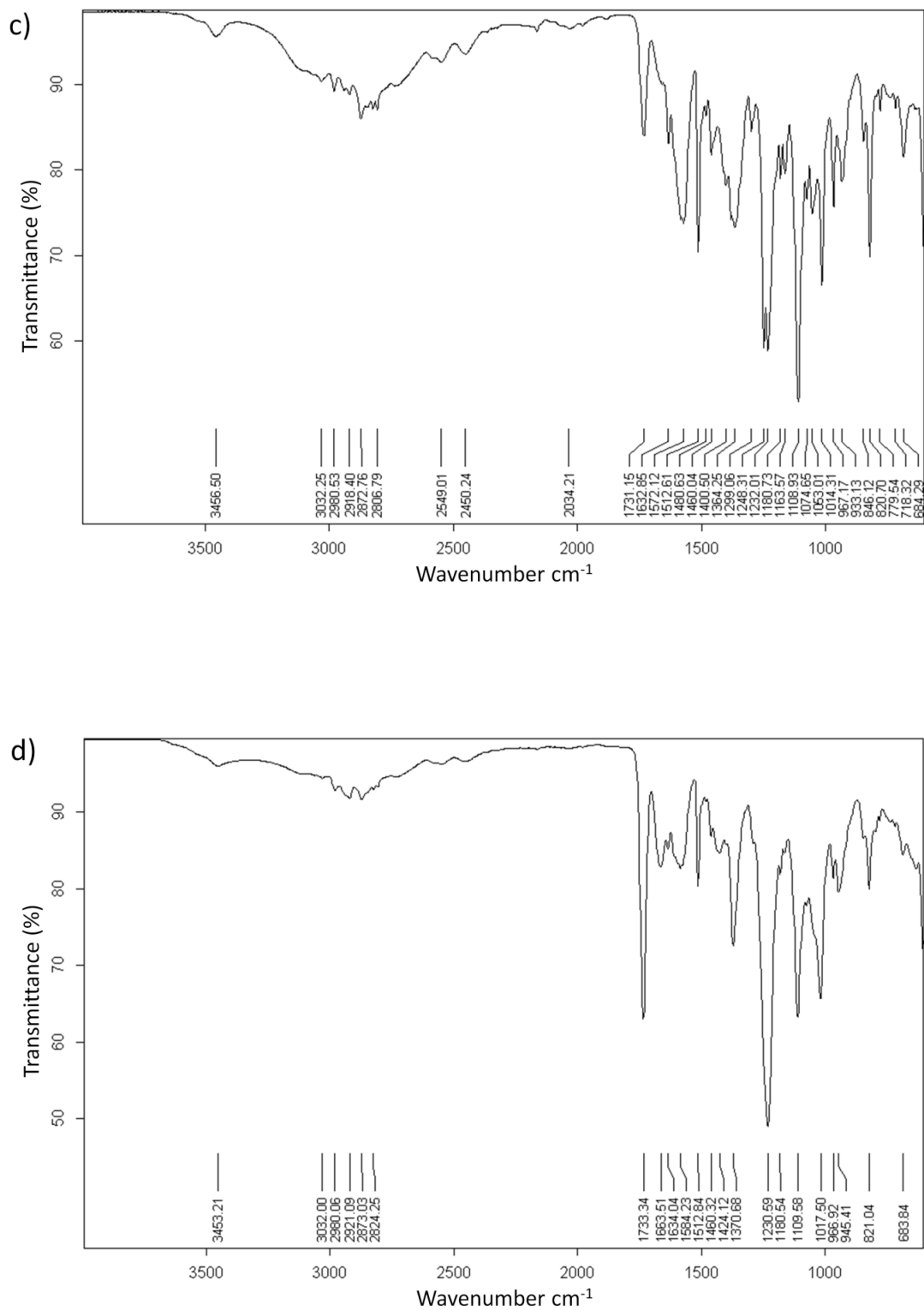


Figure 8.7. ATR FT-IR spectra of a) pure MPT, b) pure Kollidon® SR.



**Figure 8.7.** ATR FT-IR spectra of c) the physical mixture containing 40% MPT and 60% Kollidon® SR (w/w) and d) the extrudate of the physical mixture produced at 105°C.

### 8.3.2.4. Raman spectroscopy

Both DSC analysis and the ATR FT-IR results confirm each other, but none of these off-line techniques confirm the differences in interaction level and amount between the extrudates as seen with NIR spectroscopy. Figure 8.8 shows the in-line collected Raman spectra of the extrudates of the mixture at 105°C and 135°C, together with the spectrum of the physical mixture itself. The peaks of MPT broaden in the extrudates, indicating the transition from crystalline to amorphous MPT. This trend is more distinct in the spectra of the extrudates produced at 135°C, suggesting the presence of a larger fraction of amorphous MPT than in the extrudates produced at 105°C. Furthermore, peak shifts emerge in the spectra of the extrudates compared to the physical mixture. These shifts arise from changes in vibrational frequencies, caused by interactions between the polymer and the drug. Hydrogen bonding in Raman spectra can be mainly observed as a shift of the spectral bands to lower frequencies [35]. The shifts to lower Raman shifts are more explicit in the extrudates produced at 135°C, than in the extrudates created at 105°C. This confirms the NIR observations, implying that there is a difference in interaction strength between both extrudates.

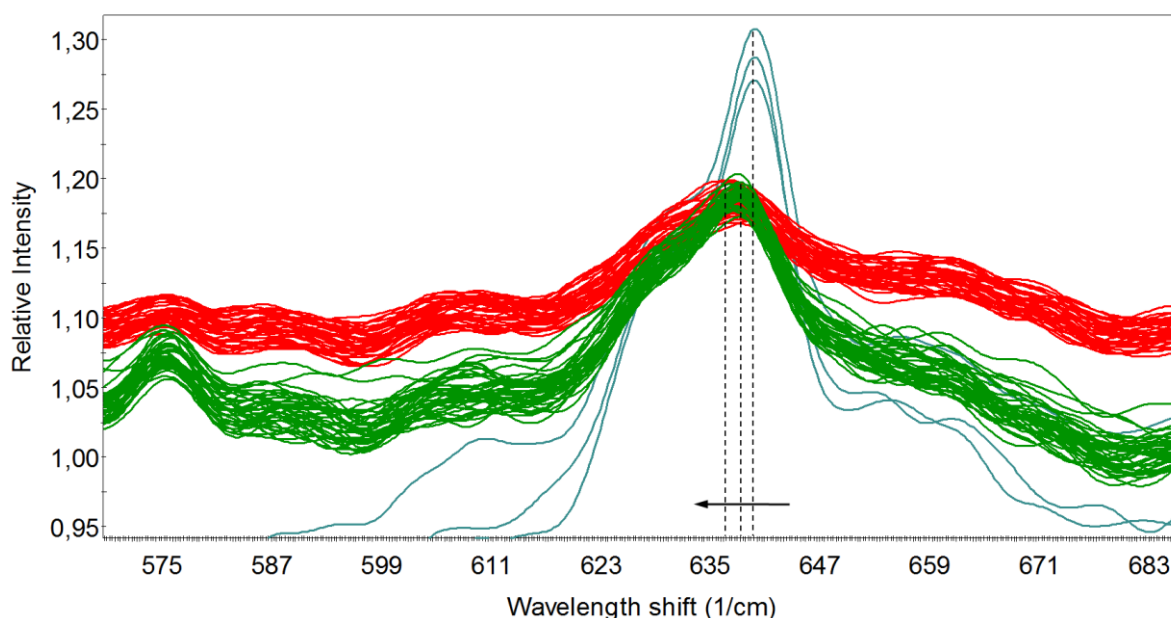


**Figure 8.8.** In-line collected Raman spectra. Blue = physical mixture (60% Kollidon® SR and 40% MPT, w/w), green = extrudate produced at 105°C, red = extrudate produced at 135°C.

It has been demonstrated that NIR spectroscopy is a more reliable technique to determine the hydrogen bond interaction level and amount for the studied formulation compared to DSC analysis and FT-IR. Furthermore, NIR spectroscopy can be used to monitor the stability over time of a certain formulation. When the extrudates produced at 105°C and 135°C were continuously monitored with NIR spectroscopy immediately after hot-melt processing, it was demonstrated that this is an unstable formulation. The extrudates were monitored for 20 minutes at room temperature (Figure 8.9). In these spectra, the peak at 6495 cm<sup>-1</sup> (1540 nm), attributed to hydrogen bonded hydroxyl groups, reduces, indicating the loss of hydrogen bond interactions between drug and polymer, and thus the separation of polymer and drug phase. The peaks in the NIR spectra attributed to MPT become more distinct and sharp, since the amorphous MPT starts to recrystallize. As recrystallization occurred rapidly, DSC analysis and FT-IR spectra were unable to differentiate between both extrudates since the sample preparation time for these techniques is longer than the time needed for the destabilization process.

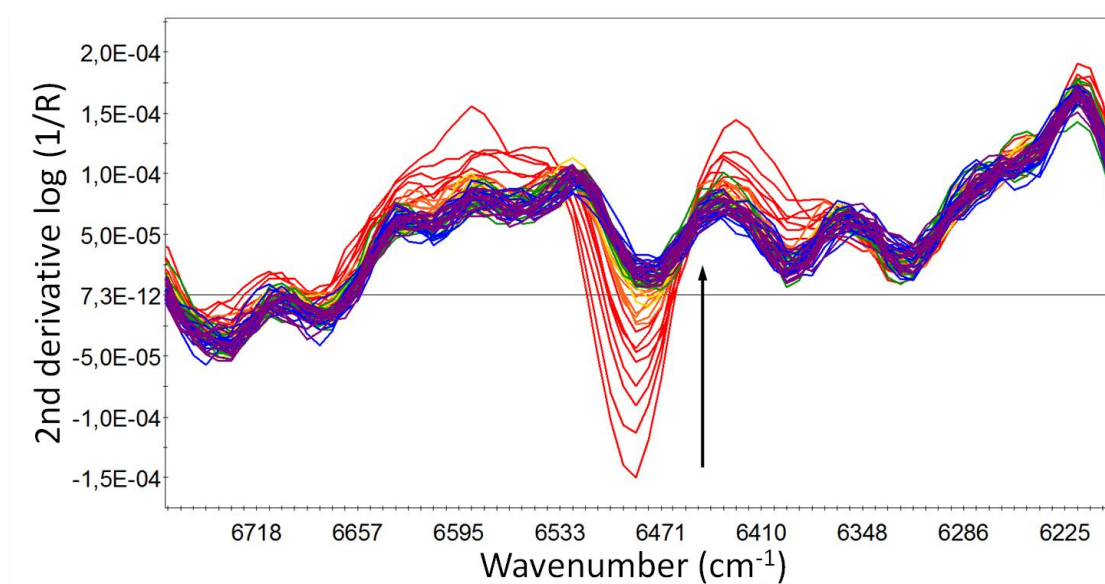


**Figure 8.9.** Pre-processed off-line collected NIR spectra of the extrudate produced at 135°C at room temperature, immediately after processing, as a function of time.



## 8.4. CONCLUSION

In this chapter, NIR spectroscopy was evaluated to monitor the API concentration and the polymer-drug melt behaviour during a pharmaceutical hot-melt extrusion process. With NIR spectroscopy, it was possible to detect variations in drug concentrations. A PLS model was developed and validated, allowing continuous drug concentration monitoring. It was possible to predict drug concentrations with an RMSEP of 1.54% (w/w).

With respect to the polymer-drug behaviour during extrusion, in-line NIR spectroscopy was able to detect changes in physicochemical state of the extrudates, as well as in amount and strength of the intermolecular interactions during processing. Furthermore, the use of NIR spectroscopy allowed the determination of the type of interactions occurring during hot-melt extrusion. These interactions are manifested as hydrogen bonds between Kollidon® SR and MPT molecules.

In-line Raman spectroscopy confirmed these NIR observations. The collected spectra displayed similar peak shifts and peak broadening, demonstrating the equivalent changes in solid state and interactions during melt extrusion. Comparison of the in-line collected NIR spectra and the off-line DSC analysis and off-line collected ATR FT-IR spectra showed that NIR is a more powerful process analyzer, able to differentiate between extrudates being processed under varying conditions, whereas DSC analysis and ATR FT-IR indicated no differences in occurring interactions between extrudates produced at different temperatures.

## 8.5. REFERENCES

- [1] R. Chokshi, H. Zia, *Iran J Pharm Res* 3 (2004) 3-16.
- [2] J. Breitenbach, *Eur J Pharm Biopharm* 54 (2002) 107-117.
- [3] M.M. Crowley, F. Zhang, M.A. Repka, S. Thumma, S.B. Upadhye, S.K. Battu, J.W. McGinity, C. Martin, *Drug Dev Ind Pharm* 33 (2007) 909-926.
- [4] M.A. Repka, S.K. Battu, S.B. Upadhye, S. Thumma, M.M. Crowley, F. Zhang, C. Martin, J.W. McGinity, *Drug Dev Ind Pharm* 33 (2007) 1043-1057.
- [5] M.A. Repka, S. Majumdar, S.K. Battu, R. Srirangam, S.B. Upadhye, *Expert Opin Drug Delivery* 5 (2008) 1357-1376.
- [6] T. Vasconcelos, B. Sarmiento, P. Costa, *Drug Discovery Today* 12 (2007) 1068-1075.
- [7] K. Dhirendra, S. Lewis, N. Udupa, K. Atkin, *Pak J Pharm Sci* 22 (2009) 234-246.
- [8] B.C. Hancock, G. Zografis, *J Pharm Sci* 86 (1997) 1-12.
- [9] L. Saerens, L. Dierickx, B. Lenain, C. Vervaet, J.P. Remon, T. De Beer, *Eur J Pharm Biopharm* 77 (2011) 158-163.
- [10] E.I. Keleb, A. Vermeire, C. Vervaet, J.P. Remon, *Int J Pharm* 273 (2004) 183-194.
- [11] C. Vervaet, J.P. Remon, *Chem Eng Sci* 60 (2005) 3949-3957.
- [12] Food and Drug Administration, Process Analytical Technology Initiative, Guidance for Industry; PAT - A Framework for Innovative Pharmaceutical development, Manufacturing and Quality Assurance, 2004.
- [13] Y. Roggo, P. Chalus, L. Maurer, C. Lema-Martinez, A. Edmond, N. Jent, *J Pharm Biomed Anal* 44 (2007) 683-700.
- [14] J. Luypaert, D.S. Massart, Y. Vander Heyden, *Talanta* 72 (2007) 865-883.
- [15] E. Räsänen, N. Sandler, *J Pharm Pharmacol* 59 (2007) 147-159.
- [16] S.E. Barnes, E.C. Brown, M.G. Sibley, H.G.M. Edwards, I.J. Scowen, P.D. Coates, *Appl Spectrosc* 59 (2005) 611-619.
- [17] P.C. Coates, S.E. Barnes, M.G. Sibley, E.C. Brown, H.G.M. Edwards, I.J. Scowen, *Polymer* 44 (2003) 5937-5949.
- [18] T. Rohe, W. Becker, S. Kölle, N. Eisenreich, P. Eyerer, *Talanta* 50 (1999) 283-290.
- [19] S.E. Barnes, E.C. Brown, M.G. Sibley, H.G.M. Edwards, P.D. Coates, *Analyst* 130 (2005) 286-292.

- [20] S.E. Barnes, M.G. Sibley, H.G.M. Edwards, P.D. Coates, *Trans Inst Meas Control* 29 (2007) 453-465.
- [21] M.G. Hansen, S. Vedula, *J Appl Polym Sci* 68 (1998) 859-872.
- [22] D. Fischer, T. Bayer, K.J. Eichhorn, M. Otto, *Fresenius' J Anal Chem* 359 (1997) 74-77.
- [23] I. Alig, D. Fischer, D. Lellinger, B. Steinhoff, *Macromol Symp* 230 (2005) 51-58.
- [24] S.E. Barnes, G.D. Smith, E.C. Brown, H.G.M. Edwards, P.D. Coates, *ANTEC* 3 (2004) 3813-3817.
- [25] D. Fischer, K. Sahre, M. Abdelrhim, B. Voit, V.B. Sadhu, J. Pionteck, H. Komber, J. Hutschenreuter, *C R Chim* 9 (2006) 1419-1424.
- [26] J. Breitzkreutz, *Pharm Res* 15 (1998) 1370-1375.
- [27] L. Eriksson, E. Johansson, N. Kettaneh-Wold, J. Trygg, C. Wikström, S. Wold, *Multi- and megavariate data analysis part I: basic principles and applications*, 3<sup>rd</sup> ed. Umetrics Academy, Umeå, Sweden, 2006.
- [28] D.E. Honigs, *Anal Instrum* 14 (1985) 1-62.
- [29] A. Forster, J. Hempenstall, I. Tucker, T. Rades, *Int J Pharm* 226 (2001) 147-161.
- [30] I. Ghebre-Sellassie, C. Martin, *Pharmaceutical Extrusion Technology*, 1<sup>st</sup> ed., Marcel Dekker, New York, USA, 2003.
- [31] L. Weyer, S.C. Lo, *Spectra – Structure Correlations in the Near-Infrared*, In: *Handbook of Vibrational Spectroscopy*, 1<sup>st</sup> ed., John Wiley and Sons, Ltd., Chichester, UK, 2006.
- [32] K. Izutsu, Y. Hiyama, C. Yomota, T. Kawanishi, *AAPS PharmSciTech* 10 (2009) 524-529.
- [33] V.B. Mathot, *Calorimetry and Thermal Analysis of Polymers*, 1<sup>st</sup> ed., Hanser Publishers, New York, USA, 1994.
- [34] S. Qi, A. Gryczke, P. Belton, D.Q.M. Craig, *Int J Pharm* 354 (2008) 158-167.
- [35] G. Socrates, *Infrared and Raman Characteristic Group Frequencies: Tables and Charts*, 3<sup>rd</sup> ed., John Wiley & Sons Ltd., Chichester, UK, 2004.



**CHAPTER 9**

**IN-LINE ULTRASOUND MONITORING OF  
DRUG CONCENTRATION DURING  
PHARMACEUTICAL HOT-MELT  
EXTRUSION**

## **ABSTRACT**

The aim of this chapter is to evaluate the suitability of ultrasonic techniques as PAT tools for the in-line monitoring of drug concentration during a pharmaceutical hot-melt extrusion process.

Physical mixtures of metoprolol tartrate (MPT) and Eudragit<sup>®</sup> RS PO were extruded with a rotational screw speed of 175 rpm, a feed rate of 0.75 kg/h and at a temperature of 110°C. Ultrasonic transit time and peak height were measured by the implementation of two ultrasound transducers in a die adapter. Die pressure and extrusion torque were also monitored during processing.

A PLS model, regressing the MPT concentrations versus the in-line measured ultrasonic transit time and peak height, was created to allow MPT concentration monitoring. A second set of experiments was performed to validate this model, resulting in a root mean square error of prediction (RMSEP) of 1.47% (w/w). When regressing the MPT content versus the monitored torque and die pressure, a similar RMSEP was obtained (1.48% (w/w)). When combining all factors (torque, die pressure and ultrasound data), an RMSEP prediction error of 0.94 % (w/w) was obtained. Ultrasound monitoring techniques are potential tools for the in-line determination of the drug content in pharmaceutical hot-melt extrusion processes.

## CHAPTER 9

# IN-LINE ULTRASOUND MONITORING OF DRUG CONCENTRATION DURING PHARMACEUTICAL HOT-MELT EXTRUSION

---

### 9.1. INTRODUCTION

In addition to optical spectroscopy, ultrasonic monitoring is one of the potential techniques for in-line monitoring and control during polymer extrusion [1]. It is a fast, robust, non-invasive and non-destructive technique which can easily be implemented in the extrusion equipment. Ultrasonic vibrations have a frequency higher than that detectable by the human ear, typically above 20 kHz. This technique has been used in polymer processing to monitor melt temperature and pressure, changes in material type, effects of process settings on rheological characteristics of the melt and filler concentration [2]. Ultrasound monitoring has also been applied to monitor residence time distributions in the extrusion die [3, 4] and at various melting, mixing and pumping zones in the barrel [3]. The melt density has been assessed using ultrasound monitoring in the extrusion die [5], and occurring melting phenomena throughout the barrel have been evaluated [6].

The results in this chapter are used to evaluate whether ultrasonic techniques, using longitudinal waves, can be applied as PAT tools for the in-line monitoring of drug concentrations in a pharmaceutical hot-melt extrusion process. During monitoring with the ultrasound technique, the velocity and attenuation of an ultrasound wave traversing a polymer melt during extrusion can be measured [7]. These values are related to the melt viscosity and elastic moduli, which are associated with the drug concentration in the polymer melt. In longitudinal waves, the oscillations occur in the direction of wave

propagation. The velocity of ultrasound waves is related to the type of waveform (longitudinal or shear), the elastic moduli and the density of the polymer melt. For longitudinal waves, the velocity is calculated by Eq. (9.1):

$$C_l = \sqrt{\left(\frac{E}{\rho} \frac{(1-\nu)}{(1+\nu)(1-2\nu)}\right)} \quad (9.1)$$

Where  $C_l$  is the velocity of the longitudinal wave,  $E$  is Young's modulus of elasticity (a proportionality constant between uniaxial stress and strain),  $\nu$  is Poisson's ratio (the ratio of radial strain to axial strain) and  $\rho$  is the density of the material. When an ultrasound wave travels through a melt, its intensity (peak height) will decrease with distance. This weakening is caused by attenuation, which includes absorption, reflection and scattering of the sound. Absorption is the main factor contributing to the attenuation of the signal. Ultrasonic velocity and attenuation vary with temperature and pressure, related to changes in elastic moduli and density with temperature and pressure. When temperature and pressure influences are constant, a change in velocity or attenuation indicates a change in extruded material, since the distance between transducers remains constant, and can be correlated to a variation in drug concentration in the melt.



## 9.2. MATERIALS AND METHODS

### 9.2.1. Materials

Metoprolol tartrate (MPT) (Esteve Quimica, Barcelona, Spain) was chosen as model drug. It has a melting temperature ( $T_m$ ) of 123°C. Eudragit® RS PO (Evonik, Germany) was used as polymer to form the matrix systems. Eudragit® RS PO is an amorphous copolymer of acrylic and methacrylic acid esters with a low content of quaternary ammonium groups, which are present as salts. It has a glass transition temperature ( $T_g$ ) of approximately 65°C. The solubility parameters of both components are 23.6 MPa<sup>½</sup> and 19.7 MPa<sup>½</sup> for MPT and Eudragit® RS PO, respectively, and were calculated with SPWin, version 2.11 [8]. Components with similar solubility parameters are likely to be miscible ( $\Delta\delta_t < 7$  MPa<sup>½</sup>) and components with  $\Delta\delta_t > 10$  MPa<sup>½</sup> are expected to be immiscible [9]. As the difference in total solubility parameter is less than 4 MPa<sup>½</sup>, a good miscibility and possible formation of a solid solution could be expected.

### 9.2.2. Hot-melt extrusion

Hot-melt extrusion was carried out with a Pharmalab co-rotating twin-screw extruder (Thermo Scientific, UK) with a screw diameter of 16 mm and length-to-diameter ratio of 40:1. The temperature of each segment of the extruder and of the die can be controlled separately. The hot-melt extruder was equipped with a gravimetric twin-screw feeder (Brabender® Technologie, Germany). For the development of a calibration model allowing in-line API quantification, different polymer-drug mixtures containing 10%, 20%, 30% and 40% (w/w) MPT in Eudragit® RS PO were extruded. Prior to hot-melt extrusion, the polymer and drug were blended in a Turbula mixer. Each mixture was extruded with a throughput of 0.75 kg/h and a screw speed of 150 rpm. The barrel temperature profile was set at 20-30-40-70-80-110-110-110-110°C (from hopper to die) for all mixtures. During extrusion, the torque (% of motor load), die pressure (bar) and melt temperature (°C) in the die were continuously monitored and logged every second.

### 9.2.3. Ultrasound equipment

Ultrasonic transit time ( $\mu\text{s}$ , used to calculate ultrasonic velocity) and peak height (V, related to attenuation and reflection) measurements were obtained from the melt using instrumentation designed at the University of Bradford (Figure 9.1), containing an ultrasonic pulser-receiver (Panametrics 5900), a sampling digital oscilloscope (LeCroy 9350AM) and automated process monitoring and analysis software. Data from the pulser-receiver were sampled using the oscilloscope at a frequency of 1 GHz and converted to form an array of voltage values representing the magnitude of the received sound wave, and time values calculated from the known trigger time and sampling frequency. The received wave was analysed using custom software employing a peak detection algorithm, to provide a measure of transit time and peak height of the first received echo. The method of operation was therefore ‘through transmission’, and the measured transit time is a total value through both the transducers and the melt. Data were acquired every second from the melt using custom-designed high temperature 3.5 MHz narrow band longitudinal wave transducers mounted directly opposite one another into the extrusion die adapter (Figure 9.2).

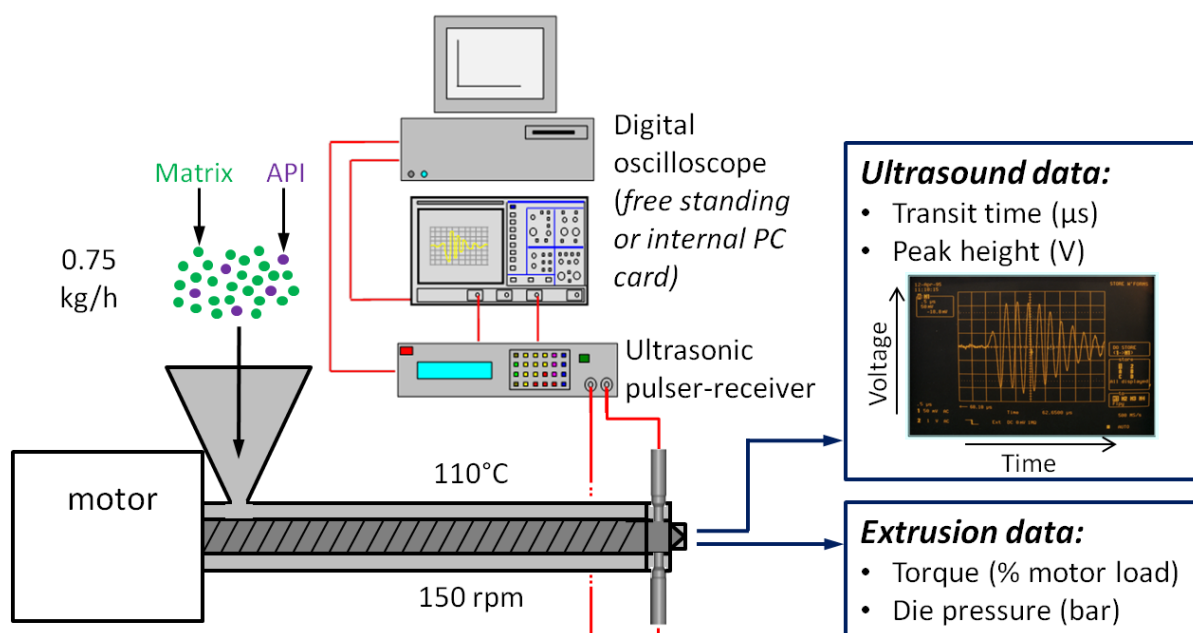


Figure 9.1. Experimental setup with instrumentation designed at the University of Bradford.



**Figure 9.2.** Experimental setup with longitudinal wave transducers mounted directly opposite one another in the extrusion die adapter. 1) Feeding unit, 2) extrusion barrel, 3) custom made die adapter, 4) ultrasound transducers.

#### 9.2.4. Data analysis

Data analysis was performed using SIMCA-P+ (version 12.0.1.0, Umetrics, Umeå, Sweden). The in-line collected ultrasound data (transit time and peak height) and/or the logged torque and die pressure measured during extrusion were used for the development of three partial least squares (PLS) regression models, which were developed by regressing the MPT-concentrations (Y) versus the corresponding in-line collected ultrasound data and/or extrusion process parameters (X). The first predictive model linked the logged extrusion parameters (torque and die pressure) to the MPT concentration, in the second model the prediction was based on the ultrasound parameters (transit time and peak height) and a third model combined both extrusion and ultrasound parameters. The predictive performance of these PLS models was validated using data gathered during new extrusion experiments of each polymer-drug mixture, with identical process settings.

### 9.3. RESULTS

Physical mixtures containing 10, 20, 30 and 40% (w/w) MPT in Eudragit® RS PO were extruded. The concentration variations were reflected in the monitored extrusion parameters, die pressure and torque, and in the ultrasound parameters, ultrasonic transit time and peak height (Table 9.1).

**Table 9.1.** Average process parameters and ultrasound parameters for each MPT concentration level.

MPT (% w/w)	Average die pressure (bar)	Average torque (% motor load)	Average melt temperature (°C)	Average transit time (μs)	Average peak height (V)
10	10.05 ±	71.78 ± 1.77	116 ± 0.24	39.202 ± 0.009	0.007 ± 0.001
20	6.15 ±	59.80 ± 1.20	113 ± 0.37	39.147 ± 0.011	0.009 ± 0.001
30	2.50 ±	48.05 ± 0.89	110 ± 0.51	39.091 ± 0.005	0.013 ± 0.002
40	1.25 ±	38.80 ± 2.78	108 ± 0.44	39.026 ± 0.005	0.016 ± 0.002

First of all, the data generated from the extrusion process were used to monitor and predict the fraction of MPT in the melt. A PLS model was developed, regressing the in-line measured torque and die pressure versus the MPT concentration. A clustering according to the MPT concentration was seen along the first principal component (Figure 9.3a), which captured 97.4% of all variation in the dataset. The validation of this predictive model with measurements performed during new extrusion experiments resulted in a root mean square error of prediction (RMSEP) of 1.48% (w/w) MPT (Table 9.2). Die pressure and torque decreased with increasing drug concentration, since MPT has a plasticizing effect on the polymer [10], making it easier to process when the MPT concentration increases.

A second PLS model was developed using the ultrasound parameters transit time and peak height as X-matrix, and the MPT concentration as Y-matrix. The first principal component, comprising 96.0% of the variation from the dataset, was related to MPT concentration

(Figure 9.3b). Validation of this second model resulted in an RMSEP of 1.47% (w/w) MPT. As the drug load in the melt increased, ultrasonic transit time decreased, and the peak height of the signal increased. When the MPT concentration in the extruded mixture increased, the average melt temperature of the melt in the die decreased (Table 9.1). This resulted in a lower free volume in the melt, increasing the intermolecular forces and thereby increasing the elastic modulus, which is represented by a higher velocity (Eq. 9.1) and thus a lower transit time [2].

**Table 9.2.** R<sup>2</sup> and RMSEP of the three different PLS models

PLS model based on:	R <sup>2</sup> (PC 1)	RMSEP
Extrusion parameters	0.974	1.48
Ultrasound parameters	0.960	1.47
Extrusion and ultrasound parameters	0.984	0.94

Finally, a third PLS model was developed combining both datasources into one matrix. The first principal component contained 98.4% of the variation from the dataset, which can be explained by differences in MPT concentration (Figure 9.3c). The combination of both ultrasound and extrusion parameters resulted in a predictive model with an RMSEP of 0.94% (w/w) MPT. The PLS biplot in Figure 9.3.c also shows clustering of the responses ultrasonic transit time, die pressure and torque. An increase in MPT concentration in the melt decreased the torque and die pressure during extrusion (Table 9.1), since MPT has a plasticizing effect on the polymer. The lower pressure increased the ultrasound velocity and therefore lowered the transit time, but also caused a decrease in attenuation of the ultrasound wave, resulting in a higher signal intensity.

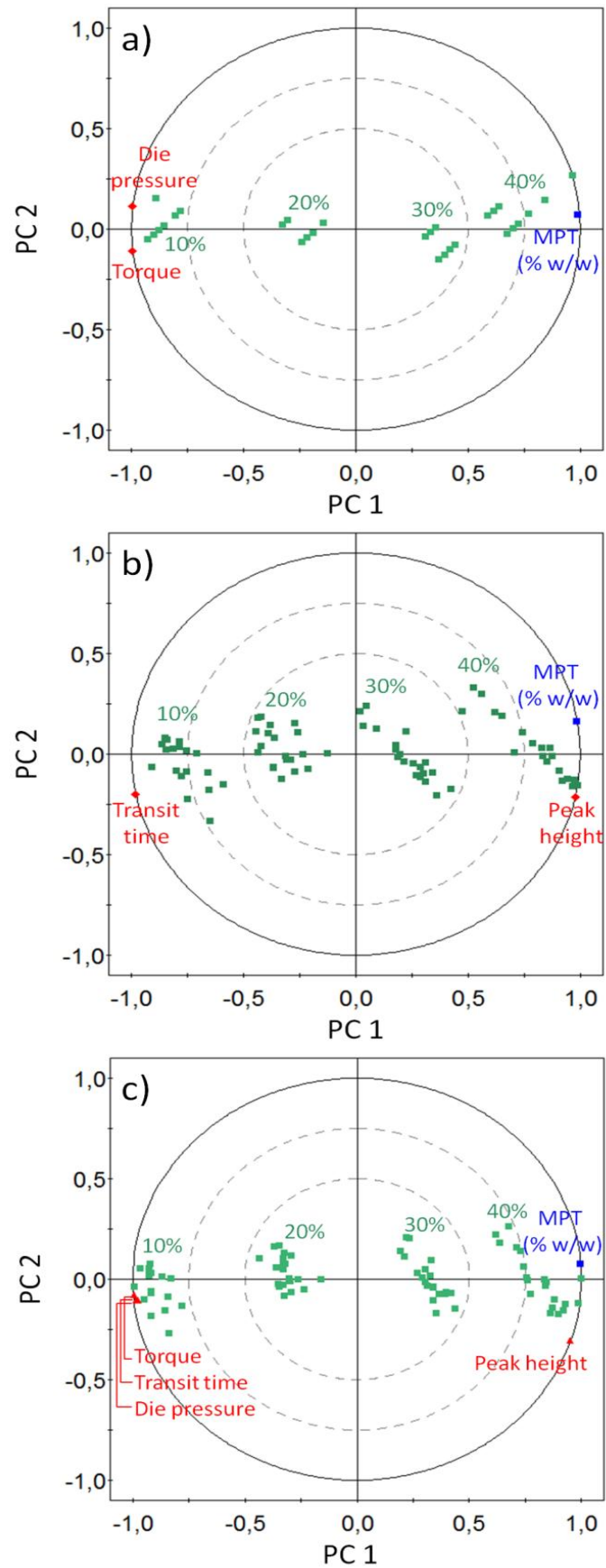


**Figure 9.3.** PLS biplots of the models developed with a) only extrusion parameters (torque and die pressure); b) only ultrasound parameters (transit time and peak height); c) both extrusion and ultrasound parameters.

## 9.4. CONCLUSION

Ultrasound monitoring techniques are potential tools for the in-line determination of the drug content in pharmaceutical hot-melt extrusion processes. The results in chapter 9 show that the use of ultrasonic techniques improved the predictive performance of the calibration model when comparing it to the model based only on die pressure and torque measurements.

The velocity of longitudinal waves through the melt can provide useful information on the elastic properties of the melt and on its density. Additionally, the attenuation also supplies information related to the concentration of the drug in the mixture during extrusion. However, both parameters are strongly influenced by temperature and pressure changes, and therefore require an extensive calibration before this technique can be applied as a monitoring tool for melt density and elasticity.

## 9.5. REFERENCES

- [1] I. Alig, B. Steinhoff, D. Lellinger, *Meas Sci Technol* 21 (2010) 1-19.
- [2] E.C. Brown, *Ultrasonic monitoring of polymer melt extrusion*, University of Bradford, Bradford, UK, 1998.
- [3] Z. Sun, C.K. Jent, C.K. Shih, D.A. Denelsbeck, *Eng Sci* 43 (2003) 102-111.
- [4] S.M. Lee, J.C. Park, S.M. Lee, Y.J. Ahn, J.W. Lee, *Korea-Aust Rheol J* 17 (2005) 87-95.
- [5] N.H. Abu-Zahra, *Int J Adv Manuf Tech* 24 (2004) 661-666.
- [6] D.B. Wang, K. Min, *Polym Eng Sci* 45 (2005) 998-1010.
- [7] R. Kažys, R. Rekuviene, *Ultragarsas* 66 (2011) 20-25.
- [8] J. Breitzkreutz, *Pharm Res* 15 (1998) 1370-1375.
- [9] A. Forster, J. Hemenstall, I. Tucker, T. Rades, *Int J Pharm* 226 (2001) 147–161.
- [10] L. Saerens, L. Dierickx, B. Lenain, C. Vervaet, J.P. Remon, T. De Beer, *Eur J Pharm Biopharm* 77 (2011) 158-163.



# FUTURE PERSPECTIVES



## FUTURE PERSPECTIVES

---

The results in this thesis demonstrate that the implementation of both Raman and NIR spectroscopy in pharmaceutical hot-melt extrusion processes allows the monitoring of drug/polymer concentration and solid state, and the visualization of solid state and interactions throughout the entire extrusion process.

The implementation of process analytical techniques in pharmaceutical hot-melt extrusion serves two purposes. The results described in this thesis regarding monitoring of solid state and interactions contribute to the first purpose of the implementation of process analytical tools in hot-melt extrusion, i.e. the improvement of process understanding by monitoring and visualizing the material behaviour. The second objective, monitoring and analyzing critical product and process parameters for process control and guaranteed end product quality, has been addressed during the development and validation of predictive models for API quantification. These models are created using data collected from a 12 or 16 mm twin-screw extruder. Both equipment types are lab scale extruders. The applicability of these monitoring models in larger, production scale extruders needs to be evaluated. To provide actual process control, the model responses from several implemented process analytical techniques, combined with the data collected from the standard sensors implemented in extrusion (temperature, pressure, torque) should trigger control loops when exceeding preset limits, to divert material with a inferior quality to waste (feed-forward control) and to allow the process to restabilize and produce extrudates with the desired quality by altering the process settings (feed-back control).

The spectroscopic process analyzers examined in this work enable the quantification of the different components in the extrudates and allow monitoring of solid state and interactions. These formulation characteristics help in defining the quality of the extrudates, but these are not the only (critical) quality attributes which need to be assessed. The application of spectroscopic techniques in extrusion can serve other purposes as well. Using spectroscopic

techniques, the detection of degradation products and reactions, the quantification and the location of formation of these products along the screws can be determined.

An additional interesting application of spectroscopic tools, since hot-melt extruded products often show modified or sustained release, is to link the drug release profiles obtained in vitro (during dissolution experiments) or in vivo to the in-line obtained process information. Since spectroscopic tools can provide information on the type and strength of interactions between drugs and polymers, it might be possible to correlate the in-line obtained spectroscopic data with the drug release profiles. Raman and NIR spectroscopy are often complementary analytical tools, and depending on the formulation used for extrusion, one technique will be more suitable than the other. Raman spectra can be strongly influenced by fluorescence and colour in the formulation, and NIR spectra, particularly in reflectance mode, contain a large amount of noise when monitoring a transparent formulation. Both tools can be applied in the reflectance or transmission mode, by using custom made die adapters, dependent on the properties of the formulation which needs to be monitored and the extrusion equipment. The transmission mode can be used to monitor across the entire melt channel, whereas the reflection mode will only monitor a fraction of the melt channel depth.

Another important (critical) characteristic of the melt is its viscosity. This is particularly relevant for further downstream processing. The melt requires a certain viscosity when being further processed to form pellets, or when injection moulding is applied. In polymer extrusion, the use of on-line rheometers (capillary, oscillatory, rotational and extensional) has been illustrated. By implementing these tools, the melt viscosity, shear stress, melt flow index, linear viscoelastic behaviour and melt strength can be evaluated. So far, these rheometers only have an on-line application, which requires elaborate adaptations to the extrusion equipment. On-line rheometers can be implemented immediately before or after the extrusion die, to assess the final rheological characteristics of the melt, but they can also be used throughout the entire barrel to determine the influence of certain kneading zones in the screw configuration on the rheological features of the melt, and to assess the effect of varying drug concentrations on these rheological parameters.

As discussed in Chapter 6, both spectroscopic and rheometric in-process measurements can provide information concerning the effect of different types of screw elements on the extruded formulation. By implementing these process analytical techniques along the extrusion barrel, the optimal screw configuration (i.e. location and number of kneading and pressure building zones) for extrusion of a certain formulation can be determined. This allows the development of the most energy-efficient screw configuration, providing both dispersive and distributive mixing with an optimal mechanical energy input.

The extrusion process on its own is only one step in a (continuous) manufacturing line. Monitoring of critical process and formulation parameters is required along the entire production process. Initially, the powder or premix feeding and liquid addition (upstream processes) need to be controlled adequately. Secondly, several downstream processes are available for further cooling, cutting, shaping and collection of the hot-melt extruded strands, and they each have a significant impact on the quality of the end product. Certain downstream process applications require the melt to be cooled. The effect of the (controlled) cooling on the quality of the extruded strands needs to be evaluated. Cooling might induce recrystallization of an amorphous drug, thereby altering its bioavailability. In addition, it also changes the viscosity of the extrudates. Other downstream equipment adds (mechanical) energy to the melt, thereby increasing its temperature, which also translates into changes in solid state and viscosity. The influence of all of these effects on the end product quality needs to be assessed, to allow production according to the 'Quality by Design' principle and to enable process control. Not only will this result in an improved product quality, but it will also enhance the process understanding and allow process optimization.



# **SUMMARY AND GENERAL CONCLUSIONS**





## SUMMARY AND GENERAL CONCLUSIONS

---

Traditionally, extruders are equipped with standard, univariate process monitoring sensors such as probes monitoring temperature and pressure, which are used to control the hot-melt extrusion process in an indirect manner by correlating the extrudate properties to these measurements. The data generated by these sensors do not suffice to assess the critical quality attributes of the extrudates, will not account for process-induced variations in material properties, cannot guarantee stable processing and are not able to ensure the production of an end product with predefined and consistent quality characteristics. Therefore, the application of spectroscopic process monitoring tools, in particular Raman spectroscopy and NIR spectroscopy, was evaluated in this thesis, to monitor, visualize and predict the drug concentration and the material behaviour of polymer-drug mixtures during hot-melt extrusion, and to improve overall process understanding.

In **Chapter 2**, the principles of hot-melt extrusion and its advantages and possible shortcomings as a non-conventional pharmaceutical manufacturing technique are discussed. Twin-screw extrusion is preferred over single-screw extrusion, since it provides a better mixing capability and allows the dispersion of an API into the polymer. Traditional monitoring and control of hot-melt extrusion processes includes the determination of barrel and product temperature, the measurement of pressure in the extrusion die, the continuous logging of torque values and the monitoring of screw speed and throughput.

The pharmaceutical industry is encouraged by several regulatory authorities to implement more advanced and innovative process analytical techniques into manufacturing processes to improve both product quality and process performance. An overview and critical evaluation of more advanced process analytical techniques (compared to the traditional monitoring sensors) for monitoring and visualizing material behaviour during processing and improving the process understanding of hot-melt extrusion is provided in **Chapter 3**. Various sensors such as spectroscopic tools, ultrasonic techniques and rheological applications are

available for observation of critical process and product parameters during extrusion. An appropriate combination of the different process analytical techniques evaluated in this chapter will lead to a thorough process understanding and will allow monitoring of the critical process and product parameters. This monitoring will eventually lead to optimization of the HME process and the formulations, and provide the possibility for improved process control in routine manufacturing.

In **Chapter 4**, the feasibility of Raman spectroscopy as a process analytical tool for the in-line monitoring and prediction of the API concentration and for the monitoring of physicochemical state of the extrudates and possible interactions between polymers and drugs during hot-melt extrusion was assessed. A Raman probe was implemented in the die of a twin-screw extruder, and spectra were collected every 5 seconds during extrusion. For the in-line API quantification, a PLS model regressing the collected Raman spectra versus the drug concentrations was developed. The predictive ability of this model was evaluated by the correlation between the predicted and real drug concentration values ( $R^2 = 0.997$ ) and the prediction error for new measurements (RMSEP = 0.59% w/w), which both demonstrated the suitability of Raman spectroscopy for the prediction of the API concentration during hot-melt extrusion. A comparison between the in-line collected Raman spectra and the off-line obtained DSC thermograms and ATR FT-IR spectra of the extrudate samples collected during processing demonstrated that information concerning the physicochemical state of a polymer-drug melt can be obtained from the Raman spectra. Broadening of peaks in the spectra indicated that the drug was present in its amorphous state, and the manifestation of peak shifts for both peaks corresponding to the API and to the polymer demonstrated that interactions between both components occurred during hot-melt extrusion.

Once the suitability of Raman spectroscopy to monitor the API concentration during hot-melt extrusion was evaluated, an advanced validation strategy for the Raman spectroscopic drug quantification method was applied in **Chapter 5**. Different models for the prediction of the API content were compared, based on the use of single spectra or averaged spectra, and using partial least squares regression or multivariate curve resolution. The predictive models were developed by extruding and monitoring five calibration mixtures, each with a different

API concentration and were validated using five other validation mixtures, each extruded on three different days by two different operators. For the validation of the different models, the accuracy profiles of the analytical procedures were calculated, based on the  $\beta$ -expectation tolerance intervals and the concept of total error (bias + standard deviation). For each of the validated API concentrations, the  $\beta$ -expectation tolerance intervals were calculated. These intervals allowed the determination of the proportion of future measurements (set at 95%) that will be found within preset acceptance limits, which were set at 10% of the relative bias. The model developed using averaged spectra and multivariate curve resolution was the only model which guaranteed that 95% of future concentration measurements will not deviate more than 10% from the reference value. The model showed good precision, trueness, linearity, specificity and accuracy over the applied concentration range. The robustness of the developed predictive model was evaluated via an experimental design varying throughput, screw speed and barrel temperature. No significant influence of any of these process settings on the predicted concentration values was found. The uncertainty of the measurements was assessed via the uncertainty of bias and the expanded uncertainty at each concentration level. The uncertainty measurements for this model showed that the unknown true value can be found at a maximum of  $\pm 7.00\%$  around the measured result, with a confidence level of 95%.

In **Chapter 6**, the Raman probe was implemented in each section of the extrusion barrel, to enhance the understanding of material behaviour during hot-melt extrusion. The influence of variations in drug concentration, barrel temperature and screw speed on the polymer-drug solid state and interactions was examined. Since hot-melt extrusion is a starve fed process, the barrel will not be completely filled with material in every segment. This causes a background signal in the in-line collected Raman spectra, which could not be corrected for. Principal component analysis was applied to separate this source of variation in the spectra from the relevant information. When a formulation with a high drug load was extruded, melting of the drug occurred in the first kneading zone, located between barrel sections 2 and 3. This was the same for a low drug load. However, an additional spectral difference was found when the melt passed through a third kneading zone, where the drug dissolved into the polymer and a solid glassy suspension was produced due to the high shear forces applied on the mixture. In the Raman spectra, this was indicated by the presence of peak shifts, and

it was confirmed by FT-IR spectra collected from samples gathered from the extrusion barrel. When extruding mixtures with a low drug load, increasing the processing temperature did not influence the solid state of the final product or the location in the barrel where the final product is attained. At a high drug load however, the solid state of the end product is reached further down the barrel when the temperature is decreased. Doubling the screw speed when processing a formulation with a low drug load did not affect the solid state of the product or the location in the barrel where it is obtained. In contrast, at a high drug load, the section where the final product is produced, is situated earlier in the barrel when applying a higher rotational speed. The performed in-barrel measurements provide real-time information about polymer/drug behaviour throughout the barrel, hence allowing the optimization of process settings and barrel and screw design required to obtain extrudates with predefined, constant solid state characteristics.

The aim of the experimental work discussed in **Chapter 7**, was to classify extrudates in-line according to their solid state. A Raman probe was implemented in the die head of an extruder, and collected spectra every 20 seconds. The influence of variations in drug concentration, changes in barrel temperature and three different screw configurations on the physicochemical state of the extrudates was assessed. Soft independent modelling of class analogy was performed to develop a model which allowed distinction between glassy solid solutions and crystalline dispersions of a poorly soluble API in a polymer, based on the in-line collected Raman spectra. Off-line analysis with DSC and XRD appeared not to be sensitive enough to detect small fractions of crystalline drug, which can later on induce recrystallization of all of the API during storage. These small crystalline fractions were detected in the Raman spectra, where the solid state characterization was based on the appearance of peak broadening and peak shifts. Modifications in screw configuration did not affect the solid state of the final products.

The influence of die pressure on the Raman spectra was also examined in **Chapter 7**. The applied drug concentration, processing temperature and feeder performance all influence the die pressure, and this effect can be found in the background signal of the Raman spectra before pre-processing. Disturbances in the feeding process can thus be observed and identified in the Raman measurements.

In **Chapter 8**, the suitability of NIR spectroscopy for the in-line determination of the drug concentration, the polymer-drug solid state and molecular interactions during extrusion was evaluated. The NIR probe was mounted in the extrusion die, and NIR spectra of the melt were collected every 30 seconds. A PLS model was developed for in-line API concentration monitoring. A good correlation between predicted and real drug concentrations was found ( $R^2 = 0.97$ ), and the prediction error for new measurements was 1.54% (w/w). The in-line collected NIR spectra showed peak broadening during extrusion, caused by the presence of amorphous API, and a new peak was found, which was not present in the spectra from the physical mixtures, indicating the formation of hydrogen bonds during processing.

In **Chapter 9**, the aim was to evaluate the suitability of ultrasonic techniques as process analytical tools for the in-line monitoring of the API concentration. Ultrasonic transit time and peak height were measured by the implementation of two ultrasound transducers in a custom made die adapter. First, a PLS model for quantification was developed based solely on the monitored die pressure and torque. It was demonstrated that adding the transit time and peak height monitored using ultrasonic techniques improved the predictive ability of this PLS model.



# **SAMENVATTING EN ALGEMEEN BESLUIT**





# SAMENVATTING EN ALGEMEEN BESLUIT

---

De procescontrole bij hot-melt extrusie wordt traditioneel uitgevoerd met behulp van standaard technieken die univariate data opleveren, zoals probes die de temperatuur en druk meten. Deze worden gebruikt om het extrusieproces op indirecte wijze onder controle te houden, door de geregistreerde parameters te correleren met bepaalde eigenschappen van het extrudaat. De metingen die door deze sensoren uitgevoerd worden, volstaan niet om de kwaliteit van extrudaten te bepalen, meten geen variaties in materiaaleigenschappen die veroorzaakt worden door veranderingen in het extrusieproces, kunnen geen stabiel proces garanderen en zijn ontoereikend om een eindproduct met een vooropgestelde en onveranderlijke kwaliteit af te leveren. Daarom werd in deze thesis het gebruik van spectroscopische technieken onderzocht, voornamelijk de toepassingen van Raman spectroscopie en nabije-infraroodspectroscopie, om de geneesmiddelconcentratie en het gedrag van materialen tijdens extrusie te monitoren, te visualiseren en te voorspellen, en om de algemene kennis van het extrusieproces te verbeteren.

In **Hoofdstuk 2** worden de principes van hot-melt extrusie, samen met de voordelen en eventuele tekortkomingen van de techniek als farmaceutisch productieproces beschreven. Dubbele-schroef extrusie wordt verkozen boven enkele-schroef extrusie, door de betere mengeigenschappen die het dispergeren van het geneesmiddel in het polymeer mogelijk maken. Het monitoren en controleren van het extrusieproces gaat gebruikelijk gepaard met het bepalen van de temperatuur van het mengsel en de schroefkamer, het meten van de druk in de matrijs, het continu monitoren van de torsie, de schroefsnelheid en de snelheid waarmee het fysisch mengsel gevoed wordt.

De regelgevende instanties moedigen de farmaceutische industrie aan om geavanceerde en innovatieve proces analytische technieken te gebruiken in productieprocessen om de kwaliteit van de ontwikkelde producten en de prestaties van de processen te perfectioneren. **Hoofdstuk 3** geeft een overzicht en kritische evaluatie van meer geavanceerde en

efficiëntere technieken (in vergelijking met de traditionele sensoren) die kunnen gebruikt worden om het gedrag van materialen tijdens extrusie te monitoren en om het extrusieproces beter te begrijpen. Een gevarieerd aanbod aan sensoren, zoals spectroscopische technieken, ultrasone technieken en reologische toepassingen zijn voorhanden om kritische proces- en productparameters te observeren tijdens extrusie. Een geschikte combinatie van de technieken die in dit hoofdstuk beschreven worden, zal leiden tot een verbeterd inzicht in het extrusieproces en laat het determineren van kritische proces- en productparameters toe. Dit zal uiteindelijk de optimalisatie van het extrusieproces en de geëxtrudeerde formulaties bevorderen, en maakt een verfijnde procescontrole in routineproductie mogelijk.

In **Hoofdstuk 4** werd de toepasbaarheid van Raman spectroscopie als proces analytische techniek geëvalueerd voor het *in-line* monitoren en voorspellen van de geneesmiddelconcentratie en voor het monitoren van de fysicochemische eigenschappen (amorficiteit, kristalliniteit, de manier waarop het geneesmiddel gedispergeerd is in de matrix) van de extrudaten en eventuele interacties tussen polymeren en geneesmiddelen tijdens extrusie. Een Raman probe werd ingebouwd in de matrijs van een dubbele-schroef extruder, en Raman spectra van het mengsel tijdens extrusie werden elke 5 seconden opgemeten. Voor de *in-line* kwantificatie werd een PLS model ontwikkeld. Het voorspellend vermogen van dit model werd geëvalueerd aan de hand van de correlatie tussen de voorspelde en 'echte' geneesmiddelconcentraties ( $R^2 = 0.997$ ) en aan de hand van de predictiefout voor nieuwe metingen (RMSEP = 0.59% w/w), die beiden de geschiktheid van Raman spectroscopie voor concentratiewaarnemingen tijdens extrusie bevestigen. Een vergelijking tussen *in-line* opgenomen Raman spectra en *off-line* resultaten van de DSC- en XRD-analyses toont aan dat de Raman spectra informatie bevatten over de fysicochemische eigenschappen van een polymeer-geneesmiddel mengsel tijdens extrusie. Het verbreden van pieken in het spectrum wijst op de overgang van het geneesmiddel van een kristallijne naar een amorse toestand, en de aanwezigheid van piekverschuivingen voor zowel pieken eigen aan het geneesmiddel als aan het polymeer duidt op het ontstaan van interacties tussen beide componenten in het mengsel tijdens extrusie.

Nadat aangetoond werd dat Raman spectroscopie kan gebruikt worden om de concentratie van het geneesmiddel te bepalen tijdens extrusie, werd een verfijnde validatiestrategie toegepast op de kwantificatiemethode gebaseerd op Raman spectroscopie in **Hoofdstuk 5**. Verschillende voorspellende modellen, opgebouwd uit de enkelvoudige of gemiddelde spectra, en ontwikkeld via PLS of MCR, werden met elkaar vergeleken. De Raman spectra die gebruikt werden om de voorspellende modellen op te stellen, werden verzameld tijdens extrusie van vijf verschillende kalibratiemengsels met elk een andere geneesmiddelconcentratie, en gevalideerd met vijf validatiemengsels, geëxtrudeerd op drie verschillende dagen door twee operatoren. Voor de validatie van deze methoden werd het totale-fout-profiel voor elke methode berekend, gebaseerd op de ' *$\beta$ -expectation tolerance intervals*' en het concept van de totale fout (= bias + standaarddeviatie). Voor elke gevalideerde concentratie werd het ' *$\beta$ -expectation tolerance interval*' bepaald. Met behulp van deze intervallen kan het aantal toekomstige metingen (ingesteld op 95%) dat binnen vooropgestelde acceptatielimiten (10% relatieve bias) zal vallen, geschat worden. Het model ontwikkeld op basis van gemiddelde spectra en MCR was het enige dat kon garanderen dat minstens 95% van de toekomstige metingen niet meer dan 10% van de 'echte' concentratie zullen afwijken. Het model heeft een goede precisie, accuraatheid, lineariteit, specificiteit en juistheid over het toegepaste concentratiebereik. De robuustheid van dit model werd nagegaan via een experimenteel design waarbij voedingssnelheid, schroefsnelheid en procestemperatuur werden gevarieerd. Geen van deze procesvariabelen bleek een significant effect te hebben op het voorspellen van de geneesmiddelconcentraties. De onzekerheid van de metingen werd geëvalueerd aan de hand van de onzekerheid van de bias en de uitgebreide onzekerheid voor elk concentratieniveau. De onbekende, 'echte' waarde ligt op maximum  $\pm 7.00\%$  van het gemeten resultaat (met een zekerheid van 95%).

In **Hoofdstuk 6** werd de Raman probe ingebouwd in elk segment van de schroefkamer, om het gedrag van materialen tijdens extrusie te visualiseren. De invloed van variaties in geneesmiddelconcentratie, schroefkamertemperatuur en schroefsnelheid op de fysicochemische eigenschappen en interacties tussen het geneesmiddel en het polymeer werd onderzocht. Bij hot-melt extrusie is de schroefkamer nooit volledig gevuld met materiaal, wat een verschil in het achtergrondsignaal in de *in-line* opgenomen Raman spectra veroorzaakte. Hiervoor kon niet gecorrigeerd worden. Daarom werd voor principale

componentenanalyse gekozen, om deze bron van variatie in de spectra te scheiden van de relevante informatie. Wanneer een formulatie met een hoge geneesmiddelconcentratie geëxtrudeerd werd, smolt het geneesmiddel in de eerste kneedzone (tussen segment 2 en 3). Dit fenomeen vond ook plaats bij formulaties met een lage geneesmiddelconcentratie. Daar werd een extra verschil in de spectra waargenomen, onder de vorm van piekverschuivingen, ter hoogte van de derde kneedzone, waar het geneesmiddel oploste in het polymeer en er een vaste oplossing gevormd werd, dankzij de hoge wrijvingskrachten in die derde kneedzone. Dit werd bevestigd door *off-line* opgenomen FT-IR spectra van stalen verzameld in de schroefkamer. Bij een lage geneesmiddelconcentratie had het verhogen van de procestemperatuur geen invloed op de fysicochemische eigenschappen van het eindproduct of op de locatie in de schroefkamer waar dit eindproduct gevormd werd. Dit was ook het geval voor het verdubbelen van de schroefsnelheid. Echter, bij extrusie van een fysisch mengsel met een hoog geneesmiddelgehalte, wordt de fysicochemische toestand van het eindproduct pas verder in de schroefkamer bereikt wanneer de temperatuur lager wordt ingesteld. Wanneer de schroefsnelheid verdubbeld wordt, bevindt het segment waar het eindproduct wordt gevormd zich vroeger in de schroefkamer. De uitgevoerde metingen doorheen de volledige schroefkamer verstrekken *real-time* informatie over het gedrag van het polymeer-geneesmiddel mengsel in de schroefkamer, wat de optimalisatie van procesparameters en procesdesign (schroeven en schroefkamer) toelaat, zodat extrudaten met een vooropgestelde en constante kwaliteit kunnen afgeleverd worden.

In **Hoofdstuk 7** werd een Raman probe ingebouwd in de matrijs van een dubbele-schroef extruder, en elke 20 seconden werd een spectrum opgenomen. Het doel was het opstellen van een model om extrudaten te classificeren op basis van hun fysicochemische toestand. Het effect van variaties in geneesmiddelconcentratie, veranderingen in procestemperatuur en drie verschillende schroefconfiguraties op de fysicochemische eigenschappen van de extrudaten werd onderzocht. Een model werd ontwikkeld, gebruik makend van '*soft independent modelling of class analogy*', waardoor het mogelijk was om *in-line* een onderscheid te maken tussen amorfe oplossingen en kristallijne dispersies van het slecht oplosbaar geneesmiddel in het polymeer, aan de hand van de opgenomen Raman spectra. *Off-line* analyse met DSC en XRD bleek niet gevoelig genoeg om kleine kristallijne fracties van het geneesmiddel te detecteren, die later de uitkristallisatie van het overige amorfe

geneesmiddel kunnen induceren. Deze kleine fracties werden wel gedetecteerd met Raman spectroscopie, aan de hand van piekvernaauwing en het voorkomen van piekverschuivingen. De verschillende schroefconfiguraties hadden geen invloed op de fysicochemische eigenschappen van de extrudaten.

Naast het opstellen van een classificatiemodel, werd ook nagegaan of de druk in de matrijs een invloed heeft op de Raman spectra. De gebruikte geneesmiddelconcentratie, procestemperatuur en de manier waarop het fysisch mengsel in de schroefkamer gevoed wordt, beïnvloeden de druk in de matrijs, en dit effect wordt teruggevonden in de niet-gecorrigeerde Raman spectra als een verschil in het achtergrondsignaal. Storingen in de voeding kunnen dus geobserveerd en geïdentificeerd worden aan de hand van de Raman spectra.

In **Hoofdstuk 8** werd het gebruik van nabije-infraroodspectroscopie geëvalueerd om de geneesmiddelconcentratie, de fysicochemische eigenschappen van de extrudaten en het ontstaan van interacties tijdens extrusie te monitoren. Een NIR probe werd gemonteerd in de matrijs, en elke 30 seconden werd een NIR spectrum opgenomen. Een PLS model werd ontwikkeld om het geneesmiddelgehalte *in-line* te bepalen. De voorspelde en echte geneesmiddelconcentraties vertoonden een goede correlatie ( $R^2 = 0.97$ ), en nieuwe metingen resulteerden in een lage predictiefout (RMSEP = 1.54% w/w). De *in-line* opgenomen NIR spectra vertoonden piekverbreding tijdens extrusie, veroorzaakt door de aanwezigheid van het geneesmiddel in de amorfe vorm, en het ontstaan van een nieuwe piek, die niet teruggevonden werd in de spectra van de fysische mengsels, wees op de vorming van waterstofbruggen tussen het polymeer en het geneesmiddel.

Het doel van **Hoofdstuk 9** was de evaluatie van ultrasone technieken als proces analytische toepassingen om de geneesmiddelconcentratie *in-line* te bepalen. De transittijd van het ultrasone signaal en de piekhoogte werden gemeten in een matrijsadapter, waarin twee ultrasone probes ingebouwd waren. Er werd eerst een PLS model voor kwantificatie opgesteld, enkel gebaseerd op de gemeten druk in de matrijs en de torsie tijdens extrusie. Er werd aangetoond dat het toevoegen van de gemeten transittijd en piekhoogte van het ultrasone signaal het voorspellend vermogen van het model verhoogde.

De resultaten in deze thesis tonen aan dat de implementatie van zowel Raman als nabije-infrarood spectroscopie in farmaceutische hot-melt extrusieprocessen toelaat de geneesmiddelconcentratie en fysicochemische eigenschappen van extrudaten te voorspellen, en de interacties tussen polymeer en geneesmiddel doorheen het volledige extrusieproces in kaart te brengen. Dit draagt bij tot de twee objectieven van het toepassen van PAT in extrusieprocessen: (i) het proces beter begrijpen aan de hand van visualisatie van het gedrag van materialen gedurende het proces en (ii) het meten en analyseren van kritische formulatie- en procesparameters om procescontrole mogelijk te maken en de kwaliteit van het eindproduct te garanderen.

Alle experimenten uit dit onderzoek werden uitgevoerd op laboschaal-extruders (12 en 16 mm). Er moet bijgevolg nagegaan worden of de ontwikkelde methodes en gebruikte modellen ook van toepassing kunnen zijn op grootschalige toestellen. Het bepalen van de geneesmiddelconcentratie en de fysicochemische eigenschappen van de extrudaten laat toe de kwaliteit van de extrudaten te definiëren, maar dit zijn niet de enige (kritische) kwaliteitseigenschappen die moeten gemeten worden. Naast deze twee karakteristieken is het nodig om mogelijke degradatieproducten en -reacties te detecteren, en eventueel om de vrijstelling *in vitro* en *in vivo* van het geneesmiddel vooraf te bepalen op basis van spectroscopische data. De viscositeit van de extrudaten is een eigenschap die van groot belang is voor het verder verwerken van de extrudaten, en die kan nagegaan worden door het implementeren van *on-line* reometers in de schroefkamer of na de matrijs. Het gebruik van spectroscopische en reologische technieken kan ook bijdragen tot de optimalisatie van de gebruikte schroefconfiguratie. De meest energie-efficiënte schroefconfiguratie voor extrusie van een bepaalde formulatie kan op deze manier ontwikkeld worden.

Het extrusieproces is slechts 1 stap in een (continue) productielijn. Het voeden van poeders of fysische poedermengsels moet voldoende gecontroleerd worden. Daarnaast moet ook de impact van de verschillende '*downstream*' processen op de kwaliteit van de extrudaten geëvalueerd worden. Het koelen of opwarmen van de extrudaten, al dan niet gecontroleerd, heeft een significant effect op de kristalliniteit, de manier waarop het geneesmiddel gedispergeerd is in de matrix en op de viscositeit van het eindproduct. Het bepalen van

kritische proces- en formulatie-eigenschappen over de gehele productielijn is noodzakelijk om productie volgens het 'Quality by Design' principe te garanderen.





# CURRICULUM VITAE



# CURRICULUM VITAE - LIEN SAERENS

---

## PERSONAL INFORMATION

---

**SURNAME:** Saerens  
**FIRST NAMES:** Lien Lieve Jan  
**NATIONALITY:** Belgian  
**DATE OF BIRTH:** 10/12/1986  
**PLACE OF BIRTH:** Dendermonde, Belgium  
**CIVIL STATUS:** unmarried  
**ADDRESS:** Albert Scheuremanspark 20  
8210 Loppem  
**EMAIL:** Lien.Saerens@UGent.be

## EDUCATION

---

**2009 – present:** PhD in Pharmaceutical Sciences: “Spectroscopic process monitoring for quality assessment, visualization and understanding of pharmaceutical hot-melt extrusion”  
Promoter: Prof. Dr. Thomas De Beer, Co-promoter: Prof. Dr. Chris Vervaet  
Laboratory of Pharmaceutical Process Analytical Technology,  
Ghent University, Belgium

**2004 – 2009:** Master in Pharmaceutical Care  
Ghent University, Belgium

**1998 – 2004:** Degree Sciences - Mathematics  
Sint Lodewijkscollege, Brugge, Belgium

## EXPERIENCE

---

- 2012:** Research exchange  
Brabender® Pharma GmbH  
Duisburg, Germany
- April – June 2011:** Research exchange  
School of Engineering, Design and Technology  
University of Bradford, United Kingdom
- August 2009:** Apotheek Van Nieuwerburgh (Lloyds Pharma), Eeklo, Belgium
- 2008 – 2009:** Pharmacist internship  
Apotheek Martin, Reep 44, 9000 Gent, Belgium
- 2008:** Master thesis: “The Effect of Moisture on the Mixing Behaviour of Granules”  
Promoter: Prof. Dr. Chris Vervaet  
Department of Pharmaceutical Technology, University of Helsinki

## PUBLICATIONS IN PEER REVIEWED JOURNALS

---

Validation of an in-line Raman spectroscopic method for continuous API quantification during pharmaceutical hot-melt extrusion

**L. Saerens, N. Segher, C. Vervaet, J.P. Remon, T. De Beer**

*Accepted for publication in Analytica Chimica Acta (2013)*

In-line solid state prediction during pharmaceutical hot-melt extrusion in a 12 mm twin screw extruder using Raman spectroscopy

**L. Saerens, D. Ghanam, C. Raemdonck, K. Francois, J. Manz, R. Krüger, S. Krüger, C. Vervaet, J.P. Remon, T. De Beer**

*Submitted to European Journal of Pharmaceutics and Biopharmaceutics (2013)*

Process monitoring and visualization solutions for hot-melt extrusion: A review

**L. Saerens, C. Vervaet, J.P. Remon, T. De Beer**

*Journal of Pharmacy and Pharmacology (2013) doi: 10.1111/jphp.12123*

Visualization and process understanding of material behavior in the extrusion barrel during a hot-melt extrusion process using Raman spectroscopy

**L. Saerens**, C. Vervaeet, J.P. Remon, T. De Beer

*Analytical Chemistry* 85 (2013) 5420-5429

Prilling of fatty acids as a continuous process for the development of controlled release multiparticulate dosage forms

A. Vervaeck, **L. Saerens**, B.G. De Geest, T. De Beer, R. Carleer, P. Adriaensens, J.P. Remon, C. Vervaeet

*European Journal of Pharmaceutics and Biopharmaceutics* (2013)doi:10.1016/j.ejpb.2013.02.003

In-line NIR spectroscopy for the understanding of polymer-drug interaction during pharmaceutical hot-melt extrusion

**L. Saerens**, L. Dierickx, T. Quinten, P. Adriaensens, R. Carleer, C. Vervaeet, J. P. Remon, T. De Beer

*European Journal of Pharmaceutics and Biopharmaceutics* 81 (2012) 230-237

Co-extrusion as manufacturing technique for fixed-dose combination mini-matrices

L. Dierickx, **L. Saerens**, A. Almeida, T. De Beer, J.P. Remon, C. Vervaeet

*European Journal of Pharmaceutics and Biopharmaceutics* 81 (2012) 683-689

Preparation and evaluation of sustained-release matrix tablets based on metoprolol and an acrylic carrier using injection moulding

T. Quinten, G.P. Andrews, T. De Beer, **L. Saerens**, W. Bouquet, D.S. Jones, P. Hornsby, J.P. Remon, C. Vervaeet

*AAPS PharmSciTech* 13 (2012) 1197-1211

Upscaling and in-line process monitoring via spectroscopic techniques of ethylene vinyl acetate hot-melt extruded formulations

A. Almeida, **L. Saerens**, T. De Beer, J.P. Remon, C. Vervaeet

*International Journal of Pharmaceutics* 439 (2012) 223-229

Raman spectroscopy for the in-line polymer-drug quantification and solid state characterization during a pharmaceutical hot-melt extrusion process

**L. Saerens**, L. Dierickx, B. Lenain, C. Vervaeet, J.P. Remon, T. De Beer

*European Journal of Pharmaceutics and Biopharmaceutics* 77 (2011) 158-163

Near infrared and Raman spectroscopy for the in-process monitoring of pharmaceutical production processes

T. De Beer, A. Burggraef, M. Fonteyne, **L. Saerens**, J.P. Remon, C. Vervaeet

*International Journal of Pharmaceutics* 417 (2011) 32-47

Detection of counterfeit Viagra<sup>®</sup> by Raman microspectroscopy imaging and multivariate analysis  
P.-Y. Sacré, E. Deconinck, **L. Saerens**, T. De Beer, P. Courselle, R. Vancauwenberghe, P. Chiap, J. Crommen, J. O. De Beer

*Journal of Pharmaceutical and Biomedical Analysis* 56 (2011) 454-461

**PRESENTATIONS AT CONFERENCES**

---

**Oral presentations**

In-line solid state prediction during pharmaceutical hot-melt extrusion in a 12 mm twin screw extruder using Raman spectroscopy

**L. Saerens, D. Ghanam, C. Raemdonck, K. Francois, R. Krüger, S. Krüger, C. Vervaet, J.P. Remon, T. De Beer**

*7<sup>th</sup> Annual PSSRC Symposium, Lille (France), 4-6 July 2013*

NIR and Raman spectroscopy as PAT tools in pharmaceutical hot-melt extrusion

**L. Saerens, T. De Beer.**

*APV Hands-on workshop on Hot Melt Extrusion, Karlsruhe (Germany), 5-6 June 2013*

In-line solid state monitoring of Celecoxib/Eudragit EPO systems during hot-melt extrusion by Raman spectroscopy

**L. Saerens, D. Ghanam, C. Raemdonck, K. Francois, R. Krüger, S. Krüger, C. Vervaet, J.P. Remon, T. De Beer**

*APV Experts' Workshop on Hot-Melt Extrusion, Ludwigshafen (Germany), 5-6 November 2012.*

Spectroscopic hot-melt extrusion in-process monitoring throughout the entire extrusion barrel

**L. Saerens, T. De Beer.**

*APS Amorphous IV: Hot-melt extrusion and powder technology in pharmaceutical industry, University of Greenwich (United Kingdom), 12-13 June 2012.*

Ultrasound and NIR monitoring of a pharmaceutical hot-melt extrusion process

**L. Saerens, E. Brown, A. Kelly, T. Gough, R. Dhumal, P. Apshingekar, A. Paradkar, C. Vervaet, J.P. Remon, T. De Beer**

*EuPAT 5, Ghent (Belgium), 9-10 May 2012*

Visualization and understanding of material behaviour in the extrusion barrel during pharmaceutical hot-melt extrusion using Raman spectroscopy

**L. Saerens, C. Vervaet, J.P. Remon, T. De Beer**

*16<sup>th</sup> Forum of Pharmaceutical Sciences, Blankenberge (Belgium), 7-8 May 2012*

In-line Raman spectroscopy for the understanding of polymer-drug behavior in the extrusion barrel during a pharmaceutical hot-melt extrusion process

**L. Saerens, C. Vervaet, J.P. Remon, T. De Beer**

*5<sup>th</sup> Annual PSSRC Symposium, Helsinki (Finland), 26-27 September 2011*

NIR spectroscopy as PAT-tool for in-line monitoring of pharmaceutical hot-melt extrusion processes

**L. Saerens, C. Vervaet, J.P. Remon, T. De Beer**

*Thermo Scientific User Meeting, Neder-over-heembeek (Belgium), 25 November 2010*

In-line determination of API content and solid state during pharmaceutical hot-melt extrusion processes using Raman spectroscopy

**L. Saerens, C. Vervaet, J.P. Remon, T. De Beer**  
*IWPCPS 12 Workshop, Lille (France) 21-24 June 2010*

NIR spectroscopy as PAT tool for in-line and real-time monitoring of pharmaceutical hot-melt extrusion processes

**L. Saerens, C. Vervaet, J.P. Remon, T. De Beer**  
*Thermo Scientific Summer Meeting, Arnhem (The Netherlands) 16 June 2010*

### **Poster presentations**

In-line solid state monitoring during pharmaceutical hot-melt extrusion using Raman spectroscopy

**L. Saerens, D. Ghanam, C. Raemdonck, K. Francois, R. Krüger, S. Krüger, C. Vervaet, J.P. Remon, T. De Beer**  
*Knowledge for growth, Ghent (Belgium), 30 May 2013*

In-line solid state monitoring during pharmaceutical hot-melt extrusion in a 12mm pharma twin screw extruder using Raman spectroscopy

**L. Saerens, D. Ghanam, C. Raemdonck, K. Francois, R. Krüger, S. Schlaefke, C. Vervaet, J.P. Remon, T. De Beer**  
*2012 AAPS annual meeting and exposition, Chicago (USA), 14-18 October 2012*

Visualization and understanding of material behaviour in the extrusion barrel during pharmaceutical hot-melt extrusion using Raman spectroscopy

**L. Saerens, C. Vervaet, J.P. Remon, T. De Beer**  
*Scientific Afternoon, Faculty of Pharmaceutical Sciences, Ghent University, Ghent (Belgium), 16 May 2012*

Visualization and understanding of material behaviour in the extrusion barrel during pharmaceutical hot-melt extrusion using Raman spectroscopy

**L. Saerens, C. Vervaet, J.P. Remon, T. De Beer**  
*EuPAT 5, Ghent (Belgium), 9-10 May 2012*

Raman spectroscopy for the in-line monitoring of a pharmaceutical hot-melt extrusion process

**L. Saerens, B. Braeckman, C. Vervaet, J.P. Remon, T. De Beer**  
*8th PBP World Meeting, Istanbul (Turkey), 19-22 March 2012*

NIR and Raman spectroscopy as Process Analytical Tools for In-Line and Real-Time Monitoring of a Pharmaceutical Hot-Melt Extrusion Process

**L. Saerens, J.P. Remon, C. Vervaet, T. De Beer**  
*Europact 2011, Glasgow (United Kingdom), 26-29 April 2011*

Raman spectroscopy as a process analytical tool for in-line and real-time monitoring of a pharmaceutical hot-melt extrusion process

**L. Saerens, J.P. Remon, C. Vervaet, T. De Beer**

*2010 AAPS annual meeting and exposition / FIP PSWC, New Orleans (USA), 14-18 November 2010*

Raman spectroscopy as a process analytical tool for in-line and real-time monitoring of a pharmaceutical hot-melt extrusion process

**L. Saerens, J.P. Remon, C. Vervaet, T. De Beer**

*PSWC 2010 Congress for students and postdoctoral fellows, New Orleans (USA), 13-14 November 2010*

Raman spectroscopy as a process analytical tool for in-line and real-time monitoring of a pharmaceutical hot-melt extrusion process

**L. Saerens, J.P. Remon, C. Vervaet, T. De Beer**

*Drug Analysis, Antwerp (Belgium), 21-24 September 2010*

Raman spectroscopy as a process analytical tool for in-line and real-time monitoring of a pharmaceutical hot-melt extrusion process

**L. Saerens, J. P. Remon, C. Vervaet, T. De Beer**

*Scientific Afternoon, Faculty of Pharmaceutical Sciences, Ghent University, Ghent (Belgium), 12 May 2010*

## **ATTENDED COURSES, CONFERENCES AND WORKSHOPS**

---

- *Conference: 11th Chemometrics symposium: Advances in Chemometrics, Belgian Chemometrics Society, 8 June 2012, Ghent (Belgium)*
- *Workshop: Continuous Processing for Tablet Manufacturing, EuPat 5 Pre-conference workshop, 8 May 2012, Ghent (Belgium)*
- *Course: Introduction to Process Control for Chemists, Pharmacists and Formulation Scientists, 27-29 June 2011, CPACT, Perceptive Engineering, Daresbury (United Kingdom)*
- *Course: Support Vector Machines: Non-linear modeling made easy, 26 April 2011, Glasgow (United Kingdom)*
- *Course: Hyperspectral Chemical Imaging for Process Analytics, 26 April 2011, Glasgow (United Kingdom)*
- *Course: Modulated Differential Scanning Calorimetry (MDSC) Training Course, 15 June 2010, TA Instruments, Ghent (Belgium)*



- *Course: Differential Scanning Calorimetry (DSC) Training Course, 7 June 2010, TA Instruments, Ghent (Belgium)*
- *Conference: EuPAT 4 – Taking PAT to the next level, 5-6 May 2010, Kuopio (Finland)*
- *Workshop: Pharmaceutical Hot Melt Extrusion, 15 April 2010, Coperion GmbH, Stuttgart (Germany)*
- *Course: Design of Experiments, January 2010, Ghent (Belgium)*
- *Course: Multivariate Data Analysis, January 2010, Ghent (Belgium)*

## LANGUAGE SKILLS

---

	<u>Speaking</u>	<u>Reading</u>	<u>Writing</u>
Dutch (native language)	very good	very good	very good
French	good	good	good
English	very good	very good	very good
German	notions	notions	notions





